a report

DEPARTMENT OF
METEOROLOGY
TEXAS A&M UNIVERSITY

TRANSFER OF THERMAL MICROWAVES IN THE ATMOSPHERE

Volume I

by

Jack F. Paris

May 1971

Funded by

National Aeronautics and Space Administration
Grant Number NASA NGR-44-001-098

Additional Support by

Office of Naval Research, Contract Nonr 2119(04)
Project Themis, Department of Defense
Water Resources Institute, Proj. No. 5013

TRANSFER OF THEMAL MICROWAVES IN THE ATMOSPHERE

Volume I

by

Jack F. Paris

May 1971

Funded by

National Aeronautics and Space Administration
Grant Number NASA NGR-44-001-098

Additional Support by

Office of Naval Research, Contract Nonr 2119(04)
Project Themis, Department of Defense
Water Resources Institute, Proj. No. 5013

Department of Meteorology
Texas A&M University
College Station, Texas 77843

FOREWARD

The primary emphasis in this investigation has been to investigate the propagation of microwave radiation in the atmosphere. The ultimate goal of this study is to determine the feasibility of utilizing microwave radiometric systems on spacecraft for use in making meaningful meteorological observations. The author has made a thorough, theoretical study of atmospheric absorption and scattering by liquid hydrometeors. The report is presented in two volumes. Volume I contains the basic theory and a brief summary of the results. Volume II contains figures and tabular information that is supplemental to Volume I.

ABSTRACT

Transfer of Thermal Microwaves in the Atmosphere. (May 1971)

Jack Frederick Paris, B.S., Texas A&M University;

B.S., University of Washington

Directed by: Dr. Robert A. Clark

The Mie theory is used to determine the absorption and scattering properties of liquid hydrometeors at 27 microwave frequencies from 500 MHz (60-cm wavelength) to 60 GHz (5-mm wavelength). Based on the Marshall-Palmer distribution of drop sizes, regression equations are developed for the volume absorption coefficient of rain as a function of its temperature and content of liquid water.

Measurements of the dielectric constant of water and aqueous sodium chloride by Lane and Saxton are used to form regression equations for the dielectric constant of water as a function of its temperature and salinity. These equations and the Fresnel equations for reflection are used to compute the polarized components of the thermal emission of sea water for a wide range of sea temperatures, sea salinities, microwave frequencies, and angles of viewing.

From the derived regression equations for the volume absorption coefficient of rain and known expressions for that of clouds, molecular oxygen, and water vapor, the direct problem of radiative

transfer is solved for 582 plane-parallel, horizontally-homogeneous, model atmospheres. The thin atmosphere approximation, in which effects of multiple scattering are ignored for both extinction and emission, is used in these calculations. The resulting fields of emission and the transmissivities are analyzed in terms of their predictability by the integrated contents of water in gaseous form, in cloud form, and in rain form. With the use of these predictors, the emission and transmissivity of the atmosphere are predictable by a set of third-degree regression equations where the multiple correlation coefficients are greater than 0.995 and the standard errors of estimate are less than 9.7%.

The effect of multiple scattering on the transfer of thermal microwaves in the atmosphere is evaluated at 37 GHz by the Monte Carlo method for a model cloud of which the thickness is 3 km, the surface rate of rainfall is 8 mm hr^{-1} (moderate rain), the optical thickness is 1.8722, and the albedo for single scattering is 0.3323. The emission of this cloud agrees with that given by the thin atmosphere approximation for zenith angles between 0 and 60 deg and between 120 and 180 deg and is essentially unpolarized. The transmitted radiation is partially polarized, especially for zenith angles near the horizon. The spectral albedo of the rain is 8.8%. As a result of multiple scattering, the intensity of upwelling radiation from the rain cloud over land is about 13% less than that from the land and about 10% less than that from a non-scattering, opaque atmosphere.

On the basis of these studies, it is concluded that (1) measurements of the dielectric constant of sea water are needed for frequencies less than 5.81 GHz, (2) a microwave radiometer can not be used to survey sea temperature, (3) an airborne radiometer operating at 1.42 GHz can be used to survey surface salinity in areas of warm water, (4) an extensive empirical study is needed to determine the effect of sea state on the emission of the sea, (5) a radiometer operating at an optimum frequency of 10.69 GHz can be used to survey the integrated content of liquid water in the rain mass over the ocean, (6) a set of radiometers operating at 5.81, 10.69, 15.375, and 19.35 GHz may be used to survey sea state, atmospheric liquid water, and precipitable water over the ocean, and (7) a radiometer operating at 37 GHz can be used to detect hail and heavy rain over land.

ACKNOWLEDGMENTS

During the course of these investigations, I have received much encouragement from friends and associates. In particular, I appreciate the support of Dr. Robert A. Clark, Dr. George L. Huebner, and Dr. Robert C. Runnels of the Department of Meteorology, Dr. John P. German of the Department of Electrical Engineering, and Dr. H. A. Luther of the Department of Mathematics. Also, I wish to thank Dr. Vance E. Moyer, Head of the Department of Meteorology, for his support and his assistance in editing this paper.

Dr. George Kattawar of the Physics Department has given many helpful suggestions in the programming of the Monte Carlo method. Dr. Charles E. Gates of the Department of Statistics provided the random number generator used in the Monte Carlo program.

This research was supported by a grant (NASA NGR-44-001-098) from the National Aeronautics and Space Administration (NASA). Other support has been received in the past years from the Office of Naval Research under Contract Nonr 2119(04), the Texas A&M Water Resources Institute, and Project Themis of the Department of Defense.

This research has received much encouragement from Dr. William Nordberg and Dr. Jack Conaway of the Laboratory for Meteorology and Earth Sciences, NASA Goddard Space Flight Center, Greenbelt, Maryland, and from Mr. Jack Sherman, Manager of the Spacecraft Oceanography Project, Naval Oceanographic Office, Washington, D. C.

Appreciation is given to my wife, Mary, and our children for their support, love, and patience throughout this period of research.

This paper was typed by Mrs. Beth Williams, and the figures were drafted in the Texas Transportation Institute, by Mr. Hector Cornelio, or by the Gerber Plotter of the Department of Industrial Engineering, Texas A&M University.

TABLE OF CONTENTS

LIST OF TABLES

LIST OF FIGURES

LIST OF SYMBOLS AND ABBREVIATIONS

SCALARS

a	drop diameter
a_{max}	maximum drop diameter in a polydispersion
a_{mode}	the drop diameter at which the content of liquid water per unit volume per unit increment of drop diameter is a maximum
a_n	complex scattering amplitude in Mie theory
b	slope parameter in M-P distribution
b_n	complex scattering amplitude in Mie theory
c	speed of light in a vacuum, 2.997925×10^8 m s^{-1}
c_1	temperature dependent constant in regression formula for α_p
c_f	number of photons per unit flux
c_n	$2 k \nu^2 c_f/c^2$
d	temperature dependent constant in regression formula for α_p
e	vapor pressure of water vapor
f	relative effectiveness factor
f_i, i=0,4	regression coefficients
g_i, i=0,4	regression coefficients
h	Planck's constant, 6.6256×10^{-34} J s
$\tilde{h}$	height of an observer above the sea surface
j	$\sqrt{-1}$, designates the imaginary part of a complex quantity.

k	Boltzmann's constant, 1.38054×10^{-23} J K^{-1}
ℓ	distance a representative photon travels from one interaction point to another
ℓ^*	distance from an interaction point to the boundary of the scattering domain.
m	complex index of refraction of water
m_w	molecular weight of water vapor, 18.016 g mol^{-1}
m'	real part of the complex index of refraction of water
m''	negative imaginary part of the complex index of refraction of water
n	integer number
p	total atmospheric pressure
q_1	normalizing factor for the probability distribution function for angular scattering
q_2	normalizing factor for the transformation of the Stokes vector of scattered radiation
t	time
u	dummy variable
v	velocity of propagation of electromagnetic waves through a medium
w_n	term used in iterative scheme of Deirmendjian (1969)
x	drop-size parameter
z	altitude
z_b	altitude of the base of the scattering medium
z_t	altitude of the top of the scattering medium
A_n	factor in the Deirmendjian method

B	intensity of emission of a black body
B_p	polarized component of the intensity of emission of a black body
E	total electric field
E_h	horizontally polarized component of the electric field vector
E_{ho}	absolute magnitude of the horizontally polarized component of the electric field vector
E_{ih}	horizontally polarized component of the electric field vector of the incident wave
E_{iv}	vertically polarized component of the electric field vector of the incident wave
E_{rh}	horizontally polarized component of the electric field vector of the reflected wave
E_{rv}	vertically polarized component of the electric field vector of the reflected wave
E_v	vertically polarized component of the electric field vector
E_{vo}	absolute magnitude of the vertically polarized component of the electric field vector
F	pressure-broadening structure-factor
$F_{N\pm}$	pressure-broadening structure-factor of molecular oxygen for resonant frequencies $\nu_{N\pm}$
F_o	pressure-broadening structure-factor of molecular oxygen for zero-frequency absorption-line.
I	(specific) intensity of a stream of electromagnetic radiation
$\bar{I}$	average or effective value of intensity over a solid-angle strip
I_h	horizontally polarized component of the intensity
I_n	intensity of the unpolarized part of a radiant energy stream

I_{rh}	horizontally polarized component of the reflection
I_{rv}	vertically polarized component of the reflection
I_v	vertically polarized component of the intensity
J	source function
K_a	efficiency of the absorption by a cloud or rain element
K_{ar}	efficiency of absorption by a cloud element given from the Rayleigh approximation
K_s	efficiency of scattering by a cloud or rain element
K_{sr}	efficiency of scattering by a cloud element given by Rayleigh approximation
K_t	efficiency of extinction by a cloud or rain element
M_c	content of liquid water in the cloud mass
M_p	content of liquid water in the rain mass
M_z	integrated content of liquid water in the atmosphere below level z
M_∞	integrated content of liquid water in the whole atmosphere
N	number of drops per unit volume per unit interval of drop diameter
N_o	number of drops per unit volume per interval of drop diameter for a diameter of zero in the M-P distribution, 8.0×10^{-6} m^{-4}
P_a	rate of absorption of energy by a cloud or rain element
P_s	rate of scattering of energy by a cloud or rain element
Q	second Stokes parameter, $I_v - I_h$

Q_a	absorption cross section of a cloud or rain element
Q_s	scattering cross section of a cloud or rain element
Q_t	total extinction cross section of a cloud or rain element
R	rainfall intensity
R_1	element of the reflection matrix
R_2	element of the reflection matrix
R_3	element of the reflection matrix
R_4	element of the reflection matrix
R_g	Universal Gas Constant, 8.3144 erg mol^{-1} K^{-1}
R_h	Fresnel reflection coefficient for horizontal polarization
R_v	Fresnel reflection coefficient for vertical polarization
S	the salinity of the surface layer of the sea
S_1	complex scattering factor for the component of the radiation scattered by a cloud or rain element parallel to the scattering plane
S_2	complex scattering factor for the component of the radiation scattered by a cloud or rain element perpendicular to the scattering plane
S_N	collection of terms given by (112)
T	temperature; often, air temperature
$\bar{T}$	mean atmospheric temperature of a horizontal layer of atmosphere
T_d	dew point temperature

$\bar{T}_d$	mean atmospheric dew point temperature of a horizontal layer of atmosphere
T_{sea}	temperature of the surface layer of the sea
T_{sfc}	surface temperature
U	third component of the Stokes vector
U_i	third component of the Stokes vector for incident radiation
U_r	third component of the Stokes vector for reflected radiation
V	fourth component of the Stokes vector
V_i	fourth component of the Stokes vector for incident radiation
V_r	fourth component of the Stokes vector for reflected radiation
W_c	equivalent depth of liquid water in the cloud mass in a vertical column
W_p	equivalent depth of liquid water in the rain mass in a vertical column
W_i	power density of incident wave
W_ℓ	equivalent depth of liquid water in the cloud and rain mass in a vertical column
W_v	equivalent depth of gaseous water in a vertical column; precipitable water
W_z	equivalent depth of liquid water in the rain mass below altitude
W_∞	equivalent depth of liquid water in a vertical column of the whole atmosphere
α	volume absorption coefficient
α_c	volume absorption coefficient of a non-raining cloud

α_g	volume absorption coefficient of atmospheric gases
α_{gold}	volume absorption coefficient of a non-raining cloud given by Goldstein (1951)
α_o	volume absorption coefficient of molecular oxygen
α_p	volume absorption coefficient of the rain mass given by the Mie theory
α_{stae}	volume absorption coefficient of a non-raining cloud given by Staelin (1966)
α_w	volume absorption coefficient of water vapor
β	volume scattering coefficient
β_c	volume scattering coefficient of a non-raining cloud
β_p	volume scattering coefficient of the rain mass
γ	the angle whose tangent is the ratio of the minor axis to the major axis of the polarization ellipse
δ_1	rotation angle (see Fig. 65)
δ_2	rotation angle (see Fig. 65)
δ_i	phase difference between ε_{iv} and ε_{ih}
δ_r	phase difference between ϕ_r and ϕ_h
ε_h	phase angle of the horizontally polarized component of the electric field vector
ε_o	permittivity of a vacuum, 8.854×10^{-12} F m^{-1}
ε_s	static dielectric constant of sea water
ε_v	phase angle of the vertically polarized component of the electric field vector
ε'	real part of the relative permittivity or complex dielectric constant

ε''	negative, imaginary part of the relative permittivity, or complex dielectric constant
ε_∞	relative permittivity of a medium at high electromagnetic frequencies
ζ	uniform, random variable having a value in the interval (0,1)
η	the normalized, probability distribution function for angular scattering of microwaves by a polydispersion
θ	angle between direction of flow of a pencil of radiation and the normal; zenith angle
θ_1	zenith angle at the top of a solid angle strip
θ_2	zenith angle at the bottom of a solid angle strip
θ_a	zenith angle of reflected or refracted ray in the atmosphere
θ_i	zenith angle of incident radiation
θ_s	zenith angle of scattered radiation
θ_w	zenith angle of the reflected or refracted ray in the ocean
κ	volume extinction coefficient
μ	cosine of the zenith angle (negative for downward traveling streams of radiation)
μ_s	cosine of the scattering angle
ν	electromagnetic frequency
$\nu_{N\pm}$	resonant frequencies of molecular oxygen
ν_w	resonant frequency of water vapor, 22.235×10^9 Hz
ξ	emissivity of the atmosphere at microwave frequencies

ξ_h	the emissivity of the sea for horizontal polarization
ξ_s	mean emissivity of a slab
ξ_v	the emissivity of the sea for vertical polarization
π	3.1415927
π_n	Pi function
ρ_l	density of liquid water, approximately 999700 g m^{-3}
ρ_w	density of water vapor
σ	conductivity of a medium
σ_i	ionic conductivity of sea water
τ	optical depth
τ_a	optical depth for absorption
τ_o	optical depth (thickness) of the entire atmosphere
τ_n	Tau function
τ_s	optical depth for scattering
τ_t	relaxation time of sea water
ϕ	azimuth angle
ϕ_h	phase angle of the Fresnel reflection coefficient for horizontal polarization
ϕ_i	azimuth angle of incident radiation
ϕ_s	azimuth angle of scattered radiation
ϕ_v	phase angle of the Fresnel reflection coefficient for vertical polarization
χ	the angle between the vertical plane and the major axis of the polarization ellipse
ω	albedo for single scattering, $\beta/(\alpha + \beta)$

ω_f	circular frequency ($2 \pi \nu$)
Γ	transmissivity of the atmosphere
Γ_s	transmissivity of a slab
Δ_a^*	optical distance for absorption between a scattering point and a boundary of the scattering medium
Δ_s^*	optical distance for scattering between a scattering point and a boundary of the scattering medium
Δ_o	line-width parameter of molecular oxygen
Δ_w	line-width parameter of water vapor
Θ	scattering angle
T	brightness temperature of microwave radiation
T_{ap}	polarized component of the anabatic emission of the atmosphere at microwave frequencies
T_{eh}	horizontal component of the brightness temperature of the thermal emission of the ocean at microwave frequenceis
T_{ev}	vertically polarized component of the brightness temperature of the thermal emission of the ocean at microwave frequencies
T_{kp}	polarized component of the katabatic emission of the atmosphere at microwave frequencies
T_p	polarized component of the brightness temperature
Ω	solid angle

VECTORS

$\vec{a}$	unit vector along direction of flow of radiant energy
$\vec{a}_x$	unit vector along x-axis
$\vec{a}_y$	unit vector along y-axis

$\vec{a}_z$	unit vector along z-axis
$\vec{n}$	unit normal vector
$\vec{B}$	Stokes vector for the intensity of emission of a black body
$\vec{E}$	electric-field vector
$\vec{E}_o$	magnitude of the electric-field vector
$\vec{H}$	magnetic-field vector
$\vec{I}$	Stokes vector
$\vec{I}_i$	Stokes vector for the intensity of the incident wave
$\vec{I}_{i,\ sea}$	Stokes vector of the intensity of the radiation incident upon the air-sea interface from below
$\vec{I}_r$	Stokes vector for reflected radiation
$\vec{I}_t$	Stokes vector for the intensity of the transmitted wave
$\vec{I}_{t,\ sea}$	Stokes vector for the intensity of the radiation originating in the ocean and transmitted through the air-sea interface
$\vec{J}$	Stokes vector of the source function
$\vec{T}$	temperature vector, $\{T,0,0,0\}$
$\vec{T}_{sea}$	column vector, $\{T_{sea},0,0,0\}$
$\vec{\upsilon}$	Stokes vector for representative photon
$\vec{\upsilon}_e$	Stokes vector for escaping photon
$\vec{\upsilon}'$	Stokes vector for remaining photon
$\vec{T}_a$	Stokes vector for the brightness temperature or the anabatic emission of the atmosphere

$\vec{T}_c$	Stokes vector for the brightness temperature of radiation incident upon the top of the atmosphere
$\vec{T}_e$	the Stokes vector for the brightness temperature of the radiation emitted by the sea into the atmosphere
$\vec{T}_k$	Stokes vector for the brightness temperature of the katabatic emission of the atmosphere
$\vec{T}_o$	Stokes vector for radiation incident upon a slab
$\vec{T}_s$	Stokes vector for the brightness temperature of the sum of the katabatic emission of the atmosphere and the transmission of radiation incident at the top of the atmosphere through the atmosphere
$\vec{T}_u$	Stokes vector for the brightness temperature of the sum of the anabatic emission of the atmosphere and the transmitted radiation originating at the surface
$\vec{T}'$	Stokes vector for the photons remaining in a scattering medium
$\vec{T}''$	Stokes vector of photons arriving at a new scattering point in a scattering medium

MATRICES

[F]	transformation matrix for angular scattering by a cloud or rain element
[I]	identity matrix
[P]	azimuthally independent phase matrix for angular scattering
$[P_o]$	phase matrix for angular scattering
[R]	reflection matrix
$[R_1]$	rotation matrix for angle δ_1

$[R_2]$	rotation matrix for angle δ_2
[T]	transmission matrix
$[\Sigma']$	transformation matrix for a polydispersion

COMPOUND SYMBOLS

Ac	altocumulus cloud
Cb	cumulonimbus cloud
Cu	cumulus cloud
CuH	cumulus humilis cloud
M-P	denotes distribution of rain drops with size given by Marshall and Palmer (1948)
ds	differential path length
dt	differential interval of time
du	dummy differential element
dz	differential height
dA	differential area
dE	differential amount of radiant energy
dF	differential element of radiative flux
$d\theta$	differential element of zenith angle
$d\nu$	differential increment of electromagnetic frequency
$d\phi$	differential element of azimuth angle
$d\tau$	differential optical path-length
$d\Omega$	differential solid angle

$d\vec{I}$	differential change in the Stokes vector for intensity due to extinction and emission processes
$d\vec{I}_{em}$	differential change in the Stokes vector for intensity due to emission processes
$d\vec{I}_{ex}$	differential change in the Stokes vector for intensity due to extinction processes
$d\vec{T}$	differential change in the Stokes vector for the brightness temperature of a stream of radiation due to extinction and emission processes
Δa	change in the optical depth for absorption from one scattering point to another
$\Delta n(\theta_1,\theta_2)$	number of photons flowing through the solid angle strip bound by zenith angles, θ_1 and θ_2, per unit time per unit band width per unit horizontal area
Δs	change in the optical depth for scattering from one scattering point to another
Δt	small time interval
Δz	thickness of a layer of atmosphere
ΔA	small area
ΔE	small amount of radiant energy
$\Delta F(\theta_1,\theta_2)$	flux passing through a solid angle strip bound by zenith angles, θ_1 and θ_2
$\Delta \nu$	bandwidth
$\Delta \Omega$	small solid angle

OPERATORS

$\log_{10}$	logarithm to the base 10
Σ	summation
$\cdot$	scalar or dot product

x	vector or cross product
$\vec{\nabla}$	del operator, $\vec{a}_x \frac{d}{dx} + \vec{a}_y \frac{d}{dy} + \vec{a}_z \frac{d}{dz}$
| |	operator indicating that absolute value of a complex quantity is to be used
*	denotes complex conjugate is being used
cos	cosine function
exp	exponential function
Im	operator indicating that the imaginary part of a complex quantity is being used
ln	logarithm to the base e
Re	operator indicating that the real part of a complex quantity is being used
sec	secant function
sin	sine function
tan	tangent function
—	average value

UNITS

cm	centimeter, 10^{-2} meters
deg	angular measure, degrees
g	grams
hr	hour
km	kilometer, 10^{3} meters
m	meter
mb	millibar
mm	millimeter, 10^{-3} meter

o/oo	parts per thousand
s	second
str	steradian
A	ampere
C	degrees Celsuis
F	farad
GHz	gigaHertz, 10^9 cycles per second
H	henry
Hz	cycles per second
J	Joule
K	degrees Kelvin
MHz	megaHertz, 10^6 cycles per second
N	normality of a solution
V	volts
W	watt, Joule per second
℧	mhos, conductivity

CHAPTER I

INTRODUCTION

A. Nature of the Problem

Meteorological studies are based upon timely observations of appropriate parameters of the atmosphere and its underlying surfaces. Remote sensing of the atmosphere and the ocean in the visible and infrared portions of the electromagnetic spectrum has provided much useful information in the past. In the 1970's, the National Aeronautics and Space Administration (NASA) will place on Earth satellites and aircraft radiometers which are capable of measuring the distribution of thermal radiation at microwave frequencies. Previous theoretical and empirical studies have shown that the thermal emission of the atmosphere at microwave frequencies depends on the spatial distribution of pressure, temperature, water vapor, and liquid hydrometeors. Also, the microwave emission of the sea depends on its surface temperature, surface salinity, and surface roughness. The relative importances of these environmental parameters in determining the microwave emission of the atmosphere and the ocean have not been determined for situations where rain is a constituent of the atmosphere. Neither have the

---

The citations on the following pages follow the style of the Journal of the Atmospheric Sciences.

quantitative relationships between the meteorological properties of the atmosphere and its microwave emissions been established for a wide range of microwave frequencies.

This study is a theoretical, calculative investigation of the thermal emission of the atmosphere and the ocean at microwave frequencies from 500 MHz (60-cm wavelength) to 60 GHz (5-mm wavelength) from a representative number of model atmospheres including rain. The radiative transfer problem is solved for each model atmosphere in order to compute the katabatic and anabatic emissions of the atmosphere at microwave frequencies. The effects of multiple scattering on the transfer of thermal microwaves in rain are evaluated by the Monte Carlo method. The resulting calculations are analyzed in terms of their predictability by a small number of basic, atmospheric parameters. The effect of the emission and reflection of thermal microwaves by the ocean is discussed, and some oceanic applications of microwave radiometry are developed. A determination of a set of optimum microwave frequencies and instrument configurations for specific meteorological applications is made. Finally, recommendations for future study are made.

B. Review of Past Studies

1. Early history of microwave radiometry. Jansky (1932) first detected thermal radiation at radio frequencies from extra-terrestrial sources in 1931, hence, the first radiowave radiometers

were called radio telescopes. In 1946, Dicke (1946) developed a technique which greatly lessened measurement errors due to fluctuations in the amplification of the radio receiver of the radiometer. By the late 1950's, radio telescopes were operating at frequencies in the microwave region, and scientists became aware of the interference of the atmosphere at these frequencies. Straiton et al. (1958), Castelli et al. (1959), and Hogg (1959) noted that the katabatic emission of the atmosphere at microwave frequencies varied greatly for different meteorological conditions. The emission of microwaves by clear atmospheres was quite small; however, on humid days, cloudy days, and especially rainy days, it was large.

In the early 1960's, scientists used an airborne microwave radiometer to survey the location of icebergs through fog in the North Atlantic Ocean (Seling and Nance, 1961; Judge, 1965). They found that sea ice emits about twice as much microwave radiation as the open ocean.

The first and only United States satellite that carried a microwave radiometer was Mariner 2 which passed within 34,350 km of Venus in December 1962. This radiometer, called the MR-62, operated at frequencies of 15.8 and 22.235 GHz. In the mid-1960's, this radiometer and another dual-frequency microwave radiometer, the MR-64, which operated at frequencies of 9.3 and 34.0 GHz, were placed in a Convair 240A aircraft by the NASA Manned Spacecraft Center. This aircraft, designated as NASA 926, was flown over

many land and sea test sites.

2. Absorption of microwaves by atmospheric gases. Van Vleck (1947a, 1947b) found that the major absorbers of microwaves among the atmospheric gases are molecular oxygen, of which the resonant frequencies lie near 60 GHz, and water vapor, of which the resonant frequency is at 22.235 GHz. Molecular oxygen has several weak absorption lines near 9.5 GHz (Mizushima, 1960; Bowers et al., 1959), and carbon dioxide has weak absorption lines at 9 and 22 GHz (Derr, 1967); however, these lines are negligible. The allowable transitions in these molecules are changed by the presence of other molecules during collisions. As a result, the absorption lines are broadened so that microwave absorption occurs for all microwave frequencies rather than just for the resonant frequencies. The most commonly used collision-broadening shape-factor is that proposed by Van Vleck and Weisskopf (1945). Although other expressions have been proposed by Gross (1955) and Fröhlich (1946), the expression of Van Vleck and Weisskopf has been accepted and verified by most investigators (Anderson, 1949; Lenoir et al., 1968) and is accepted in this paper.

The best statement of the Van Vleck theory for molecular oxygen is found in the paper by Meeks and Lilley (1963). In this paper, they list the resonant frequencies of molecular oxygen and give general expressions for the volume absorption coefficient for molecular oxygen as a function of the temperature and pressure of

the air and the microwave frequency. The most complete statement of the Van Vleck theory for water vapor is found in a report by Porter and Florance (1969). Other expressions may be found in published literature by Barrett and Chung (1962), Croom (1964), and Staelin (1966).

The above authors have proposed various applications for the sensing of the microwave emission by water vapor and molecular oxygen. Included in these are the top sounding of atmospheric temperature at frequencies near the oxygen resonance and the top sounding of atmospheric water vapor at frequencies near the water vapor resonance. These applications are not discussed in this paper.

3. Extinction of microwaves by liquid hydrometeors. During World War II, scientists became interested in the effects of meteorological factors on the propagation of microwaves used by search radar. Ryde (1946) conducted the first rigorous study of the attenuation and backscattering of microwaves by spherical hydrometeors in clouds and precipitation by applying the exact theory of the scattering of plane electromagnetic waves from homogeneous dielectric spheres. This theory is called the Mie theory after one of the earliest papers on the subject by Mie (1908); however, the theory was developed earlier by Lorenz (1890) and others mentioned in Logan (1962, 1965). Goldstein (1951) continued Ryde's work. He found that the Rayleigh approximation worked well for liquid hydrometeors in clouds wherein the largest drops had

diameters less than about 0.1 mm and that scattering of microwaves by such clouds is negligible for many purposes. Aden (1951, 1952) developed a scheme for computing the scattering and absorption parameters (hereafter called the Mie parameters) for large drops and solved the problem of predicting the scattering of microwaves from layered dielectric spheres. In a series of papers by Deirmendjian (1963, 1965, 1969) and Deirmendjian et al. (1969), an iterative scheme was developed for computing the Mie parameters of individual hydrometeors.

4. Distribution of drop sizes in rain. In order to compute the absorptive and scattering properties of rain, one must know the distribution of drop dimensions. Simple expressions giving the distribution of drop diameters in rain as a function of the rainfall intensity are given by Laws and Parsons (1943), Marshall and Palmer (1948), and Best (1950). These distributions were obtained from surface measurements of steady rain and appear to be valid for average non-orographic rain (Atlas, 1953; Atlas and Plank, 1953; Blanchard, 1953). There are only slight differences among these three distributions, and investigators usually use the Marshall-Palmer distribution (hereafter called the M-P distribution). Significant departures from the M-P distribution have been noted for some types of rain (Mason and Andrews, 1960; Dingle and Hardy, 1962) in that the number of large drops is overestimated (Caton, 1966). In this paper, the M-P distribution is assumed to be representative of precipitation over the ocean. The independent variable

in the M-P distribution is rainfall intensity; it has been changed to the content of liquid water of the rain mass in this paper. Rainfall rates may be computed from the M-P distribution by using formulas giving the terminal velocity of drops at various atmospheric densities (Best, 1950; Flower, 1928; Gunn and Kinzer, 1949; Foote and Du Toit, 1969).

5. Attenuation of microwaves by rain. Although raindrops having diameters larger than about 2.5 mm tend to be flattened at the bottom (Blanchard, 1950; Magono, 1954; McDonald, 1954; Foote, 1969) and raindrops are not strictly homogeneous dielectric spheres of pure liquid water, one may use the Mie theory and the M-P distribution to predict with considerable accuracy the scattering and absorption properties of rain. These calculations have been made for many radar frequencies by many investigators (Ryde, 1946; Goldstein, 1951; Gunn and East, 1954; Imai, 1956; Atlas and Banks, 1951; Wexler and Atlas, 1963; Medhurst, 1965). Other investigators have determined the rate of attenuation of microwaves by rain through empiricism (Robertson and King, 1946; Anderson et al., 1947; Marshall et al., 1955; Funakawa and and Kato, 1962; Hogg et al., 1963; Hogg, 1967). Still others have used the theoretical implications of the Mie theory to determine the effects of rain upon communications (Bussey, 1950; Burrows and Attwood, 1949; Hathaway and Evans, 1959; Bean and Dutton, 1966; Howell and Shakeshaft, 1967; Hogg, 1968). In general, the predictions of the rate of

attenuation by rain have been verified by the measurements of attenuation. Medhurst (1965), however, found that some measured attenuation rates were higher than the maximum value possible from the Mie theory. As far as the applications of microwave radiometry to the sensing of liquid water in rain is concerned, the foregoing studies have two shortcomings. First, the calculations and measurements have been made at frequencies other than the reserved radio-astronomy bands that must be used by passive radiometers. Second, no distinction has been made between the scattering and absorption properties of rain in either the theoretical studies or the empirical studies; only the total attenuation or extinction of microwaves by rain was utilized in those studies. The best summaries of the attenuation properties of atmospheric gases, clouds, and rain are found in publications by Rosenblum (1961), Lukes (1968), LeFande (1968), and Benoit (1968).

6. Katabatic microwave emission of the atmosphere. The Van Vleck theory and the various theories for the attenuation of microwaves by clouds and rain were used in several studies of the emission of model atmospheres by Weger (1960), Hogg and Mumford (1960), Hogg and Semplak (1961, 1963), Wulfsberg (1964), Croom (1964), Edison (1966), Falcone (1966), Kreiss (1968, 1969), and Staelin (1969). In all of those studies, the atmosphere was assumed to be a non-scattering medium. In that case, the solution to the problem of radiative transfer is fairly simple. Most of those studies did not and, indeed, should not have included rain

since rain may scatter significant amounts of microwave energy. Unfortunately, those which did include rain were based on the assumption that the attenuation properties and the absorption properties of the rain mass were the same. It will be shown in this paper that this error leads to a significant overestimate in the microwave emission of rain. In addition, those investigations used only a few atmospheric models to evaluate the microwave emission of the atmosphere.

Ground-based measurements of the katabatic emission of microwaves by the atmosphere have been made by a number of the above investigators and others (Venugopal, 1963; Cummings and Hull, 1966; Haroules and Brown, 1968, 1969; Decker and Dutton, 1970; Toong and Staelin, 1970). In general, these measurements have supported the theory; that is, the microwave emissions by clouds and especially rain are much greater than that by clear atmospheres for frequencies above about 5 GHz. Also, the microwave emission by a clear atmosphere is greater on humid days than on dry days for frequencies near the absorption line of water vapor (22.235 GHz). Scientists have not been able to establish quantitative relationships between the meteorological properties of clouds and rain and their microwave emission through empiricism because they could not measure, synoptically, the spatial distribution of the liquid water in clouds and rain.

7. Microwave emission of sea water. The emission of

microwaves by sea water was studied first by Peake (1959, 1967) and Chen and Peake (1961). Marindino (1967) computed the emission by a calm sea as a function of its temperature for several microwave frequencies, angles of viewing, and polarizations. These theoretical considerations were made on the basis of the reflective properties of a flat, semi-infinite dielectric composed of sea water where the dielectric constant was assumed to be that of pure water or aqueous sodium chloride, as measured by a number of investigators (Wyman, 1930; Saxton and Lane, 1946, 1952; Saxton, 1946a, 1946b, 1946c, 1949, 1952; Collie et al., 1946, 1948a, 1948b; Hasted et al., 1948; Lane and Saxton, 1952a, 1952b; Hasted and El-Sabeh, 1953; Von Hippel, 1954a, 1954b; Mainberg and Maryott, 1956; Hasted and Roderick, 1958; and Hasted, 1961). These measurements may be fitted to a simple relaxation theory proposed by Debye (1929) such that the dielectric constant of sea water is a function of temperature, salinity, and electromagnetic frequency. Studies have shown that the microwave emission by a calm sea is small and that it is fairly independent of the physical temperature of the sea. Barrett (1966), Sirounian (1968), and the author (Paris, 1969) have studied the effect of salinity on the microwave emission by sea water. Several investigators have discussed the microwave emission by sea water at the early symposia on the applications of remote sensing (Barath, 1965; Conway and Mardon, 1965; Mardon, 1965; Staelin, 1965). The effect of wave roughness on the microwave emission by sea water has been determined by Fried (1966)

and Stogryn (1967). They used the slope spectra of the sea surface given by Cox and Munk (1954a, 1954b) to determine the effective emission of the sea for various wind speeds over the surface of a fully developed sea. In general, they found that the largest response in the microwave emission by the sea to changes in wave roughness occurs at zenith angles of viewing near 55 deg for horizontal polarization. Williams (1969) found that the effect of sea foam on the microwave emission by sea water could dominate that of wave roughness for medium and high states of the sea since the amount of coverage of sea foam on a fully developed sea increases with increasing wind speed (Blanchard, 1963). These predictions were later confirmed by Nordberg et al. (1969).

Measurements by the MR-62 (15.8 and 22.235 GHz) and MR-64 (9.3 and 34.0 GHz) radiometers of the apparent microwave emission of the sea over the outflow of the Mississippi River into the Gulf of Mexico showed that it is independent of temperature and salinity for frequencies between 9.3 and 34.0 GHz (Paris, 1969). In 1970, a set of microwave radiometers operating at 1.42, 10.69, 22.235, and 31.4 GHz and built by Aerojet General were placed on a Lockheed P3A aircraft, designated as NASA 927, by the NASA Manned Spacecraft Center. A test flight of this instrument over the Mississippi River outflow showed that the microwave emission by the sea at a frequency of 1.42 GHz decreased with increasing salinity Droppleman et al., 1970) as predicted by the author (Paris, 1969).

8. Microwave emission of the atmosphere and the ocean. Buettner (1963) suggested that liquid water in the atmosphere over the ocean could be surveyed from aloft with a microwave radiometer operating at a frequency near 18.8 GHz. In the summers of 1967 to 1970, the NASA Goddard Space Flight Center has sponsored flights of an electronically-scanned, microwave radiometer operating at a frequency of 19.35 GHz and built by Aerojet General. Test flights of this instrument over land and ocean sites have shown that clouds, precipitation, sea foam, and wave roughness greatly enhance the intensity of the upwelling microwave radiation (Catoe et al., 1967; Nordberg et al., 1969). Also, small but measureable differences between the microwave emission of humid, tropical atmospheres and dry, polar atmospheres have been noted. Flight tests of the MR-62 and MR-64 radiometers in the NASA 926 aircraft over rain at sea have shown a significant increase in the apparent microwave emission of the sea at 15.8 GHz. The other channels of the MR-62 and MR-64 apparently were inoperative (Singer and Williams, 1968).

The most extensive study of the microwave emission by the atmosphere and the ocean to date is the one made by Kreiss (1968, 1969). In that study, the microwave emission by rain was not considered. Also, the clouds were assumed to be homogeneous in their content of liquid water.

9. Soviet research in thermal microwave physics. Scientists in the USSR have been very active in theoretical and applied research in all the topics discussed above. The nature of their

research is discussed separately since it has been difficult to follow their activities due to the limited number of English translations of their articles related to microwave radiometry. Gurvich and Egorov (1966) reported that the surface temperature of the Caspian Sea was surveyed with a microwave radiometer from an aircraft in 1964. A theoretical work published later by Pereslegin (1967) indicated that the response of the emission of sea water to changes in sea temperature is greatest for frequencies in the range of 3.0 GHz to 3.75 GHz depending on water temperature. In the course of those calculations, the conductivity of sea water was held at a constant value; such is not the case for sea water, as will be seen in Chapter III. An even later paper by Rabinovich et al. (1969) stated that the radiometer used to measure the sea temperature operated at frequencies between 3.0 and 3.75 GHz. Basharinov et al. (1968) and Kutuza (1968) discussed briefly the Soviet activities in the application of microwave radiometry in sensing cloud and rain characteristics. In 1969, the NASA translated and published (Shifrin, 1969) the proceedings from a Soviet Conference on the transfer of microwave radiation in the atmosphere. This document reviews the activities of Soviet scientists in using microwave radiometers to study a variety of atmospheric and oceanic phenomena such as sea temperature, sea ice, sea roughness, water vapor, liquid water, and precipitation. The only evaluation of the role of multiple scattering in the transfer of thermal microwaves through rain has been made by Volchok and Chernyak (1969) who used

classical radiative transfer techniques. Unfortunately, they appear to have used arbitrary values for the scattering properties of their model atmosphere that are not realistic for the frequencies used in their study. Also, vital bits of information about their models were not included in their publication or were missed in the translation.

10. Radiative transfer. It is well known that scattering may account for as much as half the extinction of microwaves at any given point in rain at microwave frequencies. The theory of the transfer of electromagnetic radiation through scattering media is presented in the texts of van de Hulst (1957), Chandrasekhar (1960), Busbridge (1960), Goody (1964), Love (1968), and Kerker (1969). This classical theory has been applied to many problems involving the transfer of ultraviolet, visible, infrared, and radar radiation through scattering atmospheres. Another interesting technique known as invariant imbedding has been developed by Bellman et al. (1960, 1966). In the past few years, Plass and Kattawar (1968a, 1968b, 1968c) and Kattawar and Plass (1968a, 1968b, 1969) have solved the radiative transfer problem for visible and infrared radiation in clouds over land and sea surfaces by using the Monte Carlo method (Fleck, 1963; Shreider, 1966). In this method, the multiple scattering of electromagnetic radiation in a scattering medium can be viewed as a sequence of single-scattering encounters between representative photons and elements of the medium.

The sequence ends when a photon is either absorbed or exits the scattering domain. The probabilities for each step in the sequence can be related to the absorption and scattering properties of the medium, as obtained from classical techniques. Shreider (1966) suggests methods for reducing the number of trials needed to determine the spatial distribution of the radiation emerging from the medium. The advantages of the Monte Carlo technique lie in its directness of application, its lack of simplifying assumptions, and its versatility.

11. Modeling of the atmosphere for radiative transfer. In all of the past investigations, the models used to represent the spatial distribution of atmospheric parameters have been too few to be representative of actual meteorological conditions existing in the real atmosphere and have been too simple. Often, only one atmosphere, as, for instance, the 1962 U. S. Standard Atmosphere (Cole et al., 1965), is used. The distributions with altitude of liquid water in clouds and rain also are assumed to be simple step functions. There have been many meteorological studies of the distribution of these quantities in the atmosphere; results from these studies can be used to formulate more realistic models. Cole et al. (1965) give several distributions with height of pressure, temperature, and moisture for different latitudes and seasons. Petterssen (1956a, 1956b) and Riehl (1954) discuss these parameters for tropical storms and maritine tropical air. Lukes (1968) gives a representative sounding for maritine polar air. The variability

of precipitable water (integrated content of water vapor) in the atmosphere is discussed by Gutnick (1961), Penn and Kunkel (1963), and Benwell (1965). The vertical distribution of liquid water in clouds and rain has been measured by a number of investigators (Wexler and Donaldson, 1968; Weickmann and Aufm Kampe, 1953; Warner, 1955; Squires, 1958; Singleton, 1960; Neiburger, 1949; Durbin, 1959; Draginis, 1958; Browne et al., 1954; Aufm Kampe, 1950; Ackerman, 1959, 1963). The implications of these studies should be taken into consideration when the atmosphere is being modeled for radiative transfer.

12. Summary of the inadequacies of past studies. During the course of this lengthy review, several shortcomings of past studies related to the application of microwave radiometry to meteorological sensing have been noted. Briefly, these are as follows: (1) past studies of the attenuation properties of rain at microwave frequencies are of little use to thermal microwave studies since no distinction has been made between absorption and scattering; (2) these studies have been made for frequencies other than the bands reserved for passive sensing; (3) the relationship between the meteorological properties of clouds and rain and their thermal emissions at microwave frequencies can not be determined through empiricism since the spatial distribution of liquid water in clouds and rain can not be determined synoptically; (4) theoretical studies of the emission of thermal microwave by model atmospheres

have not considered the effects of scattering and absorption in rain or have been based on the assumption that the absorption and attenuation properties of rain are the same; and (5) the atmospheric models used in past studies have been too few and too simple.

In this paper, the absorption and scattering properties of rain are determined for 27 microwave frequencies (see Table 1) from 0.5 GHz to 60 GHz including all reserved bands. Also, the effects of multiple scattering are evaluated, and a large number (582) of model atmospheres is used. This study is limited, however, to plane-parallel, horizontally-homogeneous atmospheres containing rain having a M-P distribution of drop sizes.

C. Objective

The objective of this research is to develop quantitative relationships between the meteorological properties of clouds, rains, and gases and their thermal emissions at microwave frequencies. Subservient to this over-all goal are the goals of (1) developing an understanding of the relationship between the emission of microwaves by the sea and its temperature, salinity, and roughness, (2) solving the radiative transfer problem under known atmospheric conditions, and (3) reducing the number of predictors needed to compute the thermal emission of the atmosphere at microwave frequencies.

It must be emphasized that the conclusions of this research are based on speculative, theoretical considerations and that

Table 1. Microwave frequencies used in this study.

Frequency (GHz)	Rationale
0.5	Lower end
0.61	RAB
0.75	IF
1.0	IF
1.42	RAB, NASA 927, Skylab
1.675	RAB
2.1	IF
2.695	RAB
2.91	10.3 cm Radar
4.0	IF
4.805	RAB, ESSA-GBMR
5.81	RAB
8.0	IF
9.369	3.2 cm Radar
10.69	RAB, NASA 927, ESSA-GBMR
11.312	IF
15.375	RAB
17.2	IF
19.35	RAB, Nimbus, NASA 990
22.235	NASA 927, Water-Vapor Resonance
31.4	RAB, NASA 927
33.2	RAB
35.1	IF
37.0	RAB, Nimbus
45.248	IF
53.8	Nimbus MWS
60.0	Upper end, Molecular Oxygen Resonance

RAB - Radio Astronomy Band, a protected "quiet" band in the microwave spectrum (Smith-Rose, 1964)
IF - Intermediate frequency, used to fill in space between RAB's
NASA 927 - Multi-frequency microwave radiometers on NASA 927 aircraft
ESSA-GBMR - ESSA Ground-based microwave radiometer
Nimbus - Nimbus E or F microwave radiometer
Nimbus MWS - Nimbus microwave spectrometer
Skylab - NASA manned space station

many of the necessary assumptions are based on sketchy meteorological and physical knowledge. Nevertheless, it is hoped that these findings will lead to a better understanding of the nature of the thermal emission of the atmosphere and the ocean at microwave frequencies and that the theory can form the basis for well-planned experiments and measurement programs in the future.

CHAPTER II

FUNDAMENTAL CONCEPTS OF THERMAL MICROWAVE RADIATION

The fundamental concepts used in radiation studies are described in detail in the texts of Chandrasekhar (1960), van de Hulst (1957), and, most recently, Kerker (1969). In addition, Deirmendjian (1969) has written an excellent source book on electromagnetic scattering in spherical polydispersions -- the main topic of this paper. In the following, the basic concepts presented in these texts are couched in a form perculiar to the radiative transfer of thermal microwaves through model atmospheres and homogeneous oceans.

A. Definitions

1. Intensity and flux. The fundamental property of radiation is its intensity field. In this study, the word intensity denotes the specific, spectral, or monochromatic intensity of electromagnetic radiation. Consider the flow of radiant energy through a point in space (see Fig. 1). Let ΔE be the amount of radiant energy (J) traveling within the solid angle, $\Delta\Omega$ (str), surrounding the unit vector, $\vec{a}$, passing through the area, ΔA (m^2), during the time interval, Δt (sec), and being carried by electromagnetic waves having frequencies from $\nu - \nu/2$ to $\nu + \nu/2$ (Hz). The intensity of the pencil of radiation traveling along $\vec{a}$ is defined (Chandrasekhar,

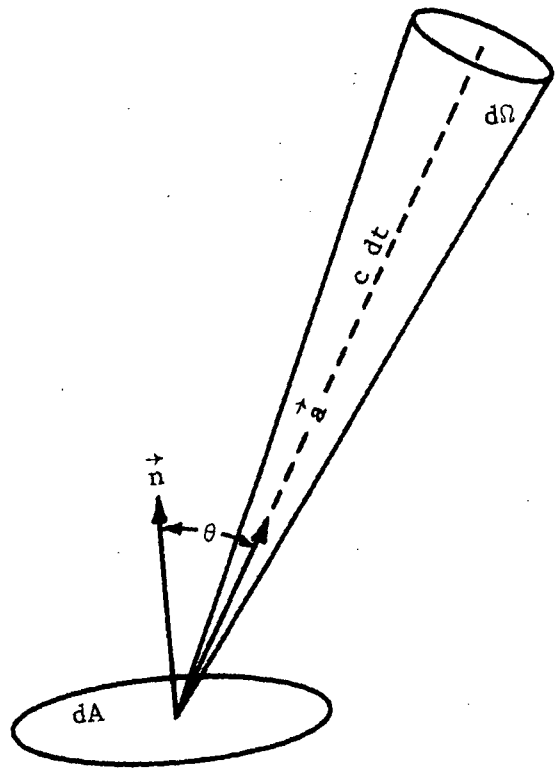

Fig. 1. Geometry of intensity.

1950, p. 1) by the expression

$$dE = I(\vec{a},\nu,t)\ \cos\theta\ d\nu\ dA\ d\Omega\ dt, \tag{1}$$

where I is the (specific) intensity (W m^{-2} str^{-1} Hz^{-1}), and θ is the angle between $\vec{a}$ and the outward unit-vector that is normal to ΔA.

The concept of intensity will be used throughout this paper to describe the nature of the emergent fields of microwave radiation from the atmosphere and the ocean. For practical considerations, one must integrate the intensity field over finite areas, solid angles, time intervals, and bandwidths to compute the flux of thermal microwave energy that may be measured by conventional microwave radiometers. In (1), one may define the differential flux dF (W m^{-2} Hz^{-1}) as

$$dF = \frac{dE}{dA\ d\nu\ dt} = I(\vec{a},\nu,t)\ \cos\theta\ d\Omega. \tag{2}$$

In polar coordinates,

$$d\Omega = \sin\theta\ d\theta\ d\phi. \tag{3}$$

Thus, (2) becomes

$$dF = I\ \cos\theta\ \sin\theta\ d\theta\ d\phi. \tag{4}$$

In this paper, the intensity will be obtained by integrating the flux over the solid-angle strip between zenith angles of θ_1 and θ_2. The flux of radiation through this solid angle is given by

$$\Delta F(\theta_1,\theta_2) = \int_0^{2\pi} \int_{\theta_1}^{\theta_2} I\ \cos\theta\ \sin\theta\ d\theta\ d\phi$$

$$= 2\ \pi\ \bar{I} \int_{\theta_1}^{\theta_2} \sin\theta\ \cos\theta\ d\theta, \tag{5}$$

where $\bar{I}$ is the effective value of I. The integral in (5) is recognized to be of the form u du where u is $\sin\theta$; thus,

$$\Delta F(\theta_1,\theta_2) = \pi \bar{I} [\sin^2\theta_2 - \sin^2\theta_1]. \quad (6)$$

If $\Delta F(\theta_1,\theta_2)$, θ_1, and θ_2 are known, then one may determine $\bar{I}$. A black-body or Lambert surface radiates isotropically (i.e., I is a constant). Thus, the flux of emission from such a surface is $\Delta F(0,\pi/2)$ or πI.

2. Brightness temperature. Scientists studying thermal radiation prefer to use some appropriate equivalent temperature to describe the intensity of a particular type of radiation. In thermal microwave studies, brightness temperature is used in place of intensity. The relationship between these two quantities is derived from the properties of a perfect emitter (black body) at microwave frequencies and terrestrial temperatures. The intensity of the thermal emission from a black body is given by Planck (1959) as

$$B(\nu,T) = 2 h \nu^3/c^2 [\exp(h \nu/k T) - 1], \quad (7)$$

where T is the temperature (K) of the black body, h is Planck's constant (6.623×10^{-34} J sec), c is the speed of light in a vacuum (2.99793×10^{8} m $\sec^{-1}$), k is Boltzman's constant (1.38×10^{-23} J K^{-1}), and ν is the electromagnetic frequency (Hz).

At microwave frequencies and terrestrial temperatures, the quantity $(h \nu/k T)$ is much less than unity, and (7) reduces to the Rayleigh-Jeans Law,

$$B(\nu,T) = 2 k \nu^2 T/c^2. \quad (8)$$

There is a linear relationship between $B(\nu,T)$ and T for a fixed microwave frequency. Suppose one is given an intensity I; there exists a unique temperature, T (K), such that $B(\nu,T)$ is equal to I. T is known as the brightness temperature of the microwave radiation under study. Mathematically,

$$T = (c^2/2\ k\ \nu^2)\ I. \tag{9}$$

A microwave radiometer is sensitive only to one component of the radiation field, that is, to radiation existing in one plane of polarization. Thus, one needs to relate intensity to the polarized component of the emission of microwaves by a black body. Since thermal emission is unpolarized, half of its energy is propagated within one plane of polarization, and half is propagated in the orthogonal plane. Therefore, any polarized component of the emission of microwave by a black body, $B_p(\nu,T)$, is given by

$$B_p(\nu,T) = k\ \nu^2\ T/c^2. \tag{10}$$

From (10), one obtains an expression for the brightness temperature, T_p (K), as follows:

$$T_p = (c^2/k\ \nu^2)\ I_p, \tag{11}$$

where I_p is some given polarized component of microwave radiation. Most investigators have chosen to resolve the microwave intensity into the vertically polarized component, I_v, and the horizontally polarized component, I_h. Vertically polarized radiation consists of those electromagnetic waves of which the electric field vector oscillates in the plane that includes the local normal and the

line of sight; horizontally polarized radiation consists of waves of which the electric field vector oscillates in the plane that includes the line of sight and that is perpendicular to the vertical plane. These two parameters alone are not adequate, however, to describe the state of polarization of the radiation under study.

The use of the word "polarized" in the phrase "polarized component" may lead one to think that the intensity is polarized, that is, that there exists a fixed phase relationship between two orthogonal components of the total electric field vector. Such is not the case in thermal microwave physics. Thermal radiation may become partially polarized upon scattering. The phrase "polarized component" refers to one component of the total stream of radiation for which the electric field vectors oscillate in one given plane of polarization. This distinction is necessary since microwave radiometers are sensitive to only one component at a time. The phrase "polarized wave," on the other hand, is meant to imply that the wave is polarized with fixed phase differences between any two orthogonal components of its electric field vector.

3. Stokes vector. Consider an eliptically polarized, electromagnetic wave. Its electric field vector may be visualized as describing an ellipse in the transverse plane (see Fig. 2). The orientation, sense of rotation, and eccentricity of this ellipse may be given by the parameters, χ and γ, where χ is the angle between the vertical or v-axis and the major axis of the ellipse

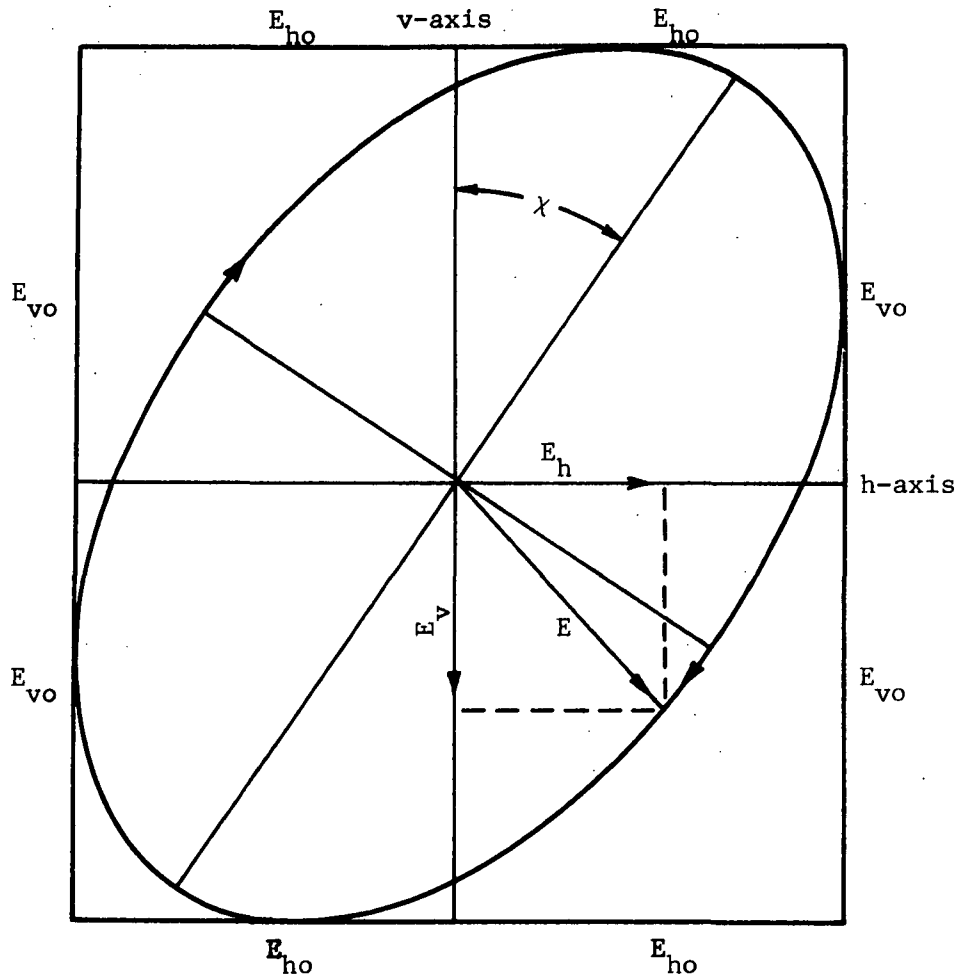

Fig. 2. Geometry of polarization.

and γ is the angle of which the tangent is the ratio of the minor axis to the major axis of the ellipse. The components of the electric field vector along the v-axis and the h-axis are $\mathrm{Re}\{E_v\}$ and $\mathrm{Re}\{E_h\}$, respectively, where

$$E_v = E_{vo} \exp[j(\omega_f t + \varepsilon_v)], \tag{12}$$

and

$$E_h = E_{ho} \exp[j(\omega_f t + \varepsilon_h)]. \tag{13}$$

E_{vo} and E_{ho} are the magnitudes of E_v and E_h, ε_v and ε_h are their respective phase angles, and ω_f is the circular frequency ($2 \pi \nu$). If the sense of rotation is clockwise (looking along the direction of propagation), then the sign of γ is taken to be positive and vice versa. Van de Hulst (1957, p. 41) suggests that four parameters be used to describe the state of polarization of an electromagnetic wave. These parameters may be expressed in the form of a column vector, known as the Stokes vector,

$$\vec{I} = \{I,Q,U,V\}, \tag{14}$$

where the components of $\vec{I}$ (having units of intensity) are given (Chandrasekhar, 1950, p. 27; van de Hulst, 1957, pp. 41-42; Kerker, 1969, p. 17) as

$$I = I_v + I_h, \tag{15}$$

$$Q = I_v - I_h, \tag{16}$$

$$U = I \cos 2\gamma \sin 2\chi = Q \tan 2\chi, \tag{17}$$

and

$$V = I \sin 2\gamma = Q \tan 2\gamma \sec 2\chi. \tag{18}$$

At any point, I is proportional to $\overline{E\ E^*}$ (note: E^* refers to the complex conjugate of E); thus,

$$I \propto \overline{E_v\ E_v^*} + \overline{E_h\ E_h^*}, \tag{19}$$

$$Q \propto \overline{E_v\ E_v^*} - \overline{E_v\ E_v^*}, \tag{20}$$

$$U \propto \overline{E_v\ E_h^*} + \overline{E_h\ E_v^*} = 2\ \mathrm{Re}\{\overline{E_v\ E_h^*}\}, \tag{21}$$

and

$$V \propto j\ (\overline{E_v\ E_h^*} - \overline{E_h\ E_v^*}) = -2\ \mathrm{Im}\{\overline{E_v\ E_h^*}\}. \tag{22}$$

Also,

$$I_v \propto \overline{E_v\ E_v^*} \tag{23}$$

and

$$I_h \propto \overline{E_h\ E_h^*}, \tag{24}$$

where the bar indicates that time averages are being taken over time periods much longer than the period of vibration of the respective electric fields. For phenomena occurring at a point, one may use the change in E_v and E_h to determine the change in the Stokes vector due to scattering, reflection, or refraction. In general, for radiation propagating from a point, the electric field strength diminishes at a rate proportional to the inverse of the distance traveled. The intensity, however, does not change with distance unless extinction or emission is occurring in the medium through which it propagates.

The important property of the Stokes vector is that the Stokes vector for the superposition of several independent streams of radiation is simply the vector formed by summing the respective

components of the Stokes vectors of the individual streams. By "independent," one means that there are no permanent phase relations among the component streams of radiation. In some processes, such as reflection from or transmission through the interface between two dielectric materials or scattering from dielectric spheres, the state of polarization may be altered.

It is important to note that for a fully-polarized wave, the intensity, I, is $\sqrt{Q^2 + U^2 + V^2}$. When Q, U, and V are zero, the intensity of the polarized part is zero and χ and γ are undefined. Thus, thermal radiation of intensity I_n may be represented by the Stokes vector $\{I_n,0,0,0\}$. In general, a partially polarized stream of radiation is the sum of an unpolarized part of which the Stokes vector is $\{I_n,0,0,0\}$ and a fully polarized part of which the Stokes vector is $\{\sqrt{Q^2 + U^2 + V^2},Q,U,V\}$.

B. Radiative Transfer

1. Extinction. A pencil of radiation may be weakened through extinction processes and strengthened through emission processes as it travels through a medium. Also, its Stokes vector may be transformed by scattering, reflection, or transmission. The fundamental law of extinction is Lambert's Law which states that the volume extinction coefficient, κ, is linear and independent of the intensity of radiation and of the amount of matter (Goody, 1964, p. 23). Lambert's Law may be stated mathematically as

$$d\vec{I}_{ex} = -\kappa \vec{I}\, ds, \tag{25}$$

where $d\vec{I}_{ex}$ is the differential change in $\vec{I}$ due to extinction processes as the radiation travels a differential path length, ds (m), and κ is the volume extinction coefficient (m^{-1}). A convenient quantity is the differential optical path-length, $d\tau$, given by

$$d\tau = -\kappa\, ds. \tag{26}$$

The negative sign in (26) is the result of the usual convention of defining the optical depth at the top of the atmosphere to be zero.

Extinction consists of absorption (conversion to heat) and scattering (redistribution with direction). Since all extinction processes are linear,

$$\kappa = \alpha + \beta, \tag{27}$$

where α is the volume absorption coefficient (m^{-1}) and β is the volume scattering coefficient (m^{-1}).

2. Emission. Formally, one may state that the differential change in $\vec{I}$ due to emission processes is given by

$$d\vec{I}_{em} = \kappa \vec{J}\, ds, \tag{28}$$

where $\vec{J}$ is the source function (vector) and has the units of intensity. If the direction of some pencil of radiation under study is specified by the zenith angle, θ, and the azimuth angle, ϕ, and (θ',ϕ') represents the direction of other pencils of radiation in the 4π solid angle around the scattering point, the source

function is given as follows:

$$\vec{J}(\theta,\phi) = \frac{\omega}{4\pi} \int_0^{2\pi} \int_0^{\pi} [P_o](\theta,\phi,\theta',\phi') \vec{I}(\theta',\phi') \sin\theta' \, d\theta' \, d\phi' + (1 - \omega) \vec{B}, \tag{29}$$

where $[P_o]$ is the phase matrix for angular scattering, $\vec{B}$ is the Planckian emission vector, $\{B(\nu,T),0,0,0\}$, and ω is β/κ. The first term of (29) represents the contribution to the emission by scattering. The second term of (29) represents the contribution by thermal emission. Goody (1964, Sec. 2.2.4) has shown that the emission of a body is Planckian if the population of energy levels is due primarily to collisions among molecules.

3. Reflection at the air-sea interface. Consider a plane polarized, electromagnetic wave incident upon a flat, semi-infinite dielectric consisting of sea water (see Fig. 3). The sea water is assumed to be characterized by a temperature and a salinity. If the complex index of refraction of the sea water, $m' - j\, m''$, is known (see Chapter III), then the reflective characteristics of the two media are prescribed by the complex Fresnel reflection coefficients, R_v and R_h, given by Kerker (1969, p. 20) as

$$R_v = \frac{\cos\theta_a - (m' - j\, m'') \cos\theta_w}{\cos\theta_a + (m' - j\, m'') \cos\theta_w} \tag{30}$$

and

$$R_h = \frac{(m' - j\, m'') \cos\theta_a - \cos\theta_w}{(m' - j\, m'') \cos\theta_a + \cos\theta_w}, \tag{31}$$

where θ_a and θ_w are the angles that the pencils of radiation make

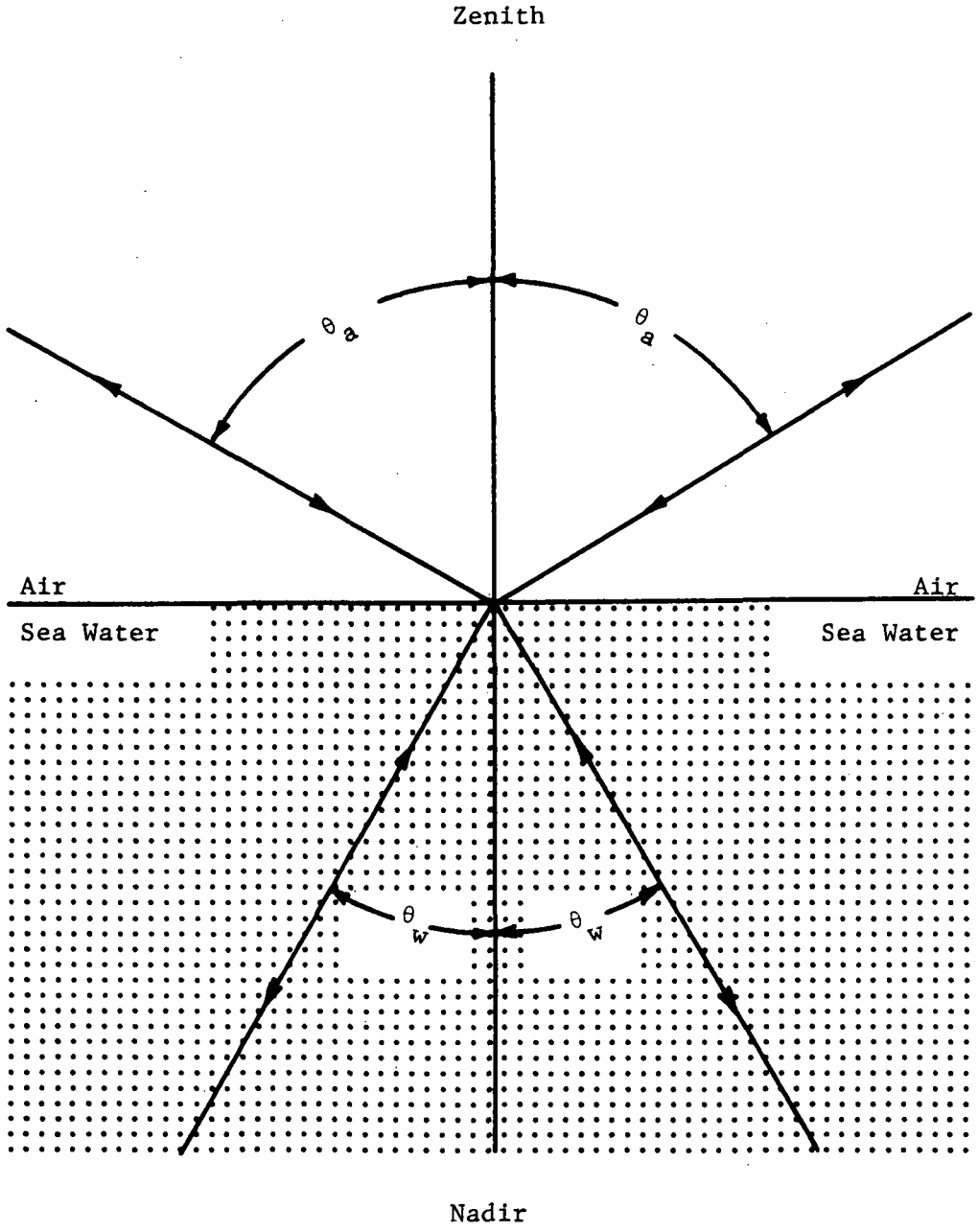

Fig. 3. Geometry of reflection and refraction at the air-sea interface.

with respect to the normal to the interface in the air and in the sea water, respectively. These angles are related through Snell's Law as follows:

$$\sin\theta_a = (m' - j\, m'') \sin\theta_w . \tag{32}$$

The components of the electric-field vector of the reflected radiation at the interface, $\mathrm{Re}\{E_{rv}\}$ and $\mathrm{Re}\{E_{rh}\}$, are related to the components of the incident radiation at the interface, $\mathrm{Re}\{E_{iv}\}$ and $\mathrm{Re}\{E_{ih}\}$, as follows:

$$E_{rv} = E_{iv}\, R_v , \tag{33}$$

and

$$E_{rh} = E_{ih}\, R_h . \tag{34}$$

The Stokes vector for the incident wave is given from (14) as

$$\vec{I}_i = \{I_i, Q_i, U_i, V_i\} , \tag{35}$$

where

$$I_i = c_p\, \overline{E_{iv}\, E_{iv}^*} + c_p\, \overline{E_{ih}\, E_{ih}^*} , \tag{36}$$

$$Q_i = c_p\, \overline{E_{iv}\, E_{iv}^*} - c_p\, \overline{E_{ih}\, E_{ih}^*} , \tag{37}$$

$$U_i = c_p\, \overline{E_{iv}\, E_{ih}^*} + c_p\, \overline{E_{ih}\, E_{iv}^*} = 2\, c_p\, \mathrm{Re}\{\overline{E_{iv}\, E_{ih}^*}\} , \tag{38}$$

and

$$V_i = j\, c_p\, (\overline{E_{iv}\, E_{ih}^*} - \overline{E_{ih}\, E_{iv}^*}) = -2\, c_p\, \mathrm{Im}\{\overline{E_{iv}\, E_{ih}^*}\} , \tag{39}$$

where c_p is the constant of proportionality between I and $\overline{E\, E^*}$ at the interface.

The Stokes vector for the reflected wave is the same as given in (35) to (39) when the i's are replaced by r's. If E_{rv} and E_{rh} are replaced by the equivalent values given by (33) and (34), then

one obtains expressions for the components of the Stokes vector for the reflected wave, I_r, as follows:

$$I_r = c_p \overline{E_{iv} R_v E^*_{iv} R^*_v} + c_p \overline{E_{ih} R_h E^*_{ih} R^*_h}$$
$$= I_{iv} \overline{R_v R^*_v} + I_{ih} \overline{R_h R^*_h}; \tag{40}$$

$$Q_r = c_p \overline{E_{iv} R_v E^*_{iv} R^*_v} - c_p \overline{E_{ih} R_h E^*_{ih} R^*_h}$$
$$= I_{iv} \overline{R_v R^*_v} - I_{ih} \overline{R_h R^*_h}; \tag{41}$$

$$U_r = c_p \overline{E_{iv} R_v E^*_{ih} R^*_h} + c_p \overline{E_{ih} R_h E^*_{iv} R^*_v}$$
$$= 2 c_p \, \mathrm{Re}\{\overline{E_{iv} R_v E^*_{ih} R^*_h}\}; \tag{42}$$

$$V_r = j c_p (\overline{E_{iv} R_v E^*_{ih} R^*_h} - \overline{E_{ih} R_h E^*_{iv} R^*_v})$$
$$= -2 c_p \, \mathrm{Im}\{\overline{E_{iv} R_v E^*_{ih} R^*_h}\}. \tag{43}$$

It was seen in (12) and (13) that E_{iv}, E_{ih} E_{rv}, and E_{rh} have associated phase angles, ε_{iv}, ε_{ih}, ε_{rv}, and ε_{rh}. Also, R_v and R_h have associated phase angles, ϕ_v and ϕ_h. If one lets

$$\delta_i = \varepsilon_{iv} - \varepsilon_{ih} \tag{44}$$

and

$$\delta_r = \phi_v - \phi_h, \tag{45}$$

then (42) and (43) become

$$U_r = 2 c_p \overline{|E_{iv}| \, |R_v| \, |E_{ih}| \, |R_h| \cos(\delta_r + \delta_i)} \tag{46}$$

and

$$V_r = -2 c_p \overline{|E_{iv}| \, |R_v| \, |E_{ih}| \, |R_h| \sin(\delta_r + \delta_i)}. \tag{47}$$

Expanding the cosine and sine terms in (46) and (47) and collecting terms, one obtains

$$U_r = (2 c_p \overline{|E_{iv}| \, |E_{ih}| \cos\delta_i}) \overline{|R_v| \, |R_h| \cos\delta_r}$$
$$+ (-2 c_p \overline{|E_{iv}| \, |E_{ih}| \sin\delta_i}) \overline{|R_v| \, |R_h| \sin\delta_r}, \tag{48}$$

and

$$V_r = (-2\, c_p\, \overline{|E_{iv}|\,|E_{ih}|\cos\delta_i})\, \overline{|R_v|\,|R_h|\sin\delta_r} + (-2\, c_p\, \overline{|E_{iv}|\,|E_{ih}|\sin\delta_i})\, \overline{|R_v|\,|R_h|\cos\delta_r}. \quad (49)$$

The terms in parentheses in (49) are recognized to be equivalent to $2\, c_p\, \mathrm{Re}\{\overline{E_{iv}\, E_{ih}^*}\}$ and $-2\, c_p\, \mathrm{Im}\{\overline{E_{iv}\, E_{ih}^*}\}$, respectively. These in turn are equivalent to U_i and V_i, respectively (see Eqs. (38) and (39)). Also, the remaining terms in (48) and (49) become as follows:

$$U_r = U_i\, \mathrm{Re}\{\overline{R_v\, R_h^*}\} + V_i\, \mathrm{Im}\{\overline{R_v\, R_h^*}\}, \quad (50)$$

$$V_r = -U_i\, \mathrm{Im}\{\overline{R_v\, R_h^*}\} + V_i\, \mathrm{Re}\{\overline{R_v\, R_h^*}\}. \quad (51)$$

Finally, one may form the reflection matrix [R] such that

$$\vec{I}_r = [R]\, \vec{I}_i, \quad (52)$$

where

$$[R] = \begin{bmatrix} R_1 & R_2 & 0 & 0 \\ R_2 & R_1 & 0 & 0 \\ 0 & 0 & R_3 & R_4 \\ 0 & 0 & -R_4 & R_3 \end{bmatrix} \quad (53)$$

and where

$$R_1 = (R_v\, R_v^* + R_h\, R_h^*)/2, \quad (54)$$

$$R_2 = (R_v\, R_v^* - R_h\, R_h^*)/2, \quad (55)$$

$$R_3 = \mathrm{Re}\{R_v\, R_h^*\}, \quad (56)$$

and

$$R_4 = \mathrm{Im}\{R_v\, R_h^*\}. \quad (57)$$

The bar has been dropped since R_v and R_h are not time-dependent quantities.

In the above derivation, one should note that the direction of travel of the radiation was not specified; the only requirement was that the radiation should travel along a pencil that is inclined to the normal of the interface at an angle, θ_a, in the air and at an angle, θ_w, in the water. The reflection matrix used to determine the Stokes vector of reflected radiation is the same for radiation originating in the water as it is for radiation originating in the air so long as angles of incidence and refraction are those specified by Snell's Law (Eq. (32)). The law of conservation of energy requires that the intensity of transmitted radiation and the intensity of reflected radiation equal the intensity of the incident radiation.

It is obvious from the form of [R] in (53) that if the incident radiation is unpolarized, then the reflected radiation will consist of an unpolarized part the intensity of which is $I_n(R_1 - R_2)$ and a linearly polarized part of intensity $I_n R_2$ with vertical orientation (i.e., $\chi = 0$). For this case, the intensities of the components of the reflected radiation are given simply as

$$I_{rv} = I_{iv} R_v R_v^* \tag{58}$$

and

$$I_{rh} = I_{ih} R_h R_h^*. \tag{59}$$

4. Transmission of thermal radiation from sea water to air.

Sea water is a highly absorptive medium for all microwave frequencies. The rate of absorption is such that almost total absorption occurs after the radiation has passed through only a few centimeters. According to Kirchoff's Law, a good absorber is also a good emitter at the same frequency, therefore, the radiation that arrives at the air-sea interface from below has an intensity that is equal to the intensity of emission of a black body the temperature of which is equal to the mean temperature of the upper few centimeters of the ocean. At the air-sea interface, a portion of this radiation is reflected back into the ocean and the rest is passed into the air. The law of conservation of energy requires that

$$\vec{I}_i = \vec{I}_r + \vec{I}_t, \tag{60}$$

where $\vec{I}_i$, $\vec{I}_r$, and $\vec{I}_t$ are the Stokes vectors for the radiation that, respectively, arrives from below at the air-sea interface, is reflected into the water, and is transmitted through the air-sea interface into the air. Through the use of (52), one may express $\vec{I}_t$ as follows:

$$\vec{I}_t = \vec{I}_i - [R]\,\vec{I}_i = [I]\,\vec{I}_i - [R]\,\vec{I}_i = ([I] - [R])\,\vec{I}_i, \tag{61}$$

where [I] is an identity matrix given as

$$[I] = \begin{bmatrix} 1 & 0 & 0 & 0 \\ 0 & 1 & 0 & 0 \\ 0 & 0 & 1 & 0 \\ 0 & 0 & 0 & 1 \end{bmatrix}. \tag{62}$$

The form of (61) suggests the formation of the transmission matrix [T] defined as

$$[T] = [I] - [R]. \tag{63}$$

It follows from (62), (63), and (53) that

$$[T] = \begin{bmatrix} 1 - R_1 & -R_2 & 0 & 0 \\ -R_2 & 1 - R_1 & 0 & 0 \\ 0 & 0 & 1 - R_3 & -R_4 \\ 0 & 0 & R_4 & 1 - R_3 \end{bmatrix} \tag{64}$$

and

$$\vec{I}_t = [T]\, \vec{I}_i. \tag{65}$$

In the above derivation, [T] is the general transmission matrix that may be used for radiation having arbitrary polarization coming from either side of the air-sea interface. Again, the only requirement is that the Fresnel coefficients used in (64) are those for radiation traveling along the path dictated by the angles, θ_a and θ_w, as described in Section B3 of this chapter.

For the ocean, the Stokes vector representing the intensity of thermal radiation arriving at the air-sea interface from below is given by

$$\vec{I}_{i,sea} = \{B(\nu,T_{sea}),0,0,0\}, \tag{66}$$

where T_{sea} is the temperature of the surface layer of the sea (K). Operating on $\vec{I}_{i,\,sea}$ by [T], one obtains the Stokes vector for the thermal radiation originating in the ocean and passing through the air-sea interface as follows:

$$\vec{I}_t = \begin{pmatrix} [1 - \frac{1}{2}(R_v R_v^* + R_h R_h^*)]\, B(\nu, T_{sea}) \\ -\frac{1}{2}(R_v R_v^* - R_h R_h^*)\, B(\nu, T_{sea}) \\ 0 \\ 0 \end{pmatrix}. \tag{67}$$

The quantity expressed in (67) has been called the intensity of emission of the sea surface by past investigators; it often is derived from the reflective properties of the sea surface by assuming detailed balance and local thermodynamic equilibrium. This concept is false since the air-sea interface cannot emit any radiation. Rather, one should think of the sea surface as passing a certain portion of the radiation emitted from its depths. One may define the emissivity of a body, such as the ocean, as the ratio of a polarized component of the radiation emerging from the body to that of a black body whose temperature is that of the body. Mathematically, the emissivities of the sea for vertical and horizontal polarization, ξ_v and ξ_h, respectively, are defined as follows:

$$\xi_v = I_{tv,sea}/B_v(\nu, T_{sea}) = 1 - R_v R_v^*, \tag{68}$$

$$\xi_h = I_{th,sea}/B_h(\nu, T_{sea}) = 1 - R_h R_h^*. \tag{69}$$

If one expresses the various intensities in terms of their equivalent brightness temperatures, and if one uses (10) to give B_v and B_h, then the Stokes vector for the emission of the sea in terms of brightness temperature, $\vec{T}_e$, is given as follows:

$$\vec{T}_e = \{(\xi_v T_{sea} + \xi_h T_{sea}),(\xi_v T_{sea} - \xi_h T_{sea}),0,0\}. \quad (70)$$

5. Equation of radiative transfer. The expression for the total differential change in the intensity of radiation as it travels along a differential optical path, $d\tau$, in a continuous medium is simply the sum of (25) and (28); that is,

$$d\vec{I} = -\kappa (\vec{I} - \vec{J})\, ds = (\vec{I} - \vec{J})\, d\tau. \quad (71)$$

Eq. (71) is known as Schwarzschild's Equation of Radiative Transfer. In a plane-parallel, horizontally-homogeneous medium, the equation of radiative transfer may be expressed as follows:

$$\mu \frac{d\vec{I}(\tau,\mu)}{d\tau} = \vec{I}(\tau,\mu) - \frac{\omega}{2} \int_{+1}^{-1} [P](\tau,\mu,\mu')\, \vec{I}(\tau,\mu')\, d\mu' - (1 - \omega)\, \vec{B}(\tau), \quad (72)$$

where τ is the optical depth, μ is the cosine of the zenith angle, θ, $[P]$ is the azimuthally independent, phase matrix defined by

$$[P] = \frac{1}{2\pi} \int_0^{2\pi} [P_o](\theta,\phi,\theta',\phi')\, d\phi', \quad (73)$$

and ω is the albedo for single scattering. The optical depth is defined by

$$\tau(z) = - \int_z^{\infty} \kappa(z')\, dz', \quad (74)$$

where z is the height (m) above sea level. The albedo for single scattering is defined by

$$\omega = \beta/\kappa; \quad (75)$$

it represents the fraction of the total extinction at a point that is due to scattering.

According to Beer's Law, radiation at some optical depth, τ, in the atmosphere will suffer some attenuation as it travels to one of the boundaries of the medium. For upward traveling radiation, the initial intensity will be reduced by the factor

$$\vec{I}(0,\mu)/\vec{I}(\tau,\mu) = \exp(-\tau/\mu). \tag{76}$$

For downward traveling radiation, this factor is

$$\vec{I}(\tau_o,\mu)/\vec{I}(\tau,\mu) = \exp[(\tau_o - \tau)/\mu], \tag{77}$$

where τ_o is the optical thickness of the entire atmosphere or the optical depth at the surface.

If one multiples (71) by the factor $c^2/k\,\nu^2$ and uses (10) to represent the components of $\vec{B}$, then one obtains the expression for the equation of radiative transfer for a plane-parallel, horizontally-homogeneous, axially-symmetric atmosphere in terms of Stokes vectors with units of brightness temperature (K) as follows:

$$\mu \frac{d\vec{T}(\tau,\mu)}{d\tau} = \vec{T}(\tau,\mu) - \frac{\omega}{2}\int_{+1}^{-1} [P](\tau,\mu,\mu')\,\vec{T}(\tau,\mu')\,d\mu' - (1 - \omega)\,\vec{T}(\tau), \tag{78}$$

where $\vec{T}$ is the temperature vector, $\{T,0,0,0\}$, in which T is the ambient temperature of the medium (K) at optical depth, τ.

The solution to (72) or (78) under appropriate boundary conditions is a difficult problem and has been obtained for only a few simple cases. The main difficulty lies in the fact that radiation incident at a point in the medium has undergone many angular scattering encounters similar to that occurring at the point. Thus, the emission of radiation due to scattering at a point depends on

the nature of emissions and extinctions occurring within the entire medium. The same can be said about every point in the medium. If reflection occurs at one or more of the boundaries of the medium, the problem of multiple scattering becomes even more complicated. Since hydrometeors scatter significant portions of microwave energy and since the ocean reflects approximately two-thirds of the radiation incident upon its surface, the effects of multiple scattering must be evaluated before one can develop relationships between the meteorological properties of the atmosphere and its thermal emissions at microwave frequencies.

The classical solution of the equation of radiative transfer for given boundary conditions was developed by Chandrasekhar (1960). In his method, certain transmission and scattering functions are developed from the invariant properties of the medium under consideration. Busbridge (1960) discusses the mathematics of such classical solutions. Almost all applications of Chandrasekhar's methods deal with media in which the source of radiation is external to the medium and in which thermal emission has been neglected. These classical techniques have been applied to the problem of the transfer of infrared radiation through clouds by Yamamoto et al. (1966). The only application of this method to the transfer of thermal microwaves through clouds has been made by Volchok and Chernyak (1969). In any classical treatment of the problem of radiative transfer, one may investigate only homogeneous media. Also,

quadrature formulas must be used to represent the phase function (matrix) for angular scattering.

Recently, an interesting technique, which employs the Monte Carlo method (Fleck, 1963; Shreider, 1966), has been applied to the problem of the transfer of visible and infrared radiation in clouds by Kattawar and Plass (1968, 1969a, 1969b). In this method, the multiple scattering of radiation in a scattering medium, such as clouds of hydrometeors, is viewed as a sequence of single-scattering encounters between representative photons and the medium. The sequence ends when a photon is either absorbed in the medium or exits the medium. The probabilities for scattering, absorption, escape, and angular scattering are predicted from classical electromagnetic theory.

The factors expressed in (76) and (77) may be viewed as being the probability that a photon at some optical depth, τ, will escape the medium without being scattered or absorbed. The phase matrix may be viewed as expressing the probability distribution function for angular scattering for a photon that is scattered at some point in the medium. Also, the probability distribution function for the distance a photon travels before interaction may be related to the distribution of the volume extinction coefficient, κ, in the medium. At that point, α/κ photons are absorbed, and β/κ photons are scattered. Shreider (1966) suggests methods for reducing the number of photon histories needed to determine the spatial

distribution of the emergent radiation fields from scattering media. The specific computational procedures used in applying the Monte Carlo method to the transfer of thermal microwaves through clouds of hydrometeors and atmospheric gases will be given in Chapter VII.

A special case of interest in this paper is the solution to (78) under the following conditions:

1. Scattering is negligible ($\beta = 0$; therefore, $\omega = 0$, $\kappa = \alpha$) (non-scattering medium).

2. Specular reflection occurs at the sea surface (specular reflection).

3. All variables in the atmosphere are explicit functions of height, z (plane-parallel, horizontally-homogeneous medium).

4. Radiation at the top of the atmosphere is isotropic and characterized by the Stokes vector, $\vec{T}_c$, where

$$\vec{T}_c = \{T_c, 0, 0, 0\} \tag{79}$$

and T_c is the cosmic brightness temperature (K).

This case is called the non-scattering case for a plane-parallel, horizontally-homogeneous, axially-symmetric atmosphere overlying a smooth, homogeneous ocean.

For the above special case, (78) becomes

$$\mu \, d\vec{T}(z,\mu) = [\alpha(z) \, \vec{T}(z) - \alpha(z) \, \vec{T}(z,\mu)] \, dz. \tag{80}$$

The microwave emission of the atmosphere may be described by two emission fields. The first field is the radiation originating as thermal radiation in the atmosphere that emerges from the top of the atmosphere; the second field is the radiation that emerges from the bottom of the atmosphere. These fields are called the anabatic

and katabatic fields, respectively, and are designated by Stokes vectors having units of brightness temperature, $\vec{T}_a$ and $\vec{T}_k$, respectively. These fields are given from the integration of (80) as

$$\vec{T}_a = \int_0^\infty \alpha(z)\, \vec{T}(z)\, \exp[-\int_0^\infty \alpha(z')\, \frac{dz'}{\mu}\,]\, \frac{dz}{\mu}\,, \tag{81}$$

and

$$\vec{T}_k = \int_0^\infty \alpha(z)\, \vec{T}(z)\, \exp[-\int_0^z \alpha(z')\, \frac{dz'}{\mu}\,]\, \frac{dz}{\mu}\,. \tag{82}$$

It is clear that $\vec{T}_a$ and $\vec{T}_k$ are functions of the zenith angle, the vertical distribution of temperature, and the vertical distribution of the volume absorption coefficient, which is, in turn, a function of the vertical distributions of temperature, dew-point temperature, pressure, liquid-water content, and drop-size distribution. If $\vec{T}_c$ is the Stokes vector that represents the isotropic microwave radiation of cosmic origin at the top of the atmosphere, then the Stokes vector representing the radiation incident on the surface of the ocean, $\vec{T}_s$, commonly called the sky brightness temperature, is calculated from

$$\vec{T}_s = \vec{T}_c\, \exp[-\int_0^\infty \alpha(z)\, \frac{dz}{\mu}\,] + \vec{T}_k. \tag{83}$$

The Stokes vector representing the radiation field at the top of the atmosphere due to the combined effects of emission and absorption in and from the atmosphere and the ocean, $\vec{T}_u$, which is designated as the upwelling brightness temperature, is calculated from

$$\vec{T}_u = \{[R]\, \vec{T}_s + [T]\, \vec{T}_{sea}\}\, \exp[-\int_0^\infty \alpha(z)\, \frac{dz}{\mu}\,] + \vec{T}_a. \tag{84}$$

where $\vec{T}_{sea}$ is the temperature vector for sea temperature, $\{T_{sea},0,0,0\}$, [R] is the reflection matrix given by (53), and [T] is the transmission matrix given by (64). For convenience, one may define a transmissivity function for the atmosphere, Γ, as

$$\Gamma = \exp[-\int_0^\infty \alpha(z)\,\frac{dz}{\mu}\,]. \tag{85}$$

Thus, it is obvious that even for this relatively simple case, the upwelling brightness temperature is a function of many environmental parameters including air temperature, dew-point temperature, liquid-water content, drop-size distribution, pressure, sea temperature, and sea salinity in addition ot the instrumental constraints of electromagnetic frequency, angle of viewing, and polarization. Of course, one or more of these parameters may be dominant for certain fixed classes. The functional relationships between $\vec{T}_a$, $\vec{T}_k$, Γ, [R], or [T] and the state of the environment will be considered in detail in the following chapters.

CHAPTER III

DIELECTRIC PROPERTIES OF LIQUID WATER

A. Theory

1. Complex dielectric constant. The meaning of the complex dielectric constant of a medium is related to the implications of Maxwell's Equations. For a medium that does not contain free charges, Maxwell's equations are as follows:

$$\vec{\nabla} \cdot \vec{E} = 0. \tag{86}$$

$$\vec{\nabla} \cdot \vec{H} = 0. \tag{87}$$

$$\vec{\nabla} \times \vec{E} = -\mu_o \frac{\partial H}{\partial t} \quad . \tag{88}$$

$$\vec{\nabla} \times \vec{H} = \sigma \vec{E} + \varepsilon' \varepsilon_o \frac{\partial E}{\partial t} \quad . \tag{89}$$

$\vec{E}$ is the electric field vector ($V\ m^{-1}$), $\vec{H}$ is the magnetic-field vector ($A\ m^{-1}$), μ_o is the permeability of a vacuum ($4\pi \times 10^{-7}\ H\ m^{-1}$), t is time (sec), σ is the conductivity ($\mho\ m^{-1}$), ε' is the real, relative permittivity, and ε_o is the permittivity of a vacuum ($8.854 \times 10^{-12}\ F\ m^{-1}$). If $\vec{E}$ and $\vec{H}$ are represented by the phasors,

$$\vec{E} = \vec{E}_o \exp(j\ \omega_f\ t) \tag{90}$$

and

$$\vec{H} = \vec{H}_o \exp(j\ \omega_f\ t), \tag{91}$$

then (89) becomes

$$\vec{\nabla} \times \vec{H} = (\sigma + j\ \omega_f\ \varepsilon'\ \varepsilon_o)\ \vec{E}. \tag{92}$$

According to Von Hippel (1954, p. 5), σ is an effective conductivity which includes all dissipative effects. The customary approach has been to define a relative loss factor, ε'', such that

$$\sigma = \omega_f \varepsilon_o \varepsilon''. \tag{93}$$

Substitution of (93) into (92) yields

$$\vec{\nabla} \times \vec{H} = (\omega_f \varepsilon_o \varepsilon'' + j \omega_f \varepsilon' \varepsilon_o) \vec{E} \tag{94a}$$

$$= j \omega_f \varepsilon_o (\varepsilon' - j \varepsilon'') \vec{E} \tag{94b}$$

$$= \varepsilon_o (\varepsilon' - j \varepsilon'') \frac{\partial E}{\partial t}. \tag{94c}$$

The parenthetical expression, $(\varepsilon' - j \varepsilon'')$, in (94c) is dimensionless and is called the complex dielectric constant of the medium. According to Sucher and Fox (1963), ε' is associated with the ability of a material to store electric energy, and ε'' is associated with the losses that occur in the material. These losses include viscous dissipation of energy in polar liquids as well as ohmic losses. It should be noted that the term, $\varepsilon_o (\varepsilon' - j \varepsilon'')$, serves the same role as $\varepsilon_o \varepsilon'$ when σ is zero. In fact, one may define the complex permittivity of the medium, ε, as

$$\varepsilon = \varepsilon_o (\varepsilon' - j \varepsilon''). \tag{95}$$

The curl of (88) is

$$\vec{\nabla} \times (\vec{\nabla} \times \vec{E}) = -\mu_o \vec{\nabla} \times \frac{\partial H}{\partial t}. \tag{96}$$

Substitution of (94c) and (95) into (96) yields

$$\vec{\nabla}(\vec{\nabla} \cdot \vec{E}) - \vec{\nabla}^2 \vec{E} = -\mu_o \varepsilon \frac{\partial^2 E}{\partial t^2}. \tag{97}$$

However, since $\vec{\nabla} \cdot \vec{E}$ is zero by (86), then

$$\vec{\nabla}^2 E = \mu_o \varepsilon \frac{\partial^2 E}{\partial t^2} . \tag{98}$$

Jordon and Balmain (1968, p. 128) show that (98) is the equation for a sinusodial electromagnetic wave propagating through space at a velocity, v, where

$$v = 1/\sqrt{\mu_o \varepsilon} = 1/\sqrt{\mu_o(\varepsilon' - j\,\varepsilon'')} . \tag{99}$$

Since the index of refraction, m, is defined as c/v, where c is the speed of propagation of electromagnetic radiation in a vacuum, $(1/\sqrt{\mu_o \varepsilon_o})$, then

$$m = m' - j\,m'' = \sqrt{\varepsilon' - j\,\varepsilon''} , \tag{100}$$

in which m' and -m" are the real and imaginary parts of the complex index of refraction.

2. Debye model for liquid water. Debye (1929, p. 94) derived the form of the dependence of the dielectric constant of polar liquids, such as water, on the electromagnetic frequency as follows:

$$\varepsilon' = \varepsilon_\infty + (\varepsilon_s - \varepsilon_\infty)/(1 + \omega_f^2 \tau_t^2) \tag{101}$$

and

$$\varepsilon'' = \omega_f \tau_t (\varepsilon_s - \varepsilon_\infty)/(1 + \omega_f^2 \tau_t^2) , \tag{102}$$

where ε_s is the static relative permittivity (i.e., the permittivity for very low frequencies), τ_t is the relaxation time (sec), and ε_∞ is the relative permittivity at high frequencies. Liquid water exhibits a resonance in the microwave region such that ε' and ε'' have large values for low microwave frequencies and small values for high microwave frequencies. In the ideal case for pure water,

ε_s and τ_t are functions of temperature only. Thus, once these values have been established for several water temperatures, one may use (101) and (102) to predict the dielectric constant of liquid water at any microwave frequency. When the medium consists of a solution of salts and water, the same form of the dependence may be used with the following alteration for ε'':

$$\varepsilon'' = \omega_f \tau_t (\varepsilon_s - \varepsilon_\infty)/(1 + \omega_f^2 \tau_t^2) + \sigma_i/\omega_f \varepsilon_o, \qquad (103)$$

where σ_i is the ionic conductivity of the medium at low frequencies.

B. Measurements

1. Pure, liquid water. The dielectric properties of pure, liquid water have been measured by a number of investigators for temperatures ranging from -8C to 100C. These measurements have been made at frequencies ranging from 3 GHz to 48.4 GHz; the specific frequencies used are itemized in Table 2 along with citations in the published literature.

The measurements of the dielectric constant of pure, liquid water are grouped around the microwave frequencies of approximately 3 GHz (S-band), 9 GHz (X-band), 22 GHz (K-band), and 48 GHz (Q-band). The specific measured values of m' and m" for pure, liquid water, as given in the literature, are listed in Tables 3 and 4.

These values are in good agreement with each other and show that (1) the real part of the complex index of refraction increases

Table 2. Frequencies at which the dielectric constant of pure, liquid water has been measured.

Frequency (GHz)	Citation in the Literature
3.0	Collie et al. (1948a)
3.25	Hasted and El-Sabeh (1953)
9.13	Hasted and El-Sabeh (1953)
9.33	Collie et al. (1948a)
9.34	Lane and Saxton (1952a)
19.0	Saxton and Lane (1946)
23.5	Collie et al. (1948a)
23.7	Hasted and El-Sabeh (1953)
24.2	Lane and Saxton (1952a)
48.4	Lane and Saxton (1952a)

with increasing temperature for frequencies in the X-, K-, and Q-bands and decreases with increasing temperature for frequencies in the S-band, and (2) the absolute value of the imaginary part of the complex index of refraction increases with increasing temperature for frequencies in the K-band, and decreases with increasing temperature for frequencies in the S- and X-bands.

2. Aqueous sodium chloride. The dielectric constant of aqueous sodium chloride has been measured by a number of investigators for temperatures ranging from -3C to 40C and for salt concentrations of 0.125N, 0.25N, 0.33N, 0.5N, 0.66N, and higher values. These measurements are not as extensive as those of pure, liquid water. The specific frequencies used are itemized in Table 5 along with citations in the published literature.

Table 3. Measured values of the complex index of refraction of pure, liquid water for frequencies in the S- and X-bands.

Temperature (C)	3.0 GHz m'	3.0 GHz m"	3.25 GHz m'	3.25 GHz m"	9.13 GHz m'	9.13 GHz m"	9.33 GHz m'	9.33 GHz m"	9.34 GHz m"
0	9.03	1.37	9.06	1.46	7.34	2.80	7.28	2.86	2.89
10	8.89	0.982	8.97	1.08	7.85	2.36	7.73	2.43	2.44
20	8.83	0.739	8.86	0.785	8.17	1.93	8.08	1.97	2.00
30	8.78	0.558	8.73	0.584	8.26	1.57	8.11	1.57	1.60

Table 4. Measured values of the complex index of refraction of pure, liquid water for frequencies in the K- and Q-bands.

Temperature (C)	19.0 GHz m'	19.0 GHz m"	23.5 GHz m'	23.5 GHz m"	23.7 GHz m'	23.7 GHz m"	24.2 GHz m'	24.2 GHz m"	48.4 GHz m"
-8	—	—	—	—	—	—	—	2.55	1.77
0	5.24	2.90	4.94	2.86	4.77	2.88	4.75	2.77	2.04
10	6.36	2.91	5.55	2.91	5.55	2.97	5.45	2.90	2.37
20	7.13	2.61	6.25	2.86	6.24	2.81	6.15	2.86	2.59
30	7.59	2.21	6.75	2.67	6.75	2.63	6.70	2.67	2.70

Table 5. Frequencies at which the dielectric constant of aqueous sodium chloride has been measured.

Frequency (GHz)	Citation in the Literature
3.0	Hasted et al. (1948)
3.01	Hasted and Roderick (1958)
3.25	Hasted and El-Sabeh (1953)
9.13	Hasted and El-Sabeh (1953)
9.31	Hasted and Roderick (1958)
9.34	Lane and Saxton (1952b)
10.0	Hasted et al. (1948)
23.7	Hasted and El-Sabeh (1953)
24.2	Lane and Saxton (1952b)
48.4	Lane and Saxton (1952b)

The specific measured values of m' and m" for aqueous sodium chloride given by the investigators listed in Table 5 (with the exception of Lane and Saxton (1952b) who did not list their measurements) are given in Tables 6 and 7.

It is impossible to determine whether or not any one set of measurements given in Tables 6 and 7 is better than any other set, since no two measurements were made at the same temperature and normality for frequencies in the same general band. The measurements given in these tables do not include any contribution to ε'' due to ohmic losses. The effects of temperature on m' and m" are similar to those observed for pure water. Since the contribution to ε'' due to ohmic losses becomes quite large at low frequencies, ε'' increases strongly with increasing normality for L-band and low S-band frequencies.

Table 6. Measured values of the complex index of refraction of aqueous sodium chloride for frequencies in the S-band.

Normality (N)	Temperature (C)	3.0 GHz m'	3.0 GHz m"	3.01 GHz m'	3.01 GHz m"	3.25 GHz m'	3.25 GHz m"
0.125	**3.0**	—	—	8.94	1.25	—	—
0.125	**25.0**	—	—	8.70	0.632	—	—
0.25	0.0	—	—	—	—	8.83	1.30
0.25	10.0	—	—	—	—	8.77	0.952
0.25	20.0	—	—	—	—	8.69	0.708
0.25	30.0	—	—	—	—	8.54	0.509
0.33	3.0	—	—	8.76	1.17	—	—
0.5	0.0	—	—	—	—	8.65	1.33
0.5	10.0	—	—	—	—	8.53	0.85
0.5	20.0	—	—	—	—	8.43	0.564
0.5	21.0	8.56	0.736	—	—	—	—
0.5	30.0	—	—	—	—	8.28	0.453
0.66	0.0	8.52	1.35	—	—	—	—
0.66	3.0	—	—	8.55	1.1	—	—
0.66	10.0	8.47	1.13	—	—	—	—
0.66	20.0	8.36	0.903	—	—	—	—
0.66	25.0	—	—	8.23	0.534	—	—
0.66	30.0	8.26	0.726	—	—	—	—

Table 7. Measured values of the complex index of refraction of aqueous sodium chloride for frequencies in the X- and K-bands.

Normality (N)	Temperature (C)	9.13 GHz m'	9.13 GHz m"	9.31 GHz m'	9.31 GHz m"	10.0 GHz m'	10.0 GHz m"	23.7 GHz m'	23.7 GHz m"
0.125	3.0	—	—	7.40	2.69	—	—	—	—
0.125	25.0	—	—	8.16	1.69	—	—	—	—
0.25	0.0	7.26	2.69	—	—	—	—	—	—
0.25	10.0	7.77	2.19	—	—	—	—	5.62	2.85
0.25	20.0	7.99	1.85	—	—	—	—	6.23	2.79
0.25	30.0	8.05	1.57	—	—	—	—	6.61	2.61
0.33	3.0	—	—	7.29	2.55	—	—	—	—
0.33	25.0	—	—	7.94	1.64	—	—	—	—
0.5	0.0	7.18	2.65	—	—	—	—	—	—
0.5	1.5	—	—	—	—	7.15	2.53	—	—
0.5	10.0	7.58	2.21	—	—	—	—	5.46	2.70
0.5	20.0	7.79	1.77	—	—	—	—	6.00	2.64
0.5	21.0	—	—	—	—	7.86	1.80	—	—
0.5	30.0	7.85	1.43	—	—	—	—	6.41	2.46
0.66	0.0	—	—	—	—	7.21	2.53	—	—
0.66	3.0	—	—	7.20	2.47	—	—	—	—
0.66	10.0	—	—	—	—	7.51	2.14	—	—
0.66	20.0	—	—	—	—	7.72	1.80	—	—
0.66	30.0	—	—	—	—	7.60	1.43	—	—

C. Practical Treatment

All of the above investigators found that the Debye model could be used to predict the measured values of the dielectric constant of pure, liquid water and aqueous sodium chloride when the static relative permittivity, ε_s, the relaxation time, τ_t, and the ionic conductivity, σ_i, were assumed to be functions of the water temperature and solution concentration only. Values of ε_s and τ_t for pure, liquid water for specific temperatures are given by Saxton (1946a, 1946b, 1949, 1952), Collie et al. (1948a), and Hasted (1961). The only values of ε_s and τ_t for supercooled, pure, liquid water given in the literature are those by Saxton (1952). Since the dielectric constant of supercooled water is of interest in this paper, the values for ε_s and τ_t given by Saxton (1952) and listed in Table 8 were used; for these values, Saxton found that the best fit was achieved when ε_∞ was taken to be 4.9 for all temperatures.

Table 8. Debye parameters of pure water at specific temperatures (after Saxton, 1952).

Temperature (C)	ε_s	$\tau_t \times 10^{12}$ (sec)
-10	92.3	27.5
0	88.2	18.7
10	84.2	13.6
20	80.4	10.1
30	76.7	7.5
40	73.1	5.9

Values of ε_s and τ_t for aqueous sodium chloride for specific temperatures and normalities are given by Hasted et al. (1948), Saxton and Lane (1952), Lane and Saxton (1952b), and Hasted and El-Sabeh (1953). The values given by Hasted et al. (1948) are only for temperatures of 1.5C and 21C. Those given by Hasted and El-Sabeh (1953) are only for normalities of 0.25N and 0.5N. Those given by Saxton and Lane (1952) and Lane and Saxton (1952b) are for temperatures of 0C, 10C, 20C, 30C, and 40C and for normalities of 0.5N, 1.0N, and 1.5N, and higher values. In addition, Saxton and Lane (1952) give values for σ_i for the same values of temperature and normality.

In this paper, a general expression is needed that gives the complex index of refraction of sea water as a function of its salinity, its temperature, and the microwave frequency. The index of refraction of pure water may be obtained from such a general expression by setting the salinity to be zero. These quantities are needed to predict the reflective and transmissive properties of sea water and the absorptive and scattering properties of liquid hydrometeors. A thorough search of the literature has shown that the complex index of refraction of sea water has not been measured. Since sodium chloride is the major constituent of sea water (McLellan, 1965, p. 16) and accounts for 85.6% of the total dissolved salts by weight in sea water, one may assume that the dielectric properties of sea water and aqueous sodium chloride are similar.

The measure of salt concentration of sea water is its salinity, S (o/oo), where S is defined as the total amount of solid material in grams contained in one kilogram of solution when all carbonate has been converted to oxide, the bromine and iodine replaced by chlorine, and all organic matter oxidized (McLellan, 1965, p. 17). This definition applies equally well to either sea water or aqueous sodium chloride.

The relationships between the mass of solute per liter of solution and the salinity of aqueous sodium chloride at 20C are as shown in Table 9 (Chemical Rubber Company, 1959, p. 2029). One gram-equivalent molecular-weight of sodium chloride is 58.448 g (ibid., pp. 401-402). The normality of aqueous sodium chloride is the number of grams of solute per liter of solution divided by 58.448. Thus, the relationship between salinity and normality in aqueous sodium chloride is as given in Table 10.

Table 9. Number of grams of sodium chloride per liter of aqueous sodium chloride versus salinity at 20C.

Salinity (o/oo)	Grams per liter
0	0.0
10	10.05
20	20.25
40	41.07

Table 10. Relationship between salinity and normality of aqueous sodium chloride.

Salinity (o/oo)	Normality (N)
0	0.0
10	0.172
20	0.346
40	0.703

Since the specific gravity of water varies only by 0.4% for temperatures ranging from 0C to 30C (ibid., p. 2114), the relationship given in Table 10 essentially is independent of temperature.

Plotting these values on a graph and drawing a smooth curve through the four points, one obtains an interpolation curve that may be used to convert normality values to salinity values. These conversions are shown in Table 11 for the normalities used in this paper.

Since sea water may have salinities as high as the upper 30's, one must use the values of ε_s, τ_t, and σ_i given by Saxton and Lane (1952) in order to allow interpolation for the usual temperatures and salinities encountered in the open ocean. These values are given in Table 12 except for pure water; in that case, the values given in Table 8 are substituted. Also, ε_∞ is assumed to be 4.9.

Table 11. Relationship between the normality and salinity of aqueous sodium chloride.

Normality (N)	Salinity (o/oo)
0.0	0.0
0.125	7.1
0.25	14.5
0.33	19.0
0.5	28.3
0.62	35.0
0.66	37.0
1.0	55.5

In order to allow one to predict ε_s, τ_t, and σ_i for any temperatures and salinities in the ranges $-10C < T_{sea} < 40C$ and 0 o/oo $< S <$ 55.5 o/oo, the data points given in Table 12 and a standard IBM Scientific, Subroutine Package were used to form a set of non-linear regression equations. The regression coefficients for these equations are given in Table 13.

These regression equations may be used with the Debye equations, (101) and (103) to predict ε' and ε'' for any given temperature, salinity, and microwave frequency. m' and m" may be obtained from ε' and ε'' through (100).

Table 12. The Debye parameters of aqueous sodium chloride for specific values of temperature and salinity (after Saxton and Lane, 1952; Saxton, 1952).

T_{sea} (C)	Debye Parameter	0.0 o/oo	28.3 o/oo	55.5 o/oo
-10	ε_s	92.3	—	—
	$\tau_t \times 10^{12}$ s	27.5	—	—
	σ_i ℧ m^{-1}	0.0	—	—
0	ε_s	88.2	77.0	69.0
	$\tau_t \times 10^{12}$ s	18.7	17.1	16.4
	σ_i ℧ m^{-1}	0.0	2.44	4.77
10	ε_s	84.2	74.0	66.0
	$\tau_t \times 10^{12}$ s	13.6	12.2	11.8
	σ_i ℧ m^{-1}	0.0	3.45	6.22
20	ε_s	80.4	71.0	63.0
	$\tau_t \times 10^{12}$ s	10.1	9.2	9.0
	σ_i ℧ m^{-1}	0.0	4.44	7.66
30	ε_s	76.7	68.0	60.0
	$\tau_t \times 10^{12}$ s	7.5	7.2	7.1
	σ_i ℧ m^{-1}	0.0	5.22	9.22
40	ε_s	73.1	65.0	58.0
	$\tau_t \times 10^{12}$ s	5.9	5.7	5.6
	σ_i ℧ m^{-1}	0.0	6.22	10.8

Table 13. Regression coefficients for the Debye parameters of aqueous sodium chloride.

Independent variable	Regression coefficients		
	ε_s	$\tau_t \times 10^{12}$ (sec)	σ_i (℧ m^{-1})
constant	0.88195 E 02	0.19390 E 02	————
T_{sea}	-0.40349 E-00	-0.68020 E-00	————
S	-0.43917 E-00	-0.11370 E-00	0.87483 E-01
T_{sea} S	0.43269 E-02	0.58629 E-02	0.45802 E-02
T_{sea}^2	0.65924 E-03	0.95865 E-02	————
S^2	0.16738 E-02	0.11417 E-02	-0.25662 E-04
T_{sea}^2 S	-0.92286 E-05	-0.87596 E-04	-0.16914 E-04
T_{sea} S^2	-0.42856 E-04	-0.54577 E-04	-0.37158 E-04
T_{sea}^2 S^2	0.44410 E-07	0.82521 E-06	0.39288 E-06
exp(T_{sea})	————	-0.65303 E-17	————

The complex index of refraction of aqueous sodium chloride was computed from the regression equation and the Debye formulas for the conditions shown in Tables 3, 6, and 7. It should be emphasized that the values of ε_s, τ_t, and σ_i on which these regression equations were based were obtained from the measurements made by Lane and Saxton. The computed values of m' and m" agree fairly well with the values measured by other investigators.

One final point needs to made: since the dielectric constant of sea water has never been measured and since aqueous sodium chloride is a good approximation to sea water as far as its electrical properties are concerned, the assumption is made hereafter that the foregoing equations may be used to predict the dielectric properties of sea water. In the following chapter, the implications of the dielectric properties of "sea water" and pure water are explored.

CHAPTER IV

MICROWAVE EMISSION OF THE OCEAN

When microwave radiation encounters the air-sea interface, it is partially reflected or transmitted. The radiation transmitted from the air to the ocean is absorbed quickly since the imaginary part of the dielectric constant of sea water is large. Since microwave radiation is absorbed completely after transversing only a few centimeters, the radiation arriving at the air-sea interface from below is the same as that from a black body the temperature of which is equal to the mean temperature of the surface layer of the ocean. If the ocean surface is calm and the ocean surface-layer is homogeneous, then the theory developed in Chapter III for the reflection and transmission of electromagnetic radiation through the flat interface between sea water and air may be used to predict the microwave emission of the sea. If the ocean surface is rough, then this theory cannot be used. The sea becomes rough when momentum and energy are being transferred from the atmosphere to the ocean, that is, when the atmosphere is applying a stress on the sea surface. Under conditions of high shearing stress, sea foam may be generated. For this case, any theoretical studies are of limited value due to the lack of knowledge of the structure of sea foam. For much of the World Ocean, the sea surface is relatively free of sea foam, and existing theory may be used to predict the

interaction of microwaves with the ocean. Three cases will be discussed: (1) the emission and reflection of calm seas, (2) the effect of wave-slope roughness, and (3) the effect of foam roughness.

A. Microwave Emission by a Calm Sea

The thermal emission of a calm ocean at microwave frequencies is visualized best as the result of the transmission of radiation originating in the surface layer of the ocean through the air-sea interface. The transmission matrix (64) may be used in this case. The elements of the transmission matrix are functions of the Fresnel coefficients which are, in turn, functions of the zenith angle in the air and the complex index of refraction of water. In Chapter III, it was shown that the complex index of refraction of water is a function of its temperature, its salinity, and the microwave frequency. In a similar manner, the reflection matrix (53) may be used to compute the reflected radiation. In addition to the dependence of the reflection matrix on the zenith angle, the sea temperature, the sea salinity, and the microwave frequency, one must know the Stokes vector for the incident radiation in order to predict that for the reflected field. On the other hand, the radiation originating in the water is a function of the sea temperature only. Thus, only the transmitted thermal radiation originating in the water will be discussed in this section. This radiation will be referred to as the microwave emission of sea

water; it is characterized by a Stokes vector for brightness temperature given by

$$\vec{T}_e = \{(T_{ev} + T_{eh}),(T_{ev} - T_{eh}),0,0\}, \tag{104}$$

where

$$T_{ev} = (1 - R_v R_v^*) T_{sea} \tag{105}$$

and

$$T_{eh} = (1 - R_h R_h^*) T_{sea} . \tag{106}$$

The polarized components of the microwave emission of sea water were calculated for a number of microwave frequencies and sea temperatures, for zenith angles of 0, 30, 55 deg, and for a salinity of 34.72 o/oo, which is the mean salinity of the surface of the World Ocean (McLellan, 1965, p. 17). These values, shown in Table 14, exhibit the following characteristics: (1) the microwave emission of sea water decreases with increasing temperature for frequencies less than 2 GHz and greater than 22 GHz, (2) the microwave emission of sea water increases with increasing temperature for frequencies between 2 GHz and 16 GHz, (3) the microwave emission of sea water is fairly independent of temperature for frequencies between 16 GHz and 22 GHz, and (4) the maximum response of the microwave emission of sea water to changes in sea temperature occurs at 0.61 GHz; secondary maxima occur at 5.81 and 60.0 GHz. The responses of the microwave emission of sea water to changes in temperature ($K\ K^{-1}$), based on the above calculations, are shown in Table 15 for the frequencies exhibiting

Table 14. Computed brightness temperatures for the polarized components of the microwave emission of sea water (34.72 o/oo) for specific frequencies, zenith angles, and temperatures.

Frequency (GHz)	Temperature (C)	Brightness Temperature (K)				
		θ = 0 deg	θ = 30 deg		θ = 55 deg	
		v or h	v	h	v	h
0.61	0	77	87	68	120	47
0.61	10	71	80	63	112	43
0.61	20	66	75	58	105	40
0.61	30	62	71	55	100	38
1.42	0	92	103	82	140	57
1.42	10	92	103	81	140	57
1.42	20	91	102	80	139	56
1.42	30	89	100	79	138	55
2.695	0	96	108	86	145	60
2.695	10	99	111	88	150	62
2.695	20	102	114	91	154	64
2.695	30	104	116	92	157	65
4.805	0	99	111	89	149	62
4.805	10	103	115	91	154	65
4.805	20	107	119	95	160	67
4.805	30	110	124	98	166	69
5.81	0	101	112	90	151	63
5.81	10	104	116	92	156	65
5.81	20	108	120	96	162	68
5.81	30	112	125	100	168	70
10.69	0	108	120	96	159	68
10.69	10	109	121	97	162	69
10.69	20	111	124	99	166	70
10.69	30	115	129	103	172	73
15.375	0	115	128	103	168	73
15.375	10	114	127	102	168	72
15.375	20	115	128	103	171	73
15.375	30	119	132	106	176	75

Table 14 (cont'd).

Frequency (GHz)	Temperature (C)	Brightness Temperature (K)				
		θ = 0 deg	θ = 30 deg		θ = 55 deg	
		v or h	v	h	v	h
19.35	0	121	134	108	174	78
19.35	10	118	132	106	173	76
19.35	20	119	132	106	175	75
19.35	30	121	135	108	179	77
22.235	0	125	138	112	179	81
22.235	10	122	135	109	177	78
22.235	20	121	135	109	178	77
22.235	30	123	137	110	182	79
31.4	0	138	151	124	192	90
31.4	10	132	146	119	189	86
31.4	20	130	144	116	187	83
31.4	30	131	145	117	190	84
33.2	0	140	154	126	195	92
33.2	10	134	148	121	191	87
33.2	20	131	145	118	189	85
33.2	30	132	146	118	191	85
37.0	0	144	158	131	199	96
37.0	10	138	152	125	195	90
37.0	20	135	149	121	193	87
37.0	30	135	150	121	195	87
45.248	0	153	168	139	208	103
45.248	10	146	161	132	203	96
45.248	20	142	156	128	200	92
45.248	30	141	156	127	202	92
53.8	0	161	176	147	215	109
53.8	10	154	169	140	211	102
53.8	20	148	163	134	207	98
53.8	30	147	163	133	208	96
60.0	0	167	181	152	220	114
60.0	10	159	174	144	215	107
60.0	20	153	168	138	212	101
60.0	30	152	167	137	213	100

maximum variations. In general, these responses are small, and an evaluation of the effects of the atmosphere must be made before any final conclusions can be reached.

Table 15. Response of the microwave emission of sea water (34.72 o/oo) to a change in the sea temperature from 0C to 30C.

Frequency (GHz)	Response ($K\ K^{-1}$)				
	θ = 0 deg	θ = 30 deg		θ = 55 deg	
	v or h	v	h	v	h
0.61	-0.478	-0.523	-0.434	-0.642	-0.319
5.81	+0.373	+0.416	+0.333	+0.560	+0.235
60.0	-0.494	-0.461	-0.508	-0.240	-0.477

The brightness temperatures of the polarized components of the microwave emission of sea water were calculated for the frequencies, temperatures, and zenith angles shown in Table 14, but for salinities ranging from 0 o/oo to 35 o/oo. These calculations show that such a change in salinity causes an absolute change in the brightness temperature of 2K or less for frequencies of 5.81 GHz or higher. For frequencies less than 5.81 GHz, the effect of salinity is appreciable especially at the lowest frequencies. The responses of the microwave emission of sea water to changes in salinity (K per o/oo) at specific temperatures, zenith angles, polarizations, and frequencies are shown in Table 16. These calculations show that a microwave radiometer operating at frequencies less than about 2 GHz and at vertical polarization may be used to survey the salinity of

Table 16. Response of the microwave emission of sea water to changes in salinity from 0 o/oo to 35 o/oo.

Frequency (GHz)	Temperature (C)	Response (K per o/oo) θ = 0 deg v or h	θ = 30 deg v	θ = 30 deg h	θ = 55 deg v	θ = 55 deg h
0.61	0	-0.528	-0.575	-0.482	-0.704	-0.357
0.61	30	-1.41	-1.54	-1.28	-1.93	-0.937
1.42	0	-0.103	-0.111	-0.095	-0.135	-0.071
1.42	30	-0.649	-0.704	-0.594	-0.852	-0.444

the sea surface from aloft if the temperature is known from an independent source (for example, an airborne, infrared radiometer). The response of the microwave emission of sea water is small; therefore, measurements of salinity in the open ocean by an airborne microwave radiometer would be of little value since the salinity of the ocean ranges over only a few parts per thousand. In the coastal zone and especially in the vicinity of the outflow of a river or estuary, the water mass changes from fresh water (less than 5 o/oo) to ocean water (34-37 o/oo) over a short distance. The corresponding changes in the microwave emissions are up to 60K at 0.61 GHz and up to 26K at 1.42 GHz. Current airborne microwave radiometers are sensitive changes in brightness temperature of 2K to 5K.

The microwave emissions of sea water are shown in Figs. 4 to 13 as a function of sea temperature and sea salinity for vertical polarization and horizontal polarization, for frequencies of 0.61 and 1.42 GHz, and for zenith angles of 0, 30, and 55 deg. The curves in these figures show that the variations of the microwave emission of sea water at these frequencies, polarizations, and zenith angles are nearly linear with respect to temperature and salinity. Also, the response of the microwave emission of sea water to changes in salinity is greatest for warm water. One should note that the effect of temperature on the microwave emission of sea water is minimal for medium values of salinity and warm temperatures. In addition, the interference of the atmosphere is negligible for these frequencies (see Chapter V). One problem that may affect adversely the interpretation of airborne measurements of the microwave emission of sea water at 0.61 GHz is the large variation in microwave radiation incident on Earth from cosmic sources which may have brightness temperatures ranging from 3K to 100K at 0.61 GHz (Kraus, 1964). The cosmic radiation at 1.42 GHz ranges from 3K to 10K. In fact, there is a constant background level of 3K or greater for frequencies above about 2 GHz (Apparao, 1968).

Recent aircraft tests by Droppleman et al. (1970) of an airborne, microwave radiometer operating at 1.42 GHz confirmed the theoretical predictions of the microwave emission of sea water as

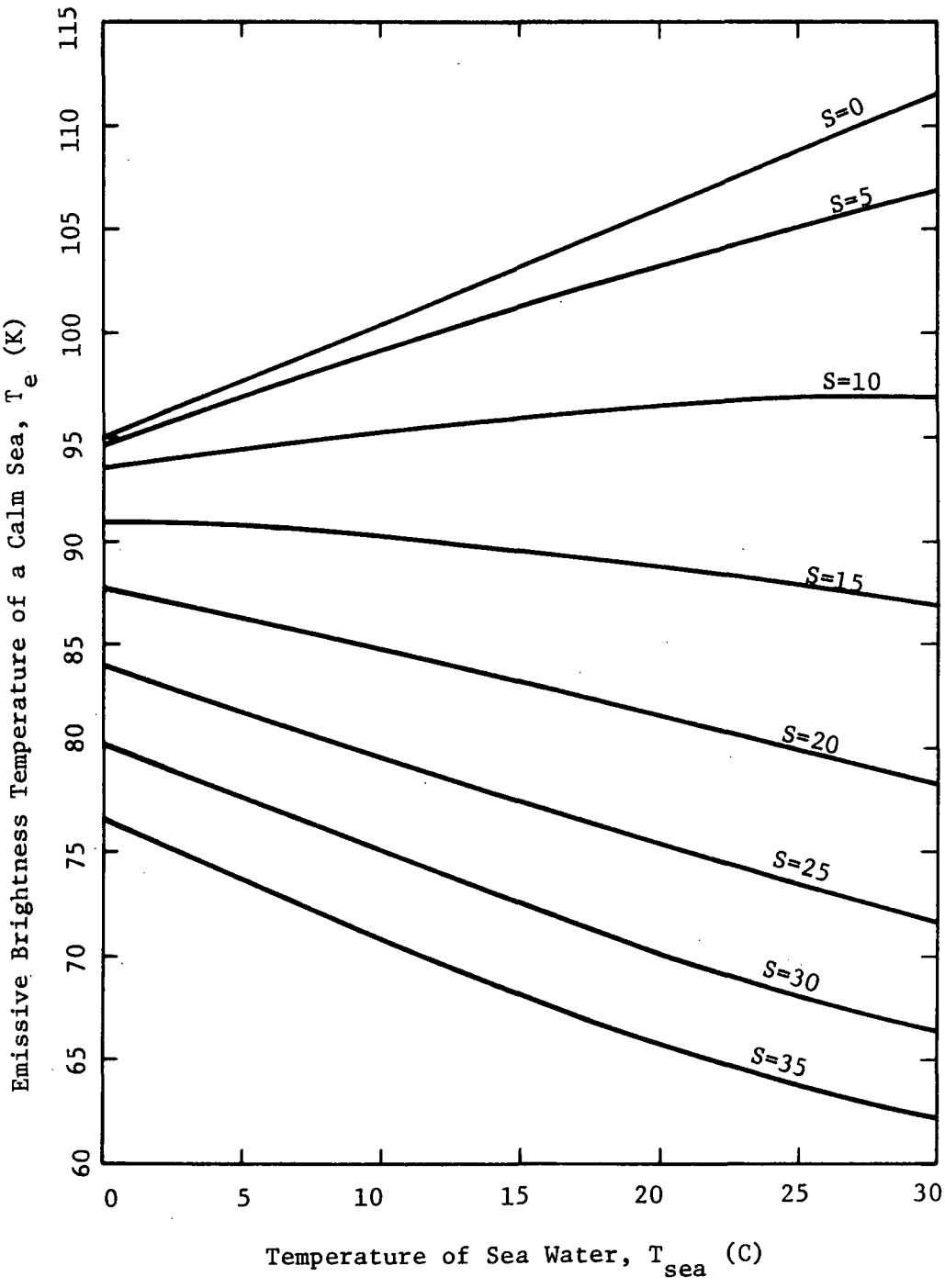

Fig. 4. Microwave emission of a calm sea: ν = 0.61 GHz, θ_a = 0 deg, vertical or horizontal polarization.

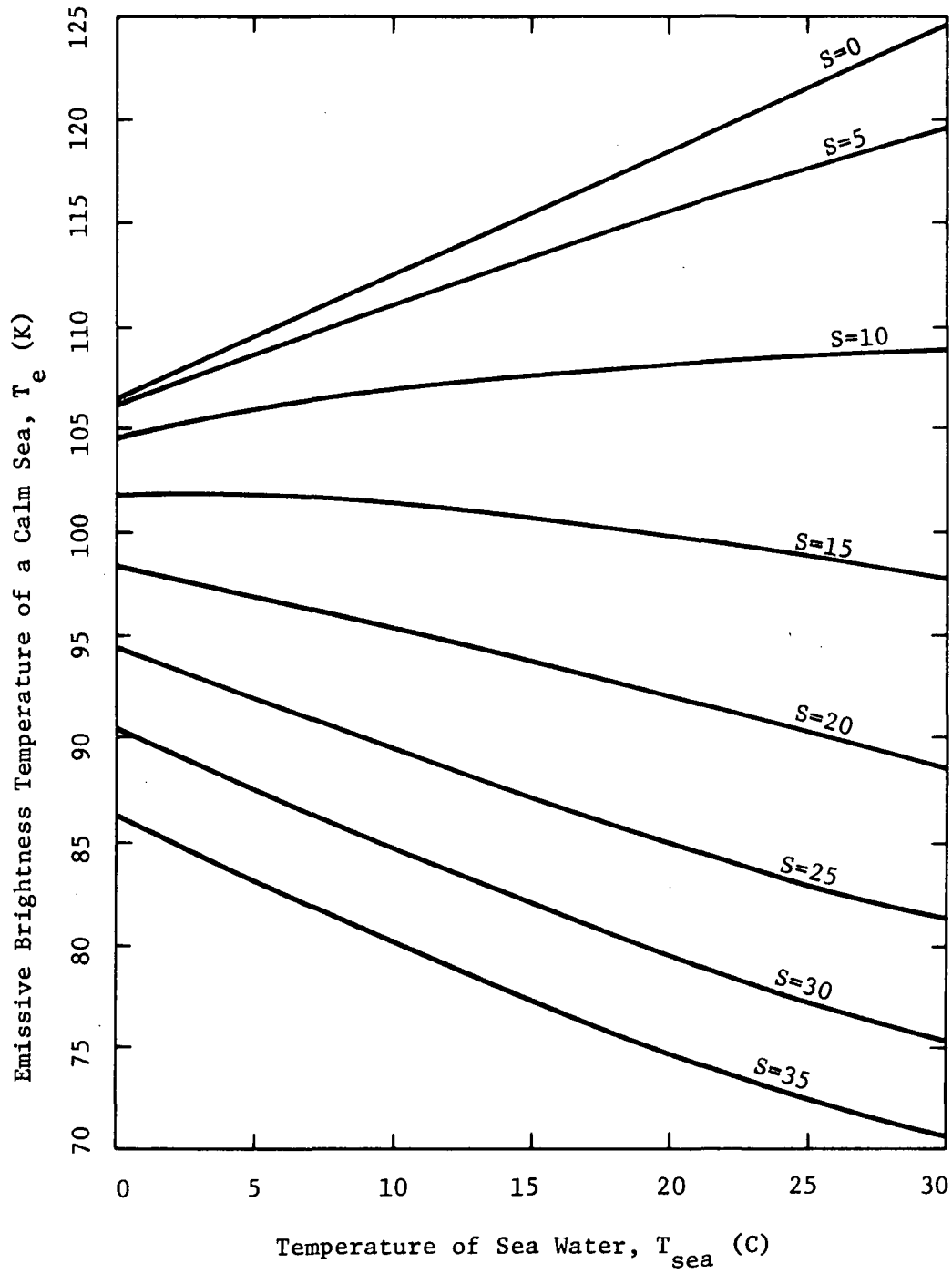

Fig. 5. Microwave emission of a calm sea: ν = 0.61 GHz, θ_a = 30 deg, vertical polarization.

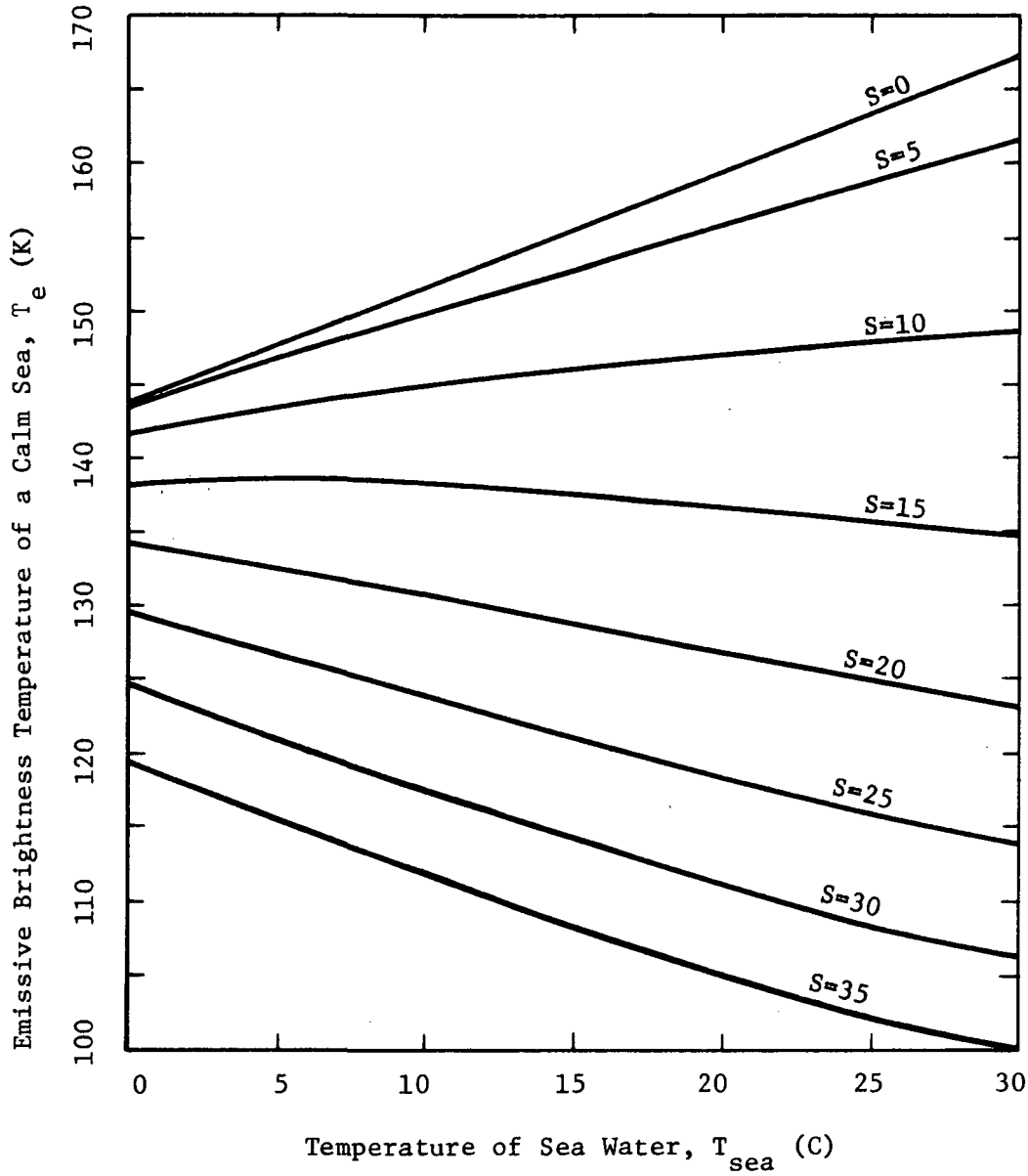

Fig. 6. Microwave emission of a calm sea: ν = 0.61 GHz, θ_a = 55 deg, vertical polarization.

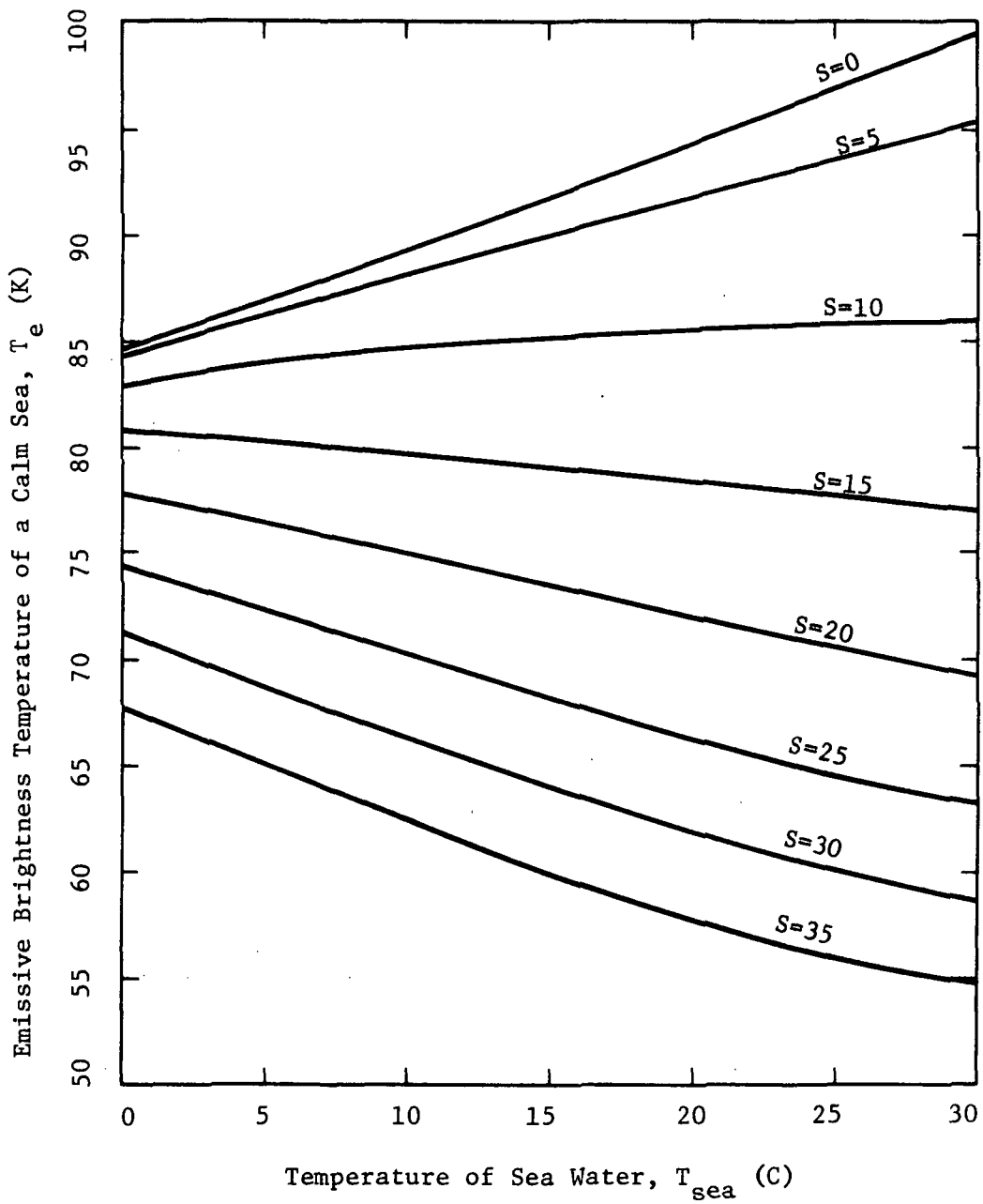

Fig. 7. Microwave emission of a calm sea: ν = 0.61 GHz, θ_a = 30 deg, horizontal polarization.

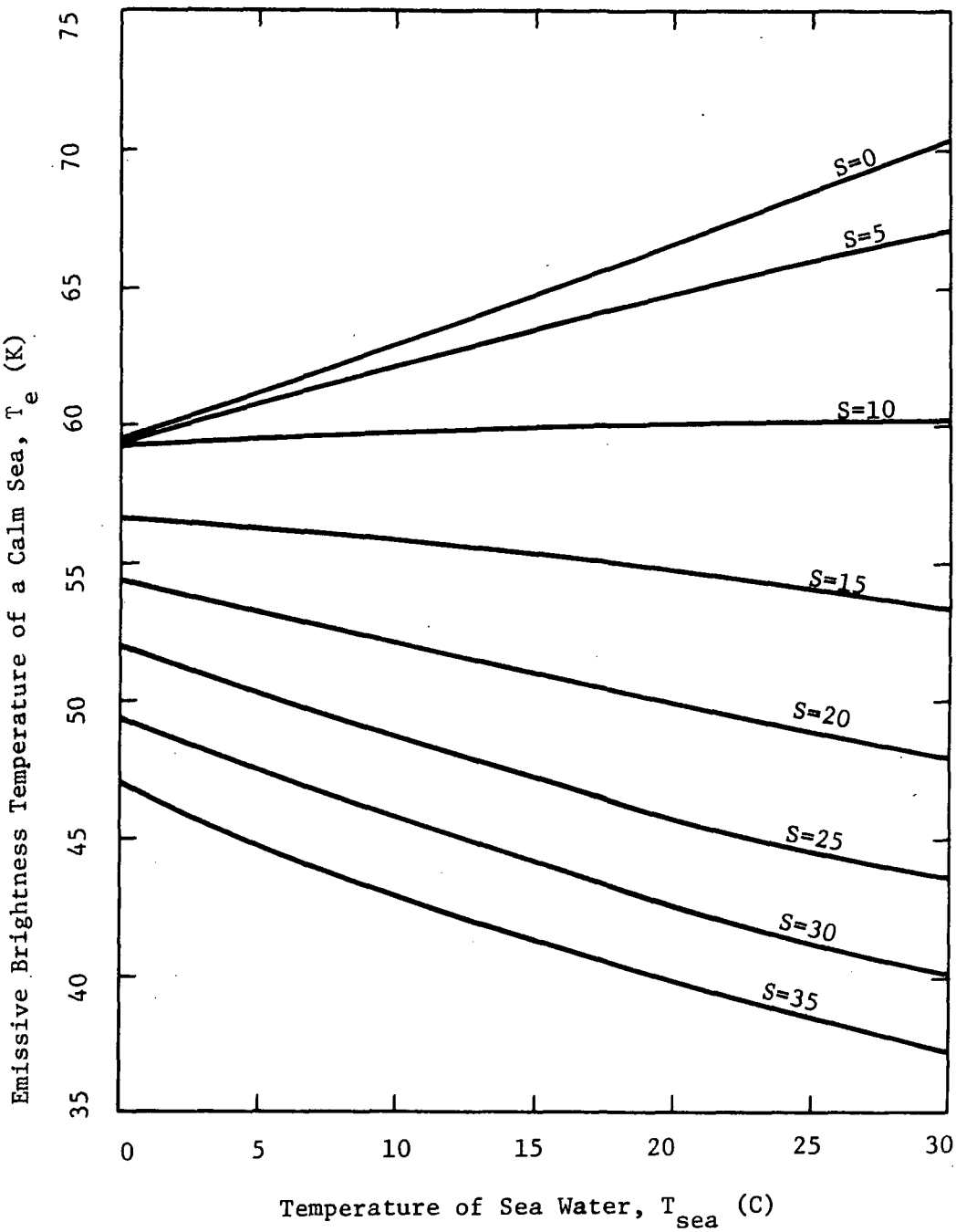

Fig. 8. Microwave emission of a calm sea: ν = 0.61 GHz, θ_a = 55 deg, horizontal polarization.

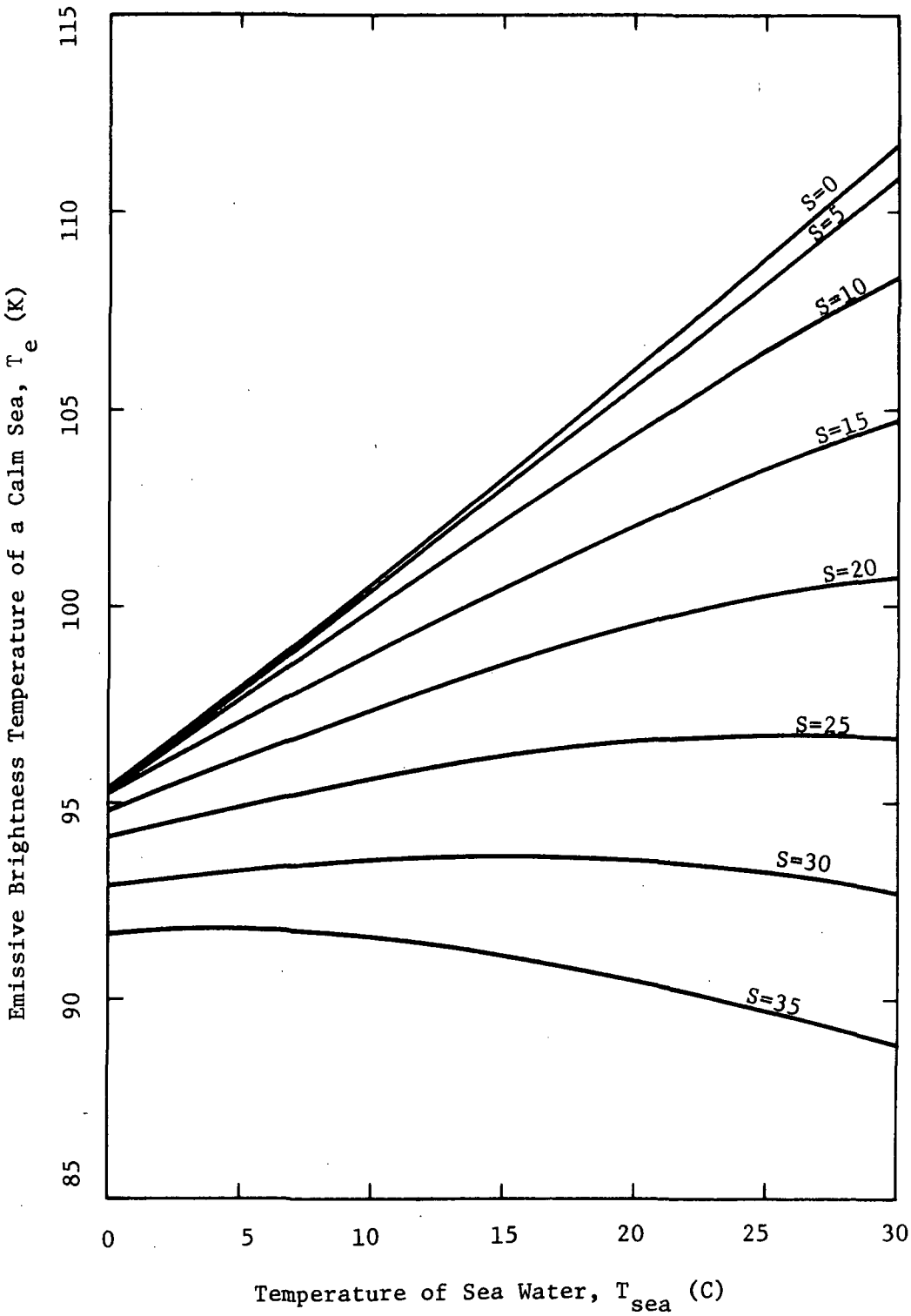

Fig. 9. Microwave emission of a calm sea: ν = 1.42 GHz, θ_a = 0 deg, vertical or horizontal polarization.

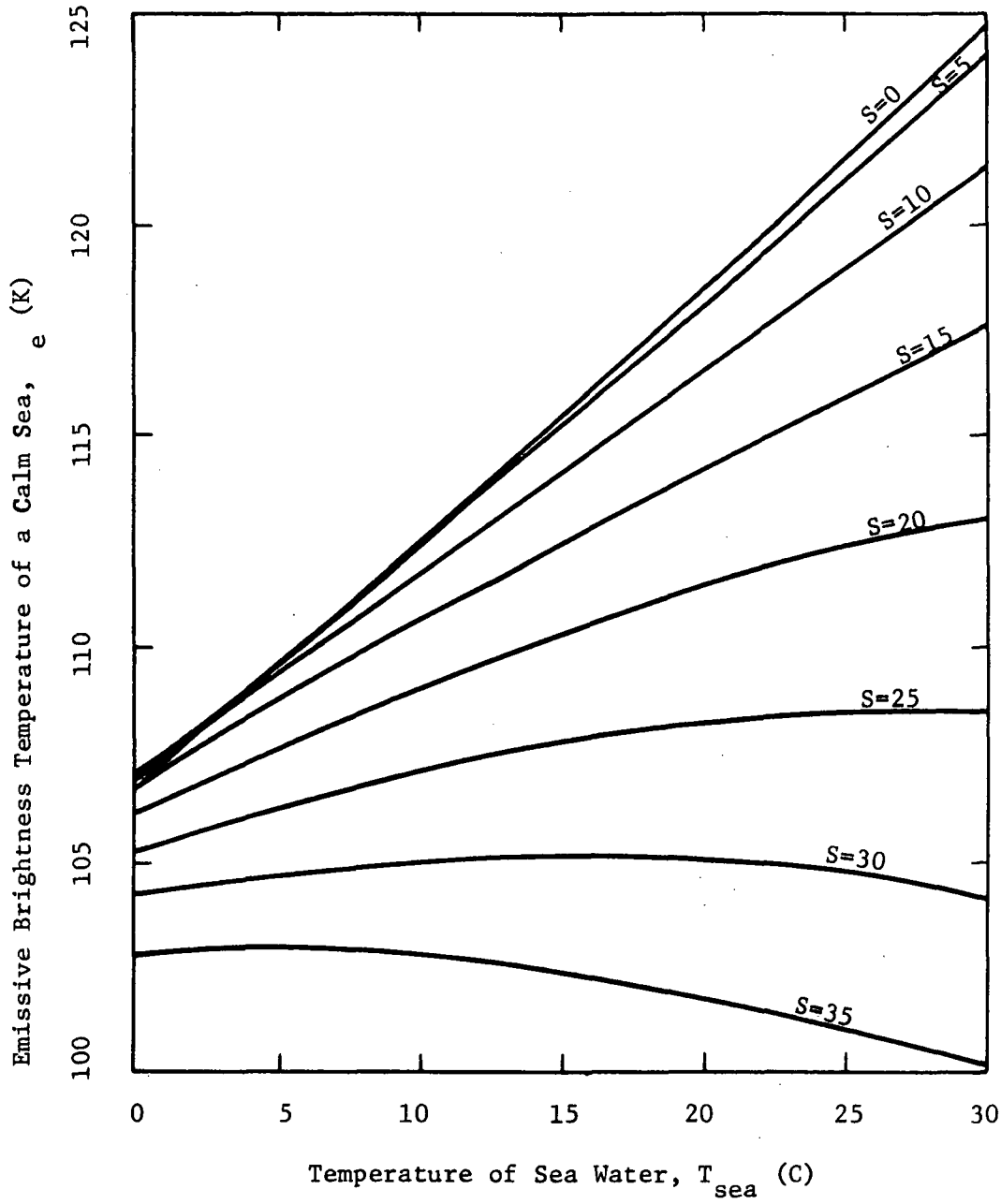

Fig. 10. Microwave emission of a calm sea: ν = 1.42 GHz, θ_a = 30 deg, vertical polarization.

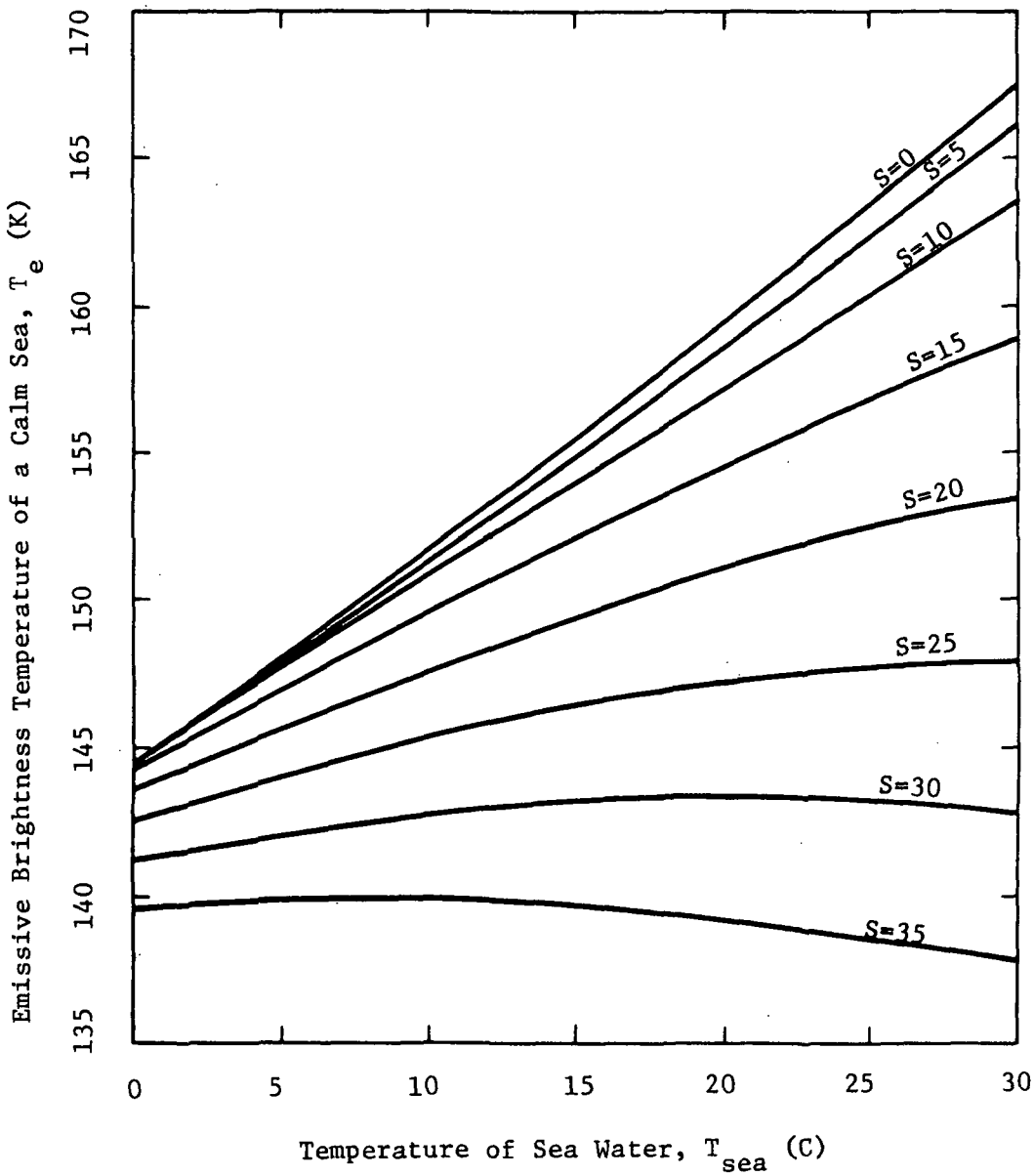

Fig. 11. Microwave emission of a calm sea: ν = 1.42 GHz, θ_a = 55 deg, vertical polarization.

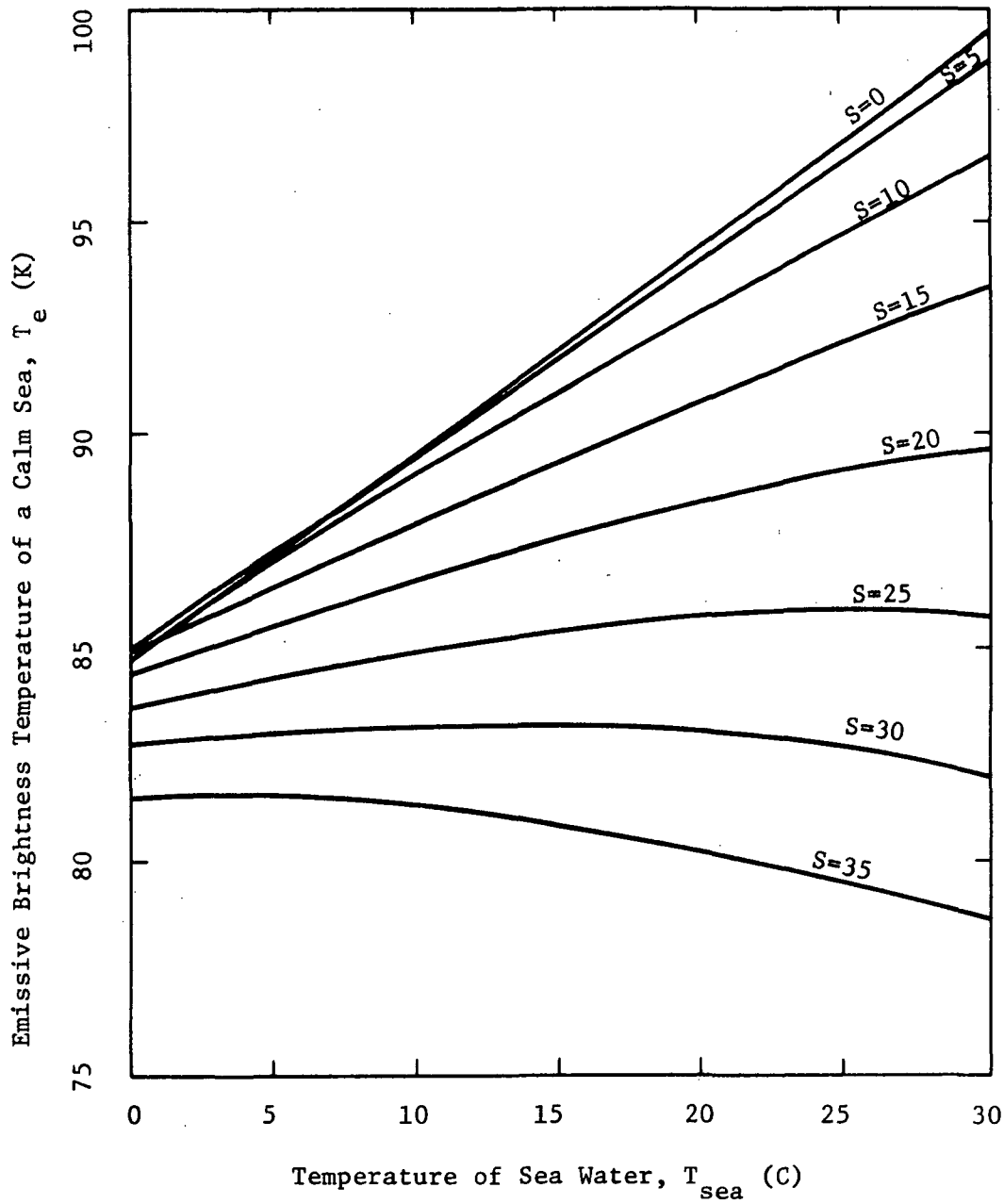

Fig. 12. Microwave emission of a calm sea: ν = 1.42 GHz, θ_a = 30 deg, horizontal polarization.

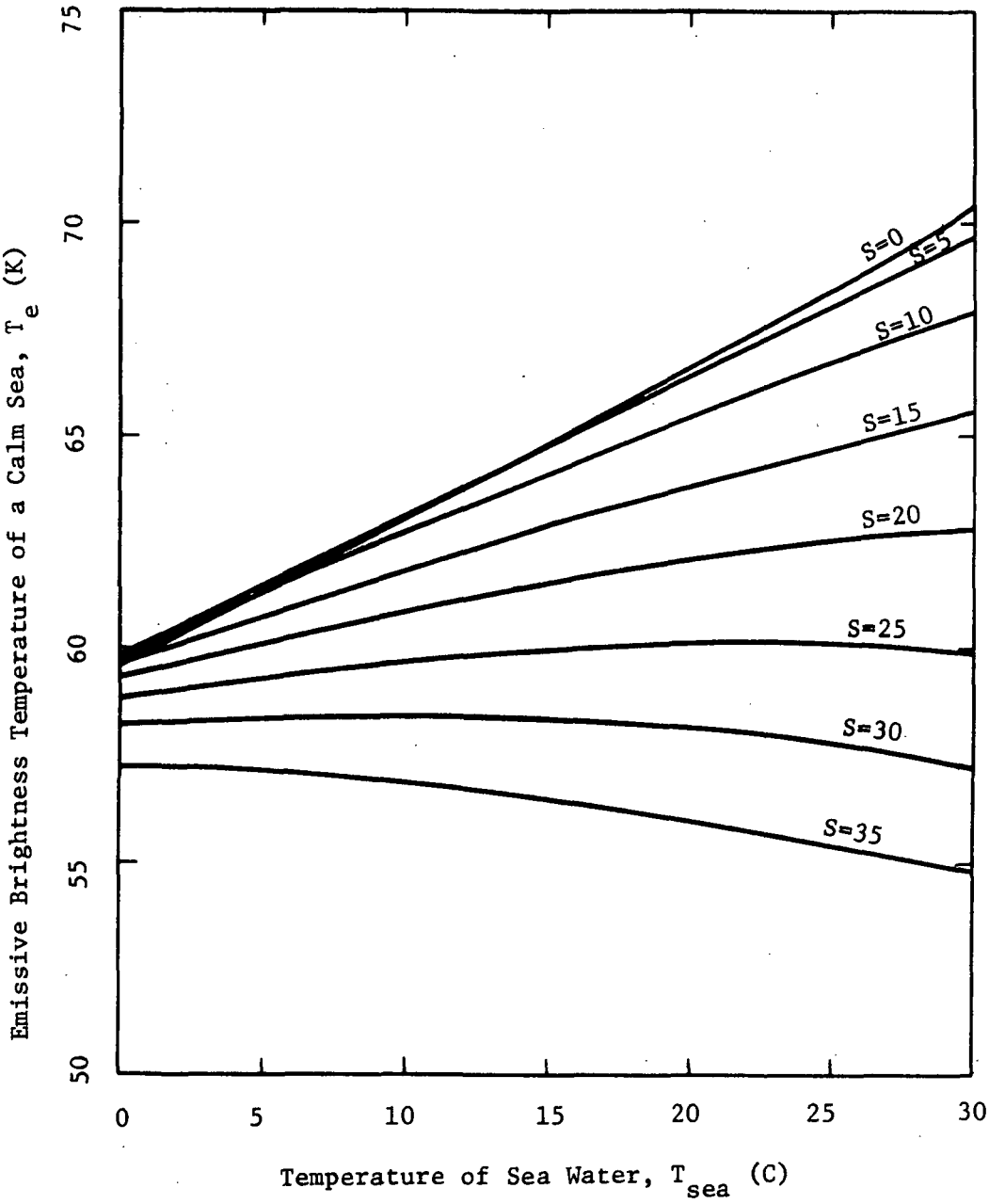

Fig. 13. Microwave emission of a calm sea: ν = 1.42 GHz, θ_a = 55 deg, horizontal polarization.

a function of salinity as shown in Fig. 9. The effects of salinity on the microwave emission of sea water were first discussed by Sirounian (1968). He considered the emission at 3 GHz and found that the effect of salinity decreased with increasing zenith angle for both vertical and horizontal polarization. The findings of this paper for vertical polarization are in disagreement with Sirounian.

The final chapters of this paper are concerned with the thermal emission of the atmosphere at microwave frequencies. It will be shown in the following chapters that the emission of the atmosphere is significant only for frequencies greater than about 2 GHz. Although there is some weak temperature dependence on the thermal emission of sea water for frequencies near 5.81 GHz, one may neglect variations in the background emission of microwave radiation due to differences in sea temperature and salinity for frequencies greater than 3 GHz. Sea foam and surface waves do have an effect at all microwave frequencies especially for high frequencies. This effect is discussed in the next section.

B. The Effects of Waves

The distribution of the slopes of the sea surface is a function of sea temperature, sea salinity, wind stress, fetch, and duration of wind stress. If the radius of curvature of a wave is many times greater than the wavelength of radiation under

consideration, then the surface may be treated as a smooth, specular surface for that particular wavelength of radiation (Beckman and Spizzichino, 1963). Such is the case for visible or infrared radiation being reflected from the sea surface. In the case of microwave radiation, however, the capillary waves and perhaps short gravity waves have radii of curvature less than microwave wavelengths.

The effect of wave roughness on the emission and scattering of microwave radiation by the sea surface has been studied by Fried (1966) and Stogryn (1967). They assumed that specular reflection is valid at any given point on the sea surface and that the effect of roughness arises from the distribution of sea slopes under various wind-stress conditions. In all cases, they used the distribution of sea slopes suggested by Cox and Munk (1954a, 1954b). Their studies may be summarized as follows: (1) the microwave emission of the sea is fairly independent of wind speed at all microwave frequencies for vertical polarization especially for a zenith angle of 55 deg; (2) the microwave emission of the sea increases with increasing wind speed for horizontal polarization and is greatest for zenith angles near 55 deg; and (3) the microwave emission of the sea is independent of wind speed for zenith angles near zero for both polarizations. Stogryn (1967) computed the combined emission and scattering of thermal microwaves from the sea and a standard atmosphere for wind speeds up to

14 m sec^{-1}, as shown in Fig. 14. The nature of the variations is similar for other frequencies. The increase in the microwave emission is approximately 10K for changes in wind speed for calm to 8 m sec^{-1} at 19.4 GHz and 35 GHz.

Measurements by Hollinger (1970) at 8.36 GHz and 19.34 GHz have shown that the theoretical predictions of Fried and Stogryn are correct except as follows: (1) the microwave emission of the sea increases slightly with increasing wind speed for zenith angles near zero; and (2) the response of the microwave emission of the sea to changes in wind speed decreases with decreasing microwave frequency.

If one wishes to minimize the effects of wave roughness, then it is clear that one should use vertical polarization. On the other hand, it is desirable that the background emission of the sea be as low as possible in order to sense atmospheric emissions. If one is willing to tolerate changes in the background emission of up to 15K due to wave roughness (wind speeds up to 14 m sec^{-1}), then one may choose horizontal polarization since the microwave emission of the sea is much less for horizontal polarization than for vertical polarization for large zenith angles. One final factor in the emission of the sea at microwave frequencies needs to be considered, viz., the effect of sea foam.

C. The Effects of Sea Foam

Williams (1969) found that sea foam has a very high emissivity

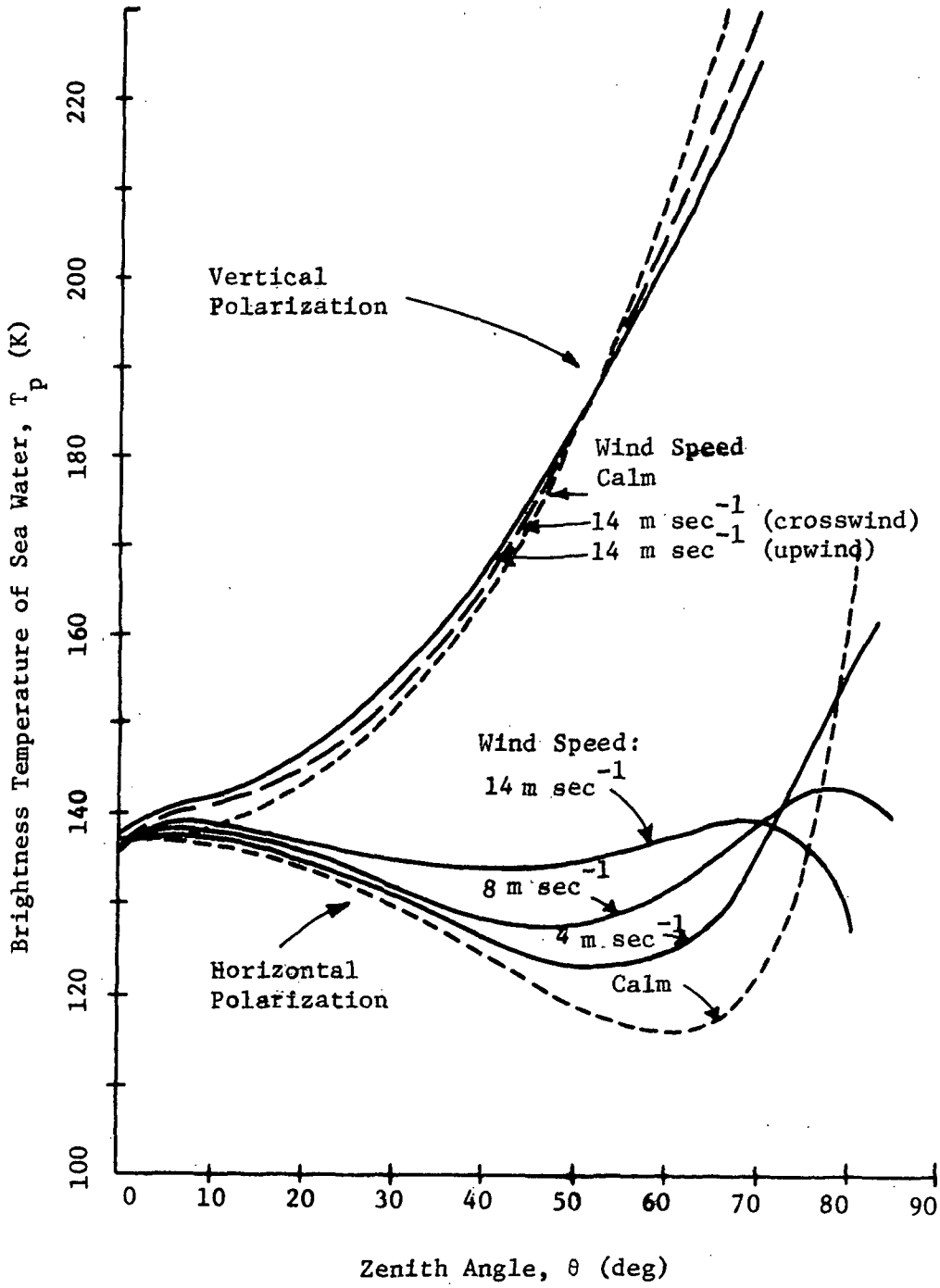

Fig. 14. Microwave emission of sea water as a function of surface roughness and zenith angle: ν = 19.35 GHz, horizontal and vertical polarization (after Stogryn, 1967).

for frequencies from 9.4 GHz to 34.0 GHz. Measurements by Hollinger (1970) from a tower at Argus Island, Bermuda, at 8.36 and 19.34 GHz indicated that the emissivity of sea foam was at least 0.6. Theoretical studies by Droppleman (1970) predicted that the emissivity of sea foam ranges from that of a specular sea surface (approximately 0.3) to near unity, which corresponds to a change in emissive brightness temperature of approximately 200K.

The percentage of cover of sea foam on the ocean's surface is a function of wind stress, fetch, duration, sea temperature, and sea salinity. An upper bound on the percentage cover of sea foam as a function of wind speed at 10 m above the sea surface has been given by Blanchard (1963). His data are shown in Table 17.

Table 17. Percentage cover of sea foam versus wind speed at 10 m above sea surface (after Blanchard, 1963).

Wind speed at 10 m ($m\ sec^{-1}$)	Percent sea-foam coverage (%)
0.0	0.0
3.0	0.0
4.0	0.6
6.0	1.8
9.0	3.7
12.5	7.2
20.0	18.5
50.0	100.0

The average wind speed over most of the World Ocean is less than 12 m sec^{-1} (Riehl, 1954, pp. 9 and 11). A change in wind speed from a calm condition to 12 m sec^{-1} could cause a change in the

microwave emission of sea water of about 15K. A change of 15K in the microwave emission of sea water due to an increase in the wind speed of 14 m sec^{-1} was observed by Nordberg et al. (1969) at 19.35 GHz over the Salton Sea.

It is clear from the above that the effects of wave roughness and sea foam on the microwave emission of the sea under various sea states may dominate those due to temperature or salinity. However, this effect is small as compared to meteorological effects for most of the World Ocean (as discussed in following chapters). At the present time, it is felt that the available body of knowledge concerning the effects of wave roughness and sea foam is inadequate to permit quantitative description. Too many environmental conditions such as atmospheric stability, duration of wind stress, fetch, wind speed, sea temperature, and sea salinity, have not been measured concurrently with airborne microwave measurements over an ocean test site. Suggestions for further research along these lines are offered in Chapter IX. Since the effects of sea roughness are dominant for some situations and are unpredictable at present, any further discussion will be left for future research. The remainder of this paper will be devoted to a description of the extinction and emissive properties of atmospheric gases and hydrometeors. The nature of the atmospheric emissions and extinctions are developed in such a manner as to allow easy computation of the combined effects of atmospheric and oceanic interactions, once the latter are described adequately.

CHAPTER V

ABSORPTION OF MICROWAVES BY ATMOSPHERIC GASES

Atmospheric gases do not scatter microwave radiation significantly. Since the emissive properties of a non-scattering medium are related directly to its absorption properties (see Eqs. 81 and 82, Chapter II, p. 45), one needs only to be concerned about the behavior of the volume absorption coefficient of atmospheric gases as a function of the variables of state. The primary absorbing and emitting gases in the atmosphere are molecular oxygen and water vapor (Van Vleck, 1947a, 1947b).

A. Absorption of Microwaves by Molecular Oxygen

Molecular oxygen possesses a permanent magnetic moment. As a result, there are 46 allowable transitions among its rotational energy states. The resonant frequencies for these transitions, ν_{N+} and ν_{N-} (N = 1, 3, 5, . . . , 45), as given by Meeks and Lilley (1963) are listed in Table 18. In addition, there is non-resonant absorption at zero frequency.

Interactions among atmospheric gases alter the allowable transitions between the rotational states of the oxygen molecules. As a result, a continuous spectrum of allowable transitions develops. This phenomenon is called pressure broadening and may be described by a pressure broadening structure factor, F.

Table 18. Resonant frequencies for the absorption of microwaves by molecular oxygen (after Meeks and Lilley, 1963).

N	ν_{N+} (GHz)	ν_{N-} (GHz)	N	ν_{N+} (GHz)	ν_{N-} (GHz)
1	56.2648	118.7505	25	65.7626	53.5960
3	58.4466	62.4863	27	66.2978	53.0695
5	59.5910	60.3061	29	66.8313	52.5458
7	60.4348	59.1642	31	67.3627	52.0259
9	61.1506	58.3239	33	67.8923	51.5091
11	61.8002	57.6125	35	68.4205	50.9949
13	62.4112	56.9682	37	68.9478	50.4830
15	62.9980	56.3634	39	69.4741	49.9730
17	63.5685	55.7839	41	70.0000	49.4648
19	64.1272	55.2214	43	70.5249	48.9582
21	64.6779	54.6728	45	71.0497	48.4530
23	65.2240	54.1294			

The accepted form for F is that given by Van Vleck and Weisskopf (1945). In the case of molecular oxygen, one needs two types of expressions for F, viz.,

$$F_o = \Delta_o/(\nu^2 + \Delta_o^2), \tag{107}$$

and

$$F_{N\pm} = \frac{\Delta_o}{(\nu_{N\pm} - \nu)^2 + \Delta_o^2} + \frac{\Delta_o}{(\nu_{N\pm} + \nu)^2 + \Delta_o^2}. \tag{108}$$

$\nu_{N\pm}$ (N = 1, 3, 5, $\cdots$, 45) are the resonant frequencies (Hz) for molecular oxygen listed in Table 18, ν is the frequency (Hz) of the radiation under consideration, and Δ_o is the line-width parameter (Hz) for molecular oxygen given by Meeks and Lilley as follows:

$$\Delta_o = 1.4625 \times 10^6 \; p \; (300/T)^{0.85} \; (0.21 + 0.78 \; f), \tag{109}$$

where p is the atmospheric pressure (mb), T is the atmospheric temperature (K), and f is a factor that expresses the relative effectiveness of nitrogen-oxygen collisions as compared to oxygen-oxygen collisions in producing pressure broadening. The value of f changes from 0.75 for very low pressures to 0.25 for high pressures. Meeks and Lilley (1963) give the following empirically-derived form for f:

$$f = \begin{cases} 0.25: & p \geq 356 \text{ mb} \\ 0.25 + 0.435\ (2.551 - \log_{10} p): & 25.3 < p < 356 \text{ mb} \\ 0.75: & p \leq 25.3 \text{ mb} \end{cases} \tag{110}$$

In meteorological units, the full expression for the volume absorption coefficient for molecular oxygen (m^{-1}) given by Meeks and Lilley (1963) is

$$\alpha_o = 4.6182 \times 10^{-13}\ (p\ \nu^2/T^3) \cdot \sum_{\substack{N=1 \\ \text{odd}}}^{45} S_N \exp[-2.06844\ N\ (N+1)/T], \tag{111}$$

where

$$S_N = F_o \frac{2\ (N^2 + N + 1)\ (2N + 1)}{N(N+1)} + F_{N+} \frac{N\ (2N + 3)}{N + 1} + F_{N-} \frac{(N+1)\ (2N - 1)}{N} . \tag{112}$$

Thus, one may predict the volume absorption coefficient for molecular oxygen for any given temperature, pressure, and frequency by using Eqs. (107) to (112) and the values of $\nu_{N\pm}$ listed in Table 18. Some investigators (e.g., LeFande, 1968, and Lenoir, 1968) give

values for $\nu_{N\pm}$ that differ in the third decimal place from those listed in Table 18. Others (Westwater, 1967; Falcone, 1966) assume a different dependence for α_o and Δ_o than that given in (111) and (109), respectively. Otherwise, there is unanimity on the question of which formulas adequately describe α_o as a function of pressure, temperature, and frequency.

It is difficult to grasp an understanding of the effects of variations in pressure, temperature, and frequency on the volume absorption coefficient of molecular oxygen from Eqs. (107) to (112), especially in the region of the resonance lines. For frequencies less than about 50 GHz, one may visualize the absorption of microwaves due to molecular oxygen as the result of two terms, one dealing with the non-resonant absorption for zero frequency and the other dealing with the combined effects of absorption for the pressure-broadened lines above 55 GHz. In general, absorption increases with increasing pressure and decreases with increasing temperature.

B. Absorption of Microwaves by Water Vapor

Water vapor possesses a single resonant transition in the microwave spectrum between the rotational-vibrational energy states of 5_{-1} and 6_{-5}. The resonant frequency for this transition is 22.235 GHz. The next highest resonant frequency is 183.3 GHz. As in the case of molecular oxygen, there is a pressure-broadening effect for water vapor. As a result, a portion of the microwave

absorption by water vapor is due to pressure-broadened absorption lines in the far infrared part of the electromagnetic spectrum. There appears to be a failure in the theory for the contribution of pressure-broadened infrared-lines to the total absorption of microwaves by water vapor as given by Van Vleck (1947b). These predictions are brought into agreement with the measured values of absorption (Becker and Autler, 1946) when a factor of five is included in the infrared portion. With this correction, the volume absorption coefficient for water vapor (m^{-1}), given by Porter and Florance (1969), is

$$\alpha_w = 3.615 \times 10^{-10} \rho_w (\nu^2/T^{1.5}) [(F/T) \exp(-642/T) + 7.07 \times 10^{-24} \Delta_w], \quad (113)$$

where

$$F = \frac{\Delta_w}{(\nu_w - \nu)^2 + \Delta_w^2} + \frac{\Delta_w}{(\nu_w + \nu)^2 + \nu_w^2} \quad (114)$$

and

$$\Delta_w = 2.62 \times 10^9 (p/1013.25) (318/T)^{0.625} [1 + 0.0147 \rho_w T/p], \quad (115)$$

in which α_w is 22.235×10^9 Hz, ρ_w is the density of water vapor (g m^{-3}), ν is the frequency (Hz), T is the atmospheric temperature (K), and p is the atmospheric pressure (mb).

The equation of state for water vapor is given by

$$e = \rho_w R_g T/m_w, \quad (116)$$

where e is the vapor pressure (dynes cm^{-2}), ρ_w is the density of water vapor (g cm^{-3}), R_g is the Universal Gas Constant (8.3144 x

10^7 ergs mol^{-1} K^{-1}), T is the temperature (K), and m_w is the molecular weight of water vapor (18.016 g mol^{-1}). Using these values and the usual meteorological units (1 mb = 10^3 dynes cm^{-2}; 1 g m^{-3} = 10^6 g cm^{-3}), one obtains from (116) the following expression for ρ_w, the density of water vapor (g m^{-3}), viz.,

$$\rho_w = 216.68\ e/T, \tag{117}$$

where e now is the vapor pressure in mb. For the range of dew-point temperatures, T_d (K), from 233K to 313K, the vapor pressure (mb) may be obtained with considerable accuracy from Teten's Equation, which is

$$e = 6.11 \times 10^{[7.5\ (T_d - 273.15)/(T_d - 35.85)]}\ . \tag{118}$$

Thus, one may predict the volume absorption coefficient for water vapor, α_w (m^{-1}), for any given frequency (Hz), atmospheric pressure (mb), atmospheric temperature (K), and dew-point temperature (K), by using (113), (114), (115), (117), and (118).

The behavior of the absorption of microwaves by water vapor is similar to that of molecular oxygen outside the region of resonance. It should be noted, however, that unlike molecular oxygen, the absorption increases with decreasing pressure for frequencies near resonance (22.235 GHz).

C. Combined Absorption by Molecular Oxygen and Water Vapor

Since extinction processes are linear, the combined absorption of microwaves by molecular oxygen and water vapor is simply the

sum of α_o and α_w, that is,

$$\alpha_g = \alpha_o + \alpha_w, \tag{119}$$

where α_g is the volume absorption coefficient of atmospheric gases (m^{-1}). The effects of pressure and electromagnetic frequency are shown in Fig. 15. These curves were formed from calculations of α_o and α_w made from the foregoing equations for a temperature of 10C, a dew-point temperature of 10C, pressures of 100 and 1013.25 mb, and for frequencies ranging from 1 GHz to 58 GHz. The effects of pressure-broadening and the factor, 1/p, in the last term of (115) are apparent. It should be noted that a dew-point temperature of 10C at 100 mb is much higher than would be found in the atmosphere. Nevertheless, the effect of pressure on the absorption of microwaves by water vapor at 22.235 GHz is significant. Croom (1966) has suggested that this property could be used to detect and measure stratospheric water vapor. This matter, however, will not be pursued further in this paper.

Extensive calculations show that frequencies for which α_w and α_o are equal fall between 2 and 18 GHz and between 38 and 55 GHz for a pressure of 100 mb, for temperatures between -10C and 30C, and for dew-point temperatures between -40C and 30C. For 1013.25 mb, these frequencies fall between 6 and 21 GHz and between 24 and 53 GHz for the same range of temperatures and dew-point temperatures. The frequency at which α_g is a minimum for frequencies greater than 22.235 GHz occurs between 28 and 32 GHz for all pressures

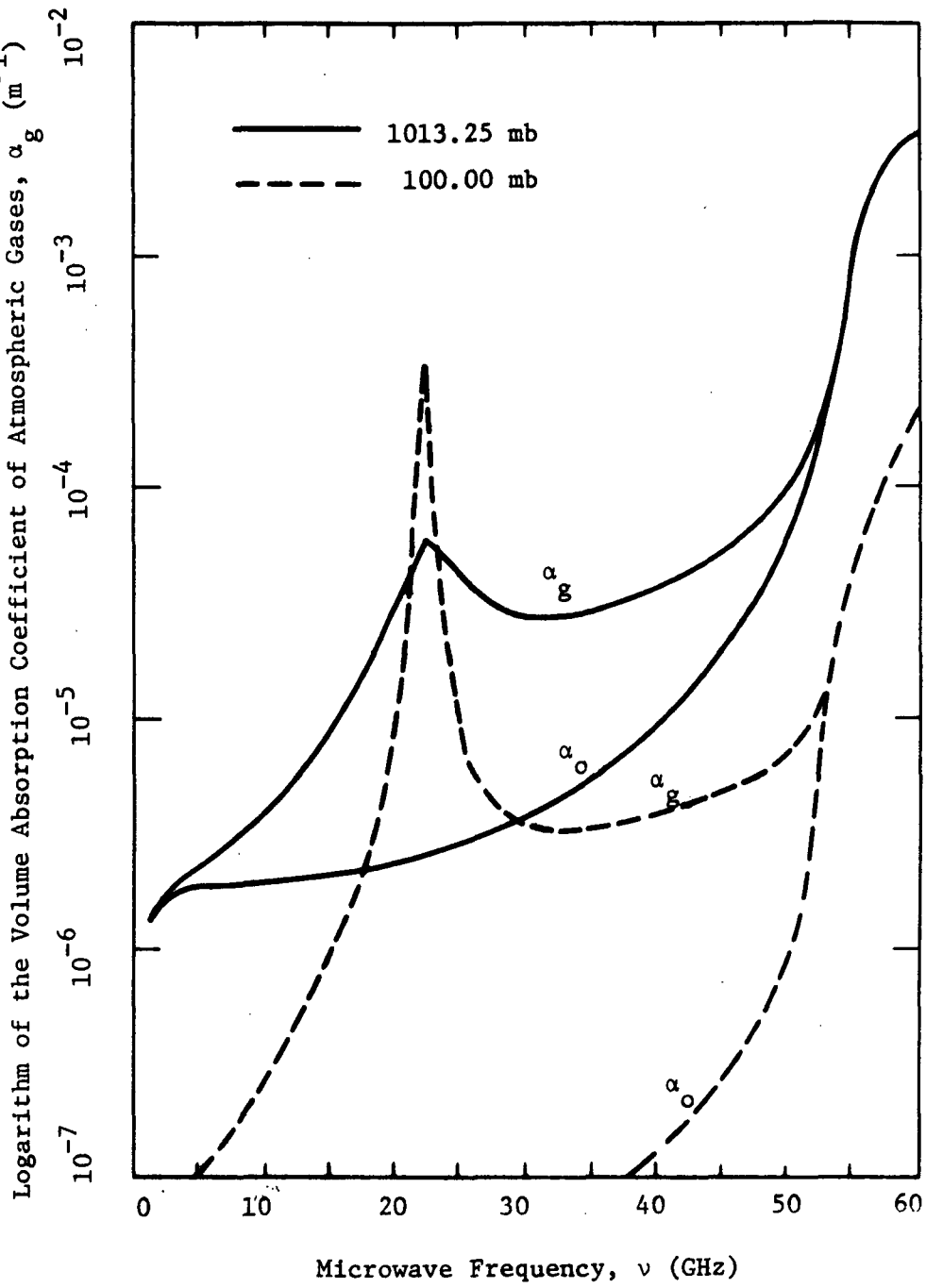

Fig. 15. Rate of absorption of microwaves by atmospheric gases: T = 10C, T_d = 10C, p = 100 mb and 1013.25 mb.

and temperatures considered.

It is important to note that the absorption of microwaves by water vapor is an important part of that by both water vapor and molecular oxygen for a large range of the microwave frequencies. The distribution of water vapor in the atmosphere is highly variable and is the object of much meteorological research. If one wishes to use the thermal emissive properties of the atmosphere at microwave frequencies to detect and measure the distribution of water vapor, then one would be wise to select frequencies near 22.235 GHz. On the other hand, if one wishes to study surface phenomena or other atmospheric parameters, then one would require that the thermal emission be as unrelated as possible to water vapor and would choose frequencies well removed from 22.235 GHz. In the case of molecular oxygen, the distribution of oxygen is well known and variations in its absorption coefficient are a function only of the distribution of temperature with altitude. Although temperature is variable in the atmosphere, water vapor is much more variable than temperature. The effects of the variability of α_o and α_w on the microwave emission of the atmosphere are considered in depth in Chapter VIII.

CHAPTER VI

ABSORPTION AND SCATTERING OF MICROWAVES BY LIQUID HYDROMETEORS

In this paper, the word cloud refers to a collection of water drops of diameters less than 0.1 mm. The word rain refers to a collection of water drops with diameters up to 6 mm (Mason, 1957, p. 438). Rain drops larger than about 2.8 mm in diameter are flattened on their lower side when falling at terminal velocity in stagnant air (Foote, 1969; Magono, 1954). Drops less than about 2.8 mm in diameter tend to be spherical in shape. Blanchard (1950) noted that large drops in turbulent air resemble ellipsoids with oscillating axes. In that case, the mean shape of the large drops approximates that of a sphere. The temperature of a water drop is fairly homogeneous but not precisely so since heat transfer is constantly taking place between the drop and its environment. Also, the temperature of the drop is probably colder than that of the ambient air. Nevertheless, in this study it is assumed that liquid hydrometeors are homogeneous, spherical masses of pure, liquid water.

Drops of liquid water in clouds and rain absorb, scatter, and emit thermal radiation at microwave frequencies. The absorption and scattering properties of homogeneous spheres in air are given precisely by Mie (1908). If the distribution of drop

diameters of a polydispersive medium is known, then the Mie theory may be used to calculate the exact absorption and scattering properties for the collection of drops. In this case, superposition may be used since the drops are randomly distributed (no fixed distance exists between individual scattering points) and are separated by distances large compared to their respective diameters.

The Mie theory was used by Ryde (1946) to predict the attenuation of radar energy by liquid and solid hydrometeors. A similar effort by Stratton (1930) had failed because the dielectric constant of water was assumed to have no imaginary part. Ryde found that the Rayleigh approximation could be used to predict the absorption properties of cloud particles smaller than 0.1 mm in diameter. Goldstein (1951) expanded the applications of the Mie theory and developed a simple expression for the volume absorption coefficient of a cloud as a function of its content of liquid water. Also, he showed that the scattering processes in a cloud can be neglected when compared to the absorption properties of the cloud. The most extensive application of the Mie theory to the problem of predicting the attenuation of microwaves by hydrometeors was conducted by Gunn and East (1954).

In the above applications of the Mie theory, these investigators gave their results in the form of simple regression equations. More importantly, no distinction was made between absorption and scattering properties in these studies. Also, the studies were

made for frequencies reserved for active radar systems. In considerations of the radiative transfer of thermal microwaves through the atmosphere, one can not ignore the distinction between absorption and scattering properties. Also, in this paper, a wide range of microwave frequencies is under consideration; most of these frequencies are in bands reserved for passive sensing and have not been discussed in the past papers dealing with the interaction of radar waves and the atmosphere. Finally, it is no longer necessary to derive simple empirical properties of hydrometeors since electronic computers may easily handle complex mathematical formulas.

The remainder of this chapter is concerned with a presentation of results of the Mie theory, an explanation of the method used to compute the Mie parameters, a discussion of the distribution of drop sizes of rain elements, and an analysis of the absorption and scattering properties of clouds and rain for the frequencies of interest in this paper.

A. Absorption and Scattering Cross Sections of an Individual Drop

An individual cloud or rain element is assumed to be a homogeneous, dielectric sphere of pure water with a diameter, a (m). Suppose that W_i is the power density ($W\ m^{-2}$) of radiation incident upon the drop. The rate of extinction of this radiation by absorption, P_a (W), or by scattering, P_s (W), may be given in terms of an absorption cross section, Q_a (m^2), or a scattering cross section,

Q_s (m^2), respectively; that is,

$$Q_a = P_a/W_i \tag{120}$$

and

$$Q_s = P_s/W_i. \tag{121}$$

It should be noted that P_s includes radiation that is scattered forward as well as radiation scattered into other directions about the drop. Thus, part of the scattered radiation may join the unextincted radiation. The extinction cross section, Q_t (m^2), is simply the sum of Q_a and Q_s.

In applying the Mie theory, it is convenient to define a drop-size parameter, x, as

$$x = \pi\ a\ \nu/c, \tag{122}$$

where a is the drop diameter (m), ν is the microwave frequency (Hz), and c is the speed of light in a vacuum (2.99793×10^8 m sec^{-1}). For frequencies less than 60 GHz and for drop diameters less than 6 mm, x is less than 3.77. In this case, an iterative scheme derived by Deirmendjian (1969) may be used to compute Q_a and Q_s from the Mie theory. The Deirmendjian method is presented below.

One may define a set of efficiency factors, K_a, K_s, and K_t, where

$$K_a = 4\ Q_a/\pi\ a^2, \tag{123}$$

$$K_s = 4\ Q_s/\pi\ a^2, \tag{124}$$

and

$$K_t = 4\ Q_t/\pi\ a^2. \tag{125}$$

From the Mie theory, Deirmendjian gives the following expressions for K_s and K_t:

$$K_s = (2/x^2) \sum_{n=1}^{\infty} (2n + 1) (|a_n|^2 + |b_n|^2) \tag{126}$$

and

$$K_t = (2/x^2) \sum_{n=1}^{\infty} (2n + 1) \, \mathrm{Re}\{a_n + b_n\}, \tag{127}$$

where a_n and b_n are the complex scattering amplitudes that are functions of the complex index of refraction, m, and the drop-size parameter, x. It was shown in Chapter III that the complex index of refraction for pure water is a function of the water temperature and the microwave frequency. Deirmendjian (op. cit.) gives the following iterative scheme to compute values of a_n and b_n for given values of m and x:

$$a_n = \frac{\left(\frac{A_n}{m} + \frac{m}{x}\right) \mathrm{Re}\{w_n\} - \mathrm{Re}\{w_{n-1}\}}{\left(\frac{A_n}{m} + \frac{m}{x}\right) w_n - w_{n-1}} \tag{128}$$

and

$$b_n = \frac{\left(m A_n + \frac{m}{x}\right) \mathrm{Re}\{w_n\} - \mathrm{Re}\{w_{n-1}\}}{\left(m A_n + \frac{m}{x}\right) w_n - w_{n-1}}, \tag{129}$$

where

$$A_n = -(n/m\,x) + 1/[(n/m\,x) - A_{n-1}], \tag{130}$$

$$A_o = \cot(m\,x), \tag{131}$$

$$w_n = [(2n - 1)/x] \, w_{n-1} - w_{n-2}, \tag{132}$$

$$w_o = \sin(x) + j \cos(x), \tag{133}$$

and

$$w_{-1} = \cos(x) - j \sin(x). \tag{134}$$

Deirmendjian (op. cit., p. 17) made a sign error in his equation that is equivalent to (133), in that he incorrectly used -j cos(x) (see Kreyszig, 1962, p. 184, prob. 12).

The efficiency factors for absorption and scattering were computed by using Eqs. (126) to (134) for the 27 microwave frequencies listed in Table 1, for drop temperatures of -10, 0, 10, 20, and 30C, and for drop diameters between 0 and 6 mm in 0.1-mm increments. The complex index of refraction of the water was computed by the method shown in Chapter III. The number of calculations (16,200) is too large to be presented in this paper in tabular form. Plots of K_a versus a and K_s versus a for temperatures of -10C (⏻), 0C (⏃), 10C (+), 20c (×), and 30C (⏀) were made by a Gerber plotter (Model 622 Automatic Graphing System) for each of the selected frequencies. Some of these plots are shown in Figs. 16 to 34. It should be noted (Eqs. 123 and 124) that if K_a or K_s is directly proportional to drop diameter, then Q_a or Q_s is directly proportional to the mass of liquid water (g) of the drop. It can be seen from the following figures that K_a is directly proportional to a for the lowest frequencies. This property is predicted by the Rayleigh Approximation which holds best when the ratio of the drop diameter to the wavelength of radiation is

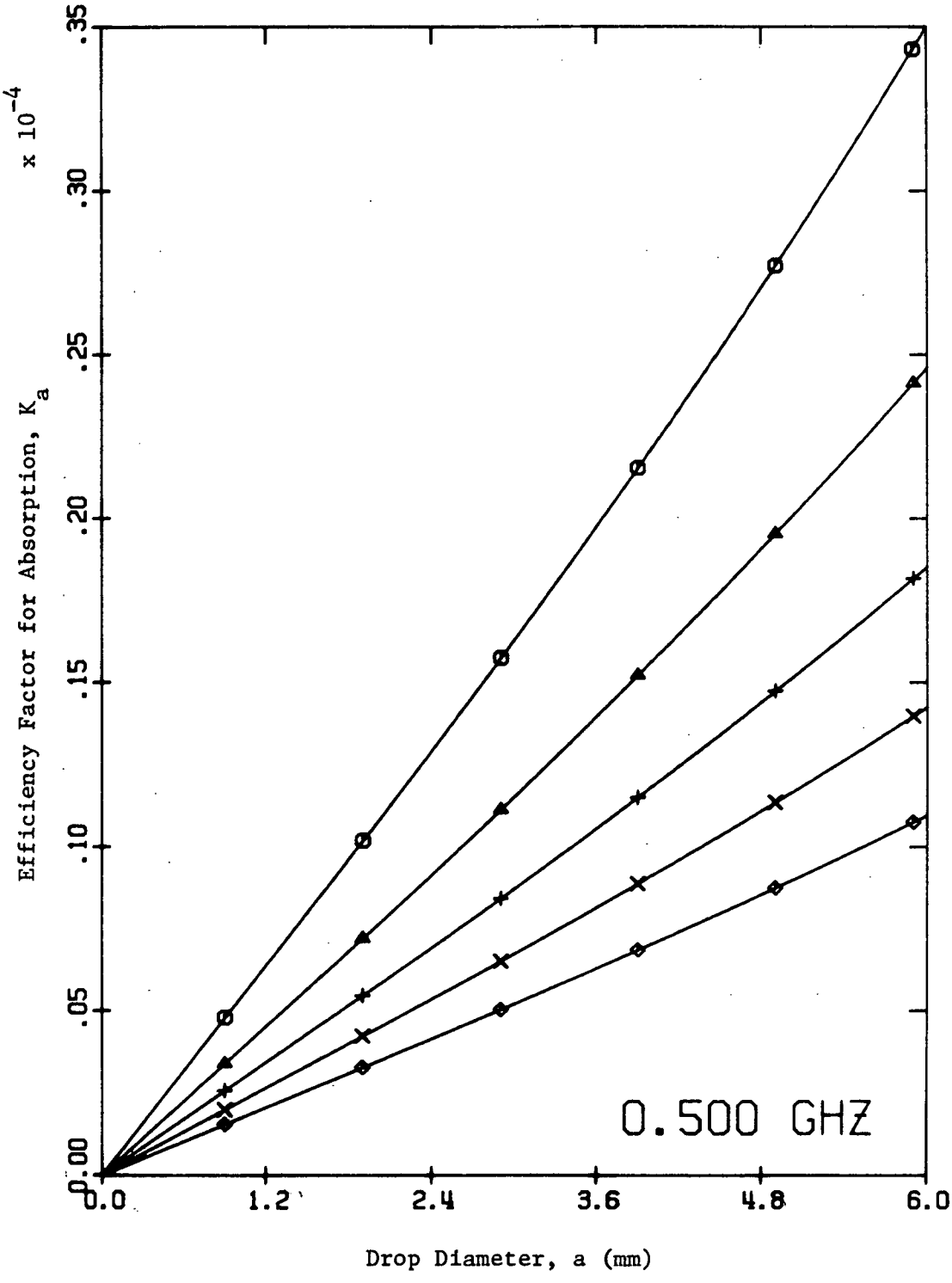

Fig. 16. Efficiency of absorption of microwaves by individual, liquid water drop: ν = 0.5 GHz.

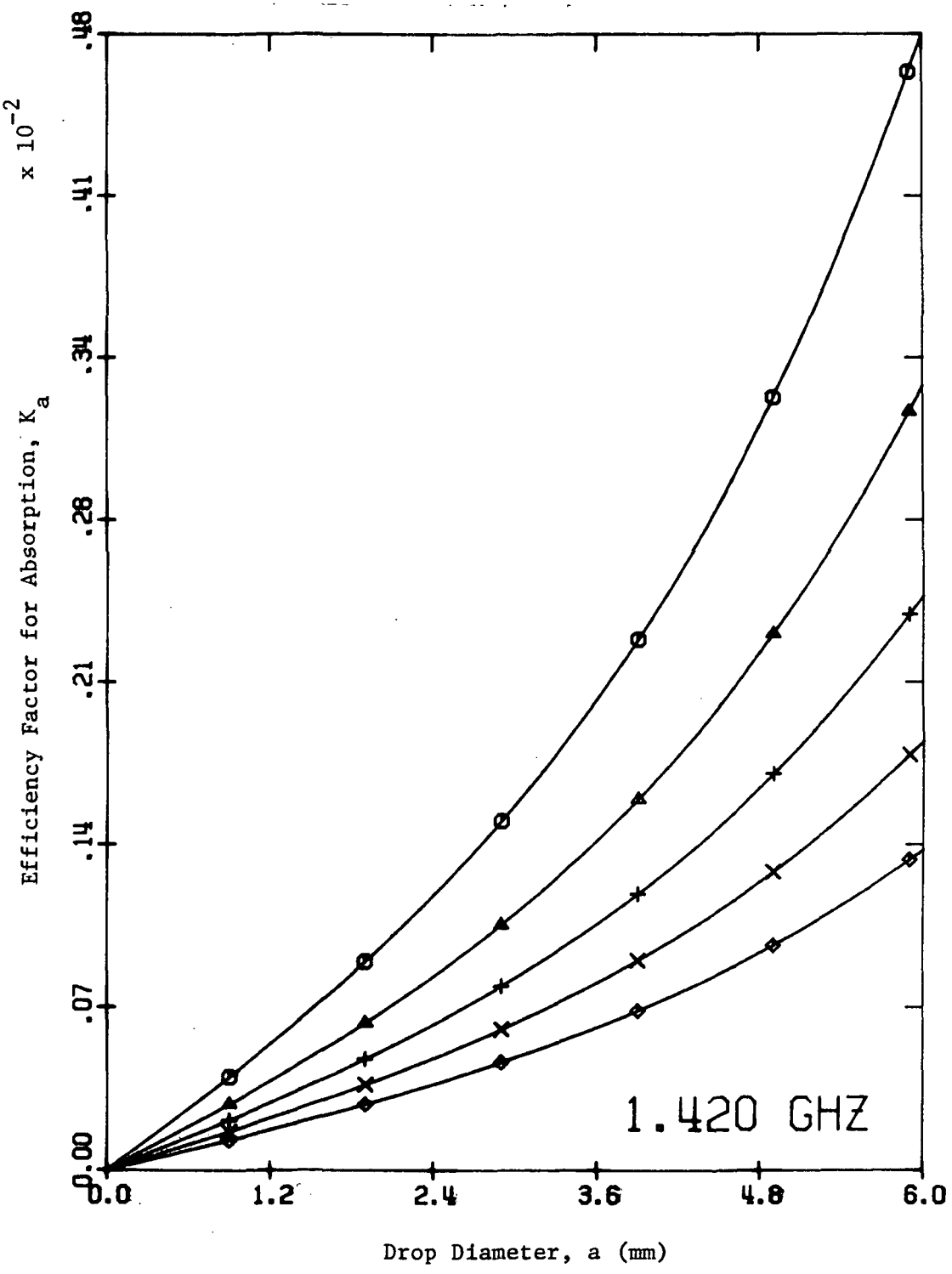

Fig. 17. Efficiency of absorption of microwaves by individual, liquid water drop: ν = 1.42 GHz.

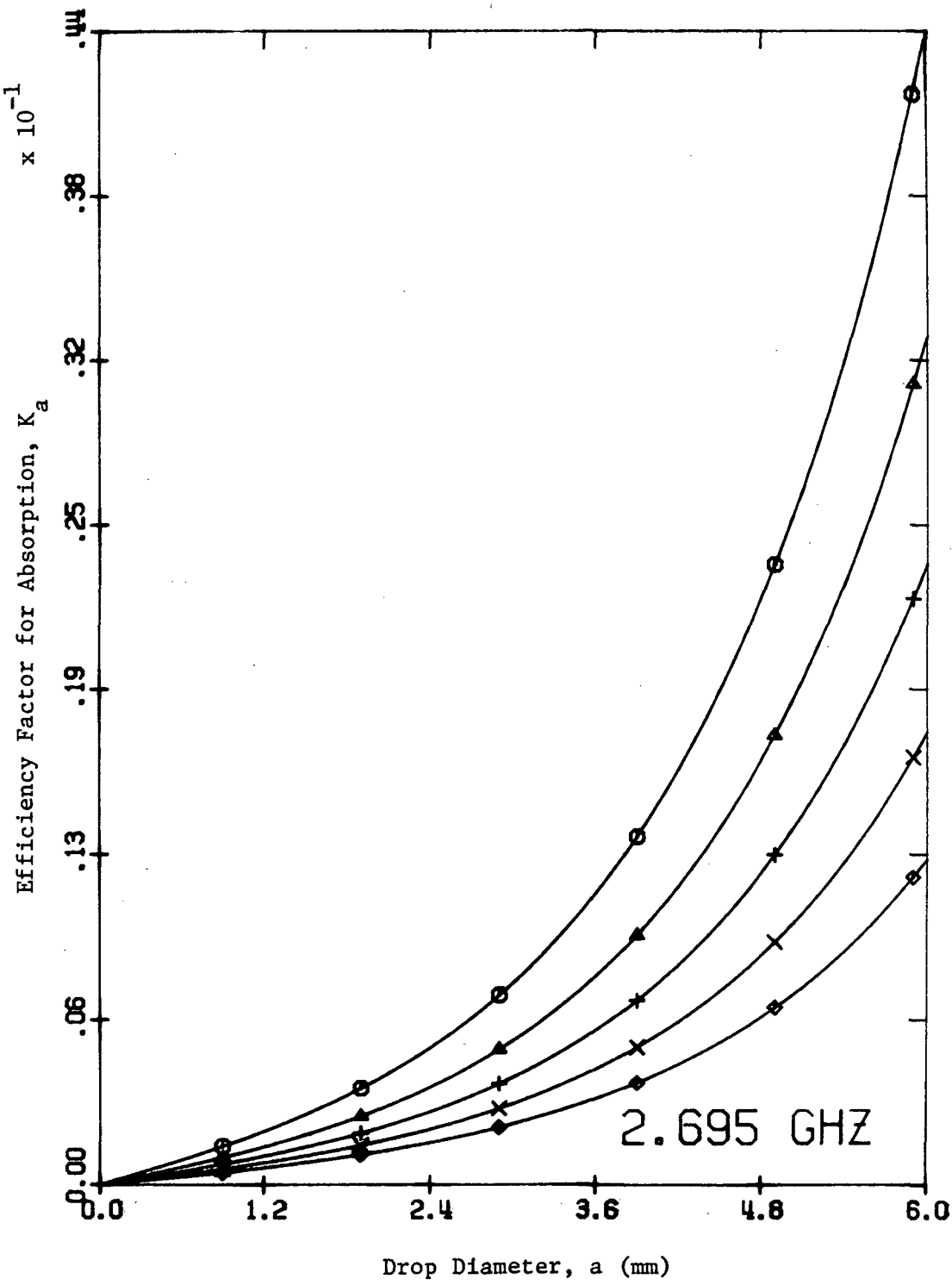

Fig. 18. Efficiency of absorption of microwaves by individual, liquid water drop: ν = 2.695 GHz.

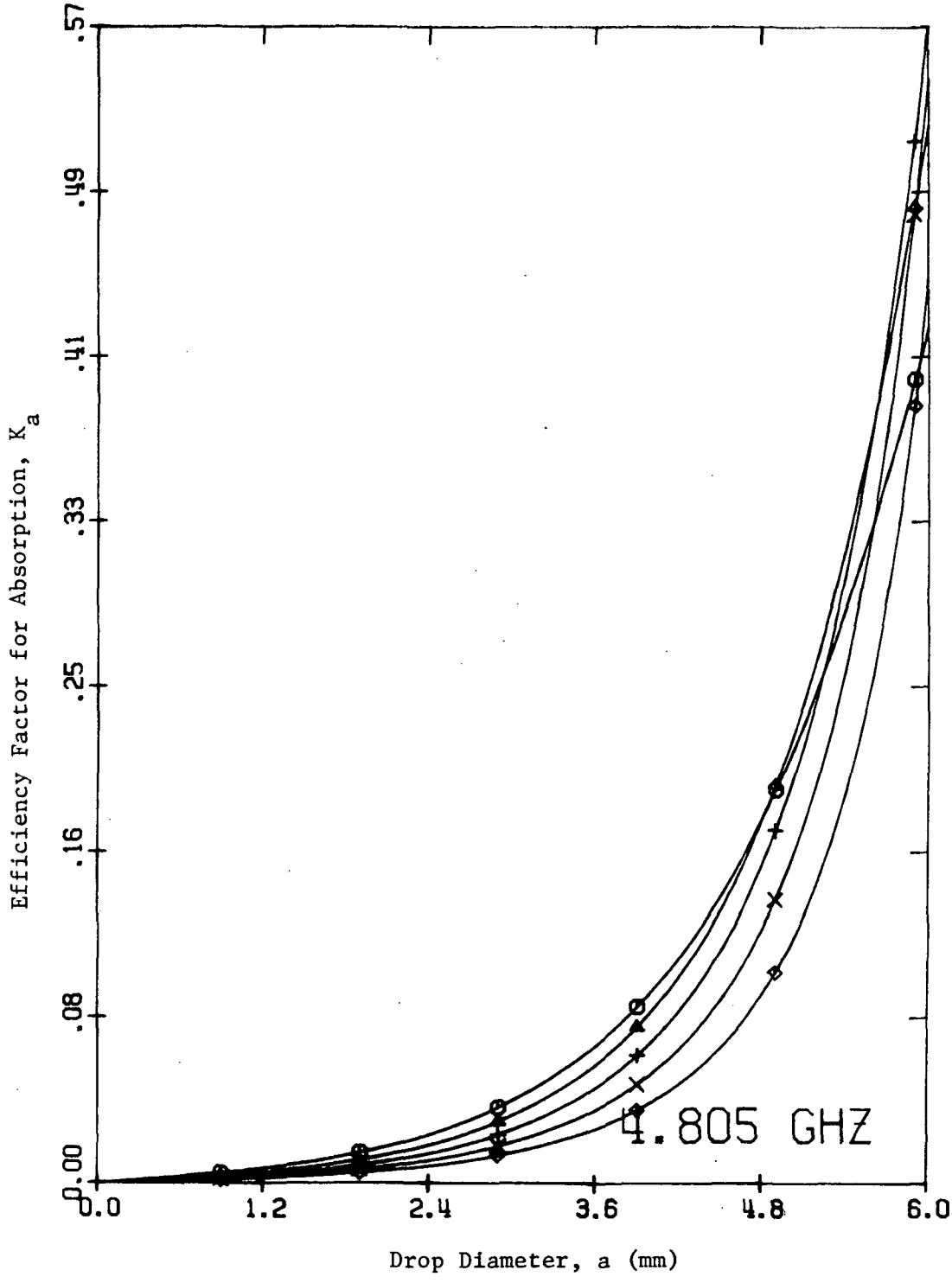

Fig. 19. Efficiency of absorption of microwaves by individual, liquid water drop: ν = 4.805 GHz.

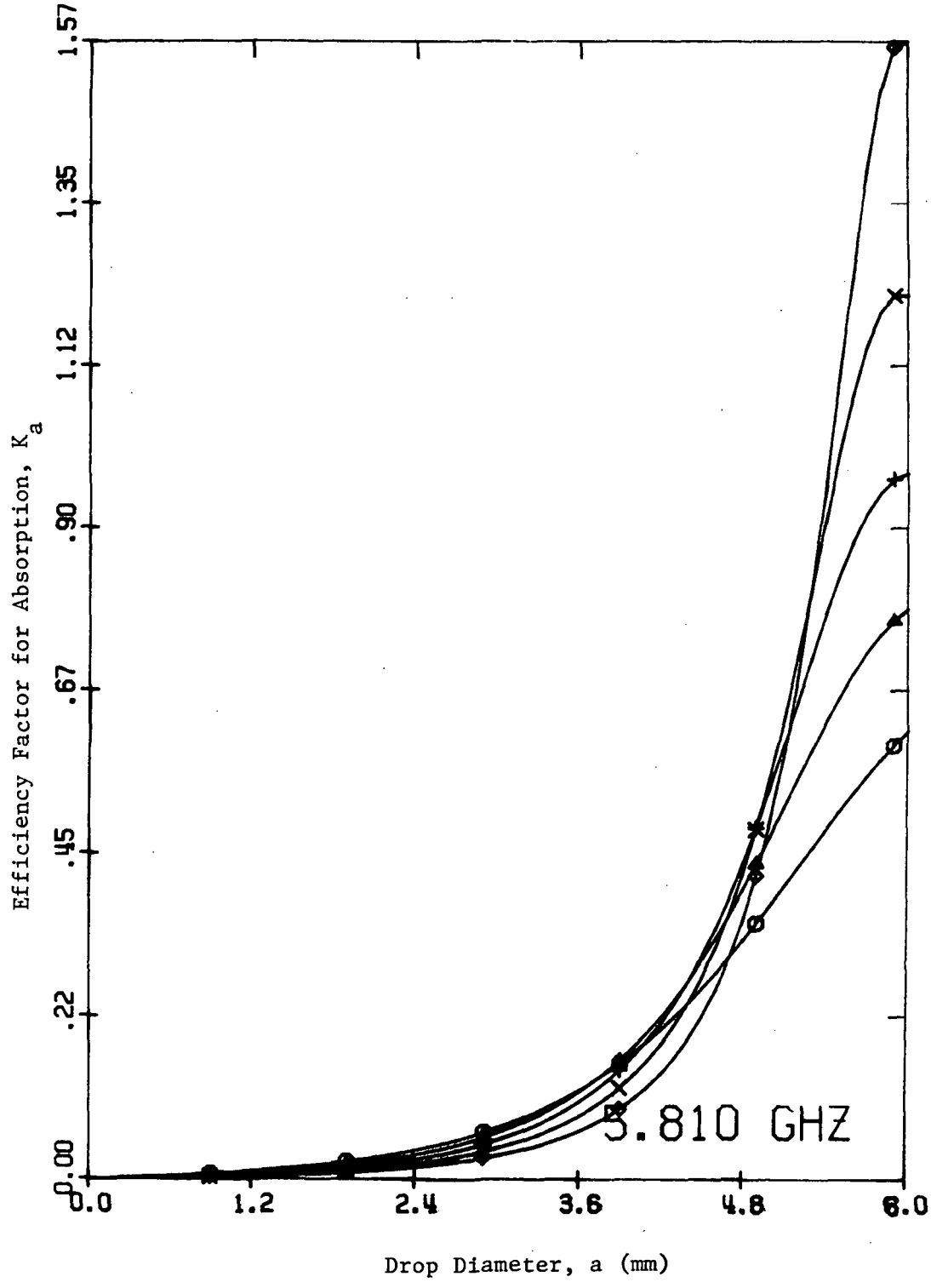

Fig. 20. Efficiency of absorption of microwaves by individual, liquid water drop: ν = 5.81 GHz.

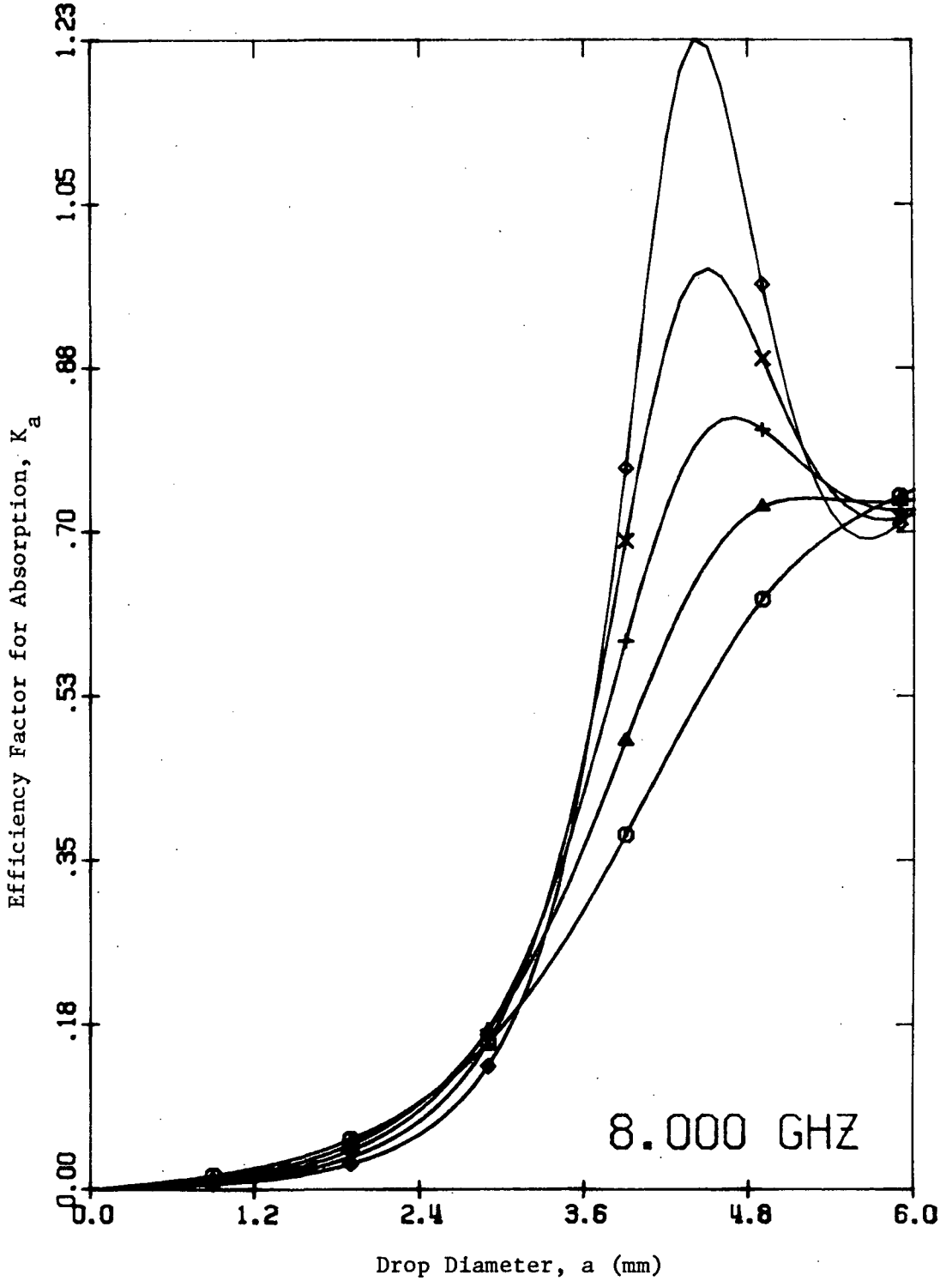

Fig. 21. Efficiency of absorption of microwaves by individual, liquid water drop: ν = 8.0 GHz.

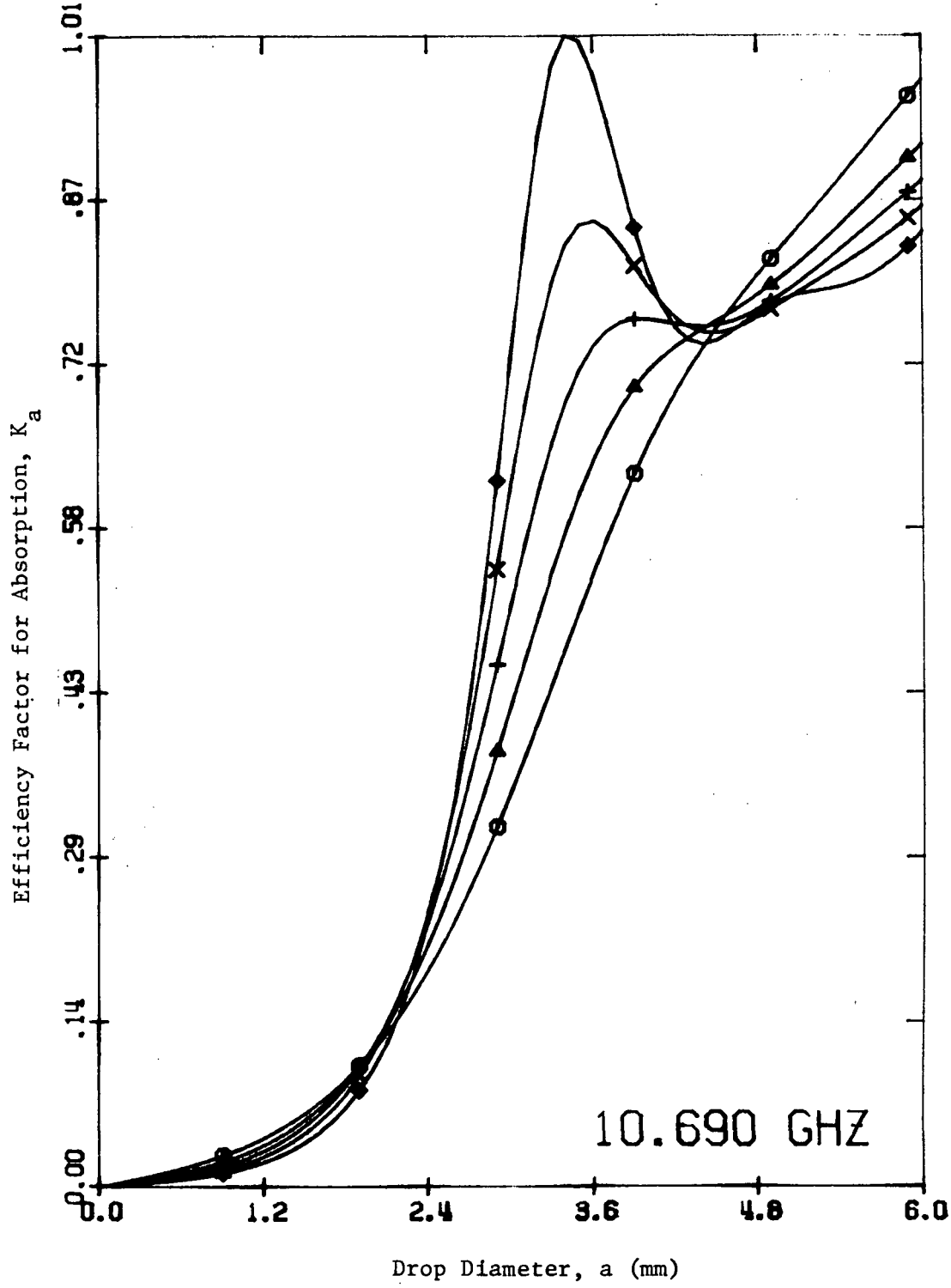

Fig. 22. Efficiency of absorption of microwaves by individual, liquid water drop: ν = 10.69 GHz.

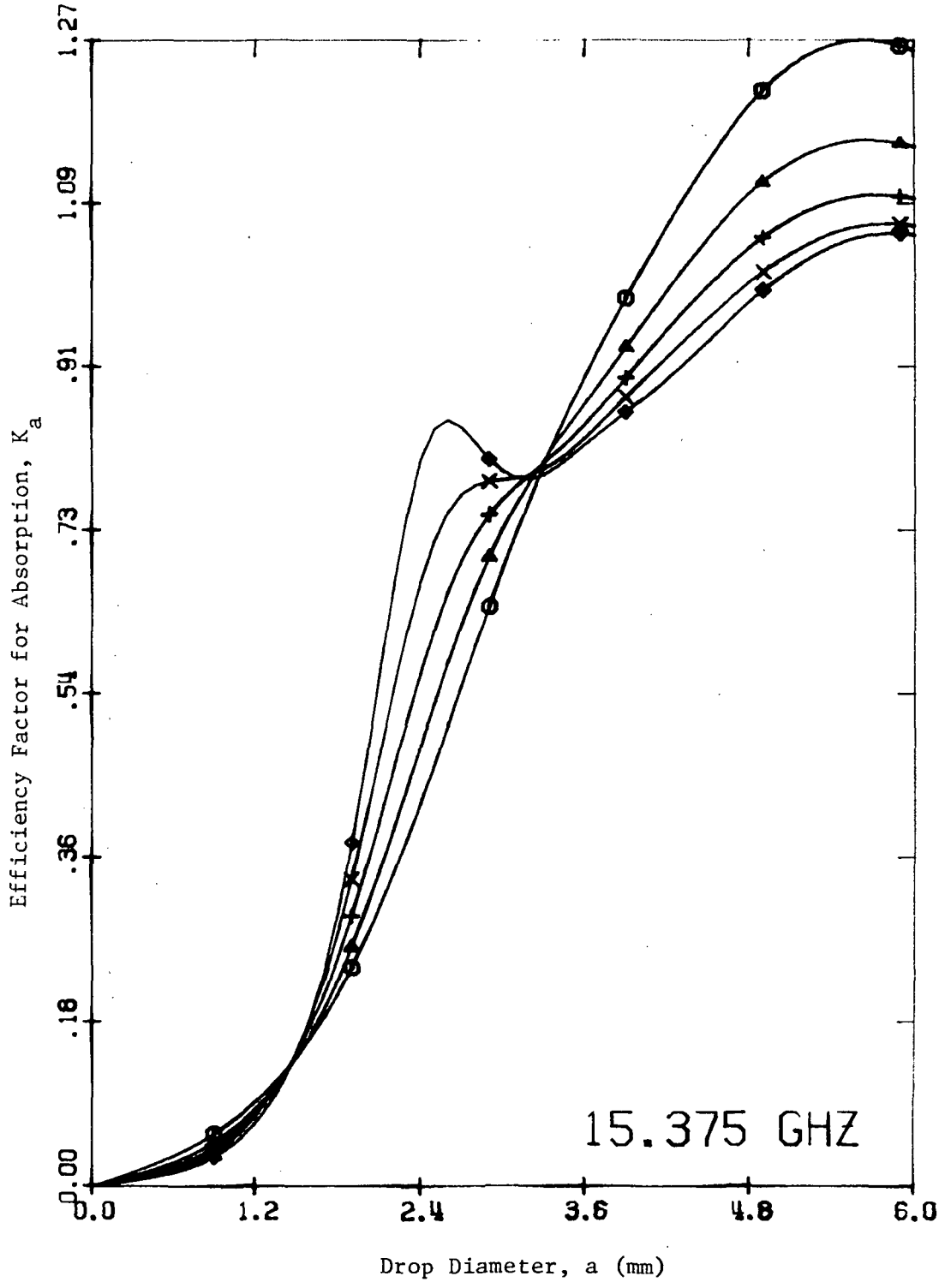

Fig. 23. Efficiency of absorption of microwaves by individual, liquid water drop: ν = 15.375 GHz.

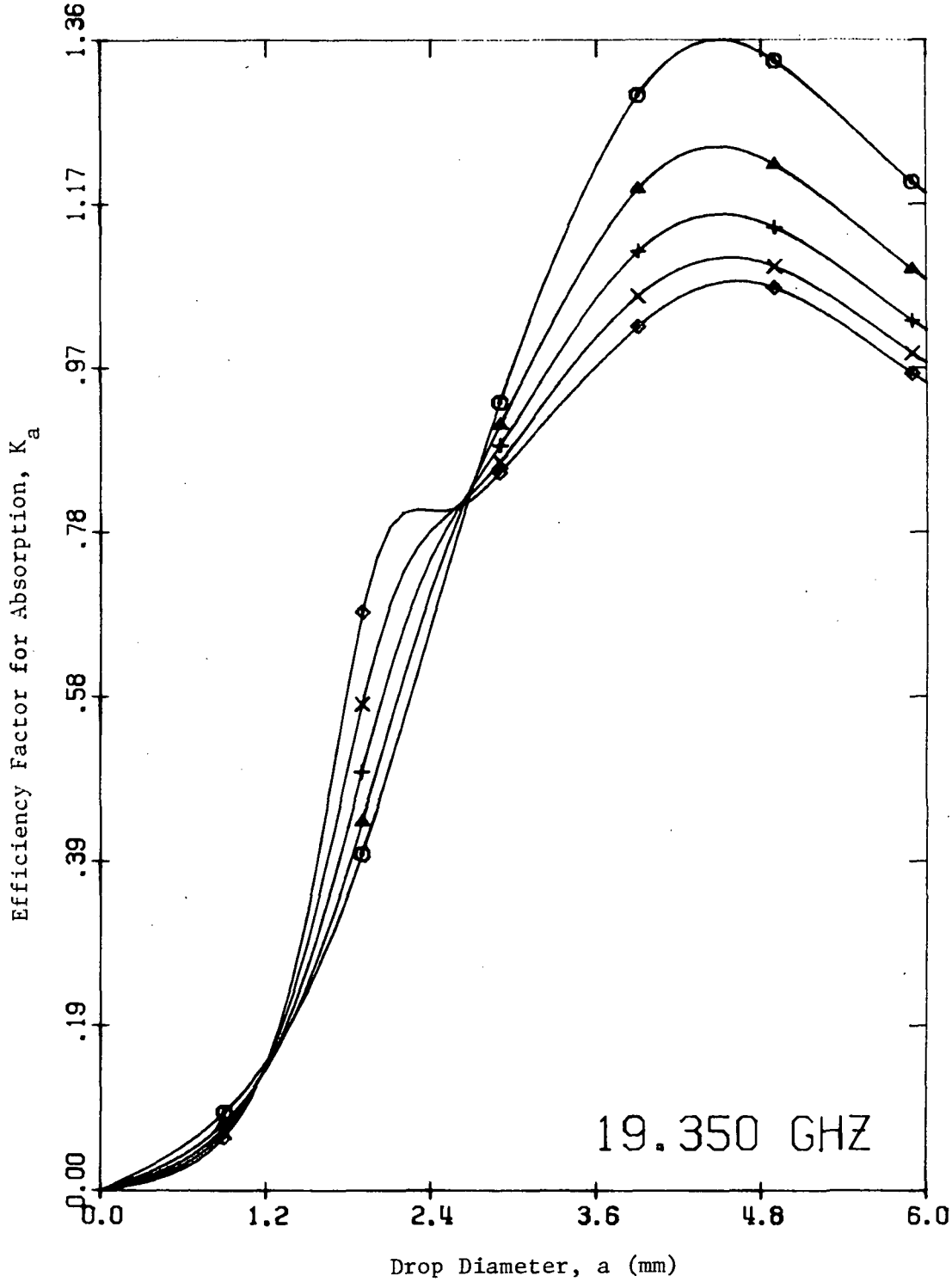

Fig. 24. Efficiency of absorption of microwaves by individual, liquid water drop: ν = 19.35 GHz.

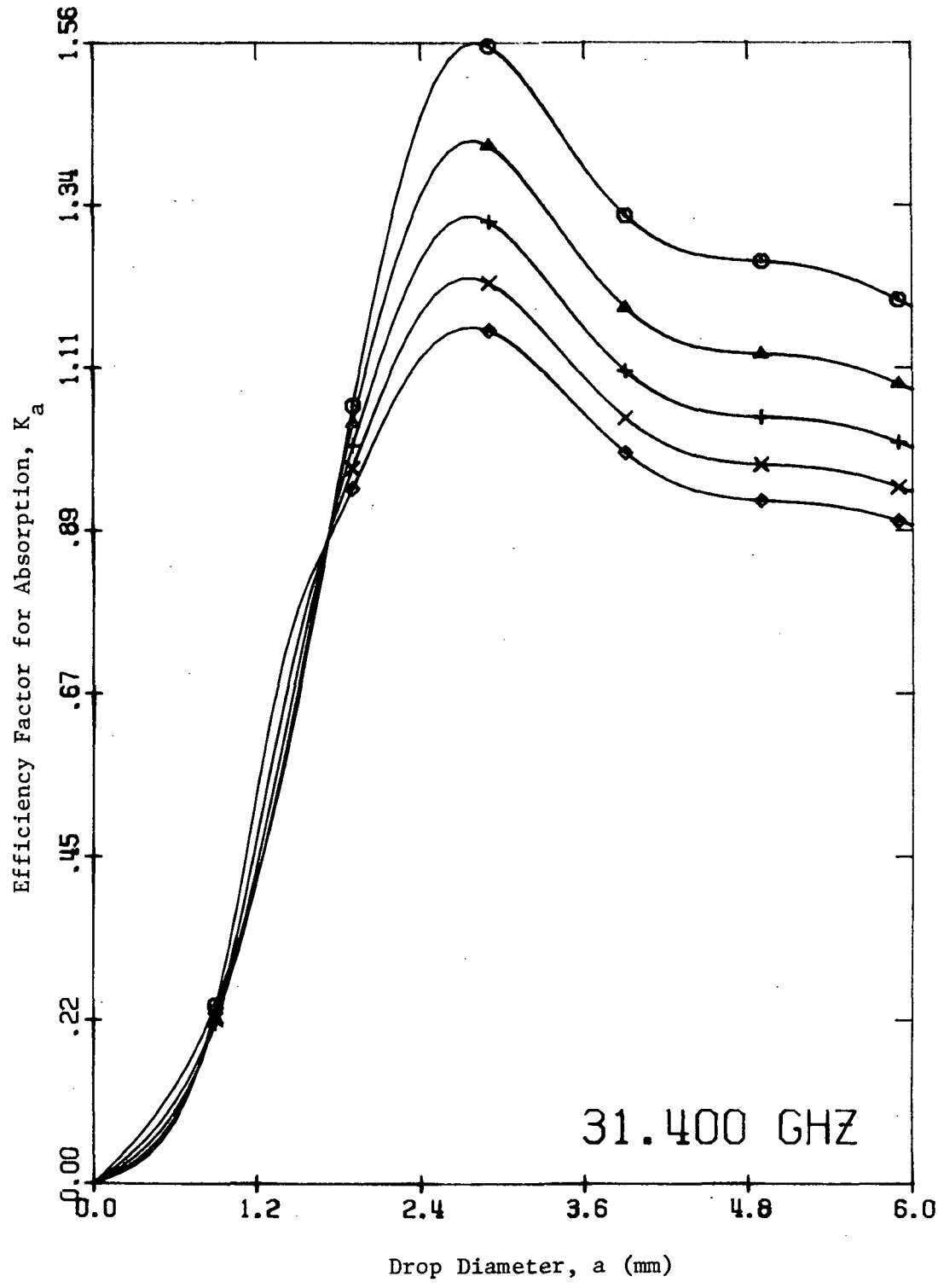

Fig. 25. Efficiency of absorption of microwaves by individual, liquid water drop: ν = 31.4 GHz.

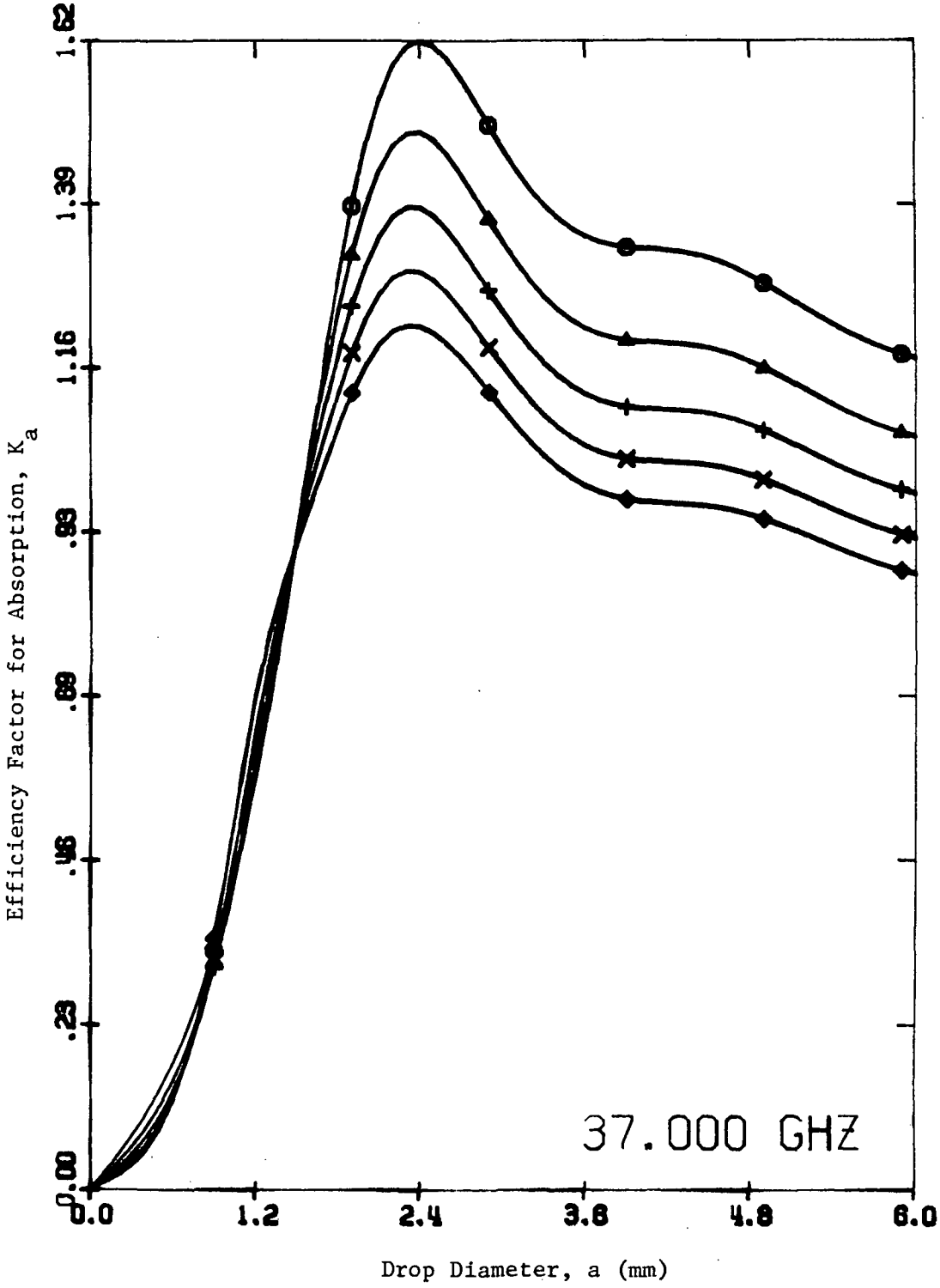

Fig. 26. Efficiency of absorption of microwaves by individual, liquid water drop: ν = 37.0 GHz.

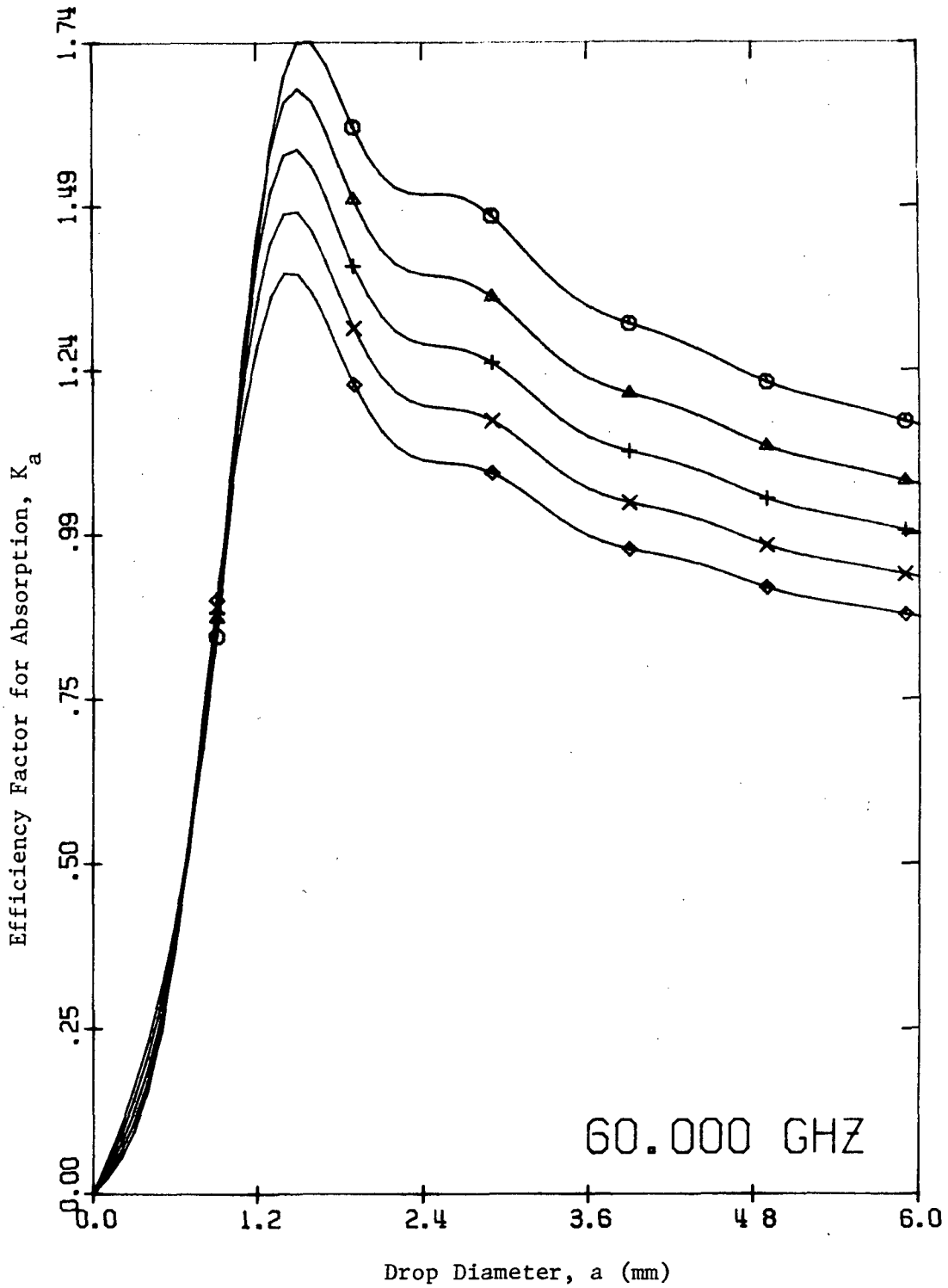

Fig. 27. Efficiency of absorption of microwaves by individual, liquid water drop: ν = 60.0 GHz.

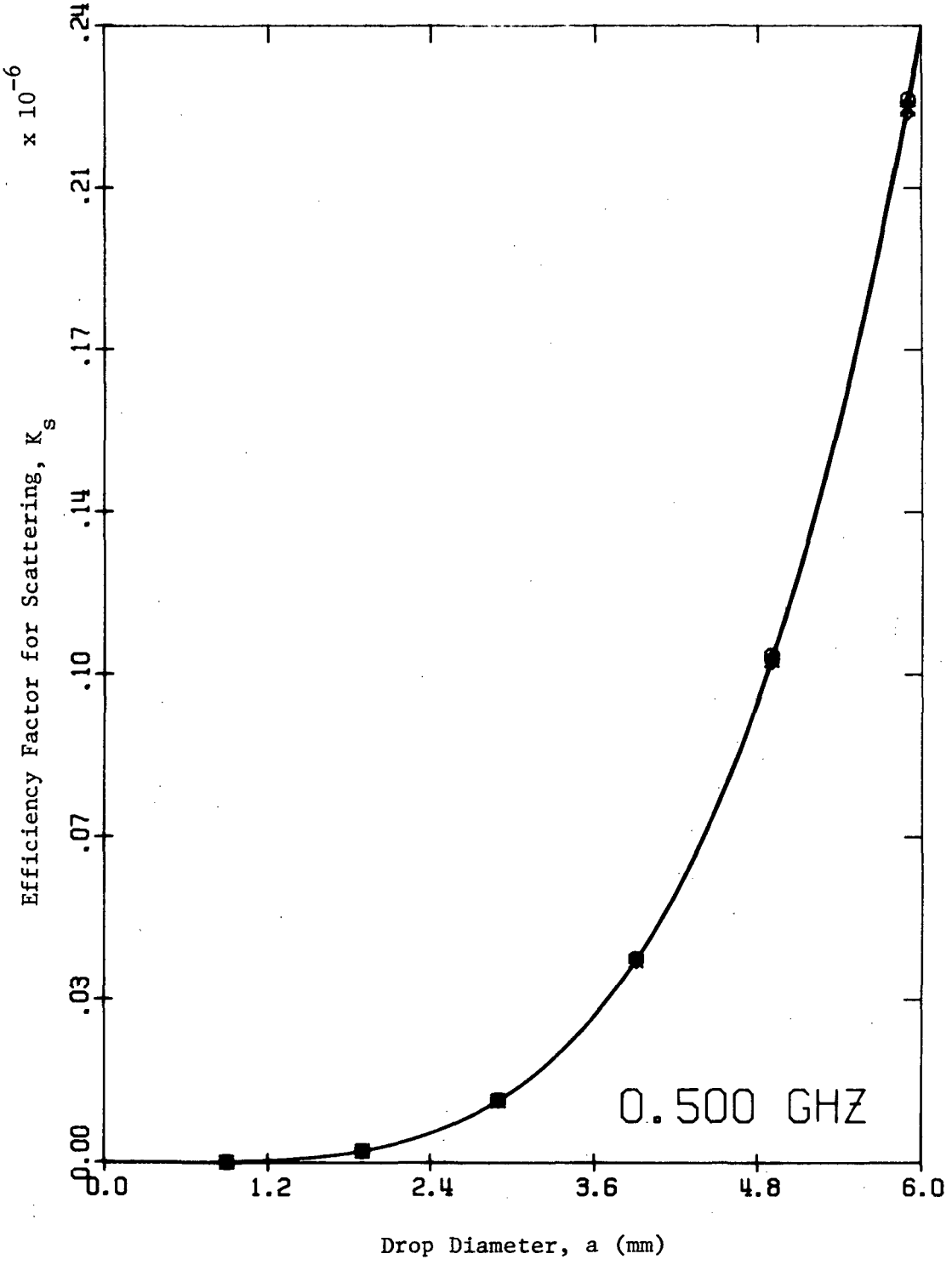

Fig. 28. Efficiency of scattering by an individual, liquid water drop: ν = 0.5 GHz.

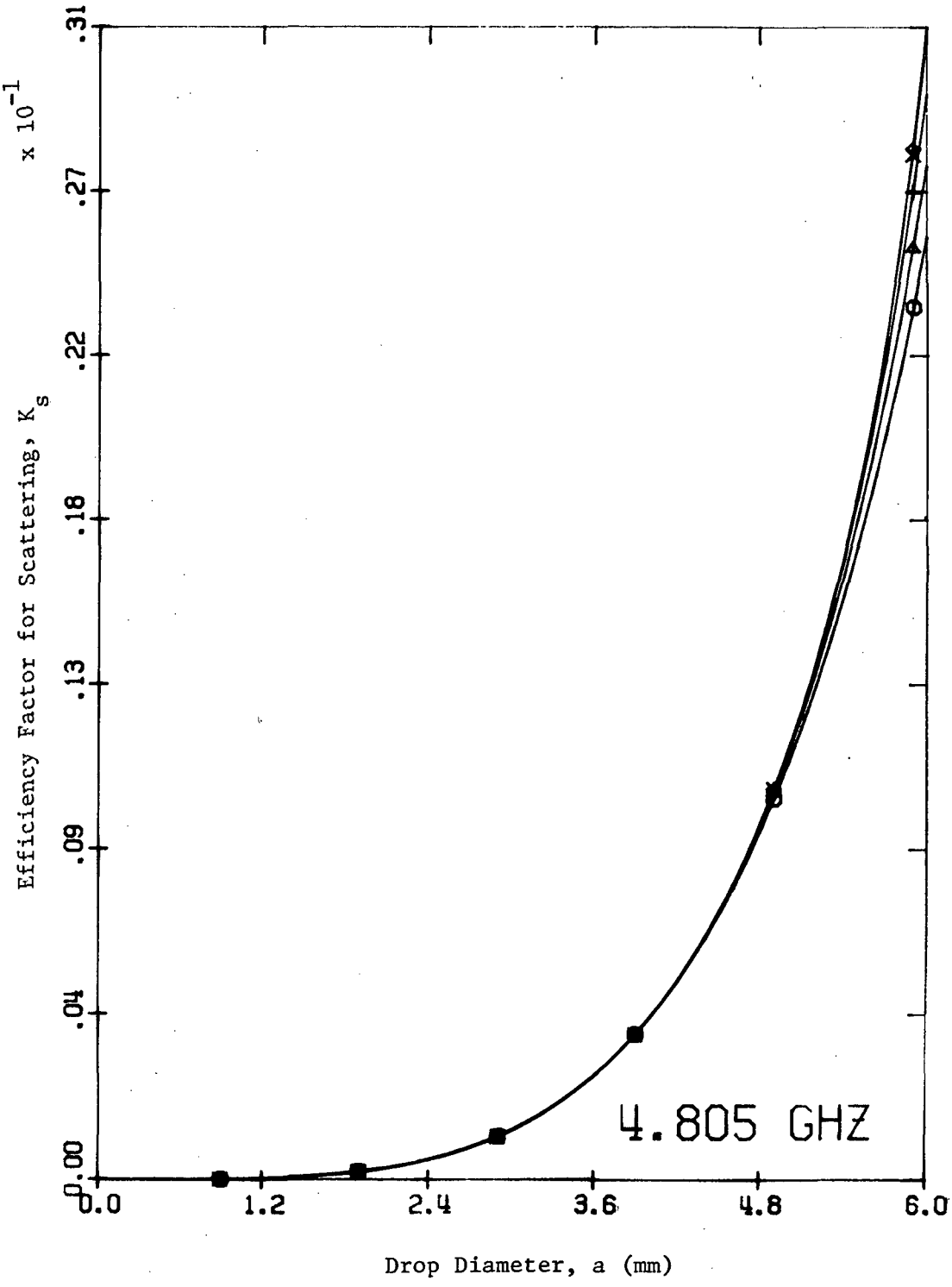

Fig. 29. Efficiency of scattering by an individual, liquid water drop: ν = 4.805 GHz.

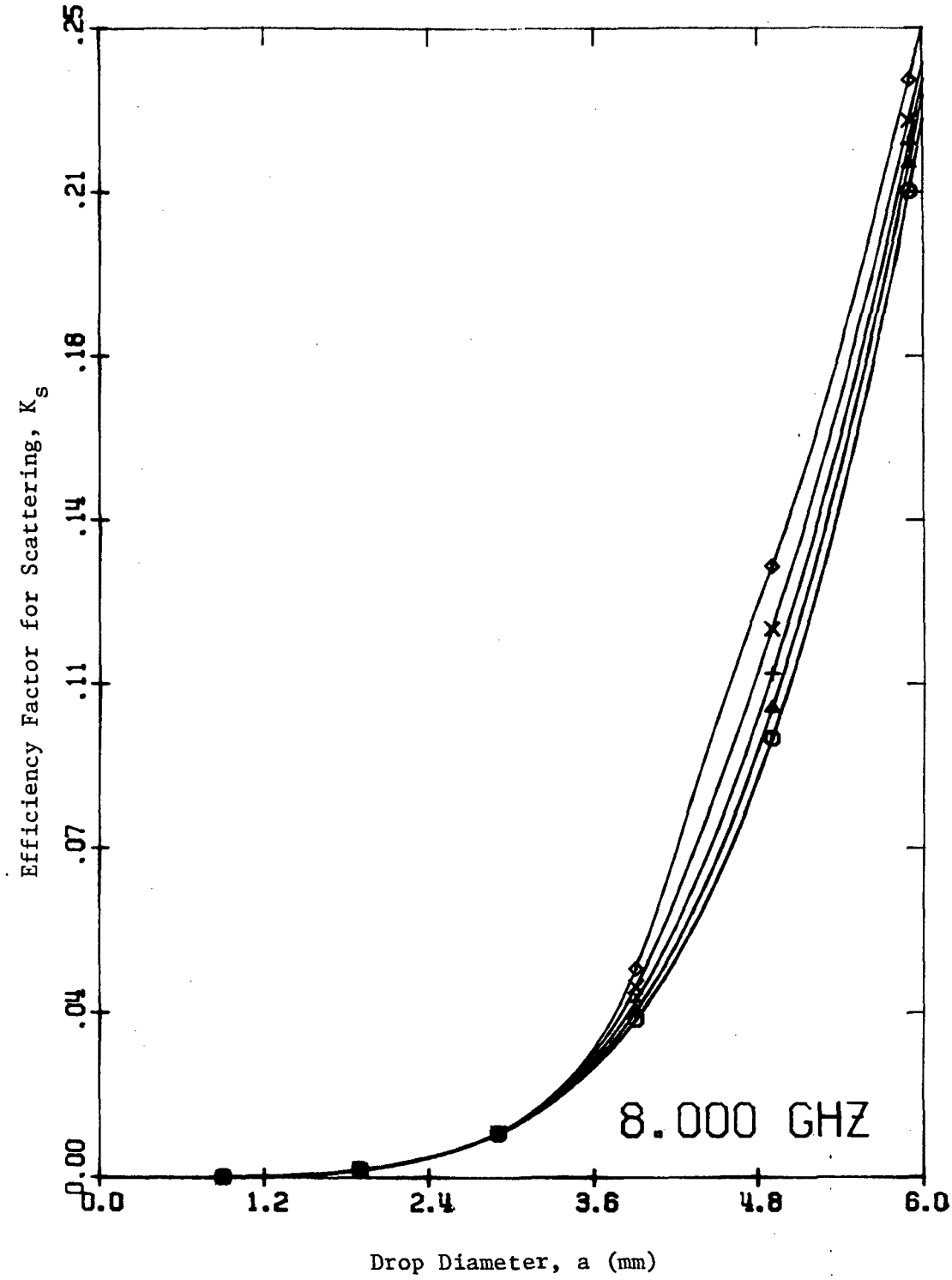

Fig. 30. Efficiency of scattering by an individual, liquid water drop: ν = 8.0 GHz.

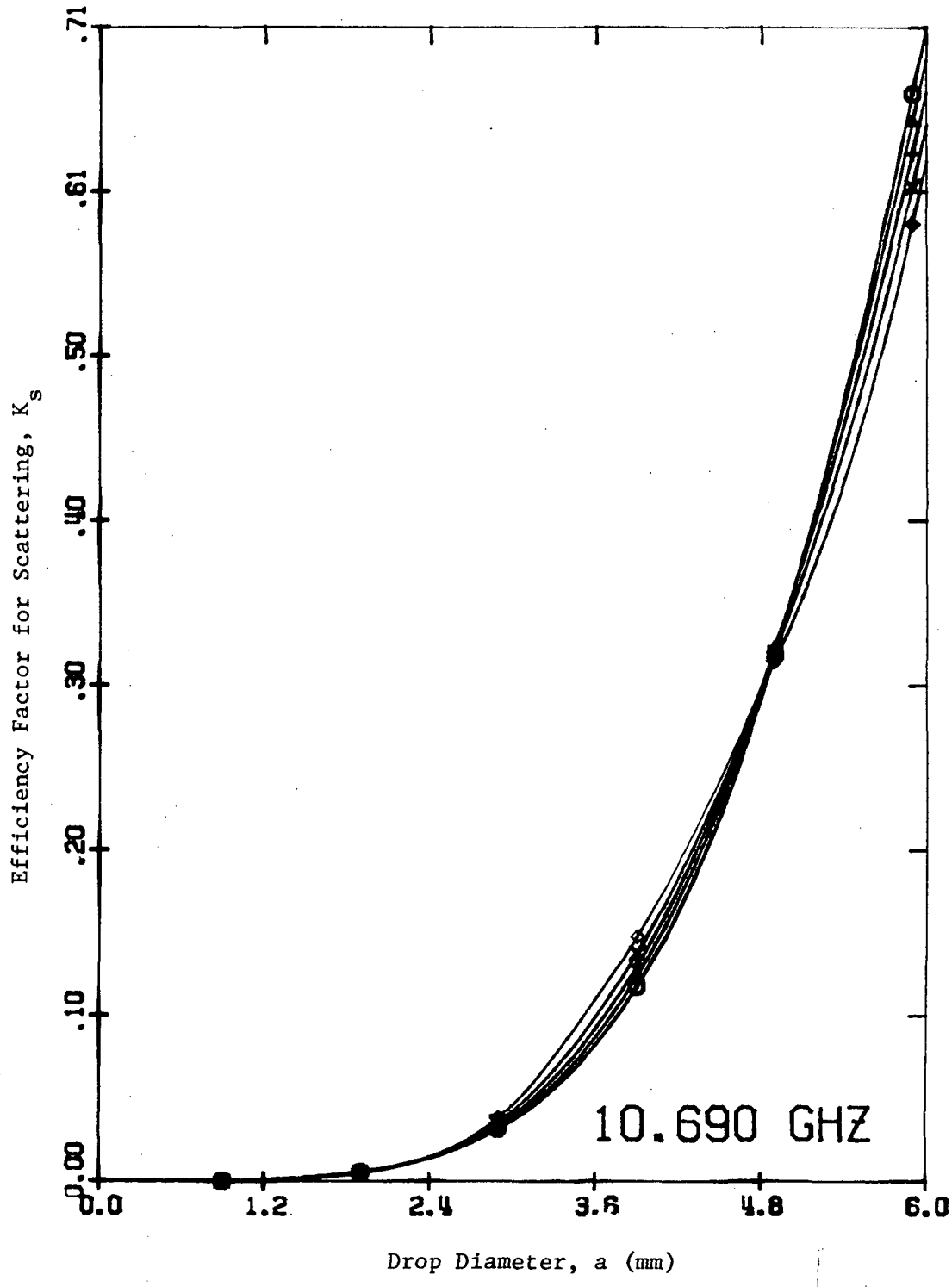

Fig. 31. Efficiency of scattering by an individual, liquid water drop: ν = 10.69 GHz.

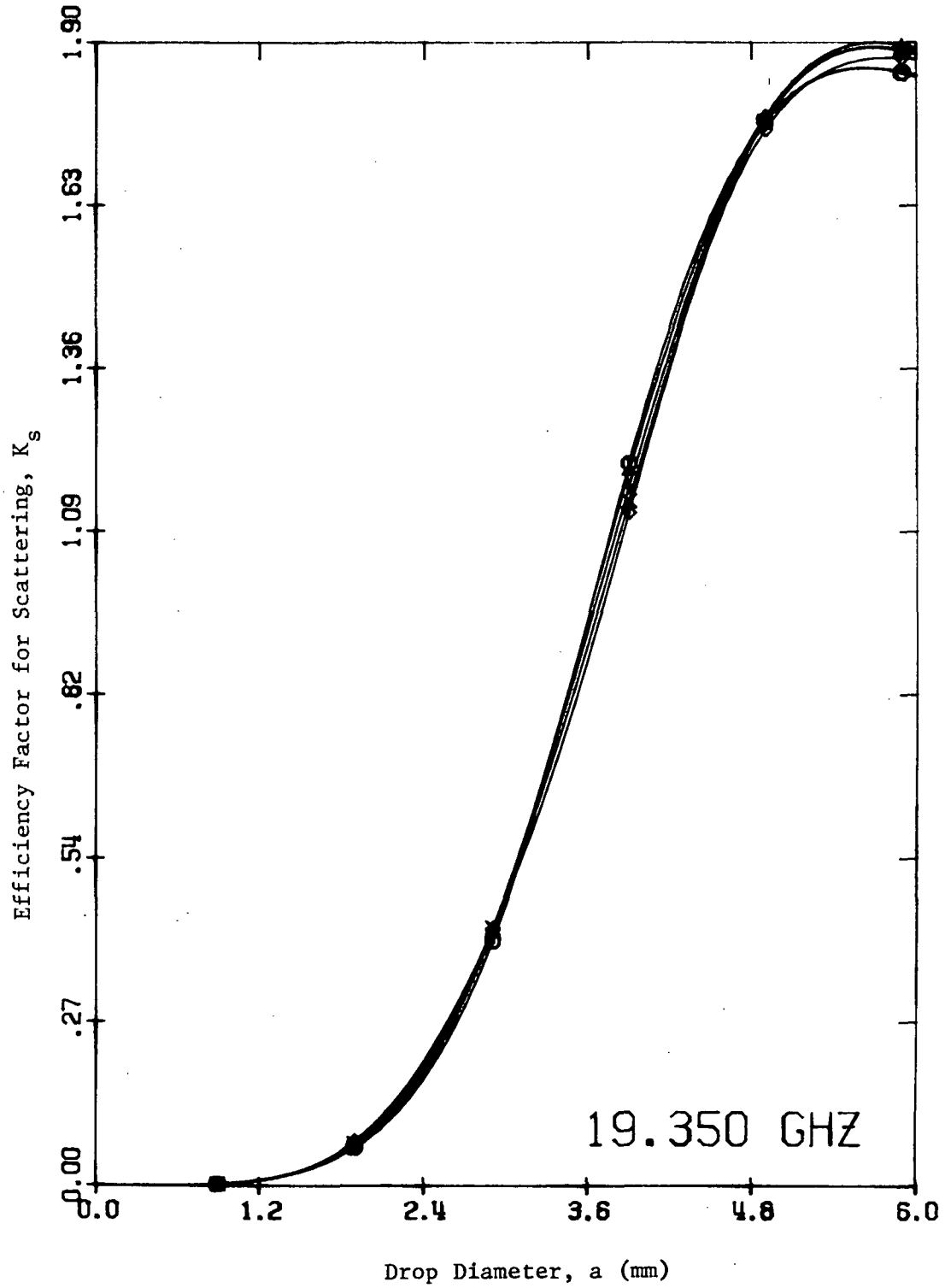

Fig. 32. Efficiency of scattering by an individual, liquid water drop: ν = 19.35 GHz.

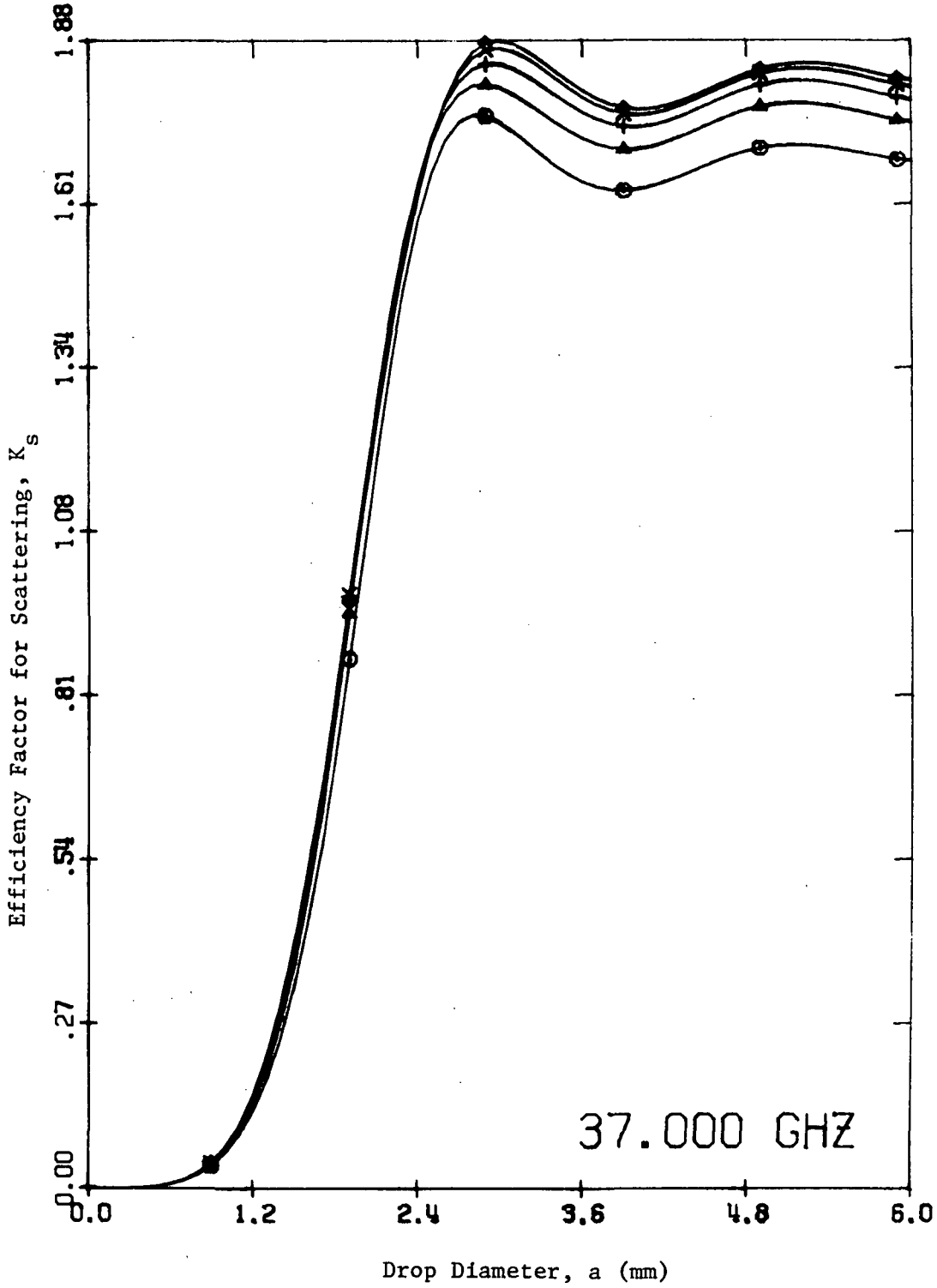

Fig. 33. Efficiency of scattering by an individual, liquid water drop: ν = 37.0 GHz.

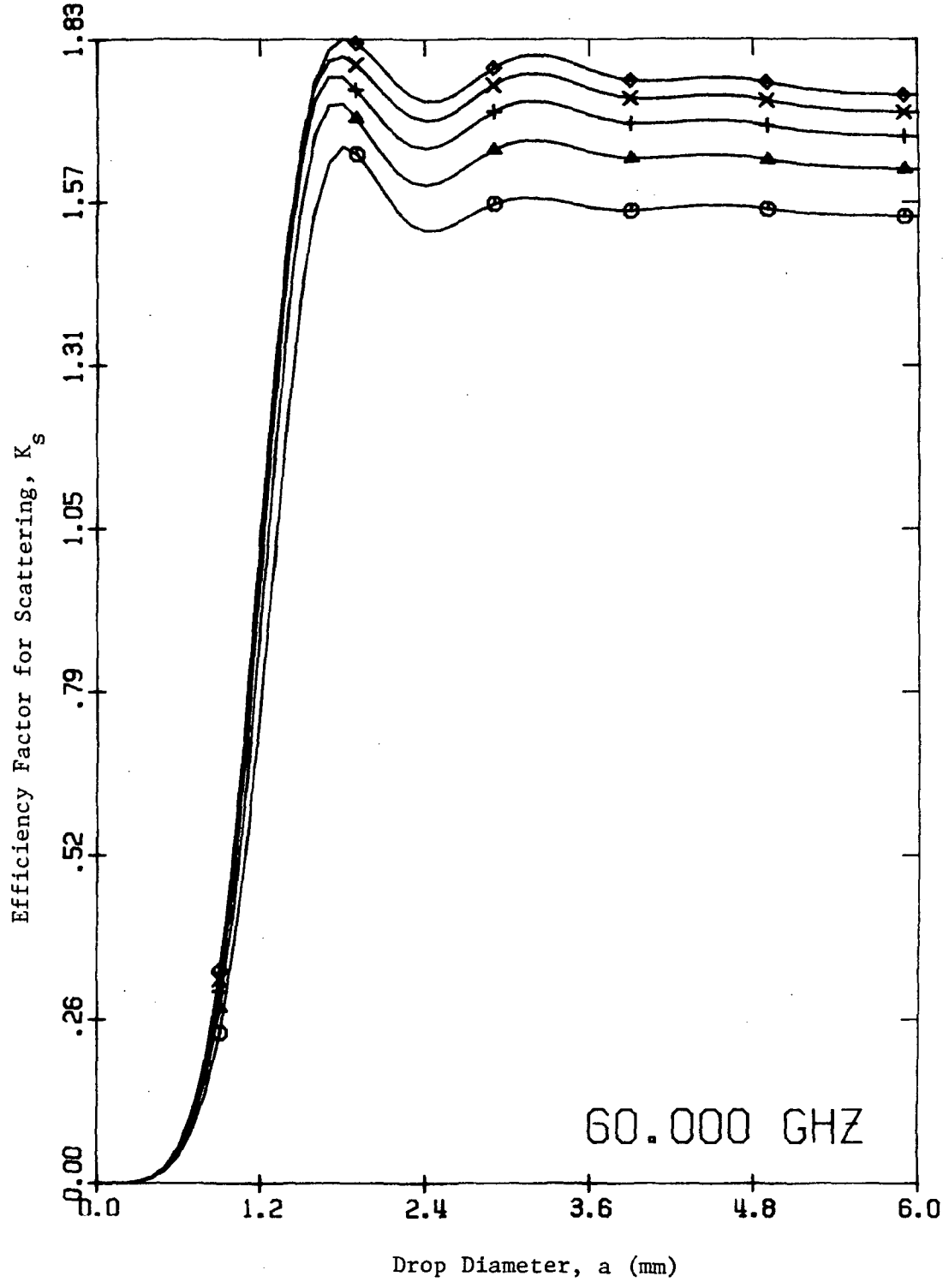

Fig. 34. Efficiency of scattering by an individual, liquid water drop: ν = 60.0 GHz.

smallest. Although the variation of K_a becomes quite non-linear with respect to a for the higher frequencies, K_a is still approximately proportional to a for small values of drop diameter. The variation of K_s with a is a non-linear function at all frequencies shown.

One may notice that K_s approaches a value greater than unity for large values of a. If there were no absorption, this limiting value would be 2. In this case, however, half of the "extincted" radiation is scattered into a small solid angle about the forward direction and becomes a part of the unextincted stream (Kerker, 1969, pp. 106-107).

A case of special interest in this paper is the situation where mx is much less than unity. In that case, the expressions for K_a and K_s are reduced to the following simple expressions, known as the Rayleigh Approximations (van de Hulst, 1957, p. 270):

$$K_{sr} = (8\, x^4/3)\, \left|(m^2 - 1)/(m^2 + 2)\right|^2 \qquad (135)$$

and

$$K_{ar} = 4 \times \mathrm{Im}\{-(m^2 - 1)/(m^2 + 2)\}. \qquad (136)$$

For clouds (drop diameters less than 0.1 mm), for frequencies less than 60 GHz, and for temperatures from -10 to 30C, mx is less than 0.327, and (135) and (136) may be expected to hold. In fact, as was mentioned earlier, K_{sr} is negligible when compared to K_{ar} for liquid water spheres at microwave frequencies. Also, K_{ar} is proportional to x which is, in turn, proportional to the drop diameter for

a given frequency. Thus, the extinction properties of clouds are such that the scattering can be neglected and the absorption is proportional to the mass of the drops regardless of the distribution of drop sizes in the cloud. The absorption and scattering of microwaves in rain can not be treated in such a simple manner since K_a and K_s are non-linear functions of a for any given drop temperature and frequency. The distribution of drop sizes is an important consideration in the case of extinction by rain.

B. Angular Scattering by an Individual Drop

The properties of angular scattering of an individual drop may be given in terms of the phase matrix [P] introduced in Chapter II (see Eqs. 72 and 73). Van de Hulst (1957, p. 45) gives an expression of a transformation matrix [F] which is related to [P] by a constant factor for any given medium and frequency of radiation. For a spherical particle, such as a drop of liquid water in a cloud or in rain, [F] is given by

$$[F] = \begin{bmatrix} \frac{1}{2}(F_1 + F_2) & \frac{1}{2}(F_1 - F_2) & 0 & 0 \\ \frac{1}{2}(F_1 - F_2) & \frac{1}{2}(F_1 + F_2) & 0 & 0 \\ 0 & 0 & F_3 & F_4 \\ 0 & 0 & -F_4 & F_3 \end{bmatrix}, \qquad (137)$$

where

$$F_1 = S_1 S_1^* , \qquad (138)$$

$$F_2 = S_2 S_2^* , \tag{139}$$

$$F_3 = \mathrm{Re}\{S_1 S_2^*\}, \tag{140}$$

and

$$F_4 = -\mathrm{Im}\{S_1 S_2^*\}, \tag{141}$$

and S_1 and S_2 are the complex scattering factors that are proportional to the amplitudes of the components of the electric field vector of the scattered radiation both parallel and perpendicular, respectively, to the scattering plane (see Fig. 35). S_1 and S_2 are given by Deirmendjian (1969, p. 13) as

$$S_1 = \sum_{n=1}^{\infty} \frac{2n+1}{n(n+1)} (a_n \pi_n + b_n \tau_n) \tag{142}$$

and

$$S_2 = \sum_{n=1}^{\infty} \frac{2n+1}{n(n+1)} (b_n \pi_n + a_n \tau_n), \tag{143}$$

where π_n and τ_n are functions of μ_s, the cosine of the scattering angle, Θ. Deirmendjian (op. cit., p. 15) gives recursion relationships which may be used to calculate π_n and τ_n for any given μ_s as follows:

$$\tau_n = \mu_s (\pi_n - \pi_{n-2}) - (2n-1)(1-\mu_s^2)\pi_{n-1} + \pi_{n-2}, \tag{144}$$

$$\pi_n = \mu_s \pi_{n-1} (2n-1)/(n-1) - n \pi_{n-2}/(n-1), \tag{145}$$

$$\pi_o = 0, \tag{146}$$

$$\pi_1 = 1, \tag{147}$$

$$\pi_2 = 3\mu_s, \tag{148}$$

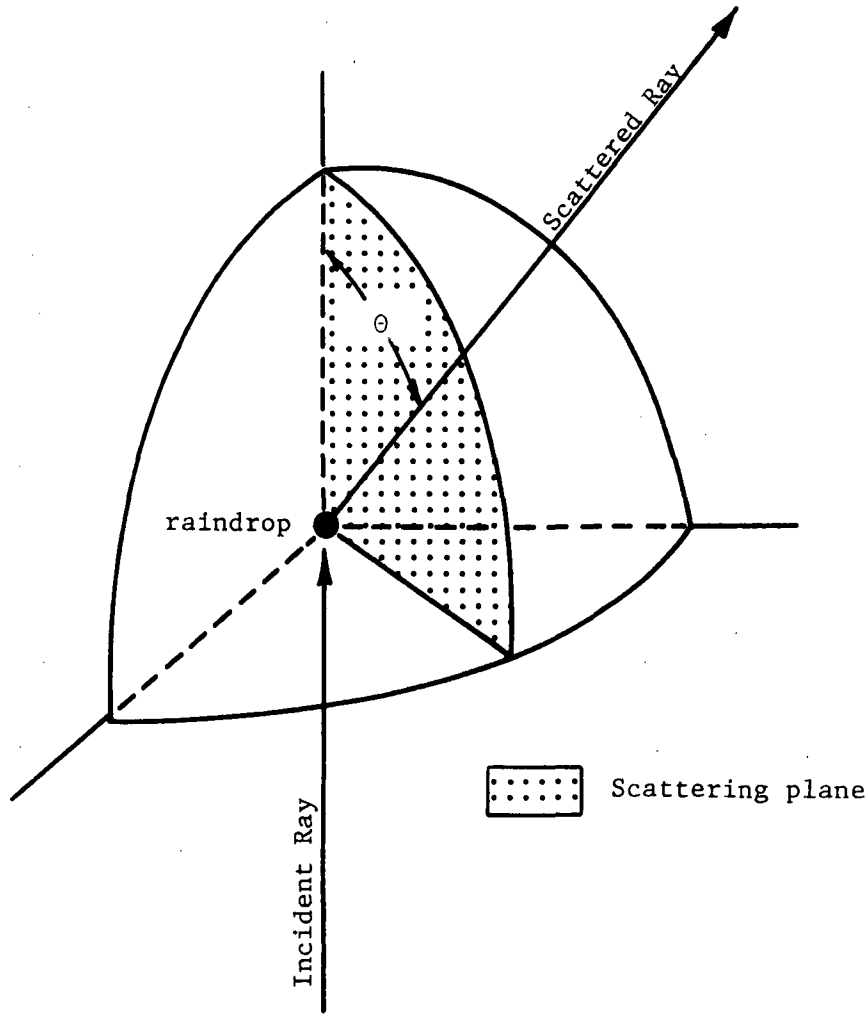

Fig. 35. Geometry of scattering.

$$\tau_o = 0, \tag{149}$$

$$\tau_1 = \mu_s, \tag{150}$$

and

$$\tau_2 = 6\,\mu_s^2 - 3. \tag{151}$$

Deirmendjian's equivalent expression for (145) omits the n in the numerator of the second term. Also, the expression of van de Hulst (1957, p. 124) equivalent to (144) is incorrect in that his $\sin\Theta$ term should read $\sin^2\Theta$.

One may use the equations developed and summarized in Sections 1 and 2 of this chapter to compute the absorption, extinction, scattering or angular scattering parameters for a single drop as a function of the microwave frequency, the drop temperature, the drop diameter, and the scattering angle. In order to compute the corresponding properties for a polydispersive medium such as rain, one must know the distribution of drop sizes.

C. Distributions of Drop Sizes in Rain

The distribution of drop diameters in precipitation has been the subject of much meteorological research during the past 30 years. The distribution used in most meteorological literature is that proposed by Marshall and Palmer (1948). The Marshall-Palmer distribution (hereafter called the M-P distribution) compares well with other distributions suggested by Laws and Parsons (1943), and Best (1950). It is based on measurements of the distribution of

drop diameters at the surface for steady rains having intensities of 1.0, 2.8, 6.3, and 23.0 mm hr^{-1}. The M-P distribution, which expresses the fact that larger drops tend to break up into smaller drops, is given by the following equation:

$$N = N_o \exp(-b\ a), \tag{152}$$

where N is the number of drops of diameter, a, per unit volume per unit drop-diameter interval (m^{-4}), N_o is 8.0 x 10^6 m^{-4}, a is the drop diameter (m), b (m^{-1}) is given by

$$b = 4100\ R^{-0.21}, \tag{153}$$

and R is the rainfall intensity (mm hr^{-1}). Fanning (1965) found that the M-P distribution worked well in subtropical precipitation but suggested that N_o is a function of R. It appears that the M-P distribution is valid for rain originating from snowflakes but fails for warm rain (Ohtake, 1970). Dingle and Hardy (1962) found that the M-P distribution tends to overestimate the number of large drops. All of these investigators and others have noted that the actual distribution of drop diameters in rain may deviate greatly from that given by the M-P distribution, but that on the average the M-P distribution fits well. It is recognized at this point that the distribution of drop sizes in actual rain may indeed deviate greatly from that given by the M-P distribution; however, the inclusion of other drop-size distributions in the considerations of this paper would only multiply and unduly complicate the analysis of the thermal emissive properties of rain. The quantitative

relationships between the meteorological properties of the atmosphere and its thermal emissions at microwave frequencies that are derived in later chapters are predicated upon the validity of the M-P distribution. One may use these relationships for interpreting actual microwave measurements by assuming that the precipitation is represented by the M-P distribution.

The properties of a M-P distribution of raindrops are considered below. Stephens (1962) suggested that the maximum drop diameter is a function of R, i.e.,

$$a_{max} = 0.0023\ R^{0.213}\ (m). \tag{154}$$

For the purposes of this paper, the content of liquid water of the rain mass, M_p (g m^{-3}), is a more convenient parameter in the M-P distribution than R. If there were no limit to the drop diameter, then M_p would be

$$M_p = \int_0^{\infty} (\rho_L\ \pi\ a^3/6)\ N_o \exp(-b\ a)\ da = \rho_L\ \pi\ N_o/b^4, \tag{155}$$

where ρ_L is the density of water (g m^{-3}). The average density of water over the range of temperatures from -10 to 30C is 99970 g m^{-3} (Chemical Rubber Company, 1959, p. 2113). If one uses the value of b given by (153), then one obtains an expression for M_p as

$$M_p = 0.0889\ R^{0.84}\ . \tag{156}$$

Thus,

$$R = 17.84\ M_p^{1.1905}\ . \tag{157}$$

Based on the criteria given in (154) for $a_{max} \leq 6.0$ mm,

values of M_p were computed by finite differences from the M-P distribution for rainfall intensities ranging up to 100 mm hr^{-1}. A plot of the resulting data on logarithmic paper shows that the following relationship may be used to compute R for any given M_p:

$$R = 18.05\ M_p^{1.19} \quad . \tag{158}$$

In this paper, M_p (g m^{-3}) will be used as the independent variable in the M-P distribution. R (mm hr^{-1}) will be computed from M_p through (158) and used in (153) and (154) to obtain values for b and a_{max}.

If one substitutes the value for b given by (153) into the integrand of (155), differentiates the result with respect to diameter, and sets the differential equal to zero, then one obtains the following expression for modal drop diameter:

$$a_{mode} = 0.7317\ R^{0.21} \quad . \tag{159}$$

The value of a_{mode} varies from 1.026 mm for a rainfall intensity of 5 mm hr^{-1} to 1.925 mm for 100 mm hr^{-1}.

An independent evaluation of the rainfall intensity was made by calculating the rainfall intensity from a M-P distribution for a pressure of 1013.25 mb and a temperature of 20C for specific values of R. In these calculations, no vertical motions of the air were assumed and the terminal velocities of the individual drops were calculated from the formulas given by Foote and du Toit (1969). The results of these calculations are shown in Table 19.

Table 19. Comparison between calculated and given values of rainfall intensity for M-P distribution of drop sizes, for a pressure of 1013.25 mb, and for a temperature of 20C.

Given Rainfall Intensity ($mm\ hr^{-1}$)	Calculated Rainfall Intensity ($mm\ hr^{-1}$)
5	5.73
10	11.35
15	16.84
20	22.29
25	27.64
30	32.91
35	38.20
40	43.35
45	48.55
50	53.64
60	63.85
70	73.81
80	83.70
90	93.51
100	103.02

Thus, it appears that R is simply a parameter to be used in the M-P distribution as a control factor and is approximately the same as the actual surface rainfall intensity of that distribution. For pressures less than 1013.25 mb, the terminal velocities increase and the resulting rainfall intensities are larger than that at the surface. The content of liquid water remains the same. Therefore, M_p is a much more useful parameter for the rain mass than R.

D. Volume Absorption and Scattering Coefficients of Clouds and Rain

It is assumed that the concentration of drops in a cloud or rain mass is sufficiently small so that there are negligible

shadowing effects, that is, the extinction caused by the collection of drops is simply the sum of the extinction of the individual drops. In this case, the volume absorption coefficient, α (m^{-1}), and the volume scattering coefficient, β (m^{-1}), are evaluated by

$$\alpha = \int_0^{a_{max}} N\, Q_a\, da \tag{160}$$

and

$$\beta = \int_0^{a_{max}} N\, Q_s\, da, \tag{161}$$

where N is the number of drops per unit volume per unit drop-size interval (m^{-4}), Q_a is the absorption cross section (m^2), Q_s is the scattering cross section (m^2), and da is the incremental drop-diameter interval (m).

In the case of a non-raining cloud, β_c, the volume scattering coefficient, is negligible, and α_c, the volume absorption coefficient, is given from (124), (136), and (161) as

$$\alpha_c = [\pi^2\, \nu\, \mathrm{Im}\{-(m^2 - 1)/(m^2 + 2)\}/c] \int_0^{a_{max}} a^3\, N\, da \tag{162a}$$

$$= [6\, \pi\, \nu\, \mathrm{Im}\{-(m^2 - 1)/(m^2 + 2)\}/\rho_L\, c] \cdot \int_0^{a_{max}} (\pi\, \rho_L\, a^3/6)\, N\, da, \tag{162b}$$

where c is the speed of light in a vacuum (2.99793×10^8 m sec^{-1}), ρ_L is the density of water (assumed to be 999700 g m^{-3}), ν is the

electromagnetic frequency (Hz), a is the drop diameter (m), and m is the complex index of refraction of the water. The parenthetical expression in the integrand of (162b) is the mass of the water drop (g). Thus, the value of the integral is simply the content of liquid water of the cloud (g m^{-3}) and is represented by the symbol, M_c. Thus,

$$\alpha_c = 6 \pi \nu M_c \, \mathrm{Im}\{-(m^2 - 1)/(m^2 + 2)\}/\rho_L \, c$$

$$= 6.2895 \times 10^{-14} \nu M_c \, \mathrm{Im}\{-(m^2 - 1)/(m^2 + 2)\}. \qquad (163)$$

Goldstein (1951) derived an expression for the volume absorption coefficient of a non-raining cloud that uses an approximation for the term dealing with the complex index of refraction of water. This expression is given as

$$\alpha_{gold} = 1.122 \times 10^{-25} \nu^2 M_c \quad (m^{-1}), \qquad (164)$$

where ν is the frequency (Hz). Staelin (1966) developed a somewhat similar expression based on the data of Goldstein (1951) and which includes a temperature factor. This expression is

$$\alpha_{stae} = 1.113 \times 10^{[0.0122 \, (291 - T) - 25]} \nu^2 M_c, \qquad (165)$$

where T is the temperature of the cloud (K). In this paper, α_c will be calculated from (163) instead of the approximations given by (164) or (165). These approximations were not meant to be valid for the entire range of frequencies from 0.5 GHz to 60 GHz. There are two important properties of the absorption of microwaves by non-raining clouds as given by the Rayleigh theory. First, the

absorption is directly proportional to the content of liquid water for a specific temperature and frequency. Second, the absorption rate decreases with increasing temperature (Gunn and East, 1954) for all microwave frequencies under consideration in this paper. It will be shown in Chapter VIII that when these two conditions hold, it follows that the emission is dependent only upon the integrated amount of liquid water and is independent of the vertical distributions of the liquid water and the temperature of the liquid water mass.

In the case of rain, it is assumed that N in (160) and (161) may be given as a function of M_p, and that Q_a and Q_s may be obtained from the Mie theory, as developed in Section A. The integrals in (160) and (161) may be evaluated using the trapozoidal rule. The corresponding values for the volume absorption coefficient of the rain mass, α_p (m^{-1}), and the volume scattering coefficient of the rain mass, β_p (m^{-1}), were computed for each of the 27 frequencies listed in Table 1 (Chapter I), for temperatures of -10, 0, 10, 20, and 30C, and for contents of liquid water ranging up to 4 g m^{-3} in steps of 0.1 g m^{-3}. The resulting values of α_p were plotted against M_p by the Gerber plotter, and these plots are shown in Figs. 36 to 53. In addition, the absorption of a non-raining cloud given by the Rayleigh theory (Y) (for a temperature of 10C) and the Goldstein approximation (★) are shown in the same figures for comparison. It can be seen that the Goldstein approximation (α_{gold}) does not agree with the Rayleigh approximation (α_c).

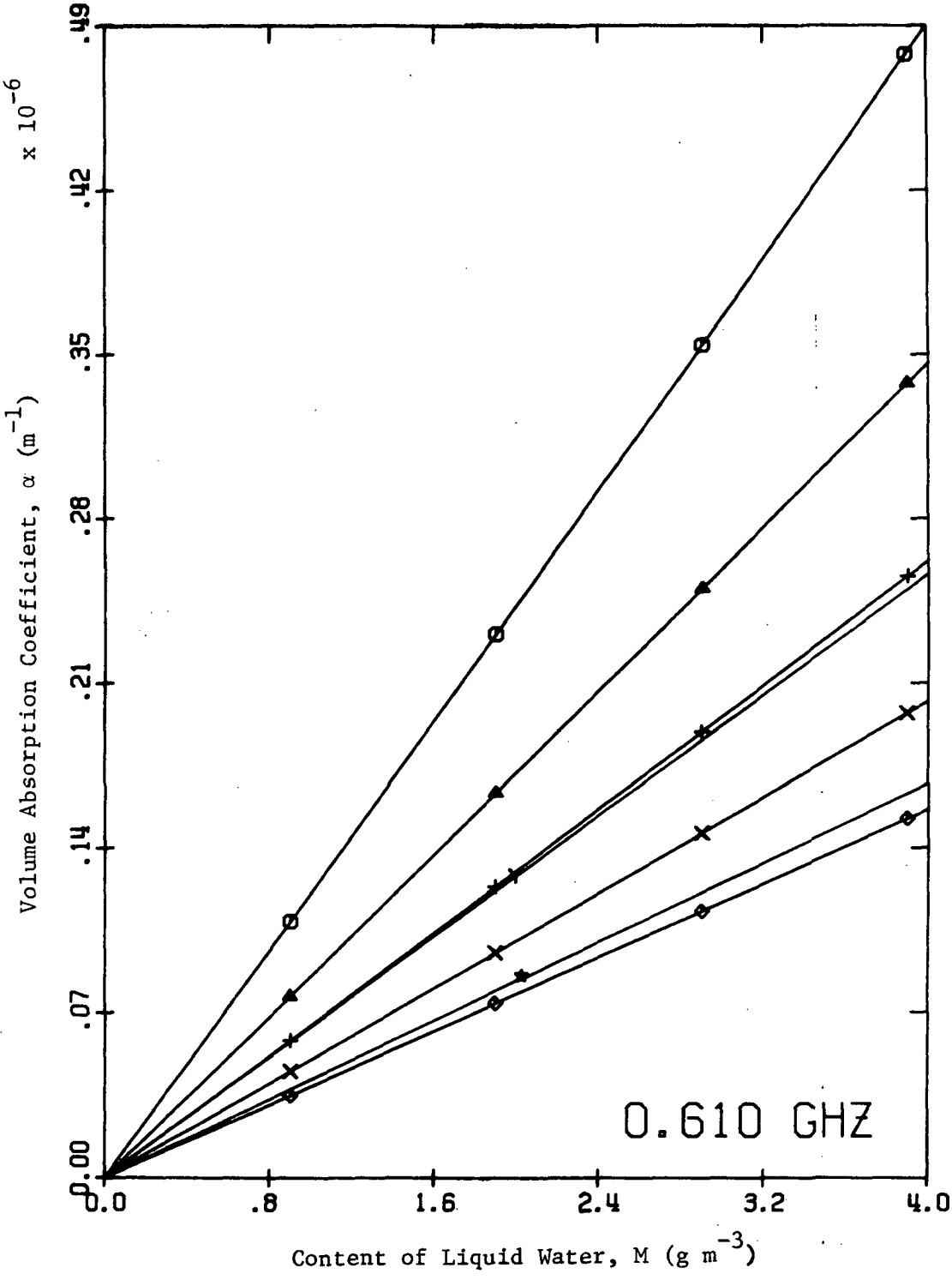

Fig. 36. Rate of absorption of microwaves by liquid water cloud and M-P rain: ν = 0.61 GHz.

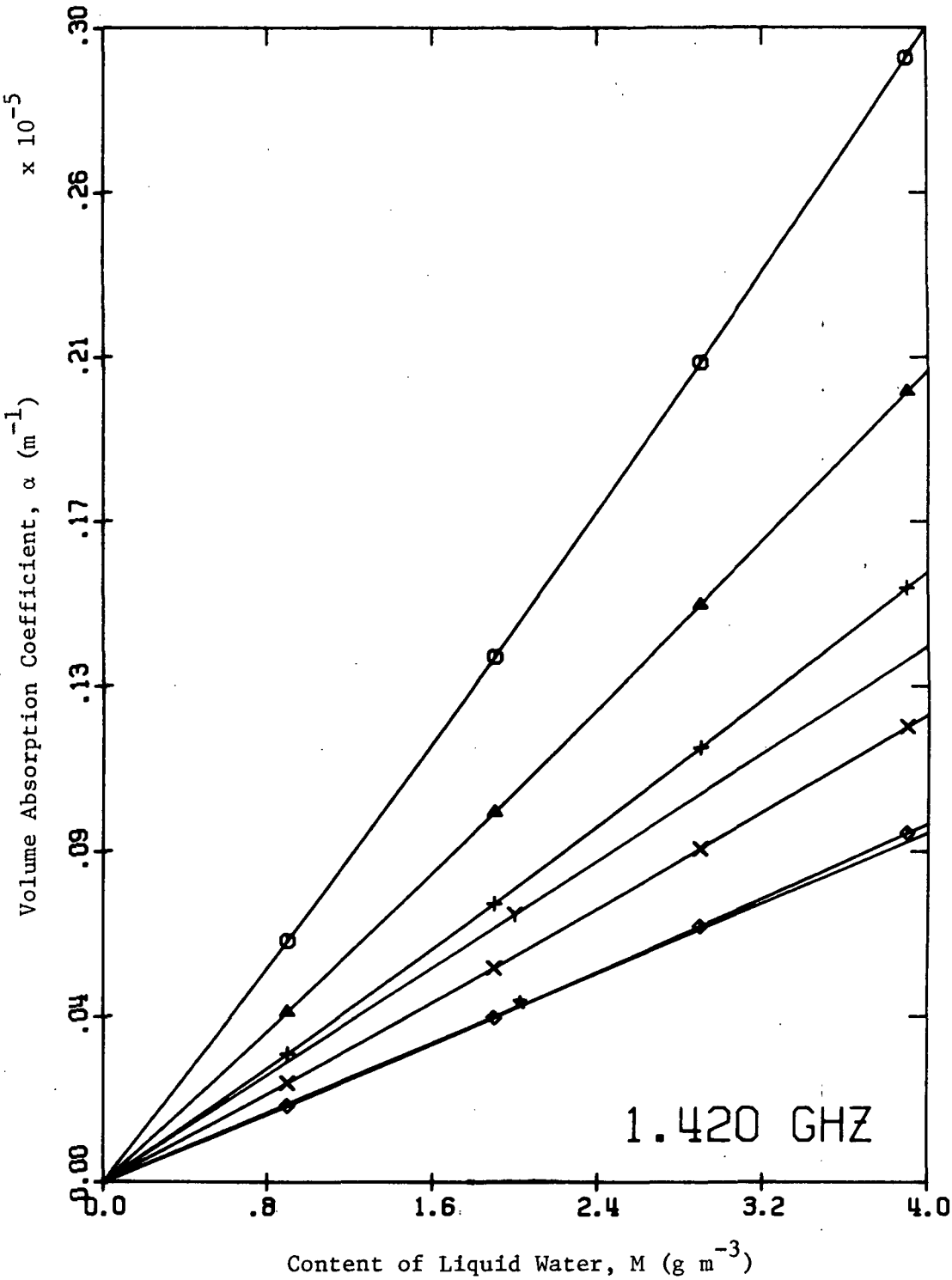

Fig. 37. Rate of absorption of microwaves by liquid water cloud and M-P rain: ν = 1.42 GHz.

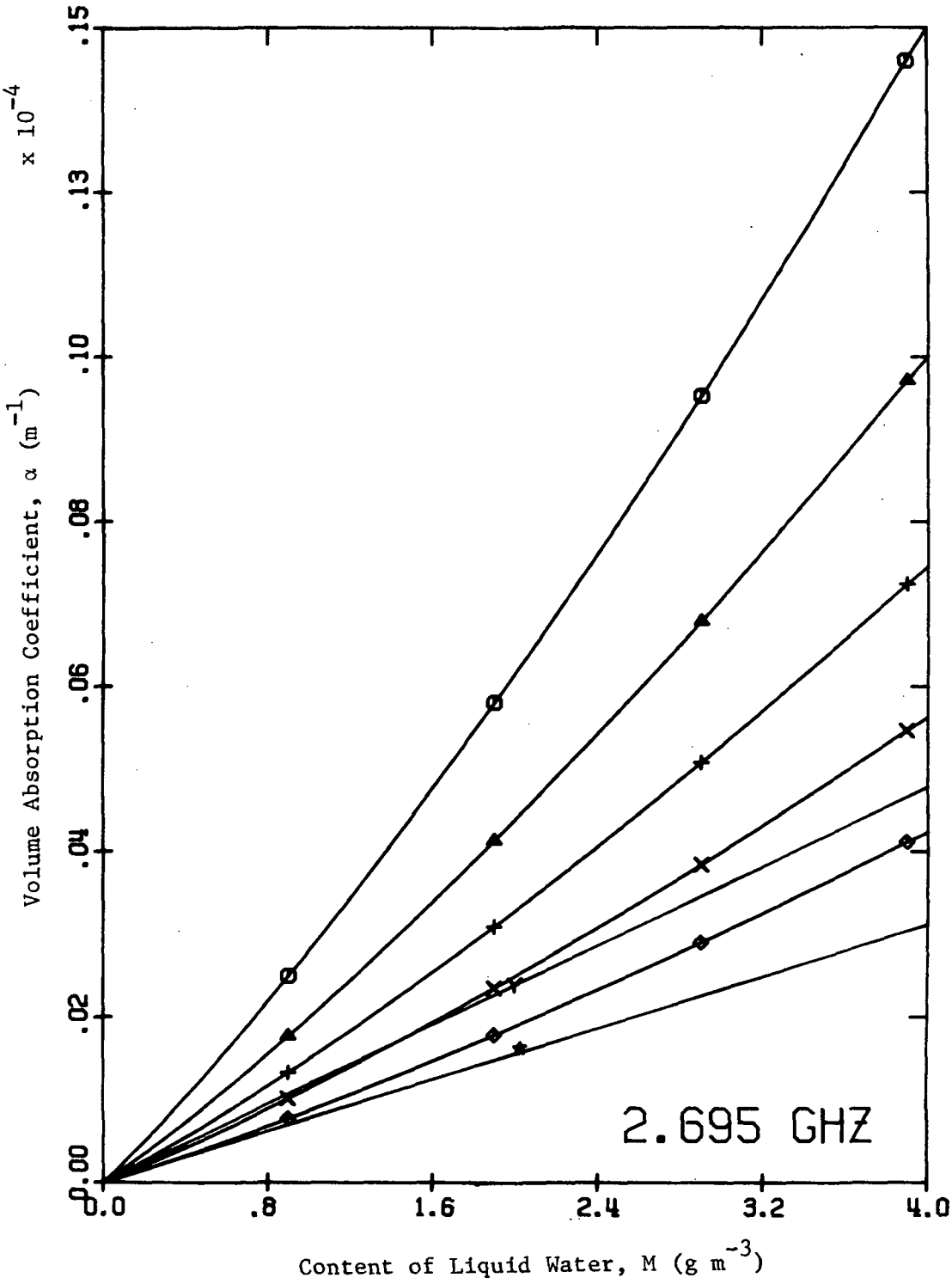

Fig. 38. Rate of absorption of microwaves by liquid water cloud and M-P rain: ν = 2.695 GHz.

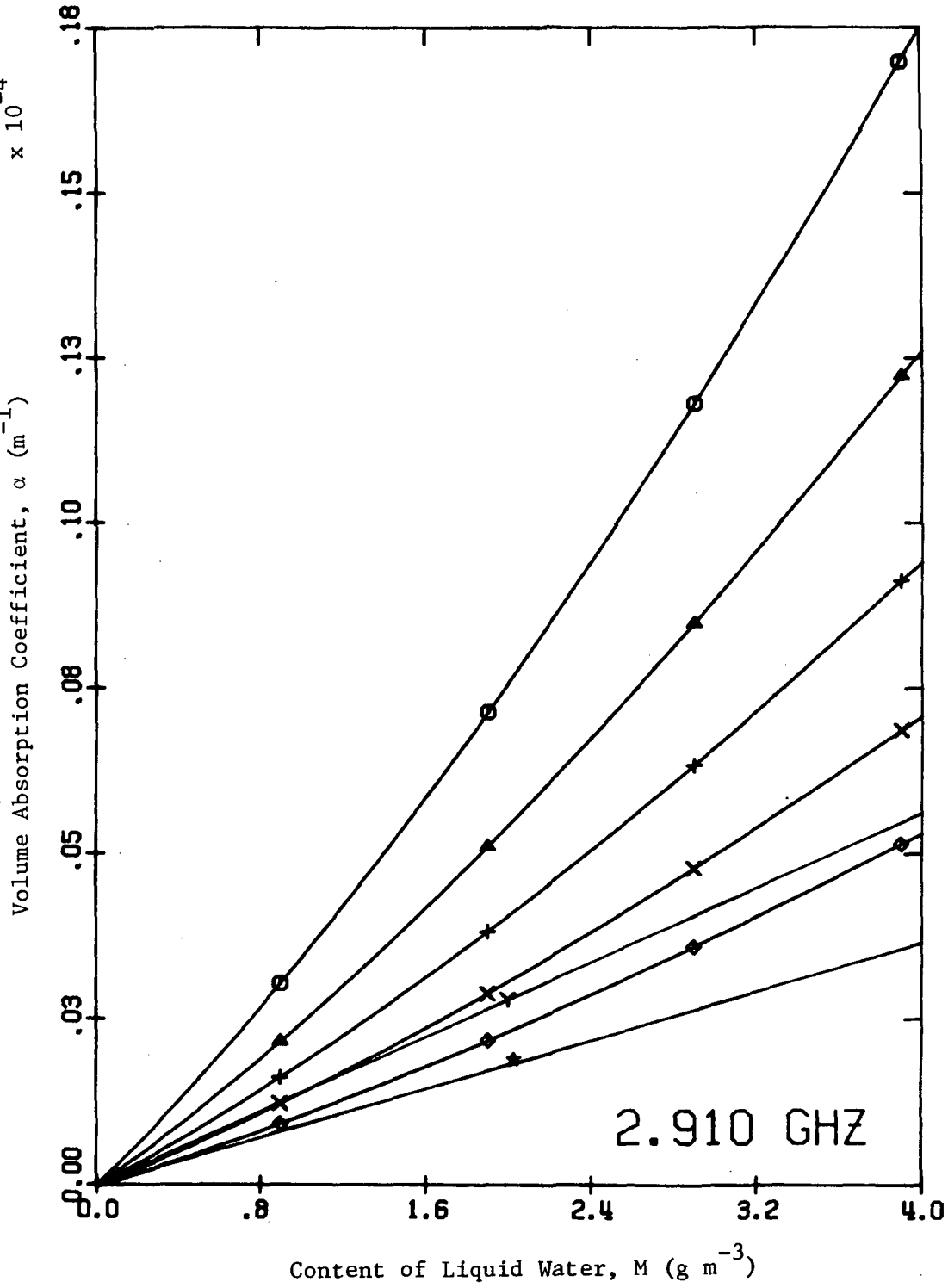

Fig. 39. Rate of absorption of microwaves by liquid water cloud and M-P rain: ν = 2.91 GHz.

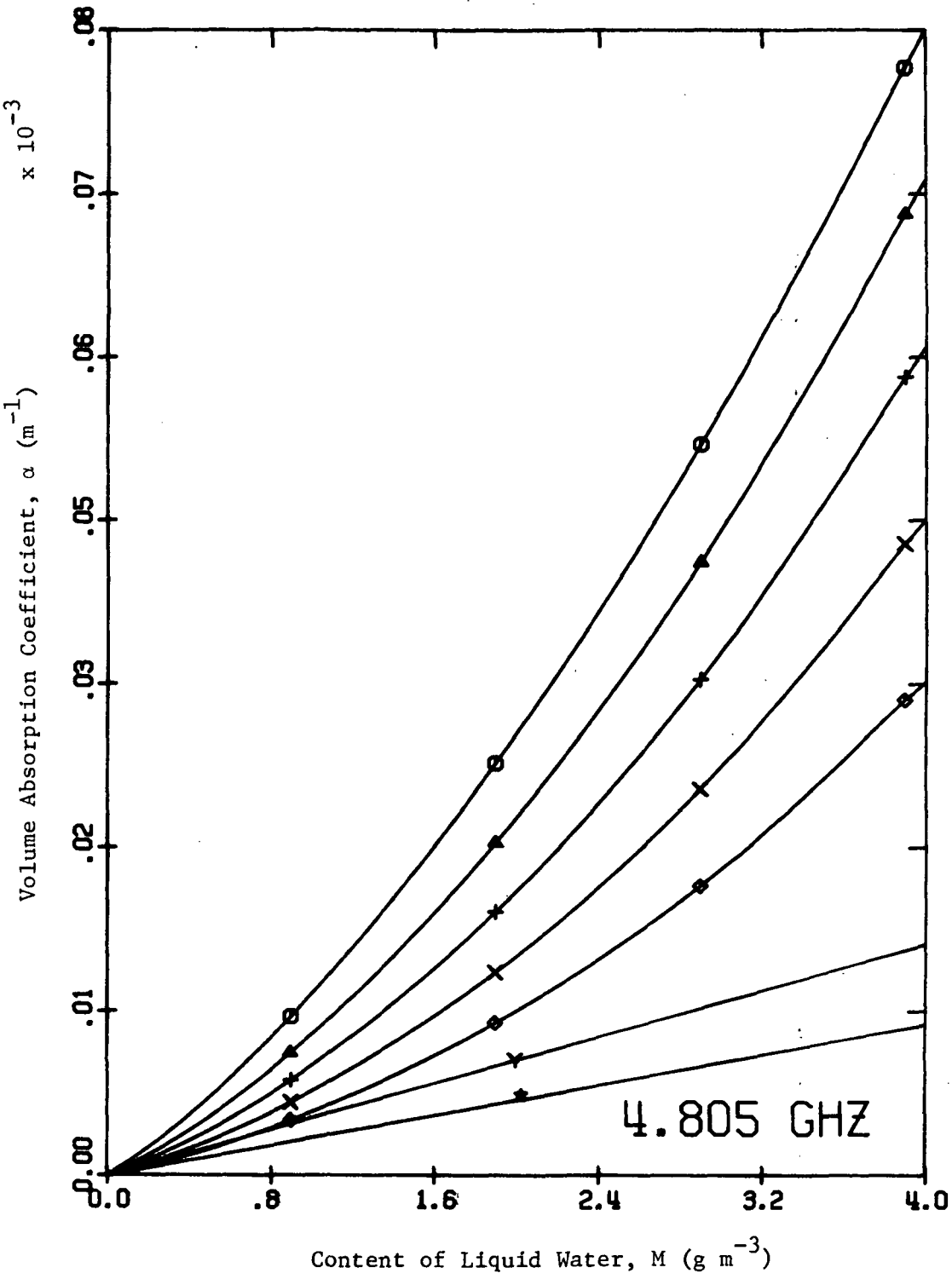

Fig. 40. Rate of absorption of microwaves by liquid water cloud and M-P rain: ν = 4.805 GHz.

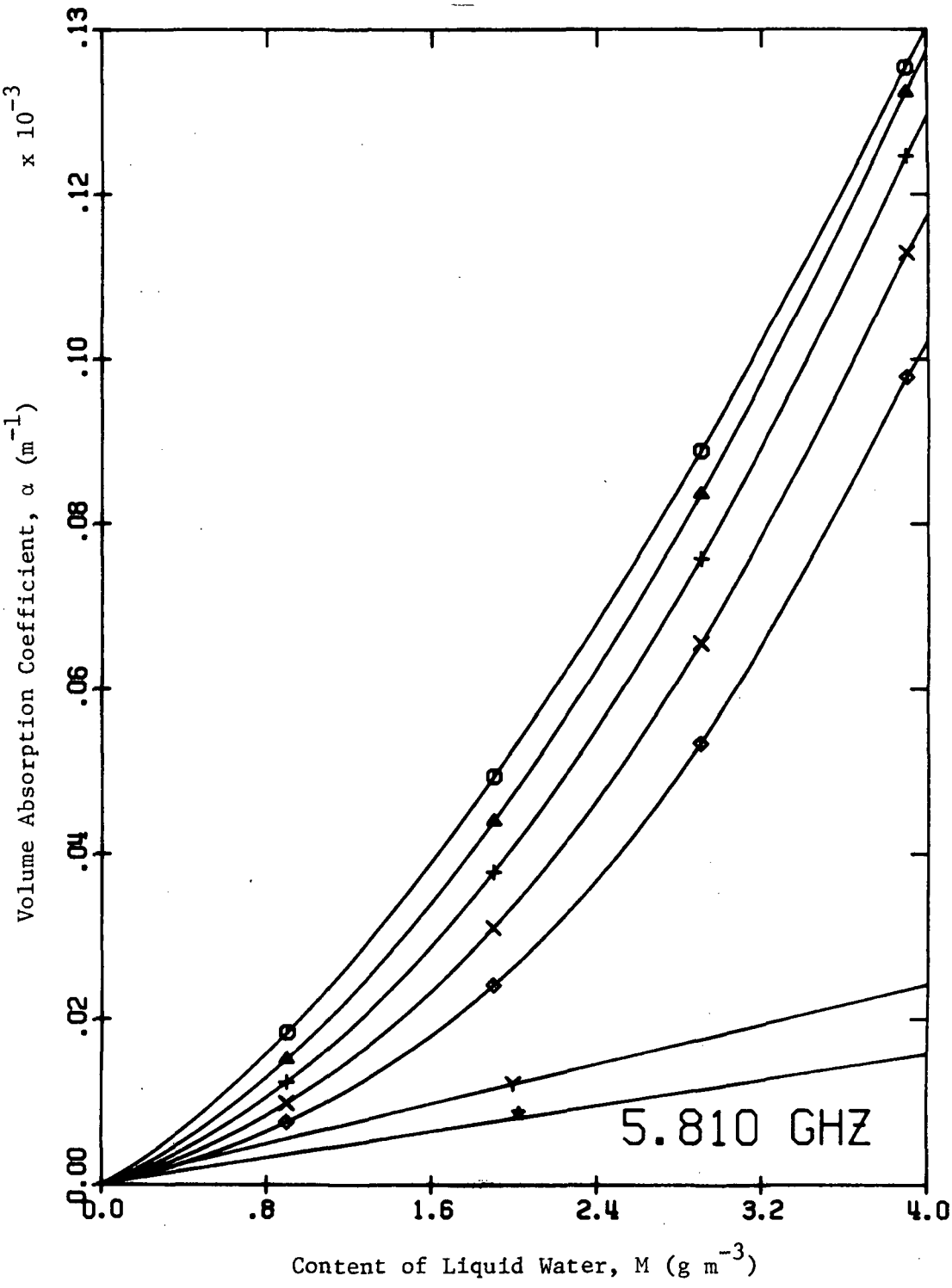

Fig. 41. Rate of absorption of microwaves by liquid water cloud and M-P rain: ν = 5.81 GHz.

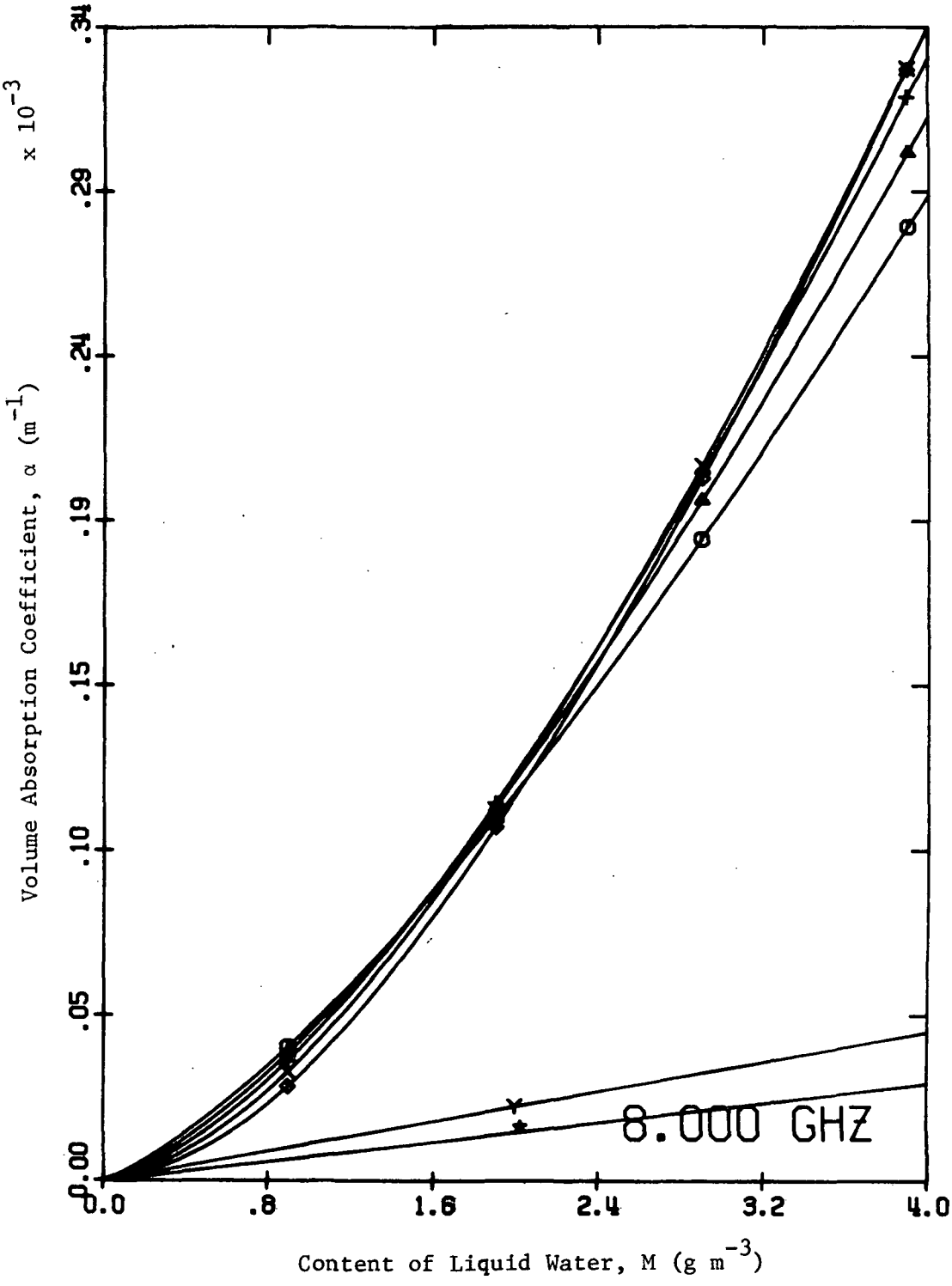

Fig. 42. Rate of absorption of microwaves by liquid water cloud and M-P rain: ν = 8.0 GHz.

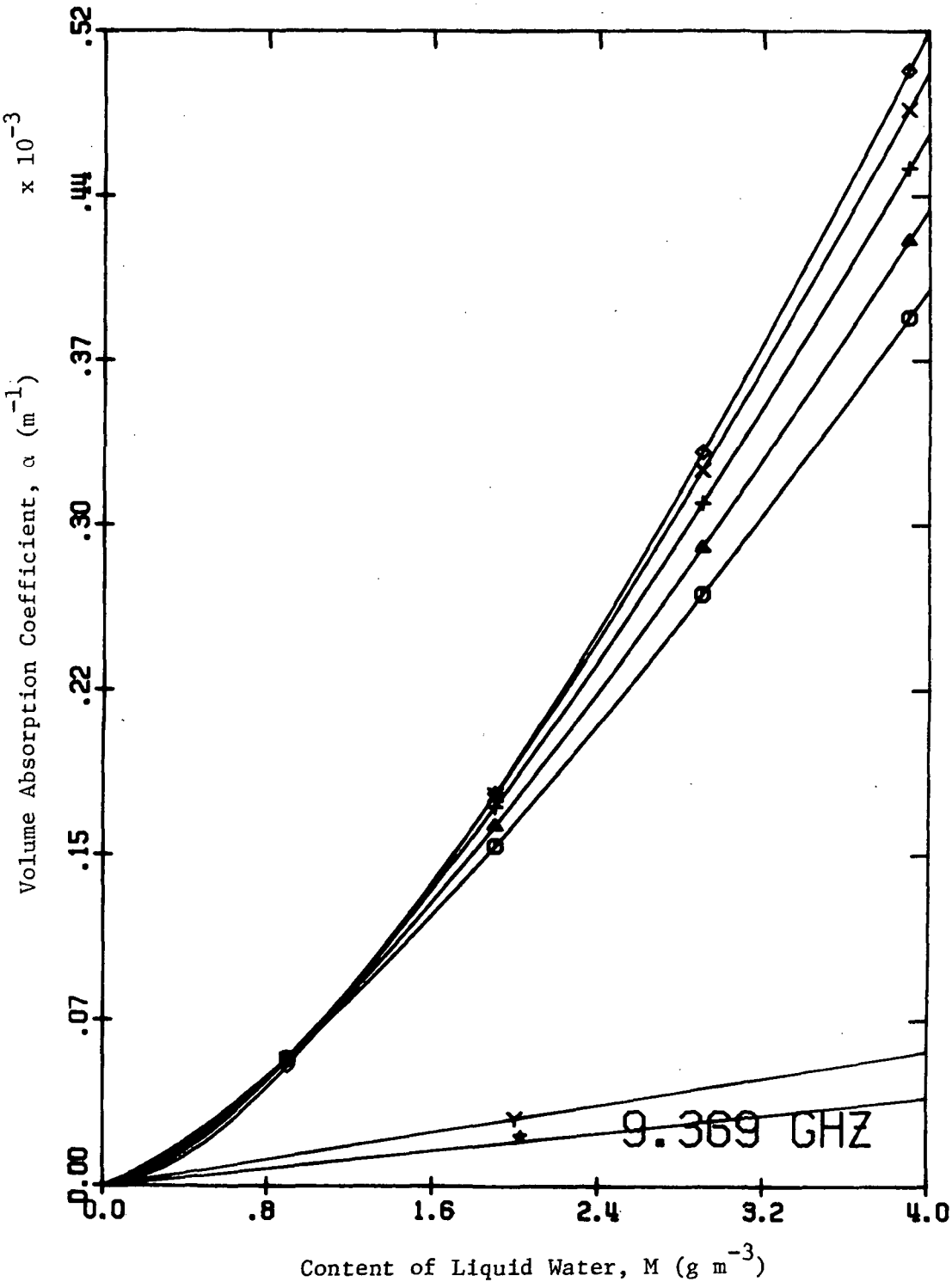

Fig. 43. Rate of absorption of microwaves by liquid water cloud and M-P rain: ν = 9.369 GHz.

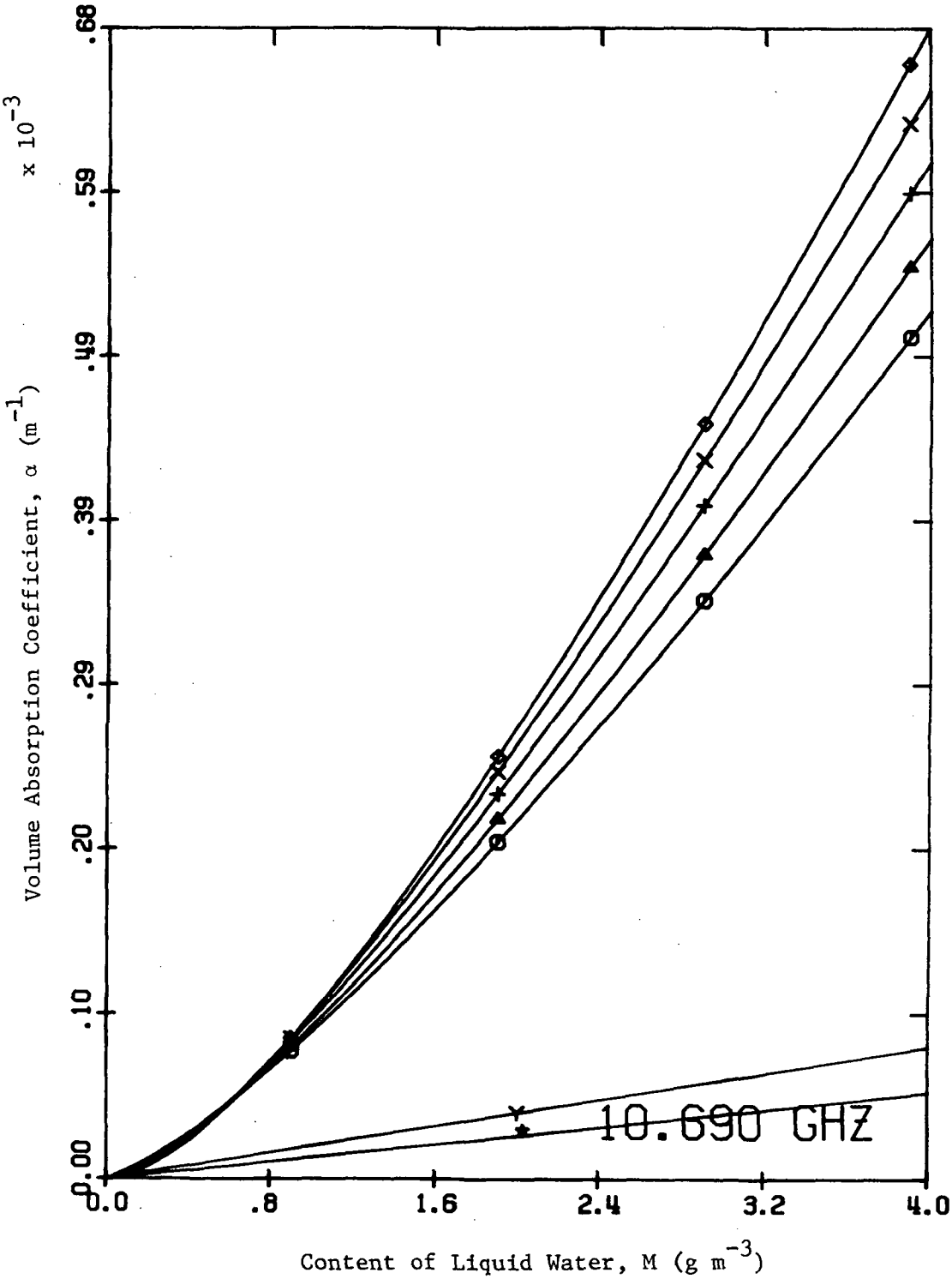

Fig. 44. Rate of absorption of microwaves by liquid water cloud and M-P rain: ν = 10.69 GHz.

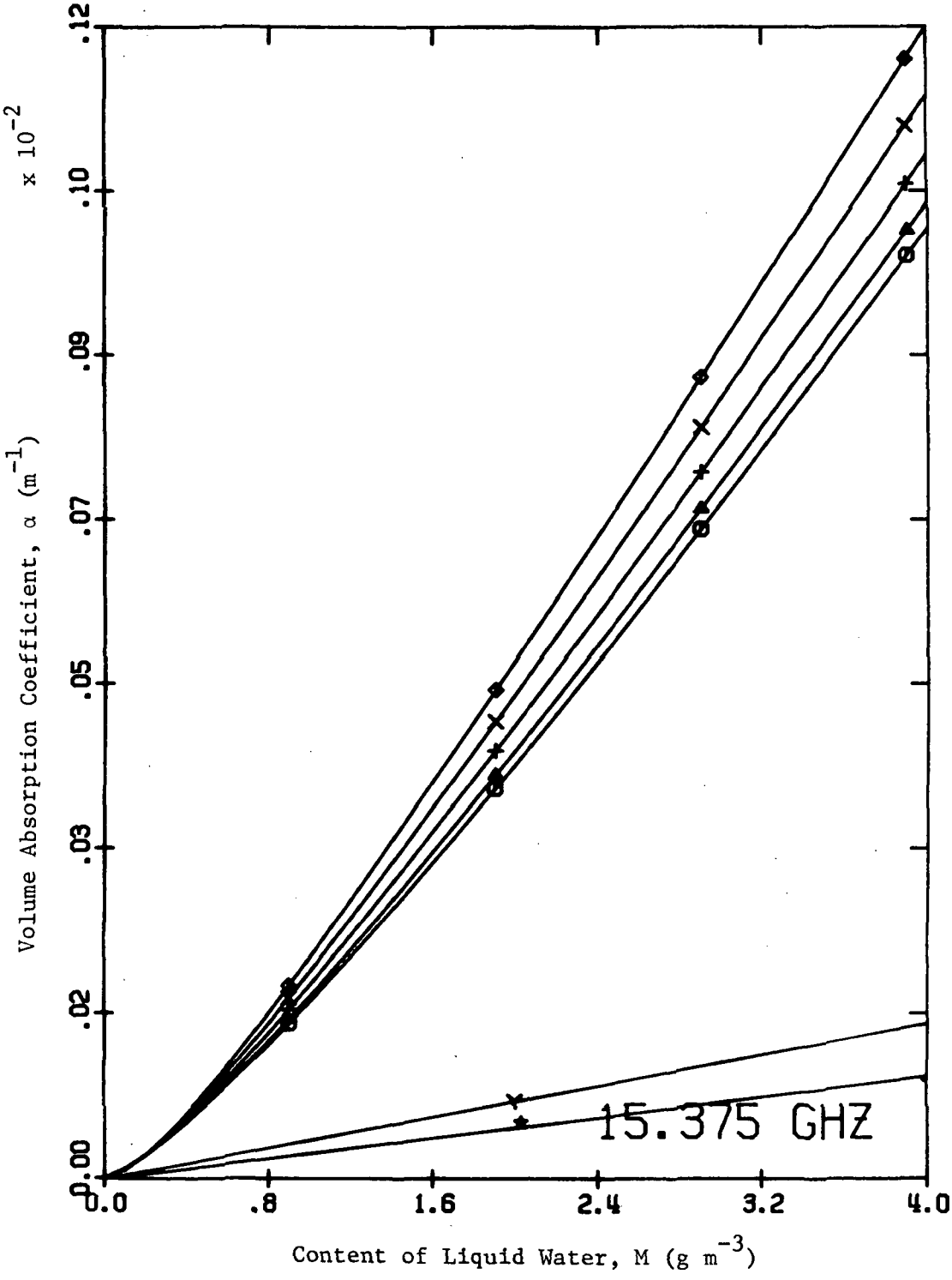

Fig. 45. Rate of absorption of microwaves by liquid water cloud and M-P rain: ν = 15.375 GHz.

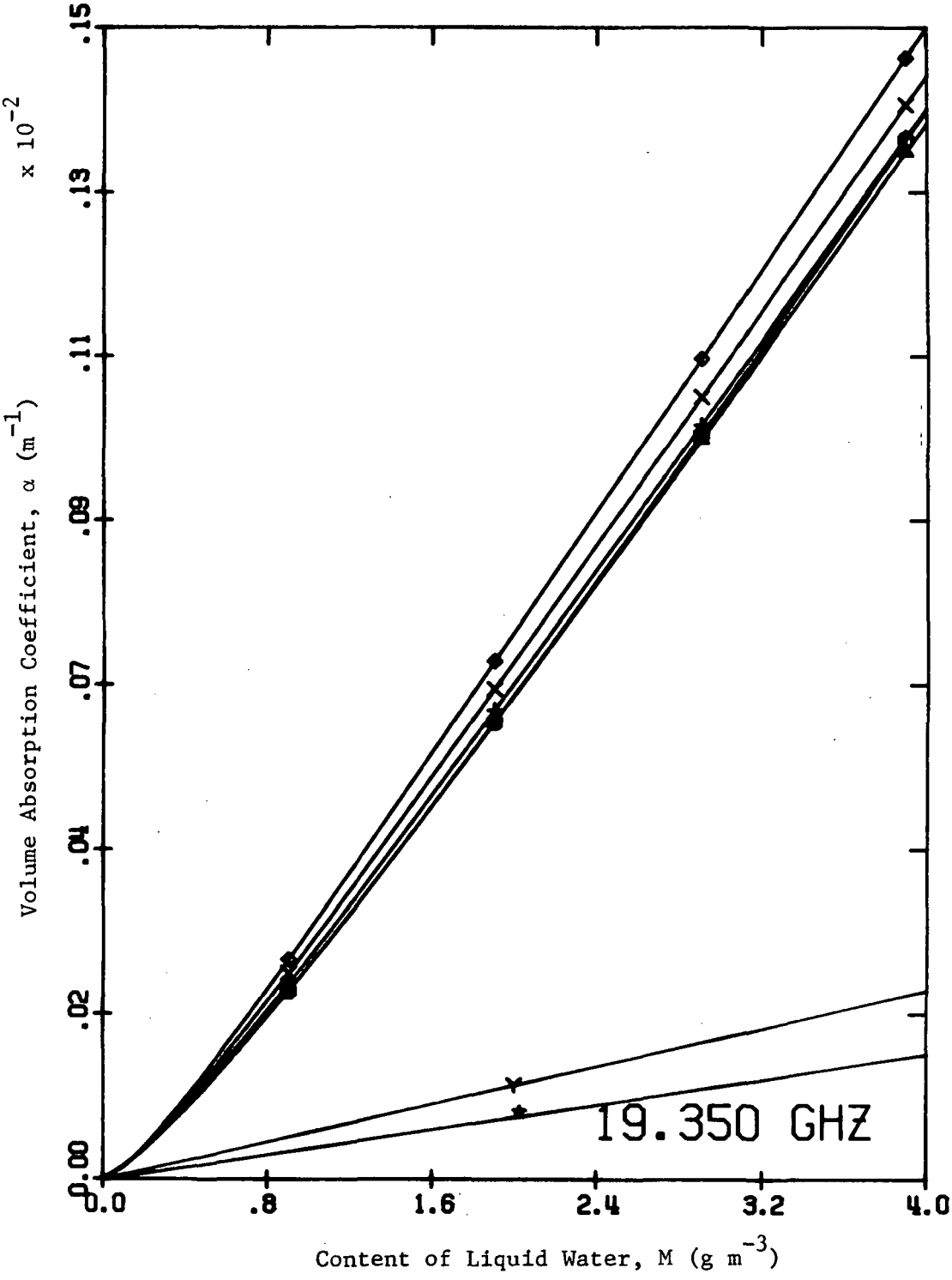

Fig. 46. Rate of absorption of microwaves by liquid water cloud and M-P rain: ν = 19.35 GHz.

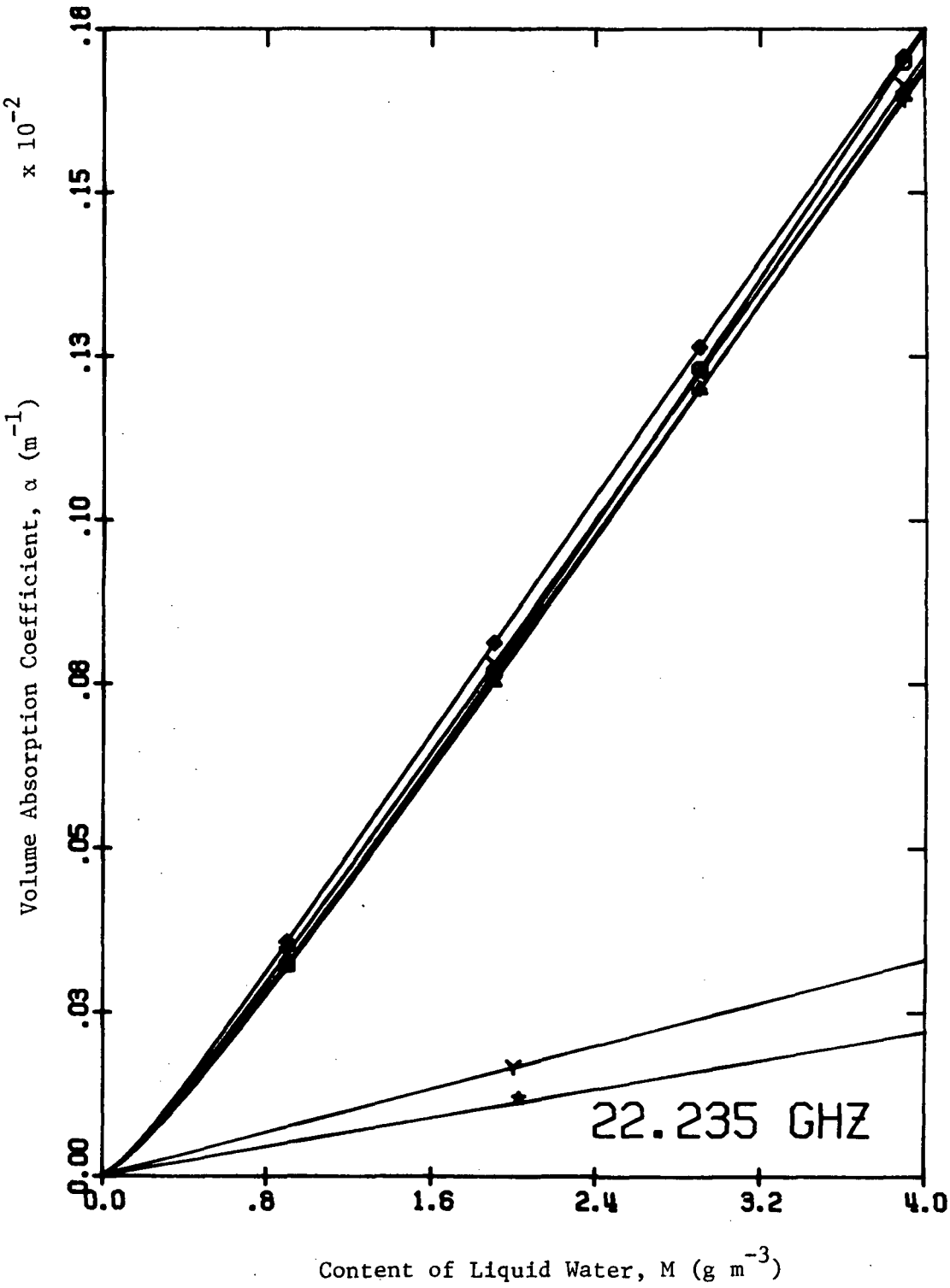

Fig. 47. Rate of absorption of microwaves by liquid water cloud and M-P rain: ν = 22.235 GHz.

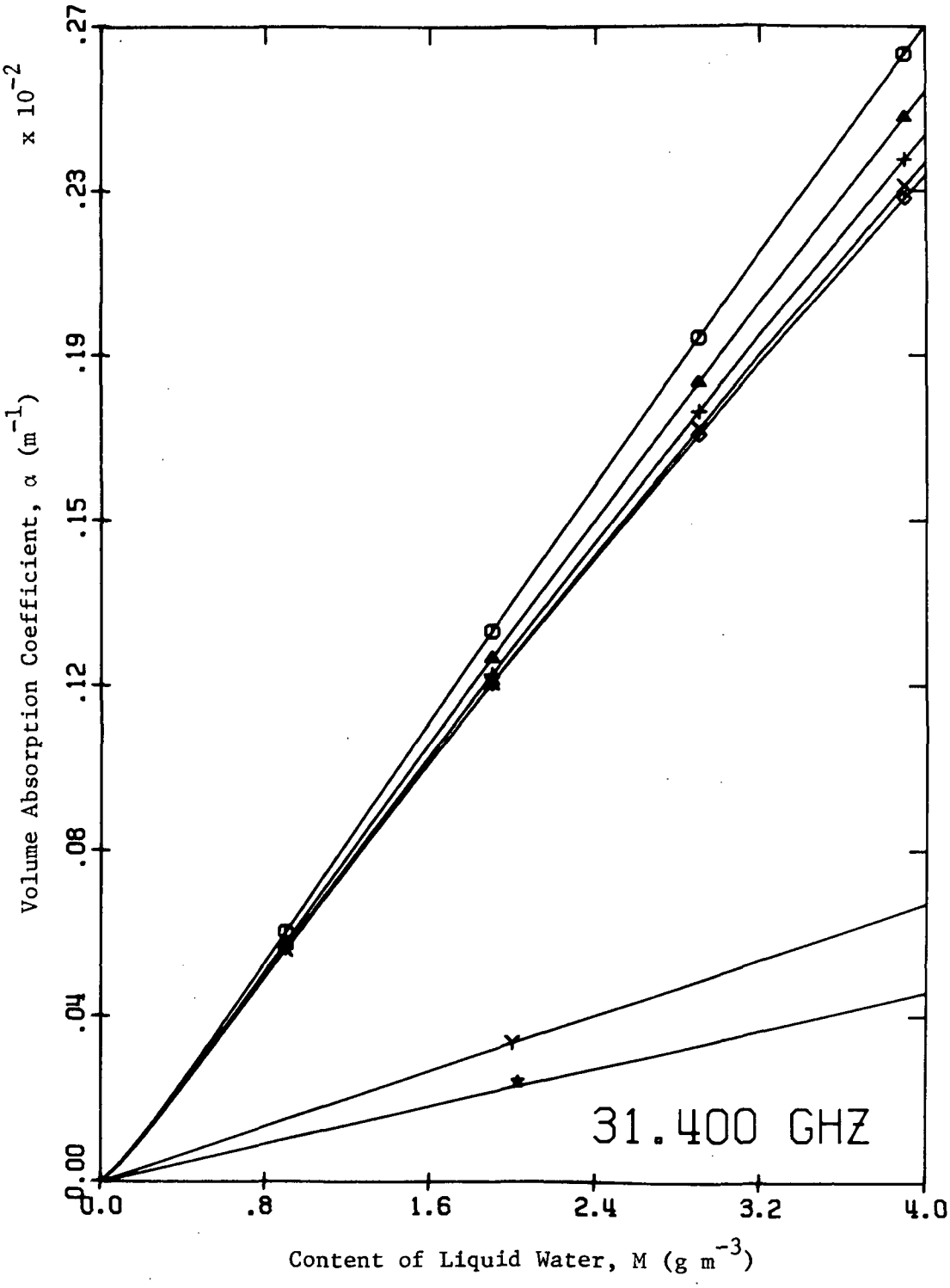

Fig. 48. Rate of absorption of microwaves by liquid water cloud and M-P rain: ν = 31.4 GHz.

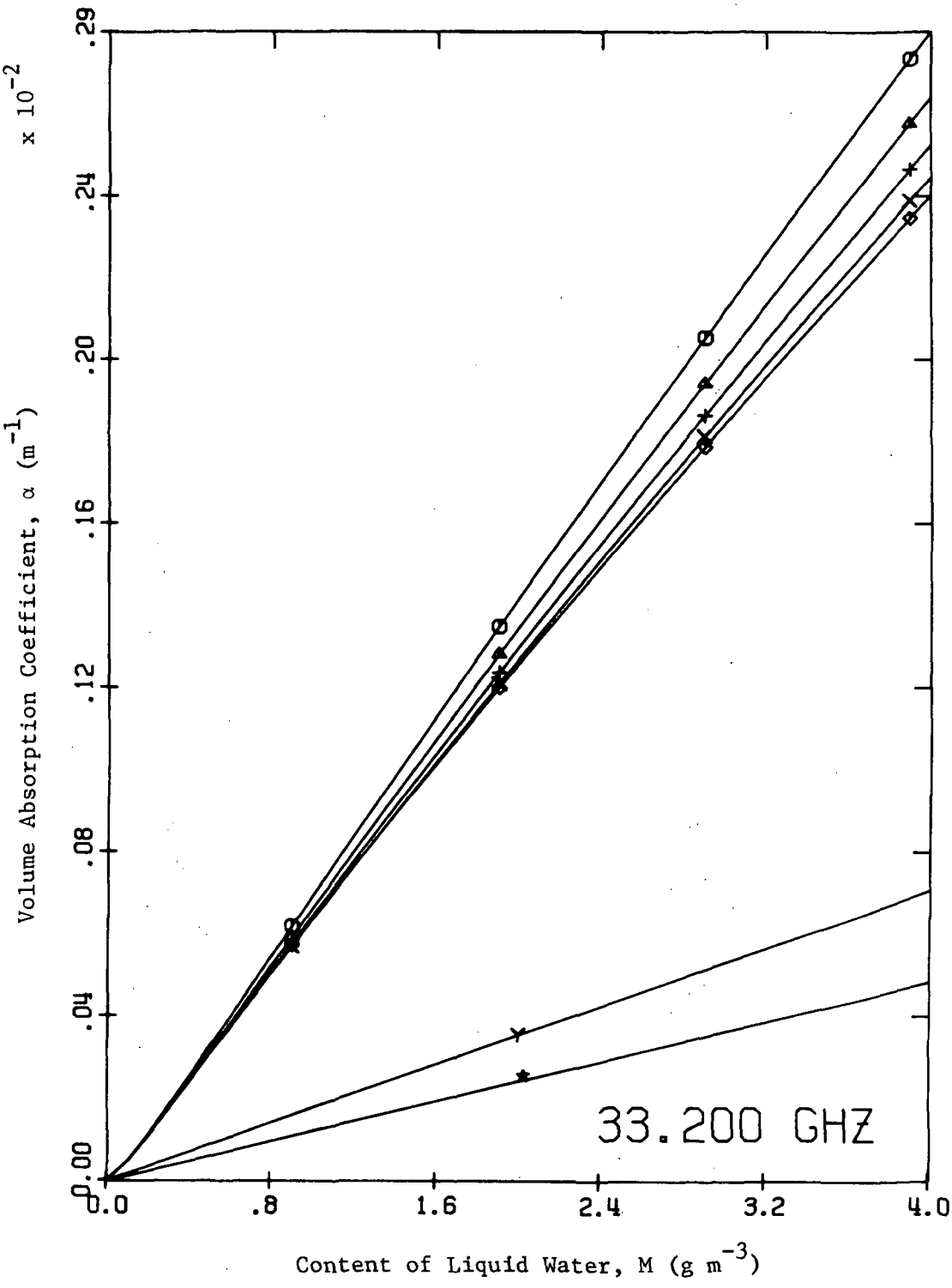

Fig. 49. Rate of absorption of microwaves by liquid water cloud and M-P rain: ν = 33.2 GHz.

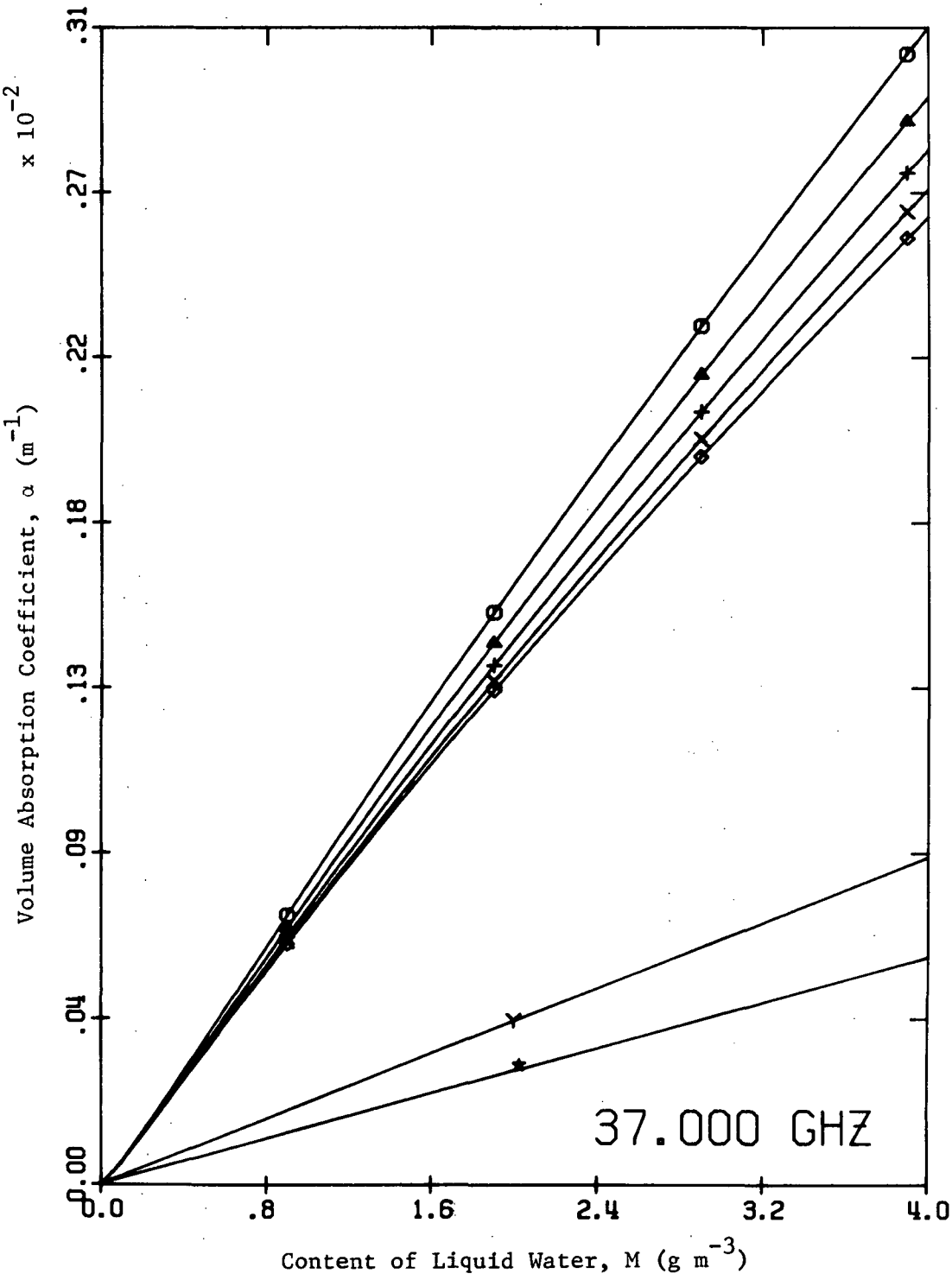

Fig. 50. Rate of absorption of microwaves by liquid water cloud and M-P rain: ν = 37.0 GHz.

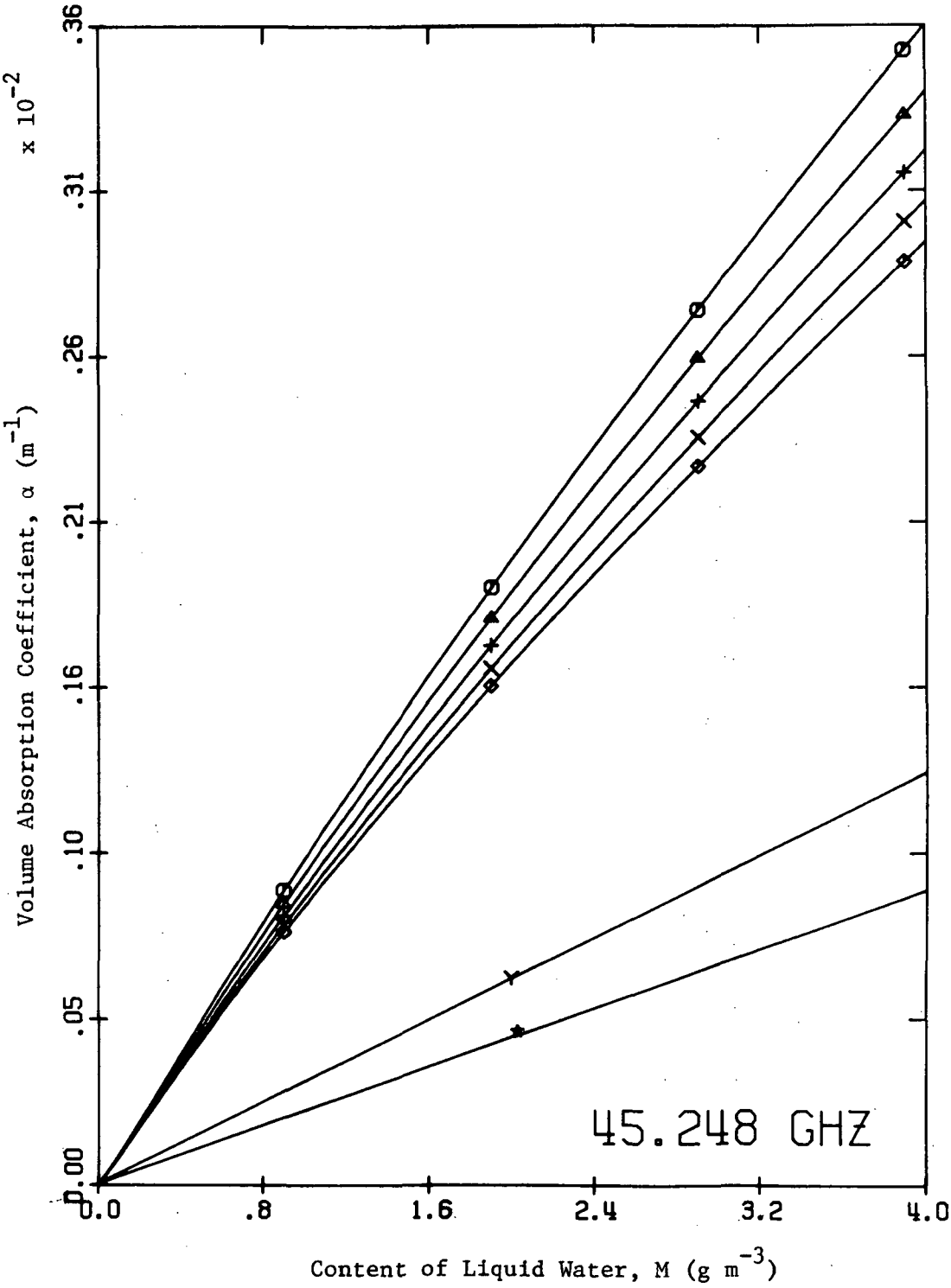

Fig. 51. Rate of absorption of microwaves by liquid water cloud and M-P rain: ν = 45.248 GHz.

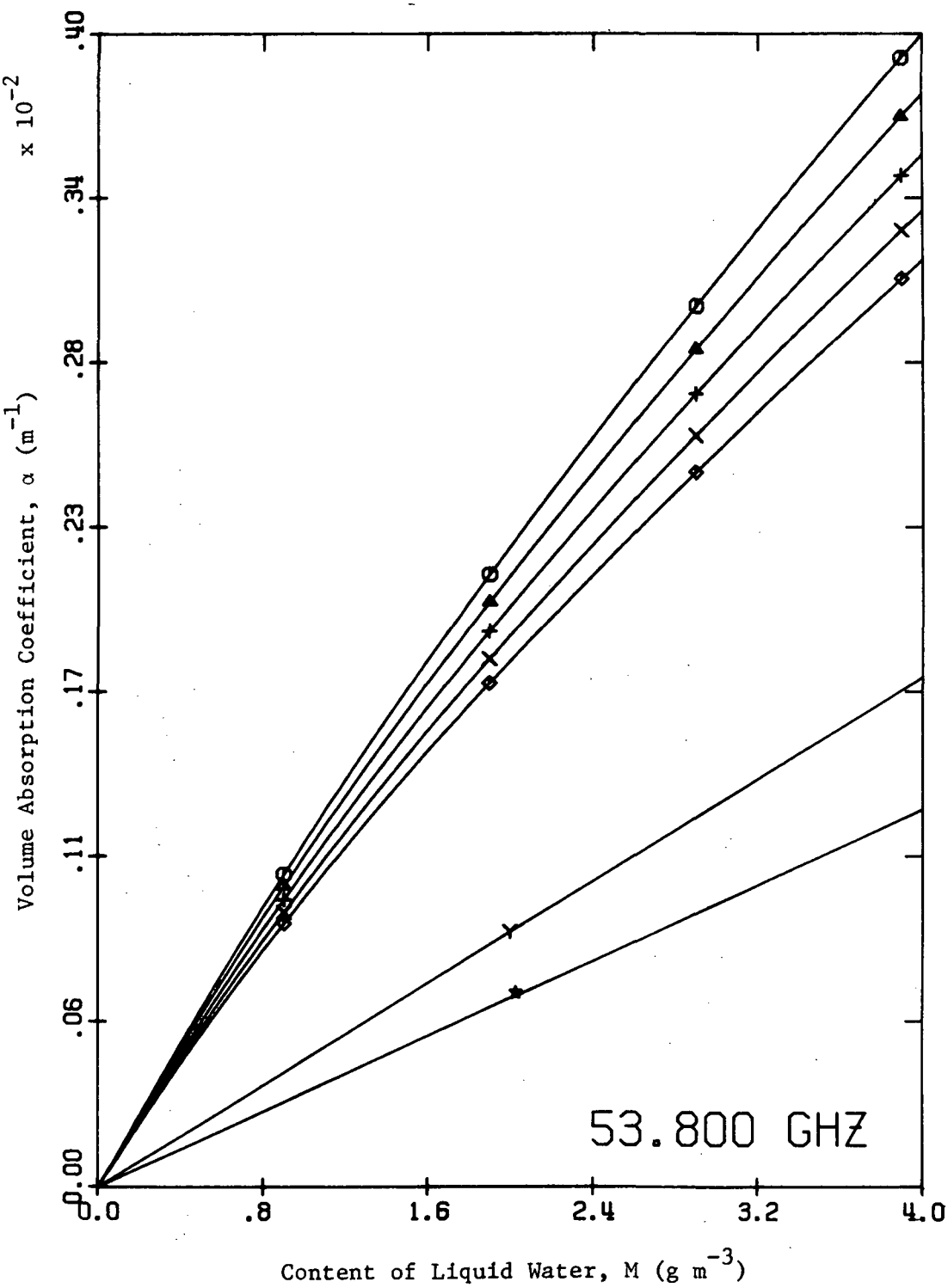

Fig. 52. Rate of absorption of microwaves by liquid water cloud and M-P rain: ν = 53.8 GHz.

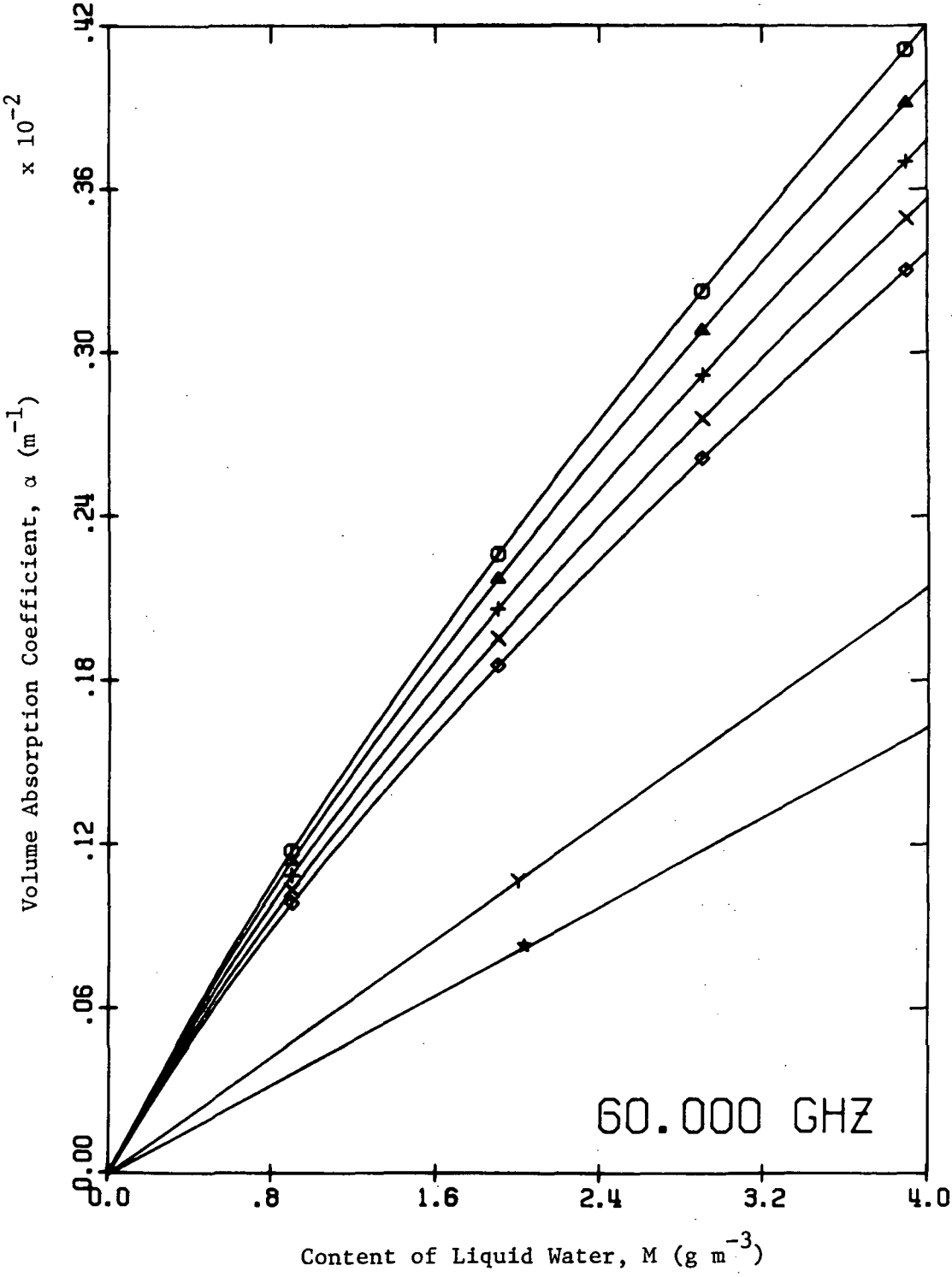

Fig. 53. Rate of absorption of microwaves by liquid water cloud and M-P rain: ν = 60.0 GHz.

An important consideration in the analysis of the microwave emission of liquid water in the atmosphere is the ratio of α_p and α_c. Values of α_p/α_c are shown in Table 20 for a temperature of 10C, for several microwave frequencies, and for several contents of liquid water. The values of α_p and α_c are nearly the same at low frequencies (i.e., $\alpha_p/\alpha_c \simeq 1.0$). This ratio reaches a maximum value at 8.05 at a frequency of 10.69 GHz. The frequency at which α_p/α_c is a maximum shifts to higher values for smaller contents of liquid water. Thus, if one wishes to sense liquid water in the form of rain and desires to minimize the effect of clouds, one would choose frequencies near 10.69 GHz.

In the Rayleigh region (small x), α_p is nearly a linear function of M_p. As the frequency increases to about 8 GHz, the shape of the curves becomes most non-linear. Then, as the frequency is increased still further to near 31.4 GHz, the curves straighten out, and α_p varies almost linearly with M_p. Above 31.4 GHz, the curves begin to show wome slight curvature, but remain quasilinear up to 60 GHz.

The albedo, ω, for single scattering in the medium is of interest in this paper. ω is defined as the ratio of the volume scattering coefficient to the volume extinction coefficient and gives the fraction of the total extinction at a point that is due to scattering. The distribution of ω as a function of the frequency and the content of liquid water in the rain mass for a temperature of 10C

Table 20. Ratio of the volume absorption coefficients of rain and clouds as a function of microwave frequency and the content of liquid water: T = 283.2K (10C).

M	R	Ratio of α_p and α_c (α_p/α_c)					
($g\ m^{-3}$)	($mm\ hr^{-1}$)	ν = 0.5 GHz	ν = 1.42 GHz	ν = 4.805 GHz	ν = 5.81 GHz	ν = 8.0 GHz	ν = 10.69 GHz
0.1	1.2	1.00	1.00	0.97	0.97	1.32	1.93
0.2	2.7	1.00	1.02	1.21	1.32	1.84	2.52
0.4	6.1	1.01	1.05	1.52	1.78	2.55	3.30
0.7	11.8	1.01	1.07	1.83	2.27	3.31	4.10
1.1	20.2	1.01	1.08	2.12	2.77	4.10	4.88
1.6	31.6	1.01	1.10	2.40	3.26	4.89	5.65
2.2	46.1	1.01	1.11	2.66	3.74	5.68	6.39
2.9	64.1	1.01	1.12	2.92	4.22	6.47	7.11
3.7	85.6	1.02	1.13	3.16	4.69	7.26	7.81
4.0	94.0	1.02	1.13	3.24	4.85	7.53	8.05

Table 20 (cont'd.)

M	R	Ratio of α_p and α_c (α_p/α_c)					
($g\ m^{-3}$)	($mm\ hr^{-1}$)	ν = 15.375 GHz	ν = 19.35 GHz	ν = 31.4 GHz	ν = 37.0 GHz	ν = 45.248 GHz	ν = 60.0 GHz
0.1	1.2	2.61	2.84	3.06	3.07	3.02	2.78
0.2	2.7	3.13	3.27	3.21	3.12	2.94	2.58
0.4	6.1	3.76	3.75	3.37	3.17	2.87	2.38
0.7	11.8	4.36	4.20	3.51	3.22	2.82	2.24
1.1	20.2	4.92	4.60	3.63	3.25	2.77	2.13
1.6	31.6	5.43	4.96	3.73	3.28	2.74	2.04
2.2	46.1	5.91	5.28	3.81	3.30	2.71	1.97
2.9	64.1	6.36	5.59	3.89	3.33	2.68	1.91
3.7	85.6	6.78	5.86	3.96	3.35	2.66	1.86
4.0	94.0	6.92	5.96	3.98	3.35	2.65	1.84

is shown in Fig. 54. It is obvious from these values that scattering of microwaves by rain may be a significant extinction process for high frequencies and large contents of liquid water. If a value of 0.1 for ω can be used as a rough guide, then one sees that scattering must be considered for frequencies of about 10 GHz or higher. If scattering is an important extinction process, then it must be an important emission process since scattered radiation must be conserved. The effects of scattering will be considered in greater detail in later chapters.

In order to show the effects of changes in temperature on α_p, the ratio of α_p (30C) to α_p (10C) was calculated for several frequencies and contents of liquid water. When this ratio is slightly less than unity, the variation of α_p with temperature is such that the thermal emission of the rain mass tends to be independent of its temperature. Such a condition exists for small values of M_p at all frequencies and for large values of M_p for frequencies less than about 15 GHz or greater than about 30 GHz. This behavior for small values of M_p is expected since the Rayleigh theory fits best for this condition.

The curves in Figs. 36 to 53 suggest that α_p may be represented by a simple power law, viz.,

$$\alpha_p = c_1 M_p^d , \tag{166}$$

where α_p is the volume absorption coefficient of the rain mass (m^{-1}), M_p is the content of liquid water of the rain mass (g m^{-3}), and c_1

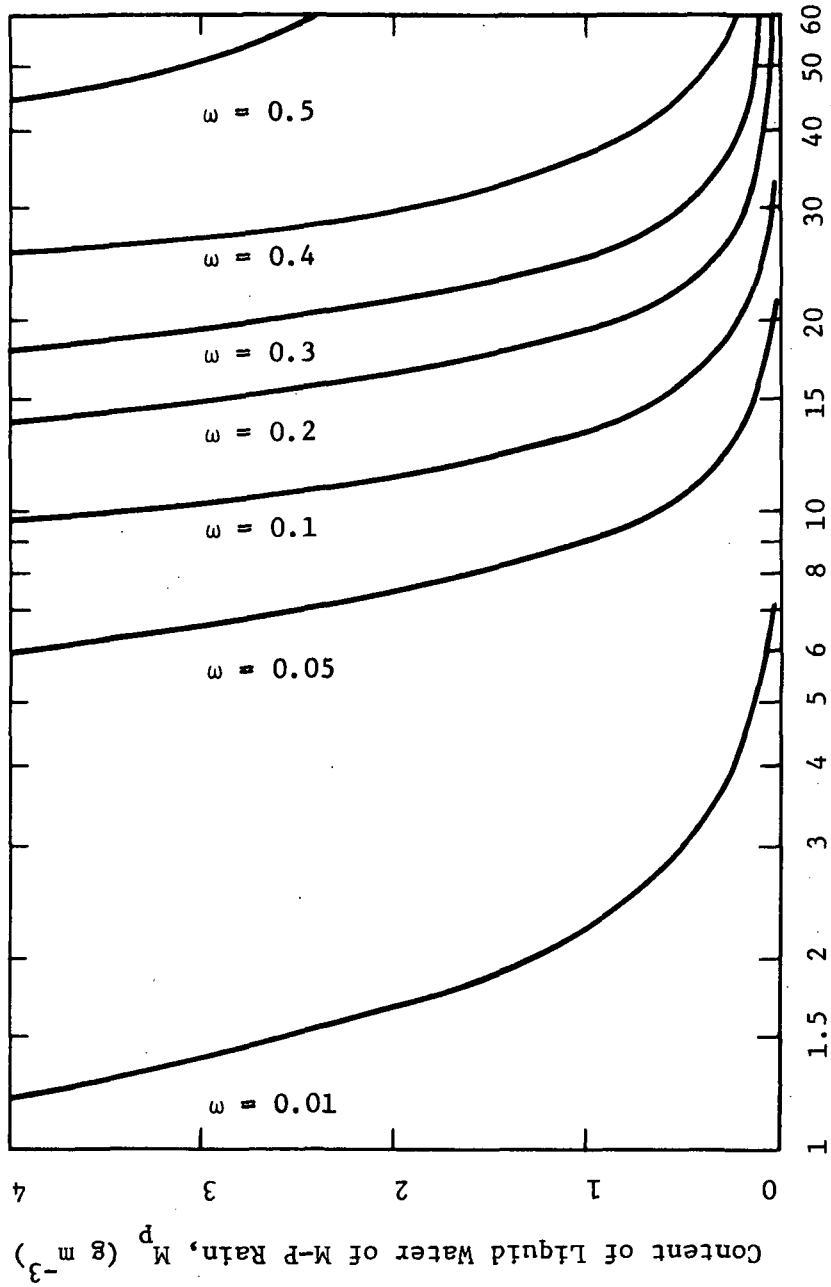

Fig. 54. Albedo for single scattering ω of M-P rain at microwave frequencies.

and d are functions of temperature and frequency. Eq. (166) may be linearized by taking the logarithm of both sides. From the resulting expression and the computed values of α_p, values of c_1 and d were found by a standard regression technique (Brooks and Carruthers, 1953). The resulting values were fit exactly to a fourth-degree polynomial in T of the form,

$$c_1 = f_o + f_1 T + f_2 T^2 + f_3 T^3 + f_4 T^4 \tag{167}$$

and

$$d = g_o + g_1 T + g_2 T^2 + g_3 T^3 + g_4 T^4, \tag{168}$$

where T is the temperature (C).

The resulting values of f_i and g_i (i = 0, 1, 2, 3, 4) are given in Appendix A. The values of d are plotted in Fig. 55 versus frequency for temperatures of -10, 0, 10, 20, and 30C. These curves may be interpreted as being a plot of the linearity of α_p as a function of temperature and frequency. From them, it is obvious that the greatest non-linearity of α_p with respect to M_p occurs at 7.3 GHz and that α_p is a linear function of M_p for low frequencies and frequencies near 39 GHz where d = 1.0.

E. Angular Scattering Matrix of Rain

Scattering in non-raining clouds is neglected in this paper. However, angular scattering will be considered for a special case of the transfer of thermal microwaves through rain. In these considerations, a knowledge will be needed of the probability

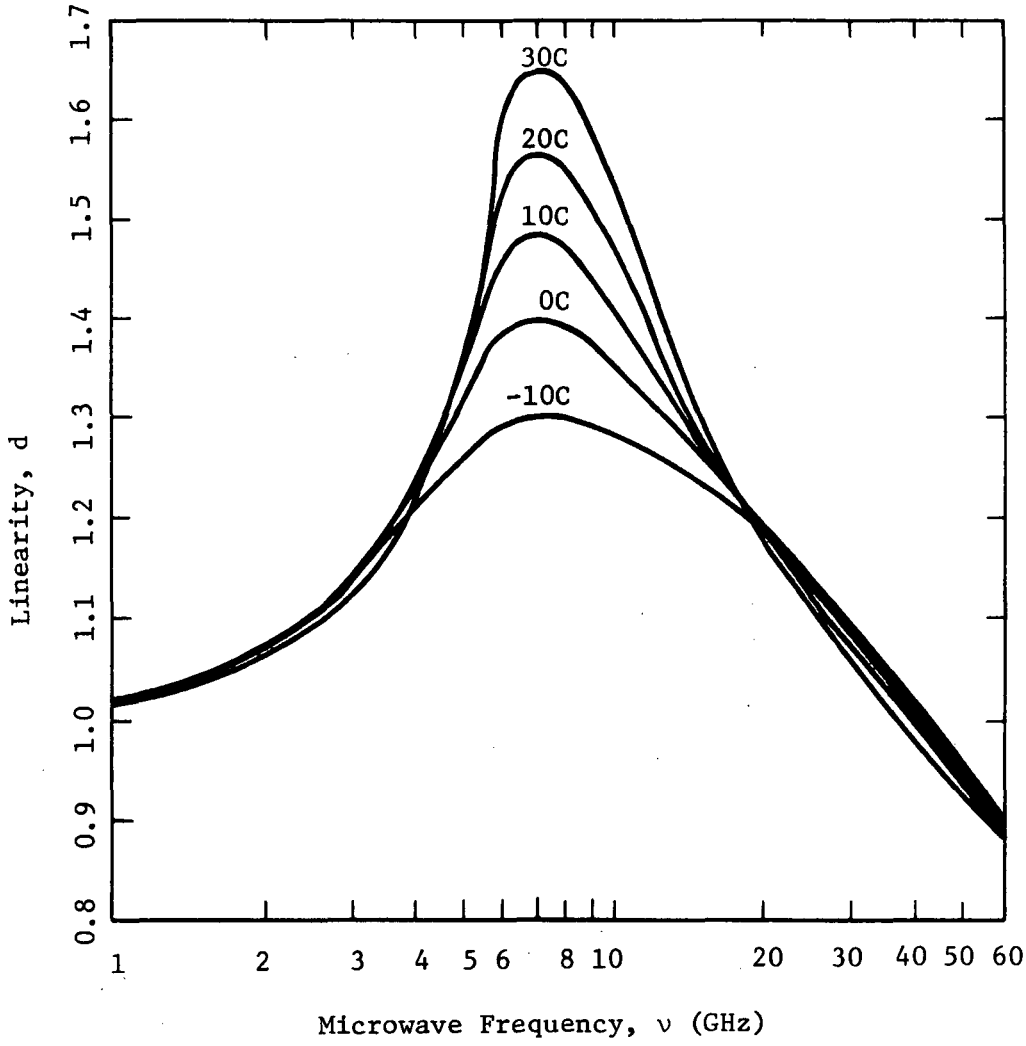

Fig. 55. Linearity of the volume absorption coefficient of a M-P rain with respect to the content of liquid water.

distribution function for angular scattering at any point of interest in the atmosphere. Since the field of microwave radiation will be represented by a set of microwave photons the states of which are described by appropriate Stokes parameters, one needs to know only how the Stokes vector is transformed for any given angular scattering encounter.

One may form a transformation matrix [Σ'] for angular scattering for a polydisperse collection of rain elements by integrating the elements of the transformation matrix [F] for angular scattering for individual drops over a given distribution of drop diameters, such as the M-P distribution. Moreover, one may view the distribution of $\frac{1}{2}(\Sigma_1' + \Sigma_2')$ with scattering angle as representing the probability distribution function for angular scattering. This distribution may be transformed to a normalized distribution, η, by dividing $\frac{1}{2}(\Sigma_1' + \Sigma_2')$ by q_1 where

$$q_1 = \int_0^{\pi} \frac{1}{2}(\Sigma_1' + \Sigma_2') \, d\theta \ . \tag{169}$$

In the Monte Carlo method, the transformation matrix [Σ'] is used to determine the state of a scattered microwave photon. In order to insure that the scattered photon has the same total intensity as the incident photon, one must normalize [Σ'] by multiplying it by the scalar quantity, q_2, where

$$q_2 = \frac{I_v + I_h}{I_v \Sigma_1' + I_h \Sigma_2'} = \frac{2I}{I(\Sigma_1' + \Sigma_2') + Q(\Sigma_1' - \Sigma_2')} \ . \tag{170}$$

Thus, the normalized transformation matrix [Σ], which is equal to q_2 [Σ'], depends on both the scattering properties of the medium and the polarized components of the radiation being scattered.

CHAPTER VII

MODELING OF THE ATMOSPHERE FOR RADIATIVE TRANSFER

In order to solve the direct problem of radiative transfer, one must specify the spatial distribution of appropriate radiational quantities (e.g., temperature, volume absorption coefficient, volume scattering coefficient, and angular scattering parameters). At microwave frequencies, one may obtain the distribution of these quantities from the spatial distribution of atmospheric parameters (e.g., temperature, dew-point temperature, liquid water in cloud form, and liquid water in precipitation form). The specific relationships between radiational and meteorological quantities were discussed in the preceding chapters. The purpose of this chapter is two-fold. First, several hundred model distributions of the atmospheric variables are selected and enumerated. These distributions are based on measurements of atmospheric parameters as reported in the literature. Second, the specific computational procedures are explained in detail for computer modeling of the atmosphere for radiative transfer.

The largest variations of atmospheric temperature and pressure occur with changes in altitude. The distribution of moisture, as represented by the distributions of dew-point temperature and the contents of liquid water, is highly variable in all three spatial dimensions. In this paper, however, the atmosphere is assumed to

be horizontally homogeneous.

A. Distributions of Temperature and Dew-Point Temperature

Cole et al. (1965) give the distributions with pressure of temperature and relative humidity for several standard atmospheres which are supplemental to the U. S. Standard Atmosphere of 1962. Distributions of temperature with pressure in several tropical storms are given by Riehl (1954, p. 328). Petterssen (1956, p. 33) gives several soundings of temperature which are representative of maritime-tropical (mT) air. Average soundings of temperature and water-vapor density in maritime-polar (mP) air are given by Lukes (1968, p. 24). All of these soundings were plotted on a Skew-T Log-P diagram. It was apparent from this plot that these soundings may be represented by seven typical distributions with pressure of temperature and dew-point temperature for a cloudless atmosphere, as enumerated in Tables 21 to 27. The coldest temperatures are found in the Mid-Latitude (Winter) model, and the warmest in the Tropical Storm model. Air colder than that of these models may be found over the World Ocean; however, there could be no significant amounts of liquid water in such air since the air would be below freezing.

B. Distributions of Liquid Water

The content of liquid water of non-raining clouds increases

Table 21. Model Number 1, Tropical Storm after Riehl (1954, p. 328) and Petterssen (1956, Vol II, p. 33).

p (mb)	T (K)	T_d (K)	$\bar{p}$ (mb)	$\bar{T}$ (K)	$\bar{T}_d$ (K)	z (m)
1013.25	303.7	300.2				
			981.6	302.3	298.9	577.7
950.0	301.0	297.6				
			925.0	299.8	296.4	479.9
900.0	298.5	295.3				
			875.0	297.3	294.2	502.8
850.0	296.1	293.1				
			825.0	294.7	291.7	528.2
800.0	293.4	290.3				
			775.0	292.0	288.8	556.5
750.0	290.7	287.3				
			725.0	289.2	286.0	588.7
700.0	287.8	284.7				
			675.0	286.1	282.9	624.9
650.0	284.4	281.2				
			625.0	282.7	279.5	666.3
600.0	281.1	277.8				
			575.0	279.1	275.9	714.5
550.0	277.2	274.0				
			525.0	275.0	272.6	770.6
500.0	272.9	271.3				
			475.0	270.4	268.2	837.0
450.0	268.0	265.2				
			425.0	265.1	262.5	916.4
400.0	262.3	259.8				
			375.0	259.1	256.5	1014.5
350.0	255.9	253.2				
			325.0	252.0	249.0	1138.5
300.0	248.2	244.9				
			275.0	243.3	239.5	1299.4
250.0	238.5	234.2				
			225.0	232.5	227.7	1519.0
200.0	226.5	221.2				
			175.0	218.8	185.6	1842.2
150.0	211.0	150.0				
			125.0	200.1	150.0	2373.0
100.0	189.2	150.0				
			75.0	189.2	150.0	3839.0
50.0	189.2	150.0				

The precipitable water of this model is 80.3 mm.

Table 22. Model Number 2, Tropical (Sub-tropical Summer) after Cole *et al.* (1965, p. 2-9) and Petterssen (1956, Vol II, p. 33).

p (mb)	T (K)	T_d (K)	$\bar{p}$ (mb)	$\bar{T}$ (K)	$\bar{T}_d$ (K)	z (m)
1013.25	300.4	295.5				
			981.6	298.7	293.9	569.0
950.0	297.1	292.4				
			925.0	295.7	291.0	472.0
900.0	294.4	289.7				
			875.0	292.9	288.3	493.8
850.0	291.5	287.0				
			825.0	290.0	285.1	518.0
800.0	288.5	283.3				
			775.0	286.9	281.3	544.9
750.0	285.3	279.4				
			725.0	283.6	277.4	575.2
700.0	281.9	275.4				
			675.0	280.0	272.5	609.5
650.0	278.2	269.7				
			625.0	276.3	266.9	648.9
600.0	274.4	264.1				
			575.0	272.3	260.6	694.8
550.0	270.3	257.2				
			525.0	268.1	255.0	748.8
500.0	265.9	252.9				
			475.0	263.4	250.8	813.0
450.0	260.9	248.7				
			425.0	258.0	246.0	890.2
400.0	255.2	243.4				
			375.0	252.1	240.2	985.8
350.0	249.0	237.0				
			325.0	245.3	233.6	1107.3
300.0	241.7	230.2				
			275.0	237.4	224.7	1267.1
250.0	233.1	219.2				
			225.0	227.9	184.6	1488.6
200.0	222.7	150.0				
			175.0	215.9	150.0	1818.5
150.0	209.2	150.0				
			125.0	202.7	150.0	2405.8
100.0	196.2	150.0				
			75.0	196.2	150.0	3980.8
50.0	196.2	150.0				

The precipitable water of this model is 45.4 mm.

Table 23. Model Number 3, Mid-latitude Summer after Cole et al. (1965, p. 2-9).

p (mb)	T (K)	T_d (K)	$\bar{p}$ (mb)	$\bar{T}$ (K)	$\bar{T}_d$ (K)	z (m)
1013.25	294.2	289.8				
			981.6	292.9	287.8	556.3
950.0	291.7	285.9				
			925.0	290.6	284.5	462.5
900.0	289.5	283.2				
			875.0	288.4	281.6	484.9
850.0	287.4	280.1				
			825.0	286.2	278.3	509.9
800.0	285.0	276.5				
			775.0	283.5	274.4	537.4
750.0	282.1	272.4				
			725.0	280.4	270.1	567.8
700.0	278.8	267.9				
			675.0	276.9	265.5	601.8
650.0	275.0	263.2				
			625.0	273.0	261.2	640.6
600.0	271.0	259.2				
			575.0	268.9	256.5	685.8
550.0	266.9	253.9				
			525.0	264.6	251.0	738.9
500.0	262.4	248.2				
			475.0	259.9	246.0	802.0
450.0	257.4	243.9				
			425.0	254.5	241.1	877.9
400.0	251.7	238.4				
			375.0	248.4	235.8	971.4
350.0	245.2	233.2				
			325.0	241.7	230.2	1090.8
300.0	238.2	227.2				
			275.0	234.1	223.3	1249.5
250.0	230.0	219.4				
			225.0	225.2	184.7	1471.0
200.0	220.4	150.0				
			175.0	218.0	150.0	1836.2
150.0	215.7	150.0				
			125.0	215.7	150.0	2560.1
100.0	215.7	150.0				
			75.0	215.7	150.0	4376.5
50.0	215.7	150.0				

The precipitable water of this model is 29.3 mm.

Table 24. Model Number 4, Sub-tropical Winter after Cole et al. (1965, p. 2-9).

p (mb)	T (K)	T_d (K)	$\bar{p}$ (mb)	$\bar{T}$ (K)	$\bar{T}_d$ (K)	z (m)
1021.0	287.2	284.1				
			985.5	286.2	282.6	606.7
950.0	285.3	281.2				
			925.0	284.6	280.1	452.3
900.0	284.0	279.1				
			875.0	283.3	277.2	475.7
850.0	282.6	275.4				
			825.0	281.8	273.5	501.5
800.0	281.0	271.7				
			775.0	279.2	269.7	528.7
750.0	277.4	267.7				
			725.0	275.6	265.6	557.6
700.0	273.8	263.6				
			675.0	271.9	261.0	590.7
650.0	270.1	258.4				
			625.0	268.0	255.8	628.6
600.0	266.0	253.2				
			575.0	263.6	250.3	671.9
550.0	261.3	247.4				
			525.0	259.1	245.4	723.2
500.0	256.9	243.4				
			475.0	254.3	241.1	784.5
450.0	251.7	238.8				
			425.0	248.7	236.0	857.6
400.0	245.7	233.2				
			375.0	242.9	230.8	949.6
350.0	240.1	228.4				
			325.0	236.6	225.4	1067.7
300.0	233.1	222.4				
			275.0	229.1	186.2	1222.7
250.0	225.1	150.0				
			225.0	220.6	150.0	1440.9
200.0	216.1	150.0				
			175.0	213.6	150.0	1799.1
150.0	211.2	150.0				
			125.0	207.9	150.0	2468.1
100.0	204.7	150.0				
			75.0	200.9	150.0	4077.2
50.0	197.2	150.0				

The precipitable water of this model is 21.2 mm.

Table 25. Model Number 5, Sub-arctic Summer after Cole et al. (1965, p. 2-9).

p (mb)	T (K)	T_d (K)	$\bar{p}$ (mb)	$\bar{T}$ (K)	$\bar{T}_d$ (K)	z (m)
1010.0	287.2	283.0				
			980.0	285.8	281.6	514.5
950.0	284.4	280.3				
			925.0	283.2	278.6	449.9
900.0	282.1	277.0				
			875.0	280.7	275.8	471.2
850.0	279.4	274.6				
			825.0	278.0	273.2	494.8
800.0	276.7	271.9				
			775.0	275.2	270.1	521.2
750.0	273.8	268.3				
			725.0	272.3	267.0	551.1
700.0	270.9	265.7				
			675.0	269.3	263.9	585.2
650.0	267.7	262.2				
			625.0	266.0	260.2	624.2
600.0	264.4	258.3				
			575.0	262.5	255.5	669.4
550.0	260.7	252.7				
			525.0	275.6	250.5	769.4
500.0	290.5	248.3				
			475.0	270.3	246.1	834.2
450.0	250.2	243.9				
			425.0	247.3	241.1	852.9
400.0	244.4	238.4				
			375.0	241.2	234.5	943.2
350.0	238.1	230.7				
			325.0	234.3	226.4	1057.6
300.0	230.6	222.2				
			275.0	227.9	186.1	1216.3
250.0	225.2	150.0				
			225.0	225.2	150.0	1471.0
200.0	225.2	150.0				
			175.0	225.2	150.0	1896.4
150.0	225.2	150.0				
			125.0	225.2	150.0	2672.8
100.0	225.2	150.0				
			75.0	225.2	150.0	4569.2
50.0	225.2	150.0				

The precipitable water of this model is 21.2 mm.

Table 26. Model Number 6, Maritime Polar after Lukes (1968).

p (mb)	T (K)	T_d (K)	$\bar{p}$ (mb)	$\bar{T}$ (K)	$\bar{T}_d$ (K)	z (m)
1013.25	282.7	278.4				
			981.6	281.0	276.2	531.7
950.0	279.3	274.0				
			925.0	277.8	272.3	440.8
900.0	276.4	270.7				
			875.0	274.9	268.8	460.9
850.0	273.5	267.0				
			825.0	271.9	264.8	483.2
800.0	270.3	262.5				
			775.0	268.6	260.5	508.1
750.0	267.0	258.5				
			725.0	265.2	256.1	536.0
700.0	263.4	253.7				
			675.0	261.5	251.5	567.7
650.0	259.7	249.3				
			625.0	257.5	246.5	603.7
600.0	255.4	243.7				
			575.0	253.2	240.8	645.1
550.0	251.0	238.0				
			525.0	248.6	235.7	693.7
500.0	246.2	233.4				
			475.0	243.7	231.0	751.7
450.0	241.2	228.7				
			425.0	238.6	226.4	822.7
400.0	236.0	224.2				
			375.0	233.2	187.1	911.5
350.0	230.4	150.0				
			325.0	227.1	150.0	1024.7
300.0	223.8	150.0				
			275.0	221.0	150.0	1179.5
250.0	218.2	150.0				
			225.0	218.2	150.0	1425.2
200.0	218.2	150.0				
			175.0	218.2	150.0	1837.5
150.0	218.2	150.0				
			125.0	218.2	150.0	2589.8
100.0	218.2	150.0				
			75.0	218.2	150.0	4427.2
50.0	218.2	150.0				

The precipitable water of this model is 11.0 mm.

Table 27. Model Number 7, Mid-latitude Winter after Cole et al. (1965, p. 2-9).

p (mb)	T (K)	T_d (K)	$\bar{p}$ (mb)	$\bar{T}$ (K)	$\bar{T}_d$ (K)	z (m)
1018.0	278.2	274.5				
			984.0	276.1	272.3	560.0
950.0	274.0	270.2				
			925.0	272.3	268.7	431.8
900.0	270.7	267.2				
			875.0	268.9	264.8	450.6
850.0	267.2	262.5				
			825.0	266.3	261.4	473.2
800.0	265.5	260.4				
			775.0	264.6	258.9	500.5
750.0	263.8	257.4				
			725.0	262.9	255.5	531.4
700.0	262.0	253.7				
			675.0	260.4	252.4	565.2
650.0	258.8	251.2				
			625.0	257.0	249.0	602.5
600.0	255.2	246.9				
			575.0	253.2	244.4	645.1
550.0	251.2	242.0				
			525.0	249.1	240.5	695.2
500.0	247.0	239.0				
			475.0	244.6	236.6	754.7
450.0	242.3	234.2				
			425.0	239.8	231.2	827.1
400.0	237.4	228.2				
			375.0	234.8	225.7	917.8
350.0	232.2	223.2				
			325.0	229.2	186.6	1034.2
300.0	226.2	150.0				
			275.0	222.8	150.0	1189.1
250.0	219.4	150.0				
			225.0	219.1	150.0	1431.4
200.0	218.9	150.0				
			175.0	218.4	150.0	1839.6
150.0	218.0	150.0				
			125.0	217.3	150.0	2579.7
100.0	216.7	150.0				
			75.0	216.0	150.0	4383.6
50.0	215.4	150.0				

The precipitable water of this model is 9.6 mm.

with altitude above the cloud base and reaches a maximum near the 0C isotherm if the upper part of the cloud is below freezing or at a level where the pressure is about 50 mb greater than the pressure at the top of the cloud if the cloud is warmer than freezing (Singleton and Smith, 1960; Warner, 1955; Ackerman, 1959). Above the maximum point, the content of liquid water decreases to zero at the top of the cloud or at the point where the temperature is less than about -20C. In this paper, the distribution of liquid water in a cloud is assumed to be linear from the base to the maximum value and from the maximum value to the top of the liquid-water cloud. Since the dielectric properties of liquid water have not been determined for temperatures colder than -10C, the top of the liquid-water cloud was not allowed to exceed the height of the -10C isotherm. The distribution of liquid water in clouds assumed in this paper is shown in Fig. 56.

The rainfall rate increases with altitude, is a maximum near the 0C isotherm, and decreases to zero near the -20C isotherm. It is assumed that M_p, the content of liquid water in the rain mass, has a constant value from the surface to the 0C isotherm or to a point where the pressure is 50 mb greater than the pressure at the top of the cloud. Also, M_p decreases linearily above that point to zero at the cloud top or at the -10C level, whichever is the lower. The schematic distribution of M_p is shown in Fig. 56.

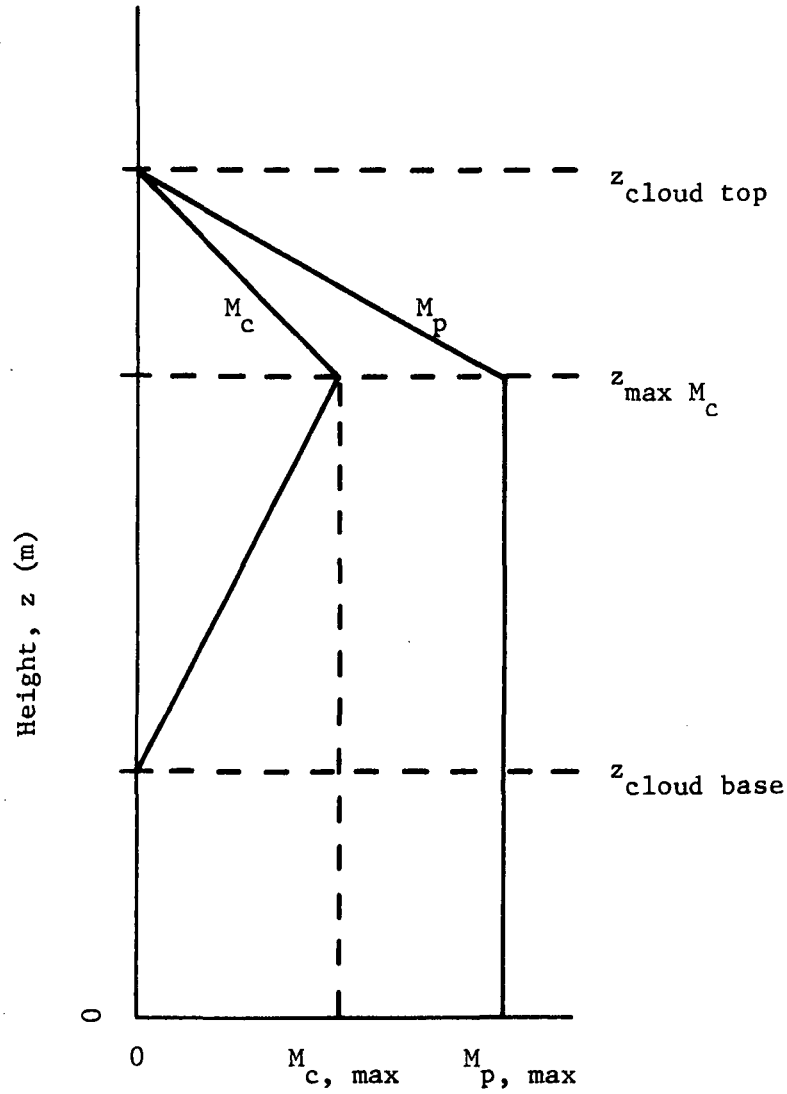

Fig. 56. Schematic distribution of liquid water with altitude in clouds and rain.

The maximum value of M_c in most clouds is less than 3.7 g m^{-3} (Ackerman, 1959; Singleton and Smith, 1960). The average value of M_c for stratiform clouds is about 0.2 g m^{-3} (Lukes, 1968, p. 93; Holzer, 1965; Aufm Kampe, 1950) and is about 0.5 g m^{-3} for cumuliform clouds (Lukes, 1968). M_c rarely exceeds 1.0 g m^{-3} for clouds less than 1 km thick. Stepanenko (1969) made a study of the average thickness and extreme thickness of various types of clouds. The most frequent thickness of altocumulus, altostratus, and stratocumulus clouds is 2 km. Thicknesses for cumuliform clouds up to 10 km were observed in his study.

On the basis of these studies and because of the limitations of the expressions relating radiative quantities and meteorological quantities, the maximum values of M_c and M_p used in this paper are presented in Table 28. The cloud types used in this paper are given in Table 29.

The tops and bases of the clouds were changed by 100-mb increments for each of the seven basic model atmospheres. Then, for each given geometry, the maximum values of M_c and M_p were set to the values listed in Table 28. The dew-point temperature was set equal to the air temperature in the clouds or rain, and the drop temperature was assumed to be equal to the air temperature. Combinations of these cloud geometries, liquid water contents, and basic distributions of temperature and dew-point temperature resulted in 582 model atmospheres. Of these, seven represented cloudless

Table 28. Maximum values of M_c and M_p used in this paper.

M_c(no rain) ($g\ m^{-3}$)	M_c(rain) ($g\ m^{-3}$)	M_p(Ac, CuH) ($g\ m^{-3}$)	M_p(Cu) ($g\ m^{-3}$)	M_p(Cb) ($g\ m^{-3}$)
0.1	0.4	0.088	0.088	0.088
0.2	1.1	0.28	0.28	0.28
0.4		0.5	0.5	0.5
0.7			0.89	0.89
1.1			1.4	1.4
1.6				1.95
2.2				3.0
2.9				4.0
3.7				

Table 29. Cloud bases and tops used in this paper.

Nomenclature	Base (mb)	Top (mb)
Cumulus Humilis (CuH)	950	900
Cumulus (Cu)	950	600 - 850
Cumulonimbus (Cb)	950	400 - 550
Altocumulus (Ac)	$\geq$ 750	400 - 700

atmospheres, 255 represented rainless atmospheres, and 320 represented atmospheres containing rain. The distributions of these model atmospheres by cloud types are shown in Table 30.

Each of these model atmospheres has a certain amount of gaseous water and liquid water. These quantities are expressed terms of equivalent depths of liquid water which are denoted by W_v, W_c, W_p,

Table 30. Distribution of the 582 model atmospheres by cloud type.

Cloud type	Number of cloud models	Number of rain models	Total
No cloud	——	——	7
CuH	35	42	77
Cu	135	150	285
Cb	45	80	125
Ac	40	48	88

and W_ℓ, where W_v is the precipitable water (mm) or equivalent depth of the total amount of water vapor in the atmosphere (mm), W_c is the equivalent depth of liquid water in the form of clouds in the atmosphere (mm), W_p is the equivalent depth of liquid water in the form of precipitation (rain) in the atmosphere (mm), and W_ℓ is the total equivalent depth of liquid water in combined cloud and rain form (mm). For the 582 model atmospheres, W_v ranges up to 97.41 mm, W_c ranges up to 14.1 mm, and W_p ranges up to 27.47 mm. One may think of these equivalent depths in terms of the areal content of liquid water (kg m^{-2}), where one mm corresponds to one kg m^{-2}. The distributions of W_c, W_p, W_ℓ, and W_v are shown in Figs. 57, 59, 61, and 63. With the exception of W_v, these distributions are skewed highly with an abundance of small values. The logarithms of W_c, W_p, and W_ℓ, however, are distributed more normally

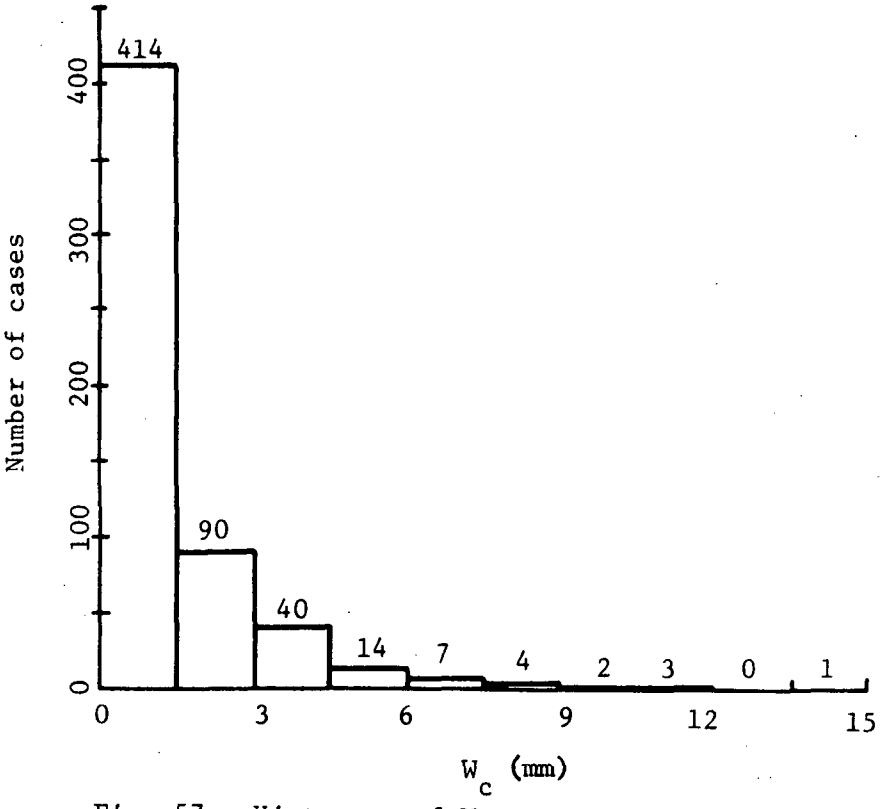

Fig. 57. Histogram of W_c.

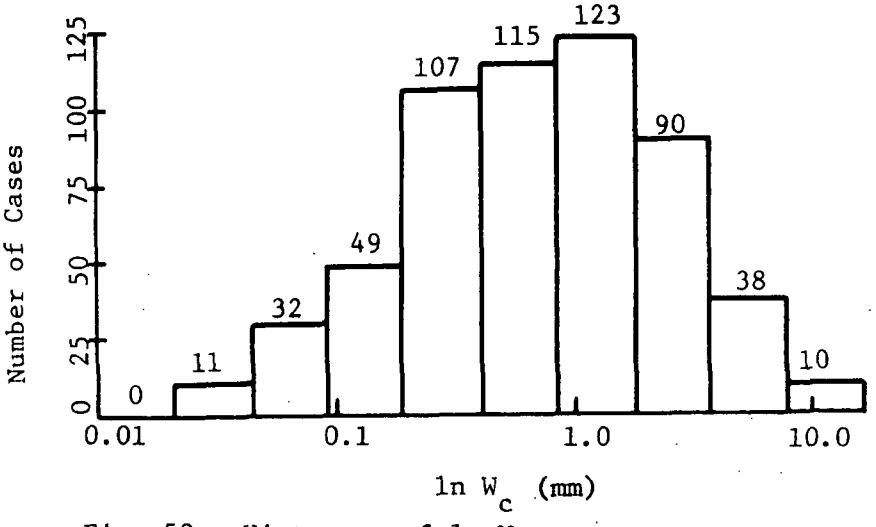

Fig. 58. Histogram of ln W_c.

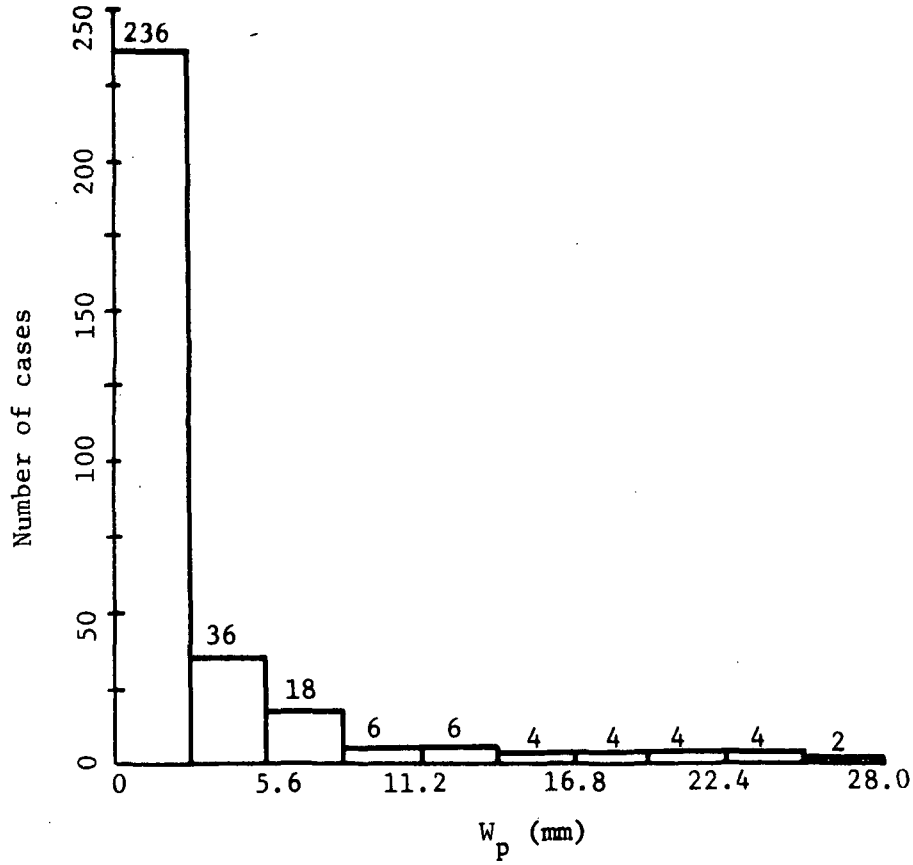

Fig. 59. Histogram of W_p.

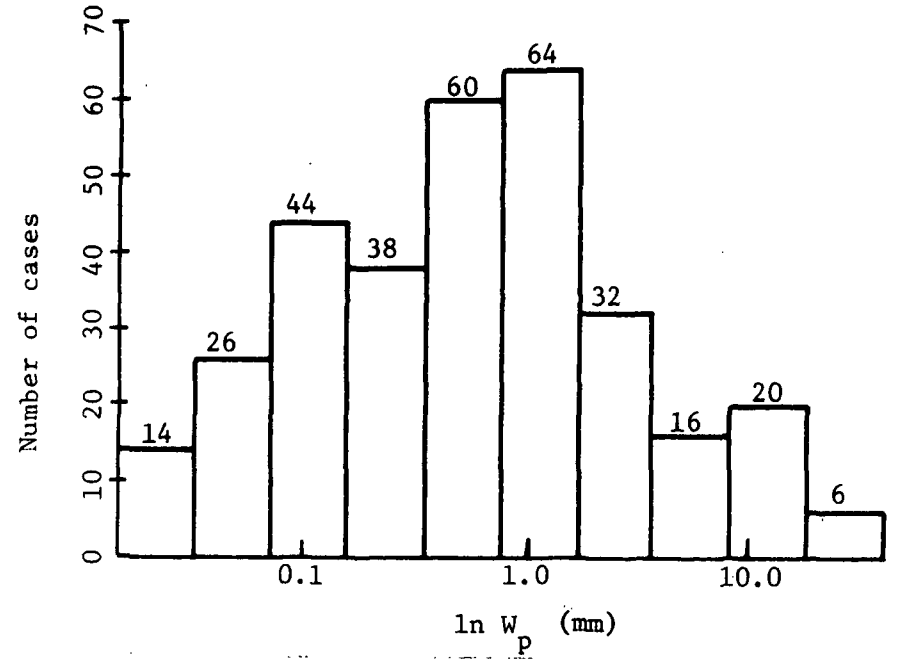

Fig. 60. Histogram of ln W_p.

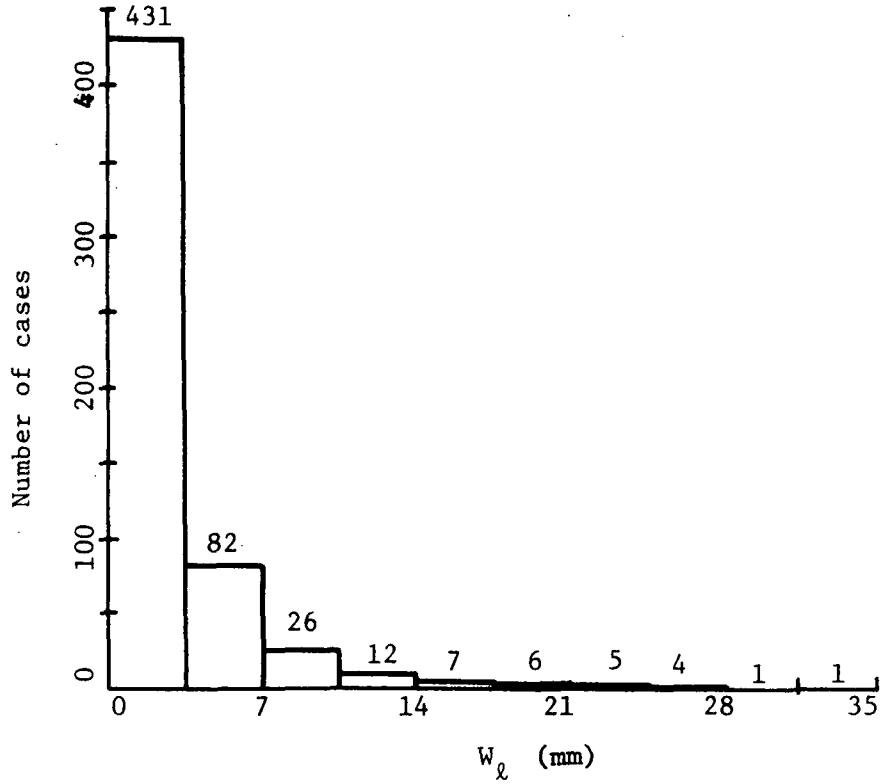

Fig. 61. Histogram of W_ℓ.

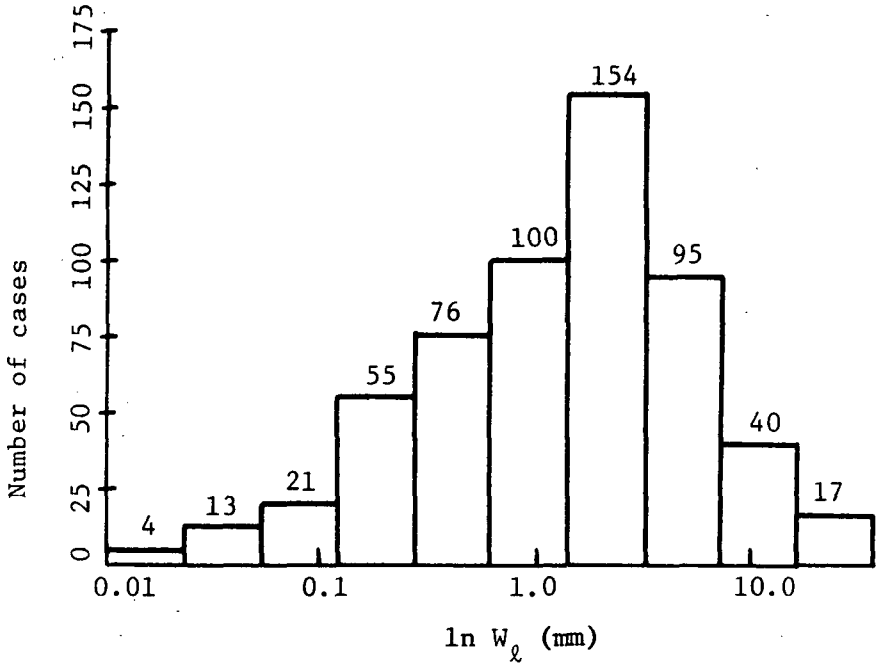

Fig. 62. Histogram of ln W_ℓ.

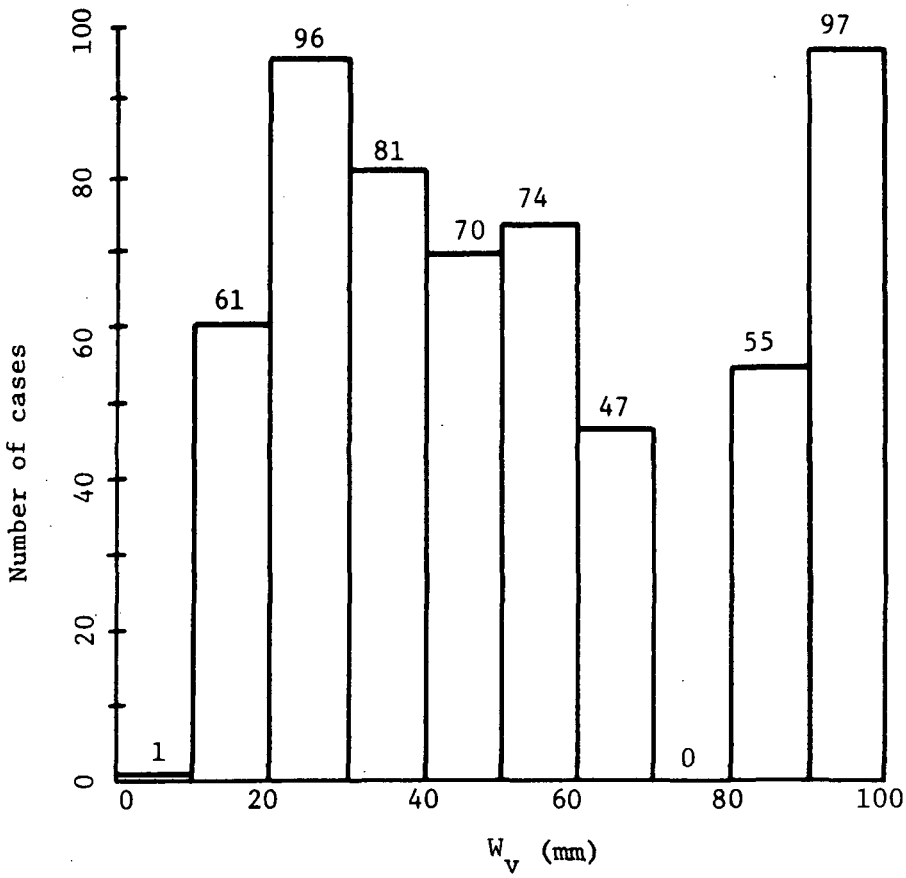

Fig. 63. Histogram of W_v.

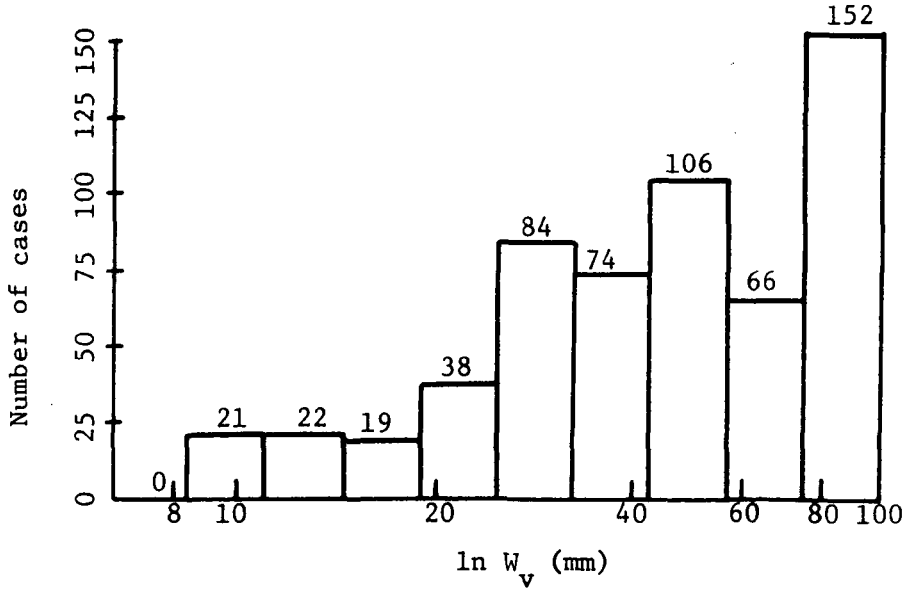

Fig. 64. Histogram of ln W_v.

than those of the variables themselves as seen in Figs. 58, 60, and 62. The distribution of the logarithm of W_v is shown in Fig. 64 for comparison. Regression analyses used in Chapter VII work best when the independent variables (predictors) are not skewed. Thus, it appears that ln W_c, ln W_p, and W_v would be the best predictors. The mean values of these variables and their standard deviations are shown in Table 31.

Table 31. Mean values and standard deviations of W_v, W_c, W_p, and W_ℓ.

Variable	Mean	Standard Deviation
W_v	52.04	27.70
W_c	1.38	1.78
W_p	3.09	4.91
W_ℓ	3.10	4.52

C. Computational Procedure for a Non-Scattering Atmosphere

As was seen in Chapter II, the solution to the problem of the transfer of thermal radiation through the atmosphere is quite simple when scattering processes may be neglected. On the other hand, one may use the solution for the non-scattering case as an approximation to the multiple-scattering case. Most investigators who have solved the radiative transfer problem have assumed that scattering can be neglected; however, they generally have retained scattering

as an extinction process while omitting scattering as an emission process. This assumption is implied when an investigator uses the volume extinction coefficient in an assumed non-scattering atmosphere. Since radiation extincted from one pencil of radiation by scattering must reappear as "emitted" radiation in other pencils of radiation, one either should neglect scattering as both an extinction process and an emission process or should include scattering in both processes. In this paper, the volume absorption coefficient is used to characterize the medium when scattering is neglected. When one approximates a scattering atmosphere by such a non-scattering scheme, one is assuming that extinction and emission by scattering are offsetting phenomena. In the case of a non-scattering atmosphere, (81) and (82) may be used to compute the katabatic and anabatic emission of thermal microwaves from the atmosphere.

Consider the transfer of microwave radiation through a homogeneous, non-scattering slab of thickness, Δz (m). If $\vec{\bar{T}}$ is the temperature vector, $\{\bar{T},0,0,0\}$, where $\bar{T}$ is the mean temperature of the slab (K), then the Stokes vector for radiation emerging from the other side of the slab is given by

$$\vec{T} = \vec{T}_o \exp(-\bar{\alpha}\,\Delta z/\mu) + \bar{T}\,[1 - \exp(-\bar{\alpha}\,\Delta z/\mu)], \qquad (171)$$

where $\bar{\alpha}$ is the mean value of the volume absorption coefficient of the slab (m^{-1}) and $\vec{T}_o$ is the Stokes vector for radiation incident on one side of the slab at a zenith angle whose cosine is μ. This

equation states that the radiation field emerging from a non-scattering slab consists of two parts. The first part is equal to the incident radiation times the transmissivity, Γ_s, of the slab. The second part is equal to the radiation emitted by the slab, i.e., the product of the temperature of the slab and its emissivity. The transmissivity, Γ_s, is $\exp(-\bar{\alpha}\ \Delta z/\mu)$, and the emissivity, ξ_s, is simply $(1 - \Gamma_s)$. In this page, (171) is used to compute the katabatic and anabatic fields of radiation from a plane-parallel, horizontally-homogeneous, non-scattering atmosphere by dividing the atmosphere into a number of homogeneous slabs and progressively transferring radiation from slab to slab. In these calculations, the incident field of radiation is assumed to be zero for the first slab. The transmissivity of the entire atmosphere is simply the product of the transmissivities of all of the slabs in the model atmosphere.

The microwave emission of the liquid-water mass is a function only of the total amount of liquid water in the atmosphere under the following conditions: (1) α is a linear function of the content of liquid water for any given temperature and frequency, and (2) α decreases with increasing temperature. This result is derived below.

The katabatic field of brightness temperatures due to microwave emission from the atmosphere is given in a form similar to (82) as

$$T_k = \lim_{\tilde{h} \to \infty} \int_0^{\tilde{h}} \alpha(z)\, T(z)\, \exp\left[-\int_0^z \alpha(z')\, \frac{dz'}{\mu}\right] \frac{dz}{\mu} \,. \qquad (172)$$

If α is represented by $c_1 M$, then

$$T_k = \lim_{\tilde{h} \to \infty} \int_0^{\tilde{h}} c_1 M(z)\, T(z)\, \exp\left[-\int_0^z c_1 M(z')\, \frac{dz'}{\mu}\right] \frac{dz}{\mu} \qquad (173a)$$

$$= \lim_{\tilde{h} \to \infty} \bar{T} \int_0^{\tilde{h}} c_1 M(z)\, \exp\left[-(c_1/\mu) \int_0^z M(z')\, dz'\right] \frac{dz}{\mu} \,, \qquad (173b)$$

where $\bar{T}$ is the mean temperature of the atmosphere.

The integral under the bracket in (173b) is the total amount of liquid water in the atmosphere below the level z and is denoted by M_z (z) (g m^{-2}). The differential of M_z (z) is simply M(z') dz' since M(0) is identically equal to zero. If one changes variables and takes the integration in (173b) over M_z rather than over z, one obtains the expression:

$$T_k = \lim_{\tilde{h} \to \infty} \bar{T} \int_{M_z(0)}^{M_z(\tilde{h})} \exp(-c_1 M_z(z)/\mu)\, \frac{c_1\, dM_z}{\mu} \,. \qquad (174)$$

The integral in (174) is now in a standard form, namely, exp(-u) du, where u is $(c_1 M_z/\mu)$. Thus,

$$T_k = \lim_{\tilde{h} \to \infty} \bar{T}\, [\exp(-c_1 M_z(0)/\mu) - \exp(-c_1 M_z(\tilde{h})/\mu]. \qquad (175)$$

However, $M_z(0)$ is zero, and $M_z(\tilde{h})$ approaches the total amount of liquid water in the atmosphere, M_∞ (g m^{-2}), as $\tilde{h}$ approaches infinity. Thus, the katabatic field of brightness temperature is dependent upon the total amount of liquid water in the atmosphere for any

given temperature distribution irrespective of the vertical distribution of the liquid water. Eq. (175) then reduces to

$$T_k = \bar{T} \left[1 - \exp(-c_1 M_\infty/\mu)\right]. \qquad (176)$$

A similar derivation could be made for the anabatic field. If c_1 decreases with increasing temperature, that is, the volume absorption coefficient decreases with increasing temperature, then the value of the bracketed term in (176) decreases. As a result, T_k, which is the product of the temperature and the mean emissivity of the atmosphere (bracketed term), tends to remain unchanged. Thus, when these conditions are met, the emission is primarily a function of the total amount of liquid water for any given zenith angle and frequency. Unfortunately, the point is rather academic, since absorption by gases, scattering by hydrometeors, and transfer of incident radiation were neglected in the derivation. In the case of katabatic radiation, the microwave radiation incident at the top of the atmosphere is small and negligible. If the frequency is low, then scattering and gaseous absorption may be neglected when clouds or, especially, rain are present. In this case, however, the absorption of microwaves by rain is non-linear. Therefore, the linearity of α with respect to M_p and the effect of temperature changes on α can not be used to determine optimum frequencies for sensing of total liquid water in the atmosphere. A thorough analysis is required that takes into consideration the effects of differences between absorption by a cloud mass and a rain mass, the effects of absorption by water vapor, and the effects of temperature.

D. Computational Procedure for a Scattering Atmosphere

The effects of scattering on the transfer of thermal radiation at microwave frequencies through a model atmosphere may be evaluated by a straightforward method of statistical trials known as the Monte Carlo method. An excellent discussion of this method is given in a book edited by Shreider (1966). In Chapter III of this book there is a detailed discussion of the application of the Monte Carlo method to the problem of neutron transport. The transfer of electromagnetic radiation is analogous to neutron transport. The concepts used in the Monte Carlo method and the procedures used to apply it to the problem of the transfer of thermal microwaves through the atmosphere are outlined below.

The field of microwave radiation at a given point in a medium may be viewed as being composed of a number of representative photons possessing certain polarizations, energies, and directions of movement, as indicated by a Stokes vector, the zenith angle, and the azimuth angle. These photons appear in the medium through a thermal emission process, interact with matter in the medium, and disappear from the medium either by being absorbed or by exiting the medium. The history of a particular photon depends on the distribution of the probabilities for scattering and absorption in the medium. These probabilities may be obtained from the electromagnetic properties of the medium given from classical considerations. The effects of multiple scattering may be evaluated by

following the history of thousands of representative photons through the medium and determining the patterns of the emergent streams of photons.

It has been noted that scattering is a significant extinction process for frequencies above about 10 GHz and in rain in which the rainfall rate is moderate to extreme. For these conditions, the absorption and scattering properties of the combined gases, cloud and rain are dominated by that of the rain elements. The extinction properties of rain are fairly homogeneous with altitude in the model used in this paper. Thus, one may assume that the scattering domain is characterized by a temperature, T (K), a volume absorption coefficient, α (m^{-1}), a volume scattering coefficient, β (m^{-1}), and a set of transformation matrices, $[\Sigma']$. These quantities are obtained from the Mie theory and the Van Vleck theory. In order to simplify further these considerations, the Monte Carlo method will be applied to one homogeneous layer of rain, cloud, and gases overlying a black-body surface of temperature, T_{sfc} (K).

The optical depth of the atmospheric layer is

$$\tau_o = -\int_{z_o}^{0} \kappa \, dz = \kappa \, z_o, \tag{177}$$

where z_o is the altitude of the top of the layer (m) and κ is the average volume extinction coefficient of the layer, $\alpha + \beta$ (m^{-1}).

1. Emission of microwave photons from a Lambert surface. The intensity of emission of a black body at temperature, T_{sfc} (K), is isotropic and is given at microwave frequencies by (8) as

$$B = 2\ k\ \nu^2\ T_{sfc}/c^2. \tag{178}$$

Therefore, the differential flux of emission of a black body is given from (4) and (178) as

$$dF = \frac{2\ k\ \nu^2}{c^2}\ T_{sfc}\ \cos\theta\ \sin\theta\ d\theta\ d\phi, \tag{179}$$

where θ is the zenith angle and ϕ is the azimuth angle. The flux of radiation between zenith angles of θ_1 and θ_2 is

$$\Delta F(\theta_1,\theta_2) = \int_0^{2\pi} \int_{\theta_1}^{\theta_2} \frac{2\ k\ \nu^2}{c^2}\ T_{sfc}\ \cos\theta\ \sin\theta\ d\theta\ d\phi \tag{180a}$$

$$= \frac{2\ \pi\ k\ \nu^2\ T_{sfc}}{c^2}\ (\sin^2\theta_2 - \sin^2\theta_1). \tag{180b}$$

Let c_f be the number of photons per unit flux, that is, c_f is the number of photons emitted per unit horizontal area per unit time per unit bandwidth. The number of photons emitted by the surface per unit time interval per unit bandwidth per unit horizontal area per unit surface termperature into the solid angle described by zenith angles θ_1 and θ_2 is $\Delta n(\theta_1,\theta_2)$, where

$$\Delta n(\theta_1,\theta_2) = c_n\ \pi\ T_{sfc}\ (\sin^2\theta_2 - \sin^2\theta_1) \tag{181}$$

and

$$c_n = \frac{2\ k\ \nu^2\ c_f}{c^2}\ . \tag{182}$$

The total number of photons emitted into the upper hemisphere from the surface is

$$\Delta n(0,\pi/2) = c_n \pi T_{sfc}. \tag{183}$$

The differential number of photons emitted in the interval of zenith angles from θ to $\theta + d\theta$ is given from (179) and (182) as

$$dn = c_n T_{sfc} \cos\theta \sin\theta \, d\theta \int_0^{2\pi} d\phi \tag{184a}$$

$$= 2 c_n \pi T_{sfc} \cos\theta \sin\theta \, d\theta. \tag{184b}$$

Thus, the probability distribution function for the zenith angle of emitted photons by a Lambert surface is $2 \cos\theta \sin\theta$. One may select values for θ from a uniformly-distributed, random number, ζ, in the interval (0,1) as follows:

$$\int_0^{\theta} 2 \cos\theta' \sin\theta' \, d\theta' = \zeta. \tag{185}$$

Thus,

$$\zeta = \sin^2\theta = 1 - \cos^2\theta, \tag{186}$$

or

$$\mu = \cos\theta = \sqrt{1 - \zeta}. \tag{187}$$

An equivalent distribution for μ would result from $\sqrt{\zeta}$ since ζ is randomly distributed over (0,1). Thus, the procedure to be used in the simulation of emission of photons from a Lambert surface is simply to have the model emit $c_n \pi T_{sfc}$ photons one at a time in random directions, as given by

$$\mu = \cos\theta = \sqrt{\zeta} \ . \tag{188}$$

2. Emission of microwave photons in the atmosphere. A small volume element dA dz (m^3) in the atmosphere of temperature, T (K), emits an amount of radiant energy (J) per unit horizontal area, dA (m^2), per unit time interval per unit bandwidth into the solid angle $d\Omega$ as given by

$$dF = \alpha \, B(\nu,T) \, dz \, d\Omega. \tag{189}$$

Substitution of the expressions for $B(\nu,T)$ and $d\Omega$ into (189) yields

$$dF = \frac{2 \, k \, \nu^2}{c^2} \ \alpha \, T \, \sin\theta \, d\theta \, d\phi \, dz. \tag{190}$$

If one integrates (190) over the entire layer of atmosphere from the surface to z_o (m) and over all solid angles, then one obtains an expression for the total amount of energy emitted in the atmosphere per unit horizontal area per unit time interval per unit bandwidth. If c_f is the number of photons per unit flux, then the total number of photons emitted in the atmosphere per unit horizontal area per unit time interval per unit bandwidth per unit of air temperature is given by

$$\Delta n(0,\pi) = 4 \, \pi \, c_n \, T \, \alpha \, z_o, \tag{191}$$

where c_n is the same as given in (182).

The probability distribution function for the zenith angle of emission of a photon at some point in the atmosphere is $(\sin\theta)/2$, that is, the distribution of θ is related to a uniformly distributed,

random number, ζ, over the interval (0,1) by

$$\int_0^{\theta} \frac{\sin\theta}{2} d\theta = \zeta. \tag{192}$$

Thus,

$$\zeta = [1 - \cos\theta]/2, \tag{193}$$

or

$$\mu = \cos\theta = 1 - 2\zeta. \tag{194}$$

The photons may be emitted at random altitudes or optical depths. One should insure, however, that μ is not too small (or zero) since division by zero is not allowed by the computer.

3. Trajectories of emitted photons. In order to reduce the number of trials necessary to determine the effects of multiple scattering on the transfer of microwaves through rain, the method of statistical weights was used as suggested in Shreider (1966). In this paper, however, the representative photons are characterized by a Stokes vector, $\vec{\upsilon}$, whose value is

$$\vec{\upsilon} = \{1,0,0,0\} \tag{195}$$

at the point of emission, since thermal emission is unpolarized. Suppose that the representative photon is found at an optical depth, τ, in the atmosphere and is traveling in a direction (θ,ϕ). It will travel a distance ℓ to the next point of interaction where ℓ is a random variable with a probability distribution function of $\kappa \exp(-\kappa \ell)$, that is,

$$\int_0^{\ell} \kappa \exp(-\kappa\, \ell')\, d\ell' = \zeta, \tag{196}$$

where ζ is a uniformly-distributed, random variable over the interval (0,1). If ℓ^* is the distance from the initial point to a boundary of the medium, then the probability that a photon will escape the medium without interaction is the probability that $\ell \geq \ell^*$. That is,

$$\int_{\ell^*}^{\infty} \kappa \exp(-\kappa\, \ell')\, d\ell' = \exp(-\kappa\, \ell^*). \tag{197}$$

Rather than allow the photon to escape without interaction, it is better to adjust the range of ζ such that $\ell \leq \ell^*$. Note that

$$\int_0^{\ell^*} \kappa \exp(-\kappa\, \ell)\, d\ell = 1 - \exp(-\kappa\, \ell^*). \tag{198}$$

Thus, as Shreider (1966) suggests, one may choose ℓ from

$$\ell = -\frac{1}{\kappa} \ln\{1 - \zeta\, [1 - \exp(-\kappa\, \ell^*)]\}. \tag{199}$$

If $\mu > 0$ (upward), then ℓ is $-\Delta\tau/\mu$ and ℓ^* is $-\tau/\mu$, where $\Delta\tau$ is the change in optical depth between points of interaction (note: $\Delta\tau$ is negative for an increase in altitude). If $\mu < 0$ (downward), then ℓ is $-\Delta\tau/\mu$ and ℓ^* is $(\tau_0 - \tau)/\mu$.

Before the photon is moved to the next point of interaction, its Stokes vector $\vec{\upsilon}$ is reduced by the amount,

$$\vec{\upsilon}_e = \begin{cases} \vec{\upsilon}\, \exp(-\tau/\mu), & \mu > 0 \\ \vec{\upsilon}\, \exp[(\tau_0 - \tau)/\mu], & \mu < 0 \end{cases}. \tag{200}$$

where $\vec{\upsilon}_e$ is the Stokes vector of the portion of the representative photon that escapes the medium without interaction. At the next point of interaction, β/κ (i.e., ω) photons are scattered and α/κ photons are absorbed. Thus, the Stokes vector of the photon at the next point of interaction is

$$\vec{\upsilon}' = \omega\ (\vec{\upsilon} - \vec{\upsilon}_e), \tag{201}$$

where ω is the albedo for single scattering of the layer.

To avoid branching trajectories, the entire remaining representative photon is scattered into some new direction (θ',ϕ'). As a result of this scattering, the relative values of the second, third, and fourth components of $\vec{\upsilon}'$ may change; however, the total intensity (first component) of $\vec{\upsilon}'$ will not change.

To determine the values of θ' and ϕ', one needs to select an angle, δ_1, and a scattering angle, Θ (see Fig. 65). δ_1 is obtained from ζ by

$$\delta_1 = 2\ \pi\ \zeta. \tag{202}$$

The scattering angle, Θ, is selected from the distribution of η discussed in Chapter VI, Section E, that is,

$$\int_0^{\Theta} \eta\ d\Theta' = \zeta, \tag{203}$$

where the integral is evaluated by the same finite-difference scheme used to calculate q_1 in (169). Using the relationships between the angles in Fig. 65 as given from spherical trigonometry (Rothrock, 1913, p. 126-127), one may state that

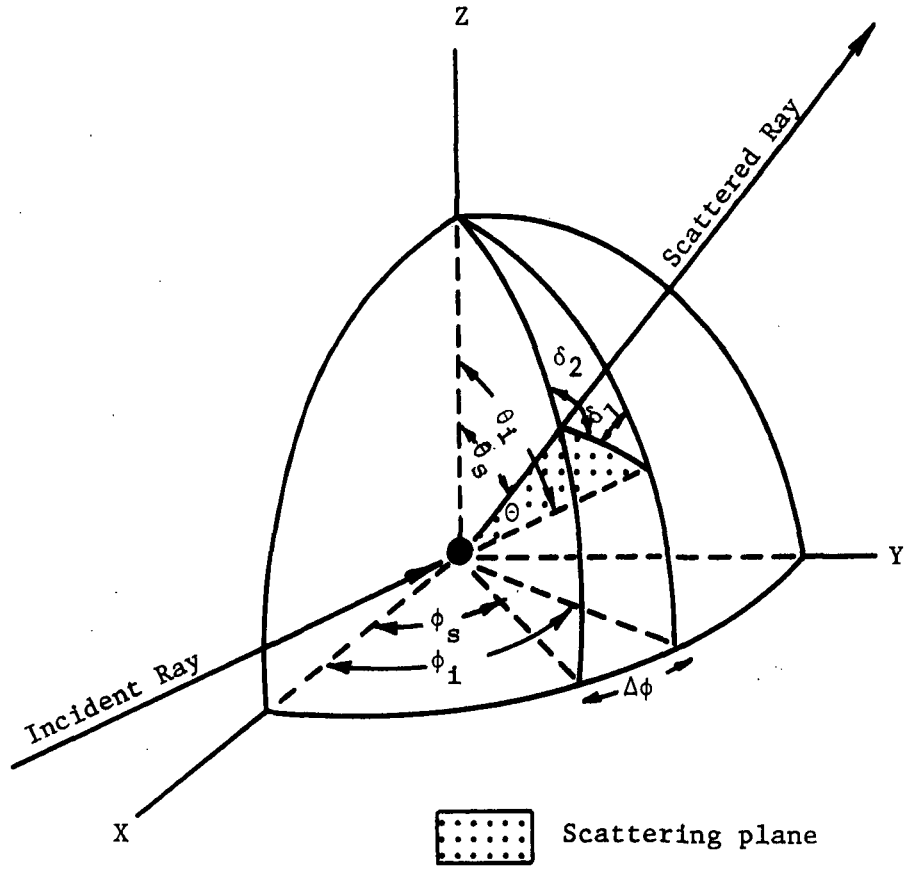

Fig. 65. Three-dimensional geometry of scattering.

$$\cos\theta_s = \cos\theta_i \cos\Theta + \sin\theta_i \sin\Theta \cos\delta_1, \tag{204}$$

$$\sin\delta_2 = \sin\theta_i \sin\delta_1/\sin\theta_s, \tag{205}$$

$$\sin(\phi_i - \phi_s) = \sin\Theta \sin\delta_2/\sin\theta_i, \tag{206}$$

and

$$\phi_s = \phi_i - (\phi_i - \phi_s). \tag{207}$$

Thus, θ_s and ϕ_s may be obtained from δ_1, Θ, θ_i, and ϕ_i.

Before the Stokes vector of the incident photon may be transformed, a rotation must be performed on $\vec{v}'$ in order to align the components properly to the scattering plane. After transformation of the resulting Stokes vector by the normalized transformation matrix for angular scattering, $[\Sigma]$, given in Chapter VI, Section E, one must rotate the Stokes vector of the scattered photon by using a second rotation matrix, $[R_2]$.

Chandrasekhar (1950, p. 40) gives the following expression for $[R_1]$:

$$[R_1] = \begin{bmatrix} 1 & 0 & 0 & 0 \\ 0 & \cos2\delta_1 & -\sin2\delta_1 & 0 \\ 0 & \sin2\delta_1 & \cos2\delta_1 & 0 \\ 0 & 0 & 0 & 1 \end{bmatrix}. \tag{208}$$

The expression for $[R_2]$ is identical to that for $[R_1]$ except that the 1's in the latter have been replaced by 2's.

The above processes are repeated to determine the next link in the scattering chain until the energy of the scattered photon is reduced below some cutoff level. After each scattering encounter,

a portion of the radiation escapes the scattering region. These escaping portions of microwave radiation are accumulated for specific ranges of the zenith angle. After a large number of photon histories are followed, one has determined the distribution of the photon emission of the atmosphere and surface with zenith angle. It is a simple matter to determine the effects of no scattering, single scattering, and multiple scattering by using different sets of accumulators at different points in the program. Similarily, one may distinguish between those photons that originate in the atmosphere and those that originate at the surface. Also, forward-scattered, back-scattered, and side-scattered photons may be counted separately. Thus, one may solve simultaneously by the Monte Carlo method a number of different scattering problems.

The number of photons counted in the accumulators is converted to an average brightness temperature by use of (181), that is,

$$\vec{T} = \frac{\Delta\vec{n}(\theta_1,\theta_2)}{c_n \pi \left|(\sin^2\theta_2 - \sin^2\theta_1)\right|} , \tag{209}$$

where $\Delta\vec{n}(\theta_1,\theta_2)$ represents the Stokes vector for the sum of all escaping photons between zenith angles θ_1 and θ_2. In this paper, θ_1 and θ_2 are taken over five-degree increments.

CHAPTER VIII

RESULTS

In this chapter, the results of the analyses of the emission of thermal microwaves from the atmosphere are given. Detailed results of the study of the emission of thermal microwaves by the sea were given in Chapter IV. One may summarize these results as follows. (1) For low states of the sea, the microwave emission by the ocean is small (brightness temperatures range between 62K and 167K for normal incidence) and is fairly independent of the temperature and salinity of the ocean for frequencies above about 5.8 GHz. (2) Salinity is an important parameter in the emission of thermal microwaves by a calm ocean for frequencies less than 5 GHz. (3) The emissivity of the ocean ranges from 0.13 to 0.81 for microwave frequencies, for low states of the sea, and for zenith angles less than 55 deg. (4) The microwave emission increases markedly when the sea becomes rough due to waves and especially to sea foam the emissivity of which appraoches unity. (5) The state of knowledge concerning the quantitative effects of sea roughness is such that the emission of the atmosphere and the ocean must be studied separately at this time.

The properties enumerated above are such that under most conditions of the sea the microwave emission is fairly predictable and small. Also, most of the katabatic emission of microwaves by

the atmosphere will be reflected upward at the sea surface and will add to the upwelling emission of microwaves by the atmosphere and the ocean. Such a reinforcing effect does not occur over land since land has a large emissivity (greater than 0.9) and small reflectivity. In some cases, the atmosphere behaves as a black body. Thus, the emission of the ocean and the atmosphere may vary by as much as 150K of brightness temperature. Current microwave radiometers are capable of sensing differences in microwave radiation on the order of 5K. Thus, some 30 levels of discrimination are possible.

A. Emission and Transmission of Thermal Microwaves by Non-Scattering Atmospheres

The general procedure for computing the katabatic and anabatic fields of microwave emission by a non-scattering atmosphere was discussed in Section C, Chapter VII. Briefly, in this procedure, one divides the atmosphere into a number of homogeneous layers, computes the volume absorption coefficient for each layer as a function of the mean temperature, dew-point temperature, content of liquid water in cloud form, and content of liquid water in precipitation form, and then transfers radiation from layer to layer by means of (171). These calculations were performed for all 582 model atmospheres described in Sections A and B of Chapter VII, for the microwave frequencies of 1.42, 2.695, 4.805, 8.0, 10.69,

15.375, 19.35, 31.4, 33.2, 37.0, and 53.8 GHz, and for zenith angles of 0.0 and 55.0 deg. In addition, the equivalent depths of water vapor, W_v (mm), of liquid water in cloud form, W_c(mm), and of liquid water in precipitation form W_p (mm), were computed for each model atmosphere. As was noted in Section B of Chapter VII, the distributions of W_c and W_p are highly skewed; however, the distributions of ln W_c and ln W_p are less skewed.

The purpose of the analyses in this section is to find the quantitative relationships between a small number of meteorological parameters of the atmosphere and the associated microwave emissions at a number of selected microwave frequencies. The ranges of the katabatic brightness temperatures of the 582 model atmospheres for each of the frequencies used are shown in Table 32 (θ = 180 deg, nadir) and in Table 33 (θ = 125 deg, 55 deg from nadir).

If one studies the values of the ranges for the clear-sky case, then one sees that the content of water vapor is an important parameter for frequencies near the water-vapor resonance line (22.235 GHz). Also, these values show that the atmosphere is nearly opaque at frequencies near 60 GHz due to the large volume absorption coefficient of molecular oxygen. Moreover, the microwave emission of rain may be significant for frequencies of 2.695 GHz or greater. In clouds, the microwave emission may be significant for frequencies of 4.805 GHz or greater. Rain is the dominant parameter for frequencies between about 2.695 and 19.35 GHz; this is due to the

Table 32. Ranges of the katabatic brightness temperature of the atmosphere: θ = 180 deg.

Frequency (GHz)	Katabatic Brightness-temperature (K)								
	Clear Sky			Clouds (No Rain)			Clouds and Rain		
1.42	2.1	(2.1)	2.2*	2.1	(2.2)	3.7	2.1	(2.3)	5.5
2.695	2.3	(2.3)	2.4	2.3	(2.7)	8.0	2.3	(3.1)	17.6
4.805	2.5	(2.6)	3.1	2.5	(3.7)	20.2	2.5	(5.4)	84.9
5.81	2.6	(2.8)	3.4	2.6	(4.4)	28.1	2.6	(7.1)	151.6
8.0	2.8	(3.2)	4.6	2.8	(6.3)	49.3	2.8	(13.4)	263.3
10.69	3.1	(4.1)	6.8	3.1	(9.7)	80.8	3.1	(26.3)	293.7
15.375	4.4	(7.6)	15.4	4.4	(19.5)	142.4	4.4	(57.9)	299.6
19.35	8.8	(20.7)	48.5	8.8	(43.2)	202.2	8.8	(88.5)	300.6
31.4	10.7	(20.9)	44.8	10.7	(62.0)	267.3	10.7	(164.0)	301.5
33.2	11.4	(21.6)	45.4	11.4	(66.0)	272.2	11.4	(173.0)	301.6
37.0	14.3	(25.0)	50.2	14.3	(76.7)	279.8	14.3	(191.3)	301.7
53.8	233.3	(252.0)	267.2	233.3	(264.0)	295.7	233.3	(282.6)	302.2

*The data are presented in the following format: Minimum Value (Value for Average Atmosphere, Cloud Condition, or Rain Condition) Maximum Value.

Table 33. Ranges of the katabatic brightness temperature of the atmosphere: θ = 125 deg.

Frequency (GHz)	Katabatic brightness-temperature (K)								
	Clear Sky			Clouds (No Rain)			Clouds and Rain		
1.42	3.7	(3.7)	3.8*	3.7	(3.9)	6.4	3.7	(4.1)	9.5
2.695	4.0	(4.0)	4.2	4.0	(4.7)	13.7	4.0	(5.4)	30.0
4.805	4.4	(4.5)	5.2	4.4	(6.5)	34.3	4.4	(9.3)	130.9
5.81	4.5	(4.8)	5.9	4.5	(7.6)	47.2	4.5	(12.3)	210.7
8.0	4.8	(5.6)	7.9	4.8	(11.0)	80.3	4.8	(23.0)	290.6
10.69	5.4	(7.1)	11.7	5.4	(16.7)	125.6	5.4	(44.3)	299.6
15.375	7.6	(13.0)	26.4	7.6	(33.1)	200.0	7.6	(93.3)	301.3
19.35	15.2	(35.1)	79.3	15.2	(71.1)	252.1	15.2	(148.5)	301.7
31.4	18.3	(35.5)	73.7	18.3	(99.2)	286.6	18.3	(221.8)	302.1
33.2	19.6	(36.6)	74.6	19.6	(104.9)	222.9	19.6	(230.0)	302.2
37.0	24.4	(42.2)	82.0	24.4	(120.0)	290.2	24.4	(245.3)	302.2
53.8	261.8	(280.5)	292.3	261.8	(284.8)	298.5	261.8	(290.2)	302.2

*The data are presented in the following format: Minimum Value (Value for Average Atmosphere, Cloud Condition, or Rain Condition) Maximum Value.

large rate of absorption by rain at these frequencies as compared to that by clouds and atmospheric gases.

In order to illustrate the correlation between the katabatic brightness temperature of the atmosphere and the equivalent depth of liquid water in precipitation form, scattergrams of the katabatic brightness temperature versus $\log_{10} W_p$ were plotted by the Gerber plotter for frequencies of 10.69, 19.35, and 37 GHz and for normal incidence. These scattergrams are shown in Figs. 66 to 68. Remarkably, there is little scatter of the plotted points in Fig. 66 (10.69 GHz). Thus, the effects of the absorption and emission of microwaves by water vapor and cloud liquid water are minimal at 10.69 GHz. Similar plots (not shown) for lower frequencies show even less scatter; however, the next lowest radio astronomy band occurs at 5.81 GHz, and the range of microwave emission of the atmosphere is too small for most observed meteorological conditions to be of practical use.

Fig. 66 suggests that one predictor, namely, W_p, the equivalent depth of liquid water in the form of precipitation (mm), may be used to predict T_{kp}, the polarized component of the katabatic brightness temperature (K) of the atmosphere at 10.69 GHz. Therefore, one may use measured values of T_{kp} to determine W_p. A third-degree ploynomial in T_{kp} was formed by means of a standard IBM Scientific Subroutine Package program. T_{kp} was taken over the range from 30K to 300K. The corresponding range of W_p is from 1.3 mm to 27.4 mm. The resulting regression equation is

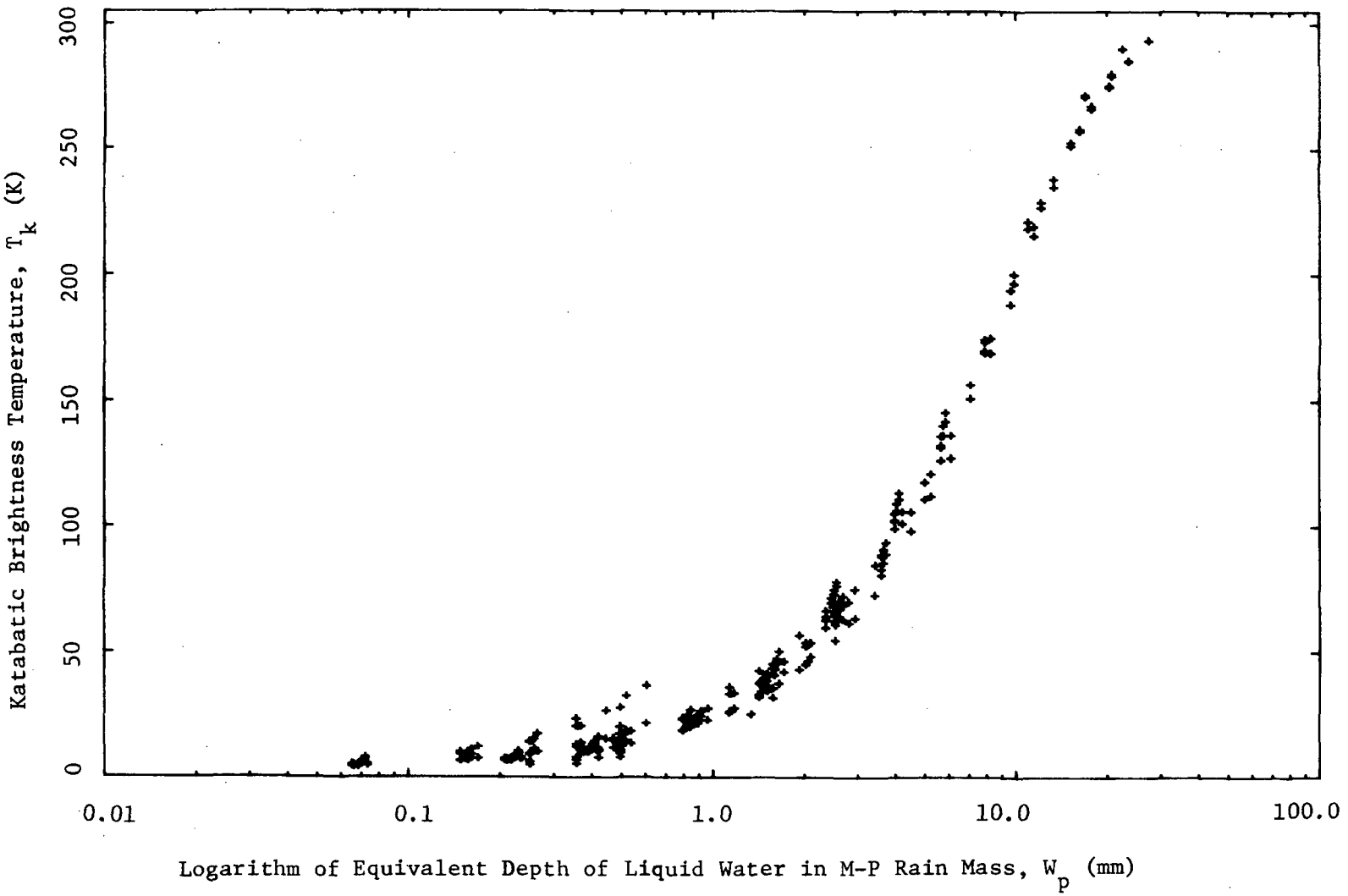

Fig. 66. Scattergram of the katabatic microwave emission of 320 model atmospheres versus their equivalent depths of liquid water in the M-P rain mass: ν = 10.69 GHz.

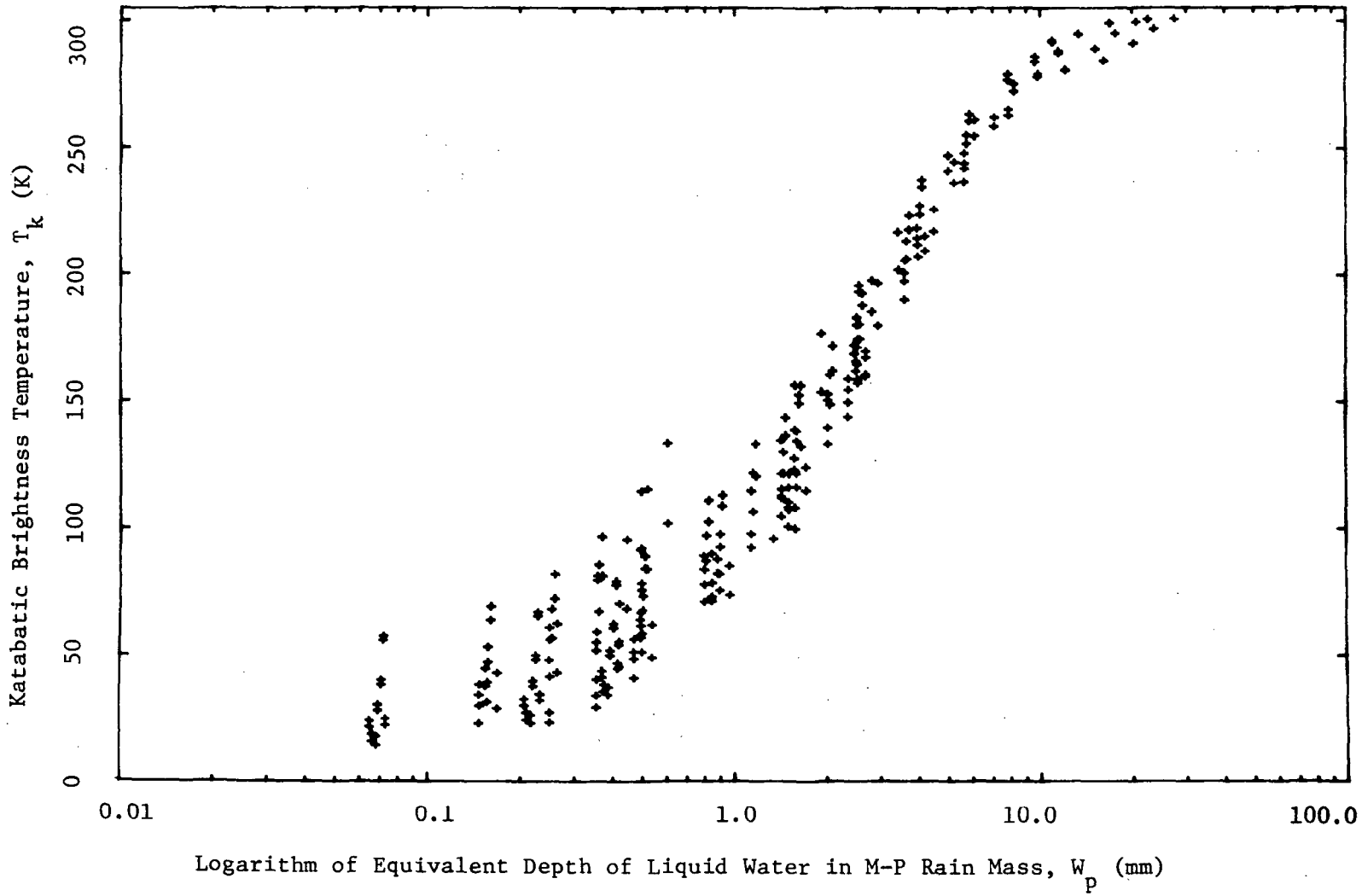

Fig. 67. Scattergram of the katabatic microwave emission of 320 model atmospheres versus their equivalent depths of liquid water in the M-P rain mass: ν = 19.35 GHz.

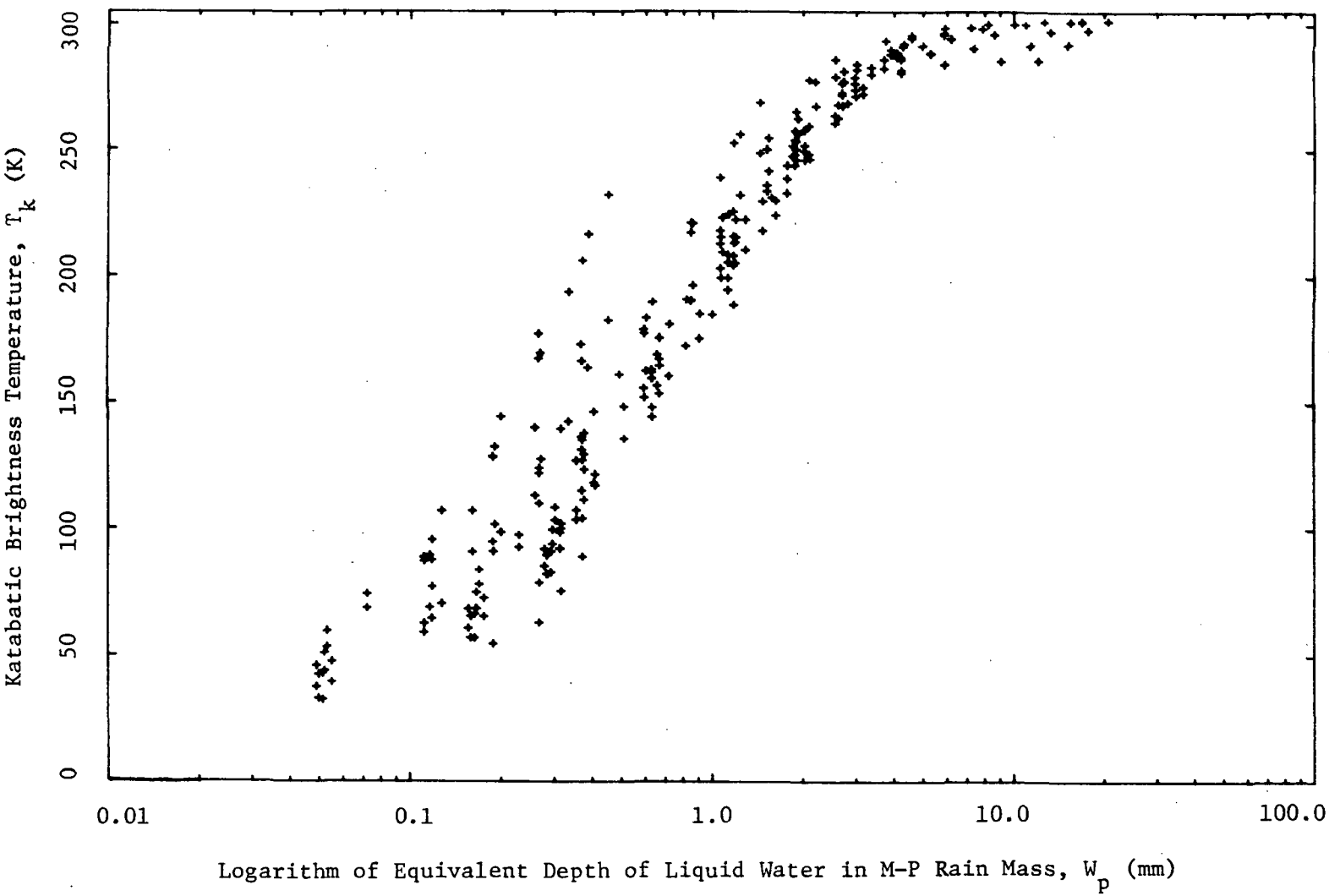

Fig. 68. Scattergram of the katabatic microwave emission of 320 model atmospheres versus their equivalent depths of liquid water in the M-P rain mass: ν = 37.0 GHz.

$$\log_{10} W_p = -0.203312 + 0.0118844\ T_{kp} - 4.604364 \times 10^{-5}\ T_{kp}^2 + 8.222227 \times 10^{-8}\ T_{kp}^3. \quad (210)$$

(The degree of significance of the various terms is not considered). Since the regression analysis minimizes the sum of the squares of the deviations of the dependent variable, $\log_{10} W_p$, one has, in effect, minimized the percent deviation of W_p. The multiple correlation coefficient for the regression specified in (210) is 0.9793, and the standard error of estimate of W_p is 18% (0.77 db).

It is clear that more than one parameter is needed to predict the values of the katabatic and anabatic brightness temperatures of the atmosphere and the transmissivity of the atmosphere at other microwave frequencies. The most logical choice of predictors appears to be W_v, W_c, and W_p. The multiple regression analysis program used in this study works best when the variables have distributions that are not highly skewed.

Since one wishes to minimize the sum of the squares of the percent deviations from regression, it appeared that $\ln W_c$, $\ln W_p$, and W_v should be the independent variables and that the logarithm of the dependent variable should be used in the regression analysis. Usually, one does not accomplish any further refinement by using regression equations of degree higher than three. Therefore, a multiple regression analysis was made of $\ln T_{kp}$, $\ln T_{ap}$, and $\ln \Gamma$ using powers of W_v, $\ln W_c$, and $\ln W_p$ and combinations of these variables such that the sum of the exponents of any particular

term did not exceed three. As a result, multiple regression equations involving 20 terms were developed; the resulting regression coefficients are listed in Appendix B. It was found that the regression on the emissivity worked better than that on the transmissivity since the emissivity increased with increasing equivalent depths. The transmissivity is related to the mean emissivity, $\bar{\xi}$, by

$$\Gamma = 1 - \bar{\xi}. \tag{211}$$

The resulting regression equations are such that no other predictors need be used. One should note in Appendix B that the multiple correlation coefficients exceed 0.995 and that the standard error of estimates are less than 9.7% (0.4019 db).

B. Emission, Transmission, and Reflection of Thermal Microwaves by a Scattering Atmosphere

The general procedure for computing the emission and scattering of thermal microwaves in a one-layer atmosphere overlying a black body surface was discussed in Section D, Chapter VII. Briefly, in this procedure, the histories of several thousand representative microwave photons are followed through the atmosphere as they interact randomly with the atmosphere. The properties of the emergent radiation are determined by summing the Stokes vectors of the escaping portions of the representative photons over 5-deg increments of zenith angle.

In order to test the Monte Carlo program, the emission of a

non-scattering atmosphere was computed using 200,000 primary photons. For this calculation, the optical depth of the atmosphere was 2.0 and its temperature was 300K. One should recall that the emission of such an atmosphere may be computed directly from (171), viz.,

$$T_e = T\,[1 - \exp(-\tau_a/\mu)], \tag{212}$$

where τ_a is the optical depth of the atmosphere for absorption, T is the temperature (K), and μ is the cosine of the zenith angle, θ (deg).

The result of the Monte Carlo solution to this problem is shown in Fig. 69 along with the corresponding theoretical solution. These solutions are in agreement. The fluctuations of the Monte Carlo solution are due to statistical fluctuations.

There are three approximations that one may use to compute the emission and transmission of a scattering and absorbing medium. In the first approximation, one assumes that the radiative properties of the medium may be predicted from the volume extinction coefficient alone. There is no physical basis for this approximation since thermal emission at some point in a medium depends on absorption processes, not on extinction or attenuation processes. This approximation is used when an investigator uses the volume extinction coefficient of a medium as if it were the volume absorption coefficient of a non-scattering medium. For a homogeneous layer of atmosphere, the extinction approximation for the microwave emission of the medium is

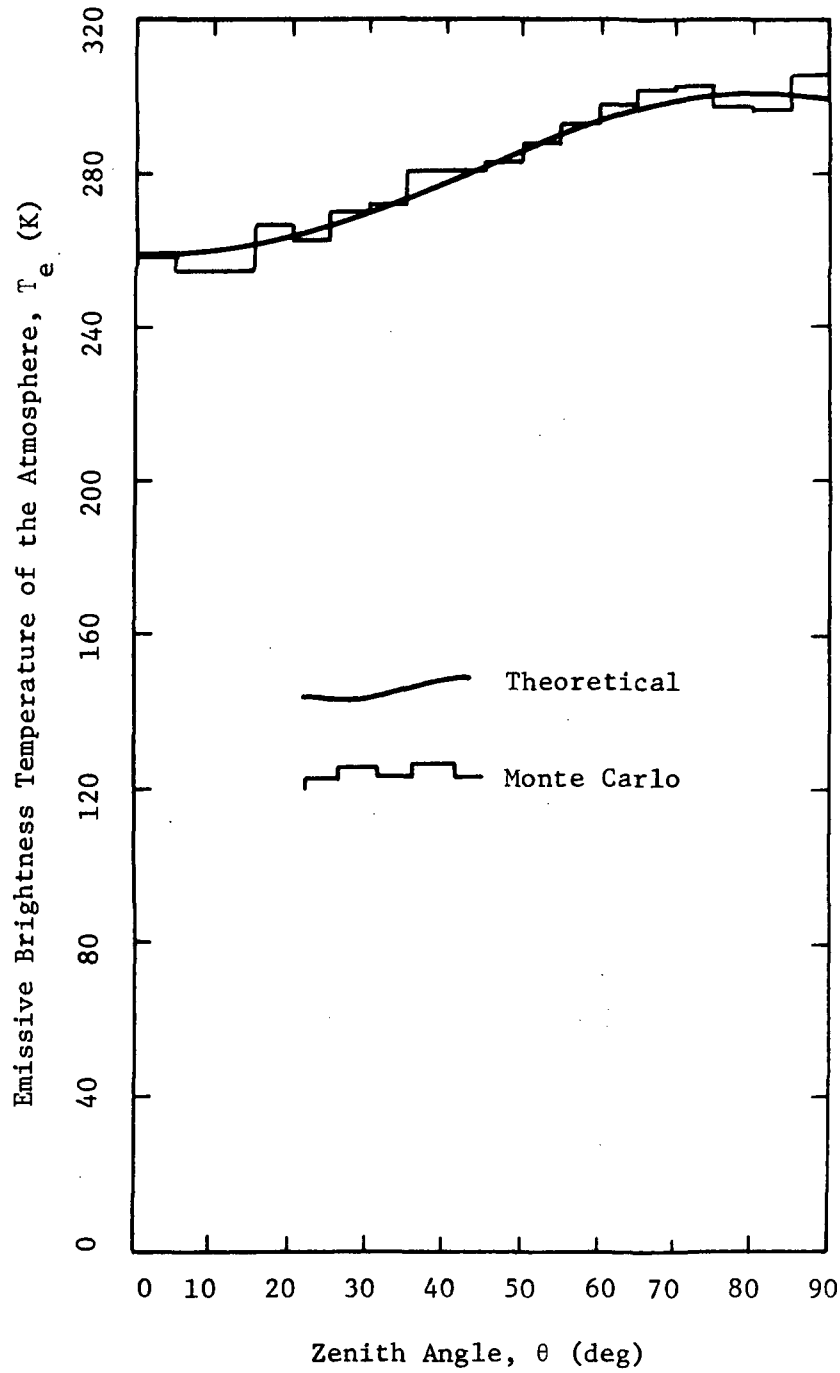

Fig. 69. Monte Carlo solution for non-scattering atmosphere.

$$T_e = T\,[1 - \exp(-\tau_o/\mu)], \tag{213}$$

where τ_o is the optical depth of the layer $\kappa\,\Delta z$, and Δz is the thickness of the layer. The transmissivity is

$$\Gamma = \exp(-\tau_o/\mu). \tag{214}$$

In the second approximation, one assumes that all radiation extincted by scattering is compensated for by radiation scattered from other pencils of radiation. In this approximation, one uses the volume absorption coefficient to describe both emission and extinction processes. This approximation, which was used throughout the investigation in this paper, is called the thin-atmosphere approximation and gives expressions for T_e and Γ as

$$T_e = T\,[1 - \exp(-\tau_a/\mu)] \tag{215}$$

and

$$\Gamma = \exp(-\tau_a/\mu), \tag{216}$$

where τ_a is the optical depth for absorption, $\alpha\,\Delta z$.

The third approximation, called the thick-atmosphere approximation, is based on the assumption that all of the scattered radiation is absorbed subsequently. In this approximation, Γ is given by (214), and T_e is given by

$$T_e = \frac{\alpha}{\kappa}\,T\,[1 - \exp(-\tau_o/\mu)]. \tag{217}$$

One should note that T_e is zero when α is zero in both the thin- and thick-atmosphere approximations. Such is not the case for the extinction approximation. All three approximations give the same values for T_e and Γ when there is no scattering. None

of the approximations, however, can be used to predict the reflection or back scattering of radiation from a scattering atmosphere.

The Monte Carlo method was used to evaluate the effects of multiple scattering on the transfer of thermal microwaves through rain. The radiative properties of the model atmosphere used in these calculations are listed in Table 34.

Table 34. Radiative properties of the atmospheric model used in multiple scattering evaluations.

Parameter	Value
Frequency	37.0 GHz
Thickness	3000 m
Rainfall intensity	8 mm hr^{-1}
Maximum M_c	0.4 g m^{-3}
Liquid content of rain mass	0.5023 g m^{-3}
Cloud temperature	283.2 K (10C)
Surface Temperature	293.2 K (20C)
Surface emissivity	1.0 (black body)
Volume absorption coefficient	0.41667 per km
Volume scattering coefficient	0.20740 per km
Volume extinction coefficient	0.62407 per km
Optical thickness	1.8722
Albedo for single scattering	0.3323

This model represents an average rain. The frequency of 37 GHz was chosen for several reasons. First, this frequency will be used by a radiometer that will be flown in a Nimbus Meteorological Satellite. Second, the excessive absorption of microwave by molecular oxygen at higher frequencies places an upper limit on the frequencies at which a radiometer might be used to sense liquid

water in the atmosphere. Third, the value of ω for this model is not far below the maximum albedo (0.47) for single scattering of a cloudburst (100 mm hr^{-1}) at 37 GHz. Last, the radiative properties of a cloudburst also are approximately the same at 19.4 GHz.

The distribution of the angular-scattering intensities for the rain mass are shown in Fig. 70. This distribution is very similar to that for Rayleigh scattering.

In the Monte Carlo program, a distinction was made between the emergent radiation before scattering and that after scattering. Also, the solutions to the emission problem and the transmission problem were calculated separately. In the former, the histories of 50,000 photons were followed, and in the latter, 20,000 photons were followed. In each case, there were an average of 5.6 scatterings before the intensity of the representative photon fell below 1/10,000 of its original value.

The angular distribution of the emission of microwaves by the model atmosphere in terms of brightness temperature is shown in Fig. 71 along with values given from each of the three approximations. It is obvious from this figure that the extinction approximation gives emissions that are much too high. The thin-atmosphere approximation holds well for zenith angles where the line of sight traverses a distance that is less than about six units of optical depth. It should be noted that these zenith angles include the useful part of the scan of a radiometer (spatial resolution is best

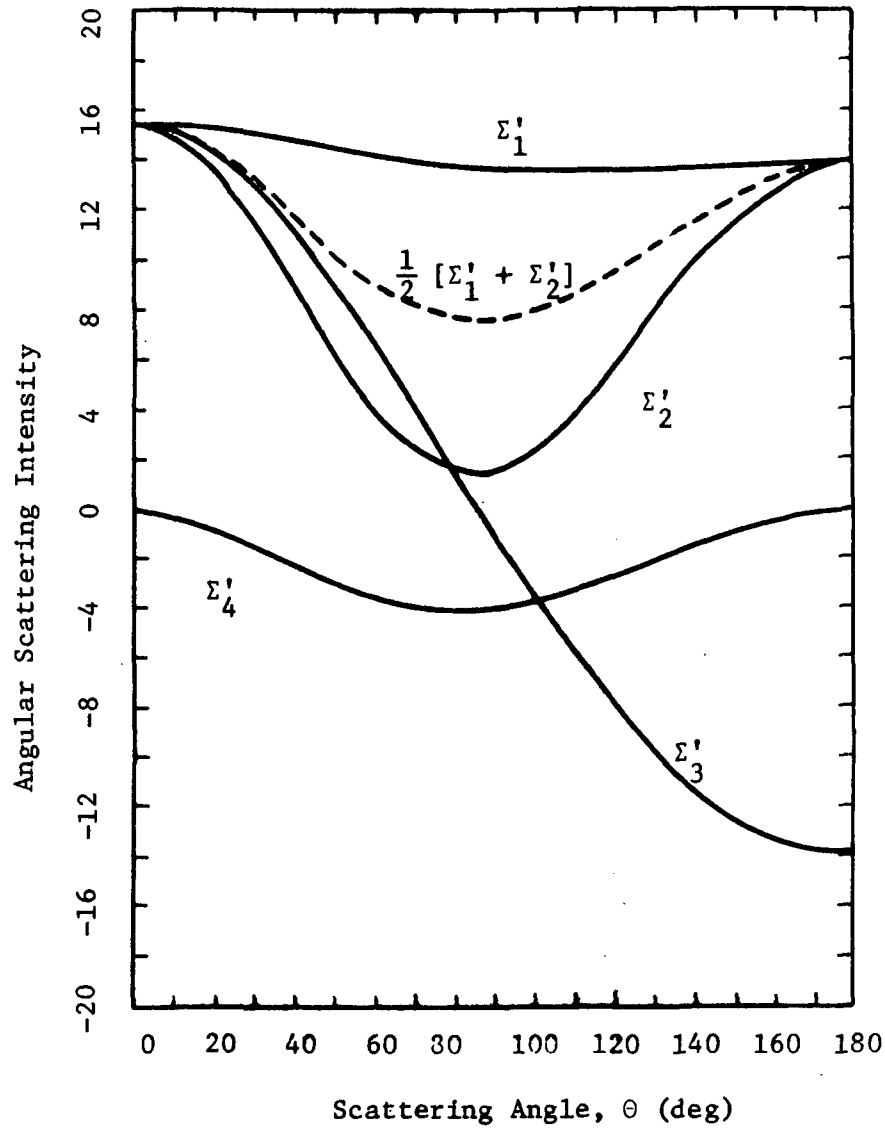

Fig. 70. Angular scattering parameters for a M-P rain: ν_1 = 37 GHz, T = 10C, R = 8 mm hr^{-1}.

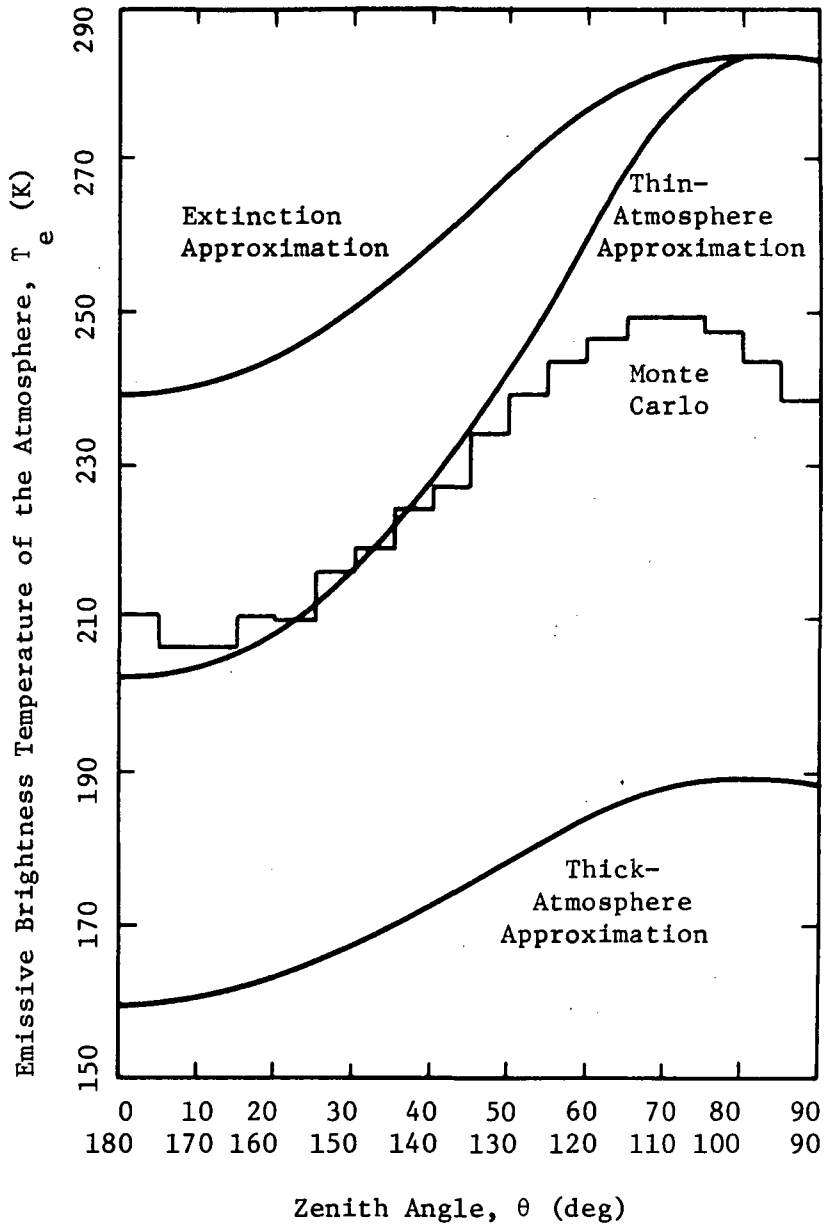

Fig. 71. Emission of thermal microwaves by the model atmosphere: ν = 37 GHz.

for low values of zenith angle). The true solution (Monte Carlo) tends toward the thick-atmosphere approximation for zenith angle near 90 deg where the path length through the atmosphere is quite long. The true solution is bounded by the thin- and thick-atmosphere approximations. Also, the percent polarization, $(\sqrt{Q^2 + U^2 + V^2}/I) \times 100\%$, of the emitted radiation was less than 0.8%

The angular distribution of the radiation originating at the surface and transferred through or scattered back from the model atmosphere is shown in Fig. 72. It appears that none of the three approximations is best for transmission, and, of course, they all fail for zenith angles from 90 to 180 deg. For this atmosphere, the spectral albedo or flux albedo is 8.8%. For a thicker atmosphere (not shown), it was 14% at the same frequency and for the same distribution of drop sizes.

The angular distribution of the combined emission, transmission, and reflection of thermal microwaves by the model atmosphere is shown in Fig. 73. One should note two important characteristics of this plot. First, the combined emission and reflection of microwaves toward the surface is larger than predicted by the thin-atmosphere approximation since the amount of reflected radiation is significant. If the surface emission is low, as in the case of sea water, the reflected component of the sky radiation would be small and the thin-atmosphere approximation still would hold for

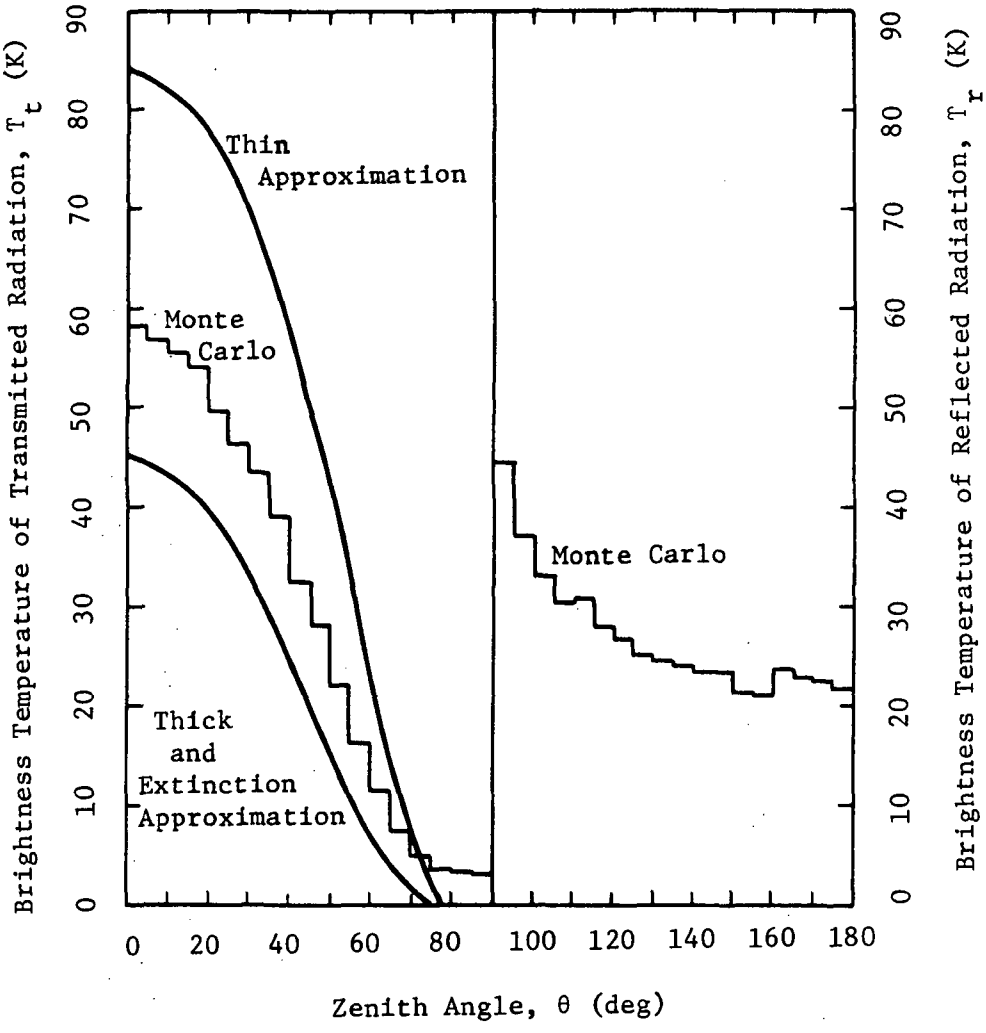

Fig. 72. Transmission and reflection of thermal microwaves from a Lambert surface by the model atmosphere: ν = 37 GHz.

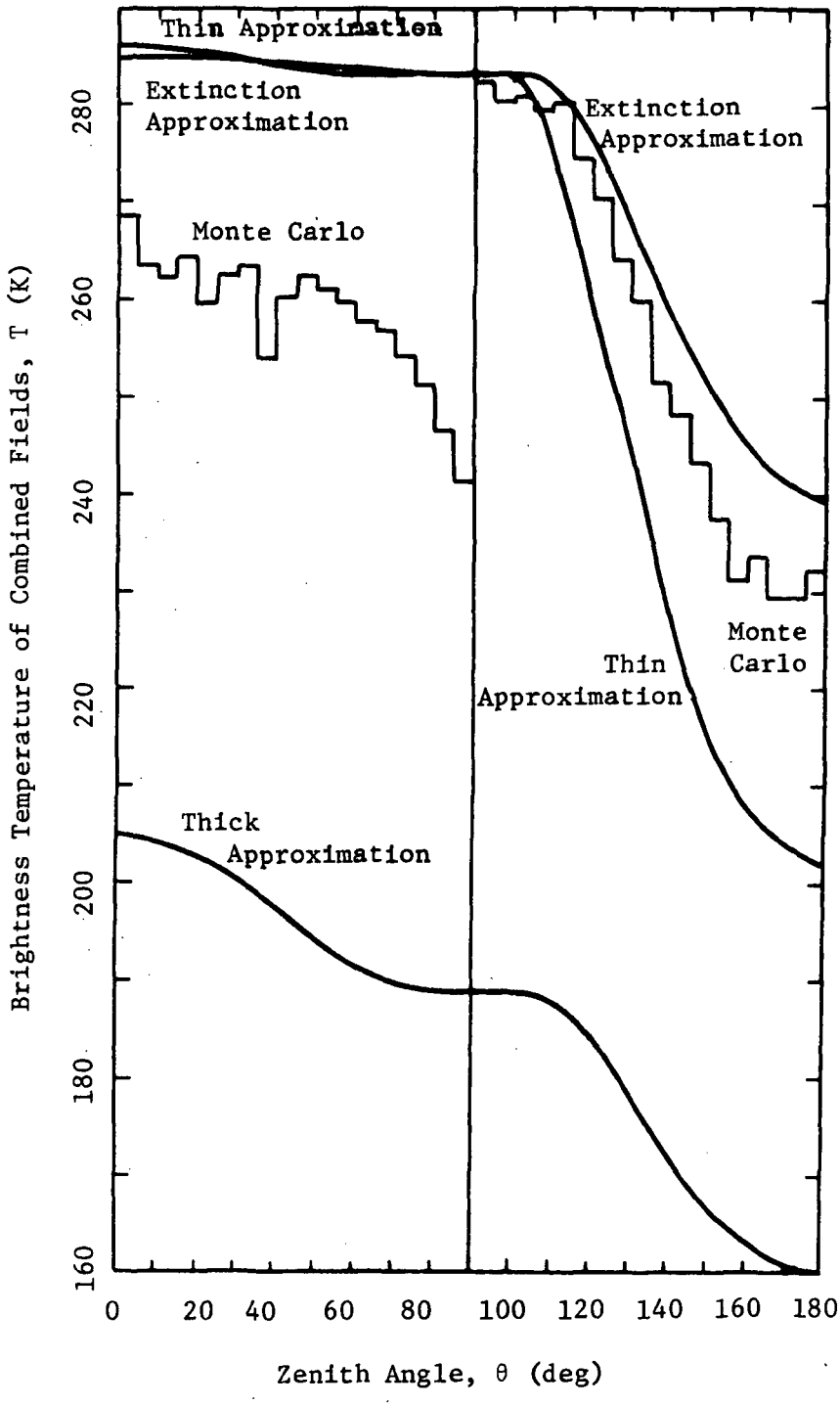

Fig. 73. Emission, transmission, and reflection of thermal microwaves by the model atmosphere and a Lambert surface: ν = 37 GHz.

medium zenith angles (viz., θ near 135 deg). Second, and perhaps more important than the first, the intensity of the upwelling radiation is significantly lower than that predicted by the thin-atmosphere and extinction approximations. All past studies have been based on these approximations and have indicated that measurements of the intensity of the microwave emission of the atmosphere over land surfaces would be of little use due to the lack of contrast between the emission of the atmosphere and the ground. The Monte Carlo calculations show, however, that, if there is significant scattering in the atmosphere, then there will be a measurable contrast between the emission of the land and the combined emission of the rain and the ground. Large rain drops and hail have large values of ω, the albedo for single scattering, and would thus appear as cold anomalies in the brightness-temperature field, as seen from overhead by a K-band microwave-radiometer in an aircraft or spacecraft. Also, the spatial resolution of a K-band radiometer is better than that of a radiometer operating at lower frequencies.

The percent polarization of the transmitted radiation ranged up to 26% for radiation with zenith angles near 90 deg. In this case, the vertical component was larger than the horizontal component, and 26% of the radiation was linearly polarized. The percent polarization of the reflected field ranged up to 5% for zenith angles near 120 deg. In all cases, the polarization was vertical.

CHAPTER IX

CONCLUSIONS AND RECOMMENDATIONS

Investigations by a number of engineers and scientists over the past decade have indicated that the remote sensing of thermal energy emitted by the atmosphere and its underlying surfaces at microwave frequencies is capable of providing needed information on the state of the environment. Due to the unique characteristics of the atmosphere and the ocean at microwave frequencies, one finds applications for remote sensing that are not possible at infrared or visible frequencies in the electromagnetic spectrum. In particular, the microwave properties of the atmosphere are functions of the distributions of water in gaseous and liquid form. Thus, microwave radiometry offers the possibility of surveying these distributions remotely from ground, ship, aircraft, or spacecraft platforms.

The present study is a theoretical, calculative study of the radiative characteristics of the ocean and several hundred model atmosphere at microwave frequencies ranging from 0.5 GHz to 60 GHz (see Table 1). This study consisted of several parts. First, the basic physical and mathematical concepts used in this study are discussed in detail, especially as they are related to the direct problem of radiative transfer through model atmospheres. Second, the basic radiational parameters of sea water, atmospheric gases,

and liquid-water clouds and rain are obtained from classical theories as a function of appropriate variables of state. In particular, the Mie theory for scattering by dielectric spheres is used to compute the absorption and scattering properties of rain. Third, the radiative transfer problem is solved for 582 non-scattering, plane-parallel, horizontally-homogeneous, model atmospheres. Fourth, the resulting anabatic and katabatic fields of microwave emission are analyzed in terms of their predictability by a small number of basic atmospheric parameters. Fifth, the solution to the radiative transfer of thermal microwaves through the atmosphere including multiple scattering and polarization is obtained through the Monte Carlo method. Last, applications to meteorology and oceanography are developed on the basis of the emissive, absorptive, and scattering properties of the atmosphere, the ocean, and the land.

A. Conclusions

The basic findings of this paper are summarized below under several topical headings. No attempt has been made to extrapolate between the frequencies listed in Table 1. Also, no attempt has been made to extrapolate between zenith angles of 0, 30, and 55 deg since most calculations were made for these angles. Many of these conclusions may be found at various places in the preceding chapters; however, those which involve the assessment of factors which extend

beyond the scope of any particular chapter are presented in this summary.

1. Complex index of refraction of water and sea water. A knowledge of the dependence of the complex index of refraction on the basic variables of state of water and sea water is essential to all studies of the absorption, scattering, reflection, and emission of microwaves by liquid hydrometeors and the ocean. Sufficient measurements of the complex index of refraction of pure water have been made by a number of investigators; however, this quantity has not been determined for sea water. The complex index of refraction of aqueous sodium chloride was used as an approximation to that of sea water. It was found that these values may be predicted when certain parameters are specified by simple expressions developed by Debye (1929). Regression equations (Table 13) involving second-degree terms of sea temperature and sea salinity were used along with the Debye equations to predict the complex index of refraction of sea water and pure water for any given sea temperature, sea salinity, and microwave frequency.

2. Emission of microwaves by a calm sea. The Fresnel equations for reflection and the Debye equations were used to compute the emission of microwaves by a calm sea. The emissivity of sea water ranges from 0.13 to 0.81 for the frequencies, polarizations, temperatures, and zenith angles used in this study. The lowest values are for low frequencies, horizontal polarization, warm water,

and large zenith angles. The highest values are for high frequencies, vertical polarization, cold water, and large zenith angles. For sea water (34.7 o/oo) and for increasing sea temperatures, the microwave emission of a calm sea increases for frequencies from 2.695 GHz to 10.69 GHz, decreases for frequencies from 0.5 GHz to 1.42 GHz and over 31.4 GHz, and remains fairly constant for frequencies from 15.375 to 22.235 GHz. The maximum rate of change in the microwave emission of a calm sea with respect to sea-temperature changes occurs at frequencies of 9.61 GHz, 5.81 GHz, and 60 GHz for vertical polarization and at a zenith angle of 55 deg; however, this response is only about 0.6K of brightness temperature per degree of change in sea temperature at these optimum frequencies. The effect of sea salinity on the microwave emission of a calm sea is small (less than 2K difference between sea water [34.72 o/oo] and pure water) for frequencies between 5.81 GHz and 60 GHz. Salinity has a large effect at low frequencies, for warm water, for vertical polarization, and at a zenith angle of 55 deg. For these configurations, the rates of change in the microwave emission of a calm sea with respect to changes in salinity range up to -1.93K of brightness temperature per part-per-thousand of salinity and -0.85K per part-per-thousand for frequencies of 0.61 GHz and 1.42 GHz, respectively.

3. Emission of microwaves by a rough sea. The effects of wave roughness and sea foam were not studied extensively in this

research. Other investigators have found that the maximum rates of change of the microwave emission of the sea with respect to changes in wave roughness occur for zenith angles near 55 deg and for horizontal polarization. This response amounts to approximately 1K of brightness temperature per m sec^{-1} of wind speed. Wave roughness has a negligible effect on the microwave emission of the sea when vertical polarization is selected, especially for zenith angles near 55 deg. The emissivity of sea foam may approach unity, especially during hurricanes when the coverage of foam may approach 100%. As a result, the microwave emission of a highly disturbed sea may be over 200K higher than that of a calm sea. At the present, no reliable, quantitative expression has been developed that may be used to predict the emission of a rough sea.

4. Extraterrestrial radiation at microwave frequencies. The background level of thermal radiation from cosmic sources is small (3K to 10K) for frequencies greater than about 1 GHz. For lower frequencies (wavelengths in excess of 30 cm), this background ranges up to 1000K and is unpredictable. This variation affects seriously microwave measurements of the ocean at these frequencies due to the large reflectivity of sea water.

5. Emission and absorption of microwaves by atmospheric gases. Molecular oxygen and water vapor absorb and emit thermal radiation at microwave frequencies as a result of resonant bands near 60 GHz and 22.235 GHz, respectively. Pressure-broadened infrared lines

also contribute to the absorption and emission of microwaves by water vapor. The atmosphere tends to become opaque for frequencies from 53.8 GHz to 60 GHz due to the large rate of absorption of microwaves by molecular oxygen; thus, sensing of microwaves emitted by the surface is severely affected by the atmosphere for these frequencies under any meteorological condition. Variations in the amount of water vapor in the atmosphere cause appreciable changes in the emission of clear atmospheres for frequencies above 11.312 GHz. For example, at normal incidence the change in the katabatic emission of microwaves by a clear atmosphere due to changes in precipitable water amounts to 0.56K of brightness temperature per mm of precipitable water at a frequency of 19.35 GHz. The air in clouds and rain is usually close to saturation. An increase in the amount of water vapor in clouds and rain causes a corresponding increase in the rate of absorption of microwaves. This contributes significantly to the combined absorption of the gases and hydrometeors for frequencies above 11.312 GHz. The microwave emission of clear atmospheres for frequencies near 22.235 GHz is related directly to the precipitable water of the atmosphere.

6. Emission and absorption of microwaves by clouds. Liquid-water clouds (drop diameters less than 0.1 mm) do not scatter significant amounts of microwave radiation. Their rates of absorption are independent of the distribution of drop sizes and can be given

from the Rayleigh Approximation. In general, the rates of absorption of microwaves by clouds increase with the square of the frequency and decrease with increasing temperature. For the 255 model clouds used in this study, the emissions of microwave have ranges greater than 10K for frequencies above 2.695 GHz. The rates of absorption of microwaves by clouds are almost an order of magnitude less than that by rain for frequencies near 10.69 GHz and approaches that by rain for frequencies near 0.5 GHz or 60 GHz. The largest range in the katabatic emissions of the 255 model clouds at normal incidence is from 14.3K to 279.8K at a frequency of 37.0 GHz. Also, these emissions are fairly independent of the cloud temperature and vertical distribution of liquid water.

7. Emission and absorption of microwaves by rain. The rate of absorption of microwaves by rain was calculated from the Mie theory by assuming a distribution of drop diameters given by Marshall and Palmer (1948) and by using the Debye equations to predict the complex index of refraction of the individual drops. This rate is a linear function of the content of liquid water in the rain mass for frequencies near 0.5 GHz and for frequencies near 39 GHz. It becomes a non-linear function for other frequences where the greatest non-linearity occurs at a frequency of 7.3 GHz and for warm rain (303K). In general, the absorption of microwaves by rain dominates that by gases for frequencies above 2.695 GHz and dominates that by clouds for frequencies between 4.805 GHz

and 31.4 GHz. The absorption and emission of microwaves by rain increases sharply with increasing frequency. For the 320 model rains used in this study and for normal incidence, the range of the katabatic emission of the atmosphere is greater than 10K and 100K for frequencies above about 2.695 GHz and 5.81 GHz, respectively. The largest range is from 4.4K to 299.6K at a frequency of 15.375 GHz.

8. Scattering of microwaves by rain. The rate of scattering of microwaves by rain and the distribution of the scattered radiation with scattering angle and polarization was calculated from the Mie theory. The ratio of the volume coefficients for scattering and extinction (the albedo for single scattering) for the rain was greater than 0.1 for frequencies greater than 10.69 GHz and for large contents of liquid water. It ranged up to 0.55 for a frequency of 60 GHz and a content of liquid water of 4.0 g m^{-3} (94 mm hr^{-1} rain). The angular distribution of scattered radiation is similar to that given by the Rayleigh scattering approximation.

An evaluation of the effect of multiple scattering on the emission of rain at microwave frequencies shows that the thin-atmosphere approximation, in which the volume absorption coefficinet is used to describe emission and extinction, may be used to compute the emission of a scattering atmosphere for zenith angles from nadir or zenith to about 60 deg toward the horizon. Beyond that

point, the emission is less than that given by the thin-atmosphere approximation and tends toward values given by the thick-atmosphere approximation, in which it is assumed that scattered photons subsequently are absorbed and do not escape the medium. The emission of microwave radiation by the atmosphere remains unpolarized in spite of the polarizing effects of scattering. This probably is due to the randomness of scattering of radiation emitted in the rain.

The effect of multiple scattering on the transmission of microwave radiation from a black body surface through a scattering atmosphere was evaluated. The true solution for the transmitted portion fell between the values given from the thin- or thick-atmosphere approximations. The flux reflectivity was appreciable and amounted to as much as 15% for the range of conditions considered in this paper. The percent polarization ranged up to 26% for the transmitted radiation for zenith angles near 90 deg and was less than 2% for zenith angles less than 50 deg.

The sum of the radiation emitted by a black-body surface and transmitted through the scattering atmosphere and the radiation emitted upward by the scattering atmosphere was less than that expected from a non-scattering atmosphere over a black-body surface. This depletion was largest at a frequency of 37 GHz and for heavy rain. The presence of hail, of which the albedo for single scattering is large, would probably greatly enhance this effect. This

depletion amounts to about 33K at 37 GHz for moderate rain (8 mm hr^{-1}) with a thickness of 3 km.

It is important to note that all approximations to the emission and transmission of rain at microwave frequencies work well when the albedo for single scattering approaches zero. In fact, it appears that multiple scattering effects may be neglected when the albedo for single scattering is 0.1 or less.

9. Predictability of the emission and transmission of the atmosphere at microwave frequencies. The calculated values of the anabatic and katabatic emissions of the 582 model atmospheres and their transmissivities were used to form third-degree regression equations where the equivalent depths of gaseous water (precipitable water), of liquid water in the cloud mass, and of liquid water in the rain mass were used as predictors. The logarithms of the latter two predictors were used to improve the skewness of the independent variables. The logarithms of the dependent variables were used to minimize the sum of the squares of the percent deviations from the line of regression. Based on these three predictors only, the resulting regression equations explain almost all of the variance. The multiple correlation coefficients are 0.995 or higher and the standard errors of estimate are 9.7% or less. Due to the fact that at 10.69 GHz absorption of microwaves by rain dominates that due to clouds and atmosphere gases, the microwave emission of the atmosphere at 10.69 GHz is dependent only upon the

equivalent depth of liquid water in the rain mass. One should note that the temperature of the atmosphere was not needed in any of the regression analyses. In a sense, the effect of temperature is included since there are correlations between the precipitable water of the atmosphere and the other equivalent depths and temperature.

B. Recommendations

On the basis of the findings of this research as summarized in the above section, the following recommendations are made:

1. Complex index of refraction of sea water. It is recommended that extensive measurements of the dielectric properties of sea water at microwave frequencies be made for a wide range of sea temperatures and sea salinities. The effects of dissolved gases and biological matter would need to be determined also. These studies are needed especially for microwave frequencies less than 5.0 GHz where salinity appears to play a major role.

2. Remote sensing of sea-surface temperature by microwave radiometry. It is recommended that the use of a microwave radiometer not be considered for surveying sea temperatures over the World Ocean from Earth satellites. Of the three possible optimum frequencies (0.61 GHz, 5.81 GHz, and 60 GHz) for such an application, the 0.61-GHz band is ruled out by the variability of radiation from cosmic sources and the extremely poor ground resolution that

could be achieved with present equipment. The 60-GHz band is not feasible due to the large absorption of microwaves by molecular oxygen. At 5.81 GHz and at the zenith angles needed to enhance the emission, the variability of the microwave emission by the atmosphere would result in fluctuations in the brightness temperature of upwelling radiation of up to 2K and clouds would cause changes of up to 70K. The range of microwave emissions by the sea surface at 5.81 GHz is from 151K to 168K -- a total change of only 17K -- for sea temperatures ranging from 0C to 30C.

3. Remote sensing of sea-surface salinity by microwave radiometry. It is recommended that a radiometer operating at 1.42 GHz, at vertical polarization, and at a zenith angle of 55 deg be used to survey surface salinity from aircraft along coastal regions where the water temperature is warm. The large amount of radiation from cosmic sources precludes such an application at lower frequencies. The effects of wave roughness would be negligible since vertical polarization is used. Such surveys would be limited to rainless conditions. In order to accomplish this survey, the sea temperature would need to be measured independently. An *infrared radiometer would be a good instrument for this purpose.* Survey of salinity from satellites is not feasible due to the poor ground resolutions that would result.

4. Remote sensing of sea-surface roughness by microwave radiometry. *It is recommended that an extensive program* be initiated

to determine the relationship between the microwave emission of the sea and its state of roughness through empiricism. Theoretical studies should be used to guide the experimentalists in selecting environmental parameters that need to be measured. It is apparent that duration, fetch, salinity, and wind stress contribute to the state of the sea both with regard to its wave spectra and to its whitecap coverage. The benefits to the forecasting efforts in both oceanography and meteorology would justify such a program. Until the effects of sea state are determined, all other applications of microwave radiometry to marine meteorology are limited to low states of the sea.

5. Remote sensing of liquid and gaseous water in the marine atmosphere by microwave radiometry. It is recommended that a radiometer operating at 10.69 GHz from aircraft or spacecraft be used to survey the equivalent depth of liquid water in rain form over the ocean when the sea state is low. There is no particular preference for viewing angle or polarization. The contributions to the emission of the atmosphere by water vapor and liquid-water clouds are minimal, the background emission of the ocean is low and predictable for low sea states, and multiple scattering may be neglected at 10.69 GHz. Such measurements are not possible at present by any other technique except direct sampling from aircraft, which is inadequate. A 10.69-GHz radiometer could differentiate between rain and clouds and give a measure of the amount of energy

being converted from latent to sensible heat in a tropical storm. Pattern recognition techniques could be applied to correlate hurricane development to the patterns of liquid precipitation observed by the radiometer. A similar application would be possible from land stations.

It is further recommended that a multifrequency radiometer be used to survey the amount of liquid water and gaseous water in the atmosphere and to measure the sea state of the ocean. These studies have shown that there is a significant change in the relative importance of the effects of the state of the sea, gaseous water, cloud liquid water, and rain liquid water on the emission of the atmosphere and the ocean as the frequency changes from 5.81 GHz to 37 GHz. Multiple scattering becomes a problem for the higher frequencies. Thus, it appears that measurement of the emission of the atmosphere and the ocean at four microwave frequencies, say 5.81 GHz, 10.69 GHz, 15.375 GHz, and 19.35 GHz, could be used to acquire information on sea state, precipitable water, cloud liquid water, and rain liquid water. Certainly, no single frequency could be used to measure the cloud liquid water under general conditions.

6. Remote sensing of severe storms over land by microwave radiometry. It is recommended that a radiometer operating at 37 GHz be used to survey the location of precipitation consisting of large hydrometeors, both liquid and solid. These conditions

would most likely be found in severe storms. Their presence would be indicated by a depletion of the radiation upwelling from the top of a storm. The relatively high ground resolution of the 37-GHz radiometer would be an additional advantage.

7. Future research. The techniques developed in this study should be applied to meteorological conditions in which the appropriate variables are a function of all three dimensions. Also, distributions of drop sizes in rain other than that given by Marshall and Palmer (1948) should be investigated. The effects of scattering in hail shafts on the upwelling radiation need to be investigated. Finally, the Monte Carlo technique should be used to investigate other multiple-scattering effects in radar propagation and the transfer of infrared and visible light through atmospheric pollution, gases, haze, clouds, and rain and through turbid oceans.

APPENDIX A

The computed values of the volume absorption coefficient of a M-P rain (α_p, m^{-1}) at fixed temperatures of -10, 0, 10, 20, and 30C were fitted to an expression of the form

$$\alpha = c_1 M^d ,$$

where M is the content of liquid water in the M-P rain mass, and c_1 and d are constants which are functions of temperature. The regression coefficients of two fourth order polynomials giving c_1 and d as a continuous function of T were obtained through the method of successive elimination (Brooks and Carruthers, 1953, pp. 297-299). These coefficients are listed in Tables A1 and A2.

Table A1. Regression coefficients for c_1 in Equation (167), Chapter VI, page 157.

Frequency (GHz)	f_0	f_1	f_2	f_3	f_4
0.5	0.57154E-07	-0.17458E-08	0.47063E-10	-0.12732E-11	0.16212E-13
0.61	0.85500E-07	-0.26155E-08	0.70540E-10	-0.19080E-11	0.24300E-13
0.75	0.13027E-06	-0.39929E-08	0.10765E-09	-0.29066E-11	0.36983E-13
1.0	0.23575E-06	-0.72553E-08	0.19554E-09	-0.52716E-11	0.67083E-13
1.42	0.49484E-06	-0.15338E-07	0.41106E-09	-0.10972E-10	0.13888E-12
1.675	0.70956E-06	-0.22068E-07	0.58678E-09	-0.15522E-10	0.19567E-12
2.1	0.11826E-05	-0.36864E-07	0.95780E-09	-0.24779E-10	0.30946E-12
2.695	0.21449E-05	-0.66252E-07	0.16202E-08	-0.39883E-10	0.48831E-12
2.91	0.25983E-05	-0.79602E-07	0.18836E-08	-0.45233E-10	0.54917E-12
4.0	0.60715E-05	-0.16883E-06	0.29724E-08	-0.57759E-10	0.66626E-12
4.805	0.10337E-04	-0.24439E-06	0.27490E-08	-0.45950E-10	0.62500E-12
5.81	0.18280E-04	-0.30217E-06	0.98253E-09	-0.41811E-10	0.92405E-12
8.0	0.44968E-04	-0.17500E-06	-0.20701E-08	-0.17999E-09	0.28998E-11
9.369	0.66376E-04	0.24100E-07	-0.17174E-09	-0.31949E-09	0.38666E-11
10.69	0.89353E-04	0.22988E-06	0.44282E-08	-0.43834E-09	0.42669E-11
11.312	0.10081E-03	0.31890E-06	0.72683E-08	-0.49101E-09	0.45169E-11
15.375	0.18398E-03	0.58708E-06	0.29554E-07	-0.70583E-09	0.59584E-11
17.2	0.22553E-03	0.51443E-06	0.39612E-07	-0.81425E-09	0.78779E-11
19.35	0.27741E-03	0.28994E-06	0.50097E-07	-0.90437E-09	0.95461E-11
22.235	0.35100E-03	-0.18483E-06	0.61842E-07	-0.10267E-08	0.12084E-10
31.4	0.59766E-03	-0.22389E-05	0.73552E-07	-0.83076E-09	0.10457E-10
33.2	0.64549E-03	-0.26320E-05	0.71025E-07	-0.69001E-09	0.87506E-11
35.1	0.69498E-03	-0.30236E-05	0.66786E-07	-0.49414E-09	0.61253E-11
37.0	0.74322E-03	-0.33730E-05	0.60416E-07	-0.35503E-09	0.63349E-11
45.248	0.93386E-03	-0.45176E-05	0.21927E-07	0.99587E-09	-0.13292E-10
53.8	0.10954E-02	-0.49912E-05	-0.29060E-07	0.23118E-08	-0.29419E-10
60.0	0.11901E-02	-0.49783E-05	-0.64000E-07	0.29333E-08	-0.34998E-10

Table A2. Regression coefficients for d in Equation (168), Chapter VI, page 157.

Frequency (GHz)	f_0	f_1	f_2	f_3	f_4
0.5	0.10043E 01	-0.46563E-04	0.58333E-06	0.16133E-07	-0.81857E-09
0.61	0.10067E 01	-0.59152E-04	-0.46094E-07	-0.81062E-08	0.41326E-09
0.75	0.10103E 01	-0.90885E-04	-0.37988E-06	0.58571E-07	-0.12517E-08
1.0	0.10184E 01	-0.14753E-03	-0.88056E-06	0.75261E-07	-0.12517E-08
1.42	0.10365E 01	-0.24669E-03	-0.23381E-05	0.11722E-06	-0.16809E-08
1.675	0.10500E 01	-0.28832E-03	-0.47509E-05	0.18318E-06	-0.24954E-08
2.1	0.10761E 01	-0.31998E-03	-0.12919E-04	0.45005E-06	-0.58333E-08
2.695	0.11187E 01	-0.19832E-03	-0.31085E-04	0.10333E-05	-0.14166E-07
2.91	0.11356E 01	-0.86570E-04	-0.40337E-04	0.12662E-05	-0.16654E-07
4.0	0.12298E 01	0.13666E-02	-0.10200E-03	0.22835E-05	-0.25002E-07
4.805	0.13023E 01	0.37951E-02	-0.13667E-03	0.19000E-05	-0.18330E-07
5.81	0.13708E 01	0.73166E-02	-0.10117E-03	0.18836E-05	-0.33339E-07
8.0	0.13905E 01	0.83510E-02	-0.50209E-04	0.24910E-05	-0.27899E-07
9.369	0.13643E 01	0.69400E-02	-0.45427E-04	0.25004E-05	-0.25836E-07
10.69	0.13351E 01	0.54467E-02	-0.45171E-04	0.23833E-05	-0.23329E-07
11.312	0.13218E 01	0.48000E-02	-0.45419E-04	0.22504E-05	-0.20846E-07
15.375	0.12515E 01	0.16658E-02	-0.48461E-04	0.17416E-05	-0.15414E-07
17.2	0.12272E 01	0.86174E-03	-0.47337E-04	0.14332E-05	-0.11663E-07
19.35	0.12018E 01	0.22507E-03	-0.47005E-04	0.12503E-05	-0.10006E-07
22.235	0.11703E 01	-0.25241E-03	-0.43712E-04	0.97481E-06	-0.79115E-08
31.4	0.10801E 01	-0.60322E-03	-0.28334E-04	0.28284E-06	-0.16530E-08
33.2	0.10639E 01	-0.59757E-03	-0.24551E-04	0.12581E-06	0.40134E-09
35.1	0.10475E 01	-0.59330E-03	-0.20758E-04	-0.16292E-07	0.24954E-08
37.0	0.10318E 01	-0.54367E-03	-0.19236E-04	-0.66322E-06	0.22333E-07
45.248	0.97185E 00	-0.63974E-03	-0.17208E-05	-0.40254E-06	0.52095E-08
53.8	0.92305E 00	-0.73783E-03	0.11750E-04	-0.69166E-06	0.84999E-08
60.0	0.89479E 00	-0.83058E-03	0.19720E-04	-0.84914E-06	0.10291E-07

APPENDIX B

This appendix presents the results of the regression analyses of the transmissivities, katabatic emissions, and anabatic emissions of the 582 model atmospheres using as predictors the equivalent depths of gaseous, cloud, and rain water. These analyses were made for a zenith angle of 55 deg. The regression equations are third order equations in the three independent variables (predictors). The multiple correlation coefficients and standard errors (db) are shown also.

Table B1. Table of symbols used in subsequent tables.

Symbol	Meaning	Units
Γ	Transmissivity	--
ξ	Emissivity, 1 - Γ	--
W_v	Equivalent depth of gaseous water	mm
W_c	Equivalent depth of liquid water in cloud mass	mm
W_p	Equivalent depth of liquid water in rain mass	mm
T_{ap}	Polarized, anabatic brightness temperature	K
T_{kp}	Polarized, katabatic brightness temperature	K
x	ln (W_c + 0.01), independent variable	--
y	ln (W_p + 0.01), independent variable	--
z	W_v, independent variable	mm
u*	ln ξ, ln T_{kp}, or ln T_{ap}; dependent variable	--

*Refer to caption of following tables for type of dependent variable.

Table B2. Regression analysis of ln ξ: θ = 55 deg.

Term	Regression Coefficients			
	ν = 2.695 GHz	ν = 4.805 GHz	ν = 5.81 GHz	ν = 10.69 GHz
Constant	-0.36644593E 01	-0.29567981E 01	-0.25997275E 01	-0.14129632E 01
x	0.16519135E 00	0.28038753E 00	0.30281772E 00	0.32372134E 00
x^2	0.68901528E-01	0.10194029E 00	0.10496589E 00	0.92652485E-01
x^3	0.96032784E-02	0.12566778E-01	0.12519162E-01	0.88152165E-02
y	0.18405517E 00	0.44209516E 00	0.55843490E 00	0.72406677E 00
y^2	0.85484260E-01	0.13326382E 00	0.13611687E 00	0.37661902E-01
y^3	0.11929187E-01	0.13688237E-01	0.10622392E-01	-0.14052468E-01
z	-0.11812625E-01	-0.18754305E-01	-0.21495645E-01	-0.19304961E-01
z^2	0.16804679E-03	0.26695868E-03	0.30894917E-03	0.32567167E-03
z^3	-0.81171735E-06	-0.12453939E-05	-0.14559254E-05	-0.17058362E-05
xy	-0.29316012E-01	-0.71810346E-01	-0.89301420E-01	-0.11067038E 00
xy^2	-0.54308808E-02	-0.10569932E-01	-0.11558357E-01	-0.58585721E-02
xz	-0.65991395E-03	-0.17120333E-02	-0.22365614E-02	-0.44880522E-02
xz^2	0.29973485E-05	0.98835588E-05	0.13893127E-04	0.29110706E-04
x^2y	-0.10054101E-02	-0.31250810E-02	-0.45975843E-02	-0.81078774E-02
x^2z	-0.89669407E-04	-0.22217930E-03	-0.26956094E-03	-0.35829423E-03
yz	-0.10099828E-02	-0.22677295E-02	-0.24649616E-02	-0.10794834E-02
yz^2	0.30261519E-05	0.79635228E-05	0.91948815E-05	0.32406388E-05
y^2z	-0.11595535E-03	-0.20497862E-03	-0.18471220E-03	-0.80170424E-05
xyz	0.33350639E-04	0.13805864E-03	0.20038833E-03	0.37563152E-03
M.C.C.*	0.9952	0.9975	0.9970	0.9960
S.E.E.**	0.1595 db	0.2206 db	0.2816 db	0.3999 db

*Multiple Correlation Coefficient
**Standard Error of Estimate

Table B2 (cont'd).

	Regression Coefficients			
	ν = 15.375 GHz	ν = 19.35 GHz	ν = 31.4 GHz	ν = 37.0 GHz
Constant	-0.85957090E 00	-0.62930076E 00	-0.12814169E 00	-0.48638063E-01
x	0.35609824E 00	0.37544394E 00	0.31449987E 00	0.26336119E 00
x^2	0.86560243E-01	0.82468019E-01	0.48667589E-01	0.31658237E-01
x^3	0.60737254E-02	0.57265346E-02	-0.48148527E-02	-0.79757083E-02
y	0.63117678E 00	0.50710265E 00	0.32089413E 00	0.24468452E 00
y^2	-0.11553895E-02	0.11601149E-02	-0.22324158E-01	-0.21768608E-01
y^3	-0.17621635E-01	-0.12378799E-01	-0.10948548E-01	-0.87892629E-02
z	-0.14848093E-01	-0.63666717E-02	-0.11212299E-01	-0.97998344E-02
z^2	0.28493800E-03	0.16679272E-03	0.20839337E-03	0.17871893E-03
z^3	-0.15364314E-05	-0.89839657E-06	-0.11107867E-05	-0.95533494E-06
xy	-0.11036024E 00	-0.86289095E-01	-0.10828291E 00	-0.10062419E 00
xy^2	-0.39924688E-02	-0.40186066E-02	-0.43687666E-02	-0.35815669E-02
xz	-0.66783752E-02	-0.89086525E-02	-0.63660414E-02	-0.49817903E-02
xz^2	0.44675413E-04	0.61195481E-04	0.44600975E-04	0.35106213E-04
x^2y	-0.68270777E-02	-0.48771419E-02	0.64498742E-03	0.23666587E-02
x^2z	-0.43130950E-03	-0.61037057E-03	-0.24907879E-03	-0.14190342E-03
yz	-0.14368837E-02	-0.32700641E-02	-0.12091416E-02	-0.75308301E-03
yz^2	0.47360138E-05	0.13585032E-04	0.52185982E-05	0.30315605E-05
y^2z	-0.24688912E-04	-0.12627921E-03	0.26098968E-04	0.39661241E-04
xyz	0.47917318E-03	0.49196194E-03	0.50502056E-03	0.45265973E-03
M.C.C.*	0.9973	0.9973	0.9968	0.9961
S.E.E.**	0.2984 db	0.2209 db	0.2291 db	0.2260 db

*Multiple Correlation Coefficient
**Standard Error of Estimate

Table B3. Regression analysis of ln T_{kp}: θ = 55 deg.

Term	Regression Coefficients			
	ν = 2.695 GHz	ν = 4.805 GHz	ν = 5.81 GHz	ν = 10.69 GHz
Constant	0.18529075E 01	0.25879323E 01	0.29532486E 01	0.41546769E 01
x	0.16692365E 00	0.28234679E 00	0.30396010E 00	0.32165577E 00
x^2	0.68289802E-01	0.10013528E 00	0.10265556E 00	0.89243007E-01
x^3	0.95404505E-02	0.12270925E-01	0.12140941E-01	0.83527195E-02
y	0.19106612E 00	0.45296402E 00	0.56942627E 00	0.73031110E 00
y^2	0.86413722E-01	0.13350311E 00	0.13621986E 00	0.37826592E-01
y^3	0.11848166E-01	0.13364735E-01	0.10278927E-01	-0.14188869E-01
z	-0.79742851E-02	-0.15416680E-01	-0.18295641E-01	-0.16206743E-01
z^2	0.11499841E-03	0.22282517E-03	0.26765512E-03	0.28914236E-03
z^3	-0.53647200E-06	-0.10237749E-05	-0.12535185E-05	-0.15442703E-05
xy	-0.29494017E-01	-0.72574154E-01	-0.90050089E-01	-0.10972615E 00
xy^2	-0.51855671E-02	-0.10190523E-01	-0.11081462E-01	-0.49003343E-02
xz	-0.77627223E-03	-0.19373417E-02	-0.24953220E-02	-0.48242992E-02
xz^2	0.37513931E-05	0.11531051E-04	0.15865163E-04	0.31927596E-04
x^2y	-0.13861963E-02	-0.36141267E-02	-0.50973301E-02	-0.85896793E-02
x^2z	-0.10251673E-03	-0.23824469E-03	-0.28473195E-03	-0.36673826E-03
yz	-0.10465757E-02	-0.23282546E-02	-0.25170348E-02	-0.10706886E-02
yz^2	0.29532740E-05	0.80434104E-05	0.92747310E-05	0.32015592E-05
y^2z	-0.12312440E-03	-0.21181841E-03	-0.18922061E-03	-0.43835552E-05
xyz	0.40532910E-04	0.15112018E-03	0.21575144E-03	0.39362024E-03
M.C.C.*	0.9966	0.9980	0.9974	0.9962
S.E.E.**	0.1380 db	0.1984 db	0.2687 db	0.3959 db

* Multiple Correlation Coefficient
**Standard Error of Estimate

Table B3 (cont'd).

	Regression Coefficients			
	ν = 15.375 GHz	ν = 19.35 GHz	ν = 31.4 GHz	ν = 37.0 GHz
Constant	0.47112574E 01	0.49417939E 01	0.54475357E 01	0.55280366E 01
x	0.35328911E 00	0.37242572E 00	0.31088178E 00	0.26005906E 00
x^2	0.83199035E-01	0.79705494E-01	0.45924642E-01	0.29071664E-01
x^3	0.57293819E-02	0.54885393E-02	-0.49253079E-02	-0.80651152E-02
y	0.63561026E 00	0.51133723E 00	0.32460963E 00	0.24837436E 00
y^2	-0.89753028E-03	0.13999331E-02	-0.22709085E-01	-0.22380850E-01
y^3	-0.17683105E-01	-0.12446891E-01	-0.11134900E-01	-0.90143769E-02
z	-0.11703564E-01	-0.31379430E-02	-0.80286401E-02	-0.66031990E-02
z^2	0.24930481E-03	0.13134758E-03	0.17431413E-03	0.14481652E-03
z^3	-0.13852767E-05	-0.75270847E-06	-0.97460889E-06	-0.82135002E-06
xy	-0.10831125E 00	-0.84117752E-01	-0.10586888E 00	-0.98565746E-01
xy^2	-0.29372002E-02	-0.31501074E-02	-0.33425922E-02	-0.25900071E-02
xz	-0.70219523E-02	-0.91986575E-02	-0.66260286E-02	-0.52246942E-02
xz^2	0.47686420E-04	0.63920922E-04	0.47028914E-04	0.37390601E-04
x^2y	-0.73166312E-02	-0.52986776E-02	0.12839789E-03	0.18604588E-02
x^2z	-0.43806275E-03	-0.61709056E-03	-0.24816143E-03	-0.13771034E-03
yz	-0.14223310E-02	-0.32716631E-02	-0.11534806E-02	-0.68630346E-03
yz^2	0.47515731E-05	0.13772549E-04	0.50435554E-05	0.27906169E-05
y^2z	-0.20681370E-04	-0.12249014E-03	0.31077333E-04	0.44903114E-04
xyz	0.49399962E-03	0.50014253E-03	0.51647544E-03	0.46510289E-03
M.C.C.*	0.9974	0.9974	0.9973	0.9969
S.E.E.**	0.2934 db	0.2189 db	0.2130 db	0.2087 db

*Multiple Correlation Coefficient
**Standard Error of Estimate

Table B4. Regression analysis of ln T_{ap}: θ = 55 deg.

Term	Regression Coefficients			
	ν = 2.695 GHz	ν = 4.805 GHz	ν = 5.81 GHz	ν = 10.69 GHz
Constant	0.18520016E 01	0.25870301E 01	0.29525646E 01	0.41552946E 01
x	0.16683984E 00	0.28214366E 00	0.30361864E 00	0.32075559E 00
x^2	0.68248876E-01	0.99996889E-01	0.10241798E 00	0.88478049E-01
x^3	0.95354519E-02	0.12257939E-01	0.12123405E-01	0.82924633E-02
y	0.19099232E 00	0.45286458E 00	0.56946881E 00	0.73053204E 00
y^2	0.86334517E-01	0.13304414E 00	0.13528243E 00	0.34394350E-01
y^3	0.11833864E-01	0.13272021E-01	0.10080112E-01	-0.14909651E-01
z	-0.79613350E-02	-0.15389923E-01	-0.18253826E-01	-0.16117884E-01
z^2	0.11465895E-03	0.22209182E-03	0.26648418E-03	0.28554335E-03
z^3	-0.53411049E-06	-0.10186374E-05	-0.12452444E-05	-0.15167286E-05
xy	-0.29481943E-01	-0.72489058E-01	-0.89850951E-01	-0.10921373E 00
xy^2	-0.51825601E-02	-0.10170878E-01	-0.11035589E-01	-0.47788934E-02
xz	-0.77520091E-03	-0.19364824E-02	-0.24934976E-02	-0.48300801E-02
xz^2	0.37399984E-05	0.11513769E-04	0.15834079E-04	0.31892130E-04
x^2y	-0.13880870E-02	-0.36273016E-02	-0.51252016E-02	-0.86823154E-02
x^2z	-0.10251642E-03	-0.23841908E-03	-0.28496975E-03	-0.36804580E-03
yz	-0.10459469E-02	-0.23296111E-02	-0.25228031E-02	-0.11211246E-02
yz^2	0.29484840E-05	0.80466828E-05	0.92873616E-05	0.33376937E-05
y^2z	-0.12308914E-03	-0.21203146E-03	-0.19019887E-03	-0.11535979E-04
xyz	0.40540153E-04	0.15098995E-03	0.21548882E-03	0.39190096E-03
M.C.C.*	0.9966	0.9980	0.9973	0.9960
S.E.E.**	0.1378 db	0.1988 db	0.2708 db	0.4019 db

*Multiple Correlation Coefficient
**Standard Error of Estimate

Table B4 (cont'd).

	Regression Coefficients			
	ν = 15.375 GHz	ν = 19.35 GHz	ν = 31.4 GHz	ν = 37.0 GHz
Constant	0.47112205E 01	0.49394567E 01	0.54393582E 01	0.55160388E 01
x	0.35224667E 00	0.37096997E 00	0.30725879E 00	0.25532809E 00
x^2	0.82052244E-01	0.78101453E-01	0.42771930E-01	0.25229128E-01
x^3	0.55864771E-02	0.52452811E-02	-0.54261839E-02	-0.86558967E-02
y	0.63390953E 00	0.50775291E 00	0.31810379E 00	0.24128952E 00
y^2	-0.47985888E-02	-0.23432396E-02	-0.25615032E-01	-0.24904727E-01
y^3	-0.18410927E-01	-0.13064635E-01	-0.11479132E-01	-0.92706968E-02
z	-0.11650845E-01	-0.30859636E-02	-0.80731028E-02	-0.66620130E-02
z^2	0.24455226E-03	0.12439371E-03	0.16690742E-03	0.13672283E-03
z^3	-0.13463125E-05	-0.69832152E-06	-0.91033014E-06	-0.75077294E-06
xy	-0.10819305E 00	-0.84232429E-01	-0.10577392E 00	-0.98092274E-01
xy^2	-0.28833221E-02	-0.31129972E-02	-0.31716413E-02	-0.23065764E-02
xz	-0.70586051E-02	-0.92617878E-02	-0.67430305E-02	-0.53572274E-02
xz^2	0.47831632E-04	0.64250718E-04	0.47792867E-04	0.38295479E-04
x^2y	-0.74184837E-02	-0.54083179E-02	-0.32711049E-04	0.16649357E-02
x^2z	-0.44192629E-03	-0.62400410E-03	-0.25894427E-03	-0.14938829E-03
yz	-0.15022671E-02	-0.33588518E-02	-0.12751720E-02	-0.81352417E-03
yz^2	0.50346321E-05	0.14119821E-04	0.55564155E-05	0.33233241E-05
y^2z	-0.29306763E-04	-0.13018496E-03	0.22011118E-04	0.35794646E-04
xyz	0.49144783E-03	0.49866051E-03	0.51691164E-03	0.46664211E-03
M.C.C.*	0.9973	0.9973	0.9971	0.9965
S.E.E.**	0.2974 db	0.2217 db	0.2191 db	0.2157 db

*Multiple Correlation Coefficient
**Standard Error of Estimate

REFERENCES

Ackerman, B., 1959: The variability of the water contents of tropical cumuli. J. Meteor., 16, 191-198.

———, 1963: Some observations of water contents in hurricanes. J. Atmos. Sci., 20, 288-298.

Aden, A. L., 1951: Electromagnetic scattering from spheres with sizes comparable to the wavelength. J. Appl. Phys., 22, 601-605.

———, 1952: Back-scattering of electromagnetic waves from spheres and spherical shells. Geophys. Res. Paper 15, Cambridge, Mass., Geophys. Res. Div., Air Force Cambridge Res. Center, 42 pp.

Anderson, L. J., J. P. Day, C. H. Freres and A. P. D. Stokes, 1947: Attenuation of 1.25-cm radiation through rain. Proc. IRE, 35, 351-354.

Anderson, P. W., 1949: On the limits of validity of the Van Vleck-Weisskopf line shape formula. Phys. Rev., 76, 417.

Apparao, M. V. K., 1968: Upper limits on universal microwave radiation below λ = 1.7 mm. Nature, 219, 709-710.

Atlas, D., 1953: Optical extinction by rainfall. J. Meteor., 10, 486-488.

———, and H. C. Banks, 1951: The interpretation of microwave reflections from rainfall. J. Meteor., 8, 271-282.

———, and V. G. Plank, 1953: Drop-size history in a shower. J. Meteor., 10, 291-295.

Aufm Kampe, H. J., 1950: Visibility and liquid water content in clouds in the free atmosphere. J. Meteor., 7, 54-57.

Barath, F. T., 1965: Microwave radiometry and applications to oceanography. Oceanography from Space, Ref. 65-10, Woods Hole, Mass., Woods Hole Oceanography Inst., 235-239.

Barrett, A. H., 1966: Semiannual report, March 1, 1966 to August 31, 1966. Contract NSR-22-009-120, Cambridge, Mass., National Aeronautics and Space Administration, Res. Lab. of Electronics, Mass. Inst. of Tech., 6 pp.

———, and V. K. Chung, 1962: A method for the determination of high altitude water vapor abundance from ground-based microwave observations. J. Geophys. Res., 67, 4259-4266.

Basharinov, A. Ye., A. B. Gorelik, V. V. Kalashnikov and B. G. Kutuza, 1968: The determination of cloud and rain characteristics by means of simultaneous microwave radiometric and radar measurements. Proc. Thirteenth Radar Meteor. Conf., Boston, Am. Meteor. Soc., 536-539.

Bean, B. R., and E. J. Dutton, 1966: Radio Meteorology. National Bu. of Standards Monograph 92., Washington, D. C., Gov. Printing Office, 435 pp.

Becker, G. E., and S. H. Autler, 1946: Water vapor absorption of electromagnetic radiation in the centimeter wave-length range. Phys. Rev., 70, 300-307.

Beckman, P., and A. Spizzichino, 1963: The Scattering of Electromagnetic Waves from Rough Surfaces. New York, Pergamon Press, 503 pp.

Bellman, R. E., H. H. Kagiwada, and R. E. Kalaba, 1966: Numerical inversion of Laplace transforms and some inverse problems in radiative transfer. J. Atmos. Sci., 23, 555-559.

———, R. Kalaba, and G. M. Wing, 1960: Invariant imbedding and mathematical physics. I. Particle processes. J. Math. Phys., 1, 280-308.

Benoit, A., 1968: Signal attenuation due to neutral oxygen and water vapour, rain and clouds. Microwave J., 11, 73-80.

Benwell, G. R. R., 1965: The estimation and variability of precipitable water. Meteor. Magazine, 94, 319-327.

Best, A. C., 1950: The size distribution of raindrops. Quart. J. Roy. Meteor. Soc., 76, 16-36.

Blanchard, D. C., 1950: The behavior of water drops at terminal velocity in air. Trans. Am. Geophys. Un., 31, 836-842.

———, 1953: Raindrop size-distribution in Hawaiian rains. J. Meteor., 10, 457-473.

———, 1963: Electrification of the atmosphere by particles from bubbles in the sea. Progress in Oceanography, Vol. 1, New York, Pergamon Press, 71-202.

Bowers, K. D., R. A. Kemper and C. D. Lustig, 1959: Paramagnetic resonance absorption in molecular oxygen. Proc. Roy. Soc. (London), A251, 565-574.

Browne, I. C., H. P. Palmer and T. W. Wormell, 1954: The physics of rainclouds. Quart. J. Roy. Meteor. Soc., 80, 291-327.

Buettner, K. J. K., 1963: Regenortung vom wettersatelliten mit hilfe von zentimeterwellen. Naturwiss., 50, 591-592.

Burrows, C. R., and S. A. Attwood, 1949: Radio Wave Propagation. New York, Academic Press, 548 pp.

Busbridge, I. W., 1960: The Mathematics of Radiative Transfer. Cambridge, England, Univ. Press, 143 pp.

Bussey, H. E., 1950: Microwave attenuation statistics estimated from rainfall and water vapor statistics. Proc. IRE, 38, 781-785.

Castelli, J. P., J. Aarons, C. Ferioli, and J. Casey, 1959: Absorption, refraction, and scintillation measurements at 4700 Mc/s with a traveling-wave tube radiometer. Planet. Space Sci., 1, 50-56.

Catoe, C., W. Nordberg, P. Thaddeus and G. Ling, 1967: Preliminary results from aircraft flight tests of an electrically scanning microwave radiometer. X-622-67-352, Greenbelt, Md., Goddard Space Flight Center, 35 pp.

Caton, P. G. F., 1966: A study of raindrop-size distribution in the free atmosphere. Quart. J. Roy. Meteor. Soc., 92, 15-30.

Chandrasekhar, S., 1960: Radiative Transfer. New York, Dover Publications, 393 pp.

Chemical Rubber Company, 1959: Handbook of Chemistry and Physics. Cleveland, Chemical Rubber Pub. Co., 3456 pp.

Chen, S. N. C., and W. H. Peake, 1961: Apparent temperatures of smooth and rough terrain. IRE Trans. Ant. Prop., AP-9, 567-572.

Cole, A. E., A. Court and A. J. Kantor, 1965: Model atmospheres. Handbook of Geophysics and Space Environments, New York, McGraw-Hill Book Co., 2-1 to 2-22.

Collie, C. H., J. B. Hasted and D. M. Ritson, 1948a: The cavity resonator method of measuring the dielectric constant of polar liquids. Proc. Phys. Soc. (London), 60, 71-82.

———, ——— and ———, 1948b: The dielectric properties of water and heavy water. Proc. Phys. Soc. (London), 60, 145-160.

———, D. M. Ritson and J. B. Hasted, 1946: Dielectric properties of water. Trans. Faraday Soc., 42A, 129-136.

Conway, W. H., and G. Mardon, 1965: Microwave radiometers for ocean and weather measurements. Oceanography from Space, Ref. 65-10, Woods Hole, Mass., Woods Hole Oceanography Inst., 241-271.

Cox, C., and W. Munk, 1954a: Measurement of the roughness of the sea surface from photographs of the sun's glitter. J. Opt. Soc. Am., 44, 838-850.

———, and ———, 1954b: Statistics of the sea surface derived from sun glitter. J. Marine Res., 13, 198-227.

Croom, D. L., 1964a: Naturally-occuring thermal radiation in the range 1-10 GHz. Proc. Inst. Elec. Eng. (London), 111, 967-980.

———, 1964b: Stratospheric thermal emission and absorption near the 22.235 Gc/s (1.35 cm) rotational line of water-vapor. J. Atmos. Terr. Phys., 27, 217-233.

———, 1966: The possible detection of atmospheric water vapor from a satellite by observation of the 13.5 mm and 1.66 mm H_2O lines. J. Atmos. Terr. Phys., 28, 323-326.

Cummings, C. A., and J. W. Hull, 1966: Microwave radiometric meteorological observations. Proc. Fourth Symp. on Remote Sensing of Environment, Ann Arbor, Mich., Univ. of Mich., 263-271.

Debye, P. 1929: Polar Molecules. New York, Dover Pub., 172 pp.

Decker, M. T., and E. J. Dutton, 1970: Radiometric observations of liquid water in thunderstorm cells. J. Atmos. Sci., 27, 785-790.

Deirmendjian, D., 1963: Complete microwave scattering and extinction properties of polydispersed cloud and rain elements. R-422-PR, Santa Monica, Calif., RAND Corp., 54 pp.

———, 1965: Complete scattering parameters of polydispersed hydrometeors in the λ 0.1 to λ 10 cm range. Radio Sci. J. Res., 893-897.

———, 1969: Electromagnetic scattering on spherical polydispersion. R-456-PR, Santa Monica, Calif., RAND Corp., 290 pp. (also available from Am. Elsevier Pub. Co., New York).

———, R. Clasen and W. Viesee, 1961: Mie scattering with complex index of refraction. J. Opt. Soc. Amer., 51, 620-633.

Derr, V. E., 1967: Propagation of millimeter and sub-millimeter waves. NASA CR-863, Washington, D. C., The Natl. Aeronautics and Space Admin., 114 pp. (available from CFSTI, Springfield, Va., 22151, price $3.00).

Dicke, R. H., 1946: The measurement of thermal radiation at microwave frequencies. Rev. Sci. Instruments, 17, 268-275.

Dingle, A. N., and K. R. Hardy, 1962: The description of rain by means of sequential raindrop-size distributions. Quart. J. Roy. Meteor. Soc., 88, 301-314.

Draginis, M., 1958: Liquid water within convective clouds. J. Meteor., 15, 481-485.

Droppleman, J. D., 1970: Apparent microwave emissivity of sea foam. J. Geophys. Res., 75, 696-698.

———, R. A. Mennella and D. E. Evans, 1970: An airborne measurement of the salinity variation of the Mississippi River outflow. J. Geophys. Res., 75, 5909-5913.

Durbin, W. G., 1959: Droplet sampling in cumulus clouds. Tellus, 11, 202-215.

Edison, A. R., 1966: Calculated cloud contributions to sky temperatures at millimeter-wave frequencies. NBS Report 9138, Boulder, Colo., National Bu. of Standards, 26 pp.

Falcone, V. J., Jr., 1966: Calculations of apparent sky temperature at millimeter wavelengths. Radio Sci., 1, 1205-1209.

Fanning, R. W., 1965: An investigation of the applicability of analytically manageable raindrop size distributions to radar observations of subtropical precipitation. M. S. Thesis, College Station, Texas, Dept. of Meteor., Texas A&M Univ., 53 pp.

Fleck, J. A., Jr., 1963: The calculation of nonlinear radiation transport by a Monte Carlo method. Methods in Computational Physics, 1 (Statistical Physics), New York, Academic Press, 43-65.

Flower, W. D., 1928: The terminal velocity of drops. Proc. Phys. Soc. (London), 40, 167-176.

Foote, G. B., 1969: On the internal circulation and shape of large raindrops. J. Atmos. Sci., 26, 179-181.

———, and P. S. Du Toit, 1969: Terminal velocity of raindrops aloft, J. Appl. Meteor., 8, 249-253.

Fried, D. L., 1966: Temperature and roughness dependence of ocean-surface emissivity. Thousand Oaks, Calif., North American Aviation Science Center, North American Aircraft Co., 30 pp.

Fröhlich, H., 1946: Shape of collision-broadened spectral lines. Nature, 157, 478.

Funakawa, K., and J. Kato, 1962: Experimental studies of propagation characteristics of 8.6 mm wave on the 24 km path. J. Radio Res. Labs. (Tokyo), 9, 351-367.

Goldstein, H., 1951: Attenuation by condensed water. Propagation of Short Radio Waves, New York, McGraw-Hill Book Co., 671-692.

Goody, R. M., 1964: Atmospheric Radiation. I. Theoretical Basis. Oxford, Clarendon Press, 436 pp.

Gross, E. P., 1955: Shape of collision-broadened spectral lines. Phys. Rev., 97, 395-403.

Gunn, K. L. S., and T. W. R. East, 1954: The microwave properties of precipitation particles. Quart. J. Roy. Meteor. Soc., 80, 522-545.

Gunn, R., and G. D. Kinzer, 1949: The terminal velocity of fall for water droplets in stagnant air. J. Meteor., 6, 243-248.

Gurvich, A. S., and S. T. Egorov, 1966: Determination of the surface temperature of the sea from its thermal radio-emission. Izv. Atm. and Oceanic Phys. (English translation), 2, 305-307.

Gutnick, M., 1961: How dry is the sky? J. Geophys. Res., 66, 2867-2871.

Haroules, G. G., and W. E. Brown, III, 1968: Radiometric measurement of attenuation and emission by the earth's atmosphere at wavelengths from 4 cm to 8 mm. IEEE Trans. on Microwave Theory and Techniques, MTT-16, 611-620.

———, and ———, 1969: The simultaneous investigation of attenuation and emission by the earth's atmosphere at wavelengths from 4 centimeters to 8 millimeters. J. Geophys. Res., 74, 4453-4471.

Hasted, J. B., 1961: The dielectric properties of water. Progress in Dielectrics, 3, 102-149.

———, and S. M. El-Sabeh, 1953: The dielectric properties of water in solutions. Trans. Faraday Soc., 49, 1003-1011.

———, D. M. Ritson and C. H. Collie, 1948: Dielectric properties of aqueous ionic solutions. J. Chem. Phys., 16, 1-21.

———, and G. W. Roderick, 1958: Dielectric properties of aqueous and alcoholic electrolytic solutions. J. Chem. Phys., 29, 17-26.

Hathaway, S. D., and H. W. Evans, 1959: Radio attenuation at 11 kmc and implications affecting relay system engineering. Bell Sys. Tech. J., 38, 73-97.

Hogg, D. C., 1959: Effective antenna temperature due to oxygen and water vapor in the atmosphere. J. Appl. Phys., 30, 1417-1419.

———, 1967: Path diversity in propagation of millimeter waves through rain. IEEE Trans. Prop., AP-15, 410-415.

———, 1968: Millimeter-wave communication through the atmosphere. Sci., 159, 39-46.

———, and W. W. Mumford, 1960: The effective noise temperature of the sky. Microwave J., 3, 80-84.

———, and R. A. Semplak, 1961: The effect of rain and water vapor on sky noise at centimeter wavelengths. Bell Sys. Tech. J., 40, 1331-1348.

———, and ———, 1963: Estimated sky temperatures due to rain for the microwave band. Proc. IEEE, 51, 499-500.

———, ——— and D. A. Gray, 1963: Measurement of microwave interference at 4 Gc due to scatter by rain. Proc. IEEE, 51, 500.

Hollinger, J. P., 1970: Passive microwave measurements of the sea surface. J. Geophys. Res., 75, 5209-5213.

Holzer, W., 1965: Atmospheric attenuation in satellite communications. Microwave J., 8, 119-125.

Howell, T. F., and J. R. Shakeshaft, 1967: Attenuation of radio waves by the troposphere over the frequency range 0.4 - 10 GHz. J. Atm. Terr. Phys., 29, 1559-1571.

Imai, I., 1957: Attenuation of microwaves through rain for various dropsize distributions. 75th Anniversary Volume of J. Meteor. Soc. (Japan), 65-71.

Jansky, K. G., 1935: A note on the source of intersteller interference. Proc. IRE, 23, 1158-1163.

Jordan, E. C., and K. G. Balmain, 1968: Electromagnetic Waves and Radiating Systems. Englewood Cliffs, N. J., Prentice-Hall Pub. Co., 753 pp.

Judge, C. W., 1965: To hunt an iceburg -- microwave radiometry. Geo-Marine Tech., (no volume), 29-31.

Kattawar, G. W., and G. N. Plass, 1968a: Influence of particle size distribution on reflected and transmitted light from clouds. Appl. Optics, 7, 869-878.

———, and ———, 1968b: Radiance and polarization of multiple scattered light from haze and clouds. Appl. Optics, 7, 1519-1527.

———, and ———, 1969: Infrared cloud radiance. Appl. Optics, 8, 1169-1178.

Kerker, M., 1969: The Scattering of Light and other Electromagnetic radiation. New York, Academic Press, 666 pp.

Kraus, J. D., 1964: Radio and radar astronomy and the exploration of the universe. IEEE Trans. Mil. Electrons, MIL-8, 232-235.

Kreiss, W. T., 1968: Meteorological observations with passive microwave systems. Doc. D1-82-0692, Seattle, Wash., Boeing Aircraft Co., 198 pp.

———, 1969: The influence of clouds on microwave brightness temperatures viewing downward over open seas. Proc. IEEE, 57, 440-446.

Kreyszig, E., 1962: Advanced Engineering Mathematics. New York, John Wiley and Sons Pub. Co., 898 pp.

Kutuza, B. G., 1968: Investigation of radiowave attenuation and radiation of rain in the microwave range. Proc. Thirteenth Radar Meteor. Conf., Boston, Am. Meteor. Soc., 540-542.

Lane, J. A., and J. A. Saxton, 1952a: Dielectric dispersion in pure polar liquids at very high radio-frequencies. I. Measurements on water, methyl and ethyl alcohols. Proc. Roy. Soc., A213, 400-408.

———, and ———, 1952b: Dielectric dispersion in pure polar liquids at very high radio frequencies. III. the effect of electrolytes in solution. Proc. Roy. Soc. (London), A214, 531-545.

Laws, J. O., and D. A. Parsons, 1943: The relationship or raindrop size to intensity. Trans. Am. Geophys. Un., 24, 452-460.

LeFande, R. A., 1968: Attenuation of microwave radiation for paths through the atmosphere. NRL Report 6766, Washington, D. C., Naval Res. Lab., 30 pp.

Lenoir, W. B., J. W. Barrett and D. Cosmo Papa, 1968: Observations of microwave emission by molecular oxygen in the stratosphere. J. Geophys. Res. 73, 119-1126.

Logan, N. A., 1962: Early history of the Mie solution. J. Opt. Soc. Am., 52, 342-343.

———, 1965: Survey of some early studies of the scattering of plane waves by a sphere. Proc. IEEE, 53, 773-785.

Lorenz, L., 1890: Selskabs Skrifter, 6.

Love, T. J., 1968: Radiative Heat Transfer. Columbus, Ohio, Ch. E. Merrill Pub. Co., 287 pp.

Lukes, G. D., 1968: Penetrability of haze, fog, clouds, and precipitations by radiant energy over the spectral range 0.1 micron to 10 cm. Study 61, New York, Center for Naval Analysis, Univ. of Rochester, 225 pp.

Magono, C., 1954: On the shape of water drops falling in stagnant air. J. Meteor., 11, 77-79.

Malmberg, C. G., and A. A. Maryott, 1956: Dielectric constant of water from 0° to 100°C. J. Res. Natl. Bur. Std., 56, 1-8.

Marandino, G. E., 1967: Microwave Signatures from Various Terrain. B. S. Thesis, Mass. Inst. of Tech., Cambridge, Mass., 54 pp.

Mardon, A., 1965: Application of microwave radiometers to oceanographic measurements. Proc. Third Symp. on Remote Sensing of Environment, Ann Arbor, Mich., Univ. of Mich., 763-779.

Marshall, J. S., W. Hitschfeld and K. L. S. Gunn, 1955: Advances in radar weather. Advances in Geophysics, Vol. 2, New York, Academic Press, 1-56.

———, and W. McK. Palmer, 1948: The distribution of raindrops with size. J. Meteor., 5, 165-166.

Mason, B. J., 1957: The Physics of Clouds. London, Oxford Univ. Press, 481 pp.

———, and J. B. Andrews, 1960: Drop-size distributions from various types of rain. Quart. J. Roy. Meteor. Soc., 86, 346-353.

McDonald, J. E., 1954: The shape and aerodynamics of large raindrops. J. Meteor., 11, 478-494.

McLellan, H. J., 1965: Elements of Physical Oceanography. New York, Pergamon Press, 150 pp.

Medhurst, R. G., 1965: Rainfall attenuation of centimeter waves: comparison of theory and measurement. IEEE Trans. Ant. Prop. AP-13, 550-564.

Meeks, M. L., and A. E. Lilley, 1963: The microwave spectrum of oxygen in the earth's atmosphere. J. Geophys. Res., 68, 1683-1703.

Mie, G., 1908: Beiträge zur Optik trüber Median, speziell kolloidaler Metallösungen. Annalen der Physik, 25, 377-445.

Mizushima, M., 1960: Theory of microwave absorption by compressed oxygen gas. J. Chem. Phys., 32, 691-697.

Neiburger, M., 1949: Reflection, absorption and transmission of insolation by stratus cloud. J. Meteor., 6, 98-104.

Nordberg, W., J. Conaway and P. Thaddeus, 1969: Microwave observations of sea state from aircraft. Quart. J. Roy. Meteor. Soc., 95, 408-413.

Ohtake, T., 1970: Factors affecting the size distribution of raindrops and snowflakes. J. Atmos. Sci., 27, 804-813.

Paris, J. F., 1969: Microwave radiometry and its application to marine meteorology and oceanography. Ref. No. 69-II, Contract Nonr 2119(04), College Station, Texas, Dept. of Oceanography, Texas A&M Univ., 210 pp.

Peake, W. H., 1959: Interaction of electromagnetic waves with some natural surfaces. IRE Trans. Ant. Prop., AP-7, S324-S329.

———, 1967: The microwave radiometer as a remote sensing instrument, with applications to geology. Notes for a Short Course on Geologic Remote Sensing, Palo Alto, Calif., Stanford Univ., 34 pp.

Penn, S., and B. Kunkel, 1963: On the prediction and variability of water vapor. J. Appl. Meteor., 2, 44-48.

Pereslegin, S. V., 1967: On the relationship between the thermal and radio brightness contrasts of the sea surface. Izv. Atm. and Oceanic Phys., (English Translation), 3, 47-57.

Petterssen, S., 1956a: Weather Analysis and Forecasting. Vol. I. Motion and Motion Systems. New York, McGraw-Hill Book Co., 428 pp.

———, 1956b: Weather Analysis and Forecasting Vol. II. Weather and Weather Systems. New York, McGraw-Hill Book Co., 266 pp.

Planck, M., 1959: The Theory of Heat Radiation. New York, Dover Pub., 224 pp.

Plass, G. N., and G. W. Kattawar, 1968a: Influence of single scattering albedo on reflected and transmitted light from clouds. Appl. Optics, 7, 361-367.

———, and ———, 1968b: Monte Carlo calculations of light scattering from clouds. Appl. Optics, 415-419.

———, and ———, 1968c: Radiant intensity of light scattered from clouds. Appl. Optics, 7, 699-704.

———, and ———, 1969: Radiative transfer in an atmospheric-ocean system. Appl. Optics, 8, 455-466.

Porter, R. A., and E. T. Florance, 1969: Feasibility study of microwave radiometric remote sensing. NASA Contract No. NAS 12-629, Cambridge, Mass., Electronics Res. Center, 836 pp.

Rabinovich, Yu. I., G. G. Shchukin and V. V. Melent'yev, 1969: Determination of the temperature of the water surface from radio emission in the centimeter range. Transfer of Microwave Radiation in the Atmosphere, NASA TT F-590, Washington, D. C., The Natl. Aeronautics and Space Admin., 51-55. (available from CFSTI, Springfield, Va., Price $3.00).

Riehl, H., 1954: Tropical Meteorology. New York, McGraw-Hill Book Co., 392 pp.

Robertson, S. D., and A. P. King, 1946: The effect of rain upon the propagation of waves in the 1- and 3-cm regions. Proc. IRE, 34, 178P-180P.

Rosenblum, E. S., 1961: Atmospheric absorption of 10-400 GHz radiation: summary and bibliography to 1961. Microwave J., 4, 91-96.

Rothrock, D. A., 1913: Elements of Plane and Spherical Trigonometry. New York, MacMillan Book Co., 147 pp.

Ryde, J. W., 1946: The attenuation and radar echoes produced at centimeter wave-lengths by various meteorological phenomena. Meteorological Factors in Radio-Wave Propagation, London, The Physical Society, 169-188.

Saxton, J. A., 1946a: The anomalous dispersion of water at very high radio frequencies. Part II: Relationship of experimental observations to theory. Meteorological Factors in Radio-Wave Propagation, London, The Physical Society, 293-306.

———, 1946b: The anomalous dispersion of water at very high radio frequencies. Part III: The dipole relaxation time and its relation to the viscosity. Meteorological Factors in Radio-Wave Propagation, London, The Physical Society, 306-316.

———, 1946c: The anomalous dispersion of water at very high frequencies. Part IV: A note on the effect of salt in solution. Meteorological Factors in Radio-Wave Propagation, London, The Physical Society, 316-325.

———, 1949: Electrical properties of water. Wireless Engineer, 26, 288-292.

———, 1952: Dielectric dispersion in pure polar liquids at very high radio-frequencies. II. Relation of experimental results to theory. Proc. Roy. Soc. (London), A213, 473-492.

———, and J. A. Lane, 1946: The anomalous dispersion of water at very high radio frequencies. Part I: Experimental determination of the dielectric perperties of water in the temperature range 0°C to 40°C for wave-lengths of 1.24 cm. and 1.58 cm. Meteorological Factors in Radio-Wave Propagation, London, The Physical Society, 278-291.

———, and ———, 1952: Electrical properties of sea water: reflection and attenuation characteristics at v. h. f. Wireless Engineer, 29, 269-275.

Seling, T. V., and D. K. Nance, 1961: Sensitive microwave radiometer detects small icebergs. Electronics, (May 12), 72-75.

Shifrin, K. S., 1969: Transfer of Microwave Radiation in the Atmosphere. NASA TT F-590, Washington, D. C., the Natl. Aeronautics and Space Admin., 185 pp. (available from CFSTI, Springfield, Va., price $3.00)

Shreider, Yu. A., 1966: The Monte Carlo Method: The Method of Statistical Trials. New York, Pergamon Press, 381 pp.

Singer, S. F., and G. F. Williams, Jr., 1968: Microwave detection of precipitation over the surface of the ocean. J. Geophys. Res., 73, 3324-3327.

Singleton, F., 1960: Aircraft observations of rain and drizzle from layer clouds. Quart. J. Roy. Meteor. Soc., 86, 195-204.

———, and D. J. Smith, 1960: Some observations of dropsize distributions in low layer clouds. Quart. J. Roy. Meteor. Soc., 86, 454-467.

Sirounian, V., 1968: The effect of temperature, angle of observation, salinity, and thin ice on the microwave emission of water. J. Geophys. Res., 73, 4481-4486.

Squires, P., 1958: The spatial variation of liquid water and droplet concentration in cumuli. Tellus, 10, 372-380.

Staelin, D. H., 1965: Microwave spectral measurements applicable to oceanography. Oceanography from Space. Ref. 65-10, Woods Hole, Mass., Woods Hole Oceanographic Inst., 229-234.

———, 1966: Measurements and interpretation of the microwave spectrum of the terrestrial atmosphere near 1-centimeter wavelength. J. Geophys. Res., 71, 2875-2881.

———, 1969: Passive remote sensing at microwave wavelengths. Proc. IEEE, 57, 427-439.

Stepanenko, V. D., 1969: Several geometric characteristics of clouds and precipitatings based on radar observations. Transfer of Microwave Radiation in the Atmosphere, NASA TT F-590, Washington, D. C., The Natl. Aero. and Space Admin., 148-151.

Stephens, J. J., 1962: Radar characteristics of an exponential drop-size distribution with application to a dual-frequency system. Austin, Tex., Elect. Eng. Res. Lab., The Univ. of Tex. 31 pp., (plus appendices).

Stogryn, A., 1967: The apparent temperature of the sea at microwave frequencies. IEEE Trans. Ant. Prop., AP-15, 278-286.

Straiton, A. W., C. W. Tolbert and C. O. Britt, 1958: Apparent temperatures of some terrestrial materials and the sun at 4.3 millimeter wavelengths. J. Appl. Phys., 29, 776-782.

Stratton, J. A., 1930: The effect of rain and fog on the propagation of very short radio waves. Proc. IRE, 18, 1064-1074.

Sucher, M., and J. Fox, 1963: Handbook of Microwave Measurements. Vols. I, II, III. New York, John Wiley and Sons Pub Co., 283 pp.

Toong, H. D., and D. H. Staelin, 1970: Passive microwave spectrum measurements of atmospheric water vapor and clouds. J. Atmos. Sci., 27, 781-784.

van de Hulst, H. C., 1957: Light Scattering by Small Particles. New York, John Wiley and Sons Pub. Co., 470 pp.

Van Vleck, J. H., 1947a: The absorption of microwaves by oxygen. Phys. Rev., 71, 413-424.

———, 1947b: The absorption of microwaves by uncondensed water vapor, Phys. Rev., 71, 425-433.

———, and V. F. Weisskopf, 1945: On the shape of collision broadened lines. Rev. Mod. Phys., 17, 227-236.

Volchok, B. A., and M. M Chernyak, 1969: Transfer of microwave radiation in clouds and precipitation. Transfer of Microwave Radiation in the Atmosphere, NASA TT F-590, 90-97.

Von Hippel, A. R., 1954a: Dielectric and Waves. Cambridge, Mass., The M. I. T. Press, 284 pp.

———, 1954b: Dielectric Materials and Applications. Cambridge, Mass., The M. I. T. Press, 438 pp.

Warner, J., 1955: The water content of cumuliform cloud. Tellus, 7, 449-457.

Weger, E., 1960: Apparent sky temperature in the microwave region. J. Meteor., 17, 159-165.

Weickmann, H. K., and H. J. Aufm Kampe, 1953: Physical properties of cumulus clouds. J. Meteor., 10, 204-211.

Westwater, E. R., 1967: An analysis of the correction of range errors due to atmospheric refraction by microwave radiometric techniques. IER 30-ITSA, Boulder, Colo., ESSA Institute for Telecommunication Sciences and Aeronomy, 66 pp.

Wexler, R., and D. Atlas, 1963: Radar reflectivity and attenuation of rain. J. Appl. Meteor., 2, 276-280.

———, and R. J. Donaldson, Jr., 1968: Comments and reply "on the modeling of cumulus clouds." J. Atmos. Sci., 25, 1168.

Williams, G. F., Jr., 1969: Microwave radiometry of the ocean and the possibility of marine wind velocity determination from satellite observation. J. Geophys. Res., 74, 4591-4594.

Wulfsberg, K. N., 1964: Sky noise measurements at millimeter wavelengths. Proc. IEEE, 52, 321-322.

Wyman, J., 1930: Measurements of the dielectric constants of conducting media. Phys. Rev., 35, 623-634.

Yamamoto, G., T. Masayuki and K. Kamitini, 1966: Radiative transfer in water clouds in the 10-micron window region. J. Atmos. Sci., 23, 305-313.